Characterization of Iron- and Zinc-containing Alcohol Dehydrogenases from Anaerobic Hyperthermophiles

by

Xiangxian Ying

A thesis
presented to the University of Waterloo
in fulfillment of the
thesis requirement for the degree of
Doctor of Philosophy
in
Biology

Waterloo, Ontario, Canada, 2007

Author's Declaration

I hereby declare that I am the sole author of this thesis. This is a true copy of the thesis, including any required final revisions, as accepted by my examiners.

I understand that my thesis may be made electronically available to the public.

Abstract

Hyperthermophiles are microorganisms that can grow at temperatures close to the boiling point of water or above. They are potential resources of thermostable enzymes including alcohol dehydrogenases (ADHs). Both *Thermococcus guaymasensis* and *Thermotoga hypogea* produce ethanol as an end product using glucose as substrate. However, the metabolic pathway and enzymes involved in alcohol production by these hyperthermophiles were not clear. ADH is a key enzyme responsible for alcohol metabolism, and the enzyme has been purified and characterized.

T. hypogea is an extremely thermophilic anaerobic bacterium capable of growing at 90°C. The $NADP^+$-dependent ADH from *T. hypogea* was purified to homogeneity and a homodimeric protein with a subunit size of 40 ± 1 kDa. A part of its encoding gene was cloned and sequenced, from which a major part of the amino acid sequence of the enzyme was deduced and found to have high similarities to iron-containing ADHs from other *Thermotoga* species and harbored typical iron and $NADP^+$-binding motifs. The conserved domain search showed that *T. hypogea* ADH was a member of the family of uncharacterized iron-containing ADHs. The iron content of the enzyme was determined to be 1.02 ± 0.06 *g*-atoms per subunit. It is the first characterized iron-containing ADH from hyperthermophilic bacteria. Similar to known iron-containing ADHs, *T. hypogea* ADH was oxygen sensitive; however, the loss of enzyme activity upon exposure to oxygen could be recovered by incubation with dithiothreitol and Fe^{2+}. The enzyme was thermostable with a half-life of about 10 h at 70°C, and its catalytic activity increased along with the rise of temperatures up to 95°C. Optimal pH values for the production and oxidation of alcohol were determined to be 8.0 and 11.0, respectively. The enzyme had a broad specificity in utilizing primary alcohols and aldehydes as substrates. Apparent *K*m values for ethanol and 1-butanol were much higher than that for acetaldehyde and butyraldehyde and thus the enzyme was likely to catalyze the reduction of aldehydes to alcohols *in vivo*.

T. guaymasensis is a hyperthermophilic anaerobic archaeon capable of catalyzing the starch degradation and producing ethanol and acetoin as end-products. The purified *T. guaymasensis* ADH was an $NADP^+$-dependent homotetramer with a subunit of 40 ± 1 kDa. The enzyme was a primary-secondary ADH, but it exhibited substrate preference on secondary alcohols and corresponding ketones. In particular, it catalyzed the reduction of diacetyl to 2, 3-butanediol *via* acetoin in which the reduction from diacetyl to acetoin was irreversible. For the oxidation of 2, 3-butanediol, the enzyme exhibited higher activities on (*2R*, *3R*)-(-)-2, 3-butanediol and *meso*-2, 3-butanediol than (*2S*, *3S*)-(+)-2, 3-butanediol while the stereoselective reduction of racemic (*R*/*S*)-acetoin produced (*2R*, *3R*)-(-)-2, 3-butanediol and *meso*-butanediol but not (*2S*, *3S*)-(+)-2, 3-butanediol. The optimal pHs for the oxidation and formation of alcohols were determined to be 10.5 and 7.5, respectively. The enzyme activity increased along with the rise of temperatures up to 95°C, and it was highly stable with a half-life of 24 hours at 95°C. The enzyme was resistant to 30% (v/v) methanol (retaining 40% of its full activity). NADPH for the ketone reduction was efficiently regenerated using isopropanol as a substrate. The apparent *K*m value for NADPH was 40 times lower than that of $NADP^+$, and the specificity constant with NADPH were 5 times higher than that of $NADP^+$. Therefore, the physiological role of the enzyme was likely to be responsible for the reactions involving the NADPH oxidation–coupled formation of ethanol and/or acetoin.

The fully active *T. guaymasensis* ADH contained 0.9 ± 0.03 *g* atom zinc per subunit determined by inductively coupled plasma mass spectrometry (ICP-MS) and was the first characterized zinc-containing ADH from *Thermococcus* species. The gene encoding this enzyme was cloned and sequenced, and the deduced amino acid sequence contained 364 amino acids showing high similarities (85%) to those ADHs from *Thermoanaerobacter* species which have only the catalytic zinc atom. The motif analyses also indicated the enzyme lacked of the structural zinc-binding motif; thus, zinc might play a catalytic role in the enzyme. Further analyses showed the presence of the conserved domains of $_L$-threonine dehydrogenases; however, the enzyme could not oxidize $_L$-threonine or $_L$-serine. Distinct

from most of zinc-containing ADHs, the enzyme activity was almost fully inhibited by 100 μM Zn^{2+} in the assay mixture. Moreover, it was sensitive to oxygen.

An $NADP^+$-dependent ADH was purified from the hyperthermophilic anaerobic archaeon *Thermococcus* strain ES1, an ethanol producer. The recombinant enzyme over-expressed in *Escherichia coli* was purified using a two-step procedure including heat treatment, and characterized in comparison with the native enzyme. The purified recombinant enzyme exhibited a specific activity of 52.8 U mg^{-1}, close to that of the native enzyme (57 U mg^{-1}). Both native and recombinant enzymes were homotetramers with a subunit size of 45 ± 1 kDa. Their optimal pHs for the ethanol oxidation and acetaldehyde reduction were determined to be 10.5 and 7.0, respectively. Both enzymes were able to oxidize a series of primary alcohols and diols. Metal contents of the fully active recombinant enzyme were determined by ICP-MS to be 1.0 ± 0.04 *g* atom iron per subunit, and both iron-containing enzymes were oxygen sensitive. Their kinetic parameters showed lower *K*m-values of acetaldehyde and NADPH than those of ethanol and $NADP^+$, suggesting the native enzyme could be involved in ethanol formation *in vivo*. The recombinant and native enzymes had almost identical characteristics and thus its encoding gene was successfully over-expressed in *E. coli*. The deduced amino acid sequence of the ADH from *Thermococcus* strain ES1 was a 406 amino acid polypeptide. Its amino acid sequence showed high identities (80%) to iron-containing ADHs from the related archaea *Thermococcus zilligii* and *Thermococcus hydrothermalis*. The conserved domain search revealed it belonged to the family of iron-containing ADHs. Moreover, the sequence of the enzyme had catalytic metal and dinucleotide-binding motifs typical for iron-containing ADHs.

In conclusion, the results indicate that iron- and zinc-containing ADHs from hyperthermophiles have significant differences in terms of biophysical, biochemical and molecular properties. The hyperthermophilic bacterial and archaeal iron-containing ADHs are divergent while the zinc-containing ADH from *T. guaymasensis* has significant similarity to thermophilic bacterial ones.

Acknowledgements

When I look back my study here in the last few years, I feel lucky and grateful for so many persons pouring kindness and help upon me. I would first like to thank Dr. Kesen Ma for his guidance and support. Dr. Ma offers great freedom and opportunities for me to tap new areas for this subject. He lifts me up often when things seem not to be reached. I would also like to thank my committee members, Dr. Trevor Charles and Dr. Owen Ward, for their attention and energy to my study.

Studying at this great city, I not only move forward to my research but also obtain plenty of friendships. I want to show my appreciations to my present and former lab members who bring me lots of good memories. In particular, I present special thanks to Dr. Xianqian Yang, a great researcher, for shared joys from either research or life. I am proud of having a friend and labmate like her.

Many friends outside of Dr. Ma's lab contributed to my study. First, friends in the Department of Biology Zhenyu Cheng, Jing Ye, Yili Sun, and Xuan Huang offer me a lot of help and cheerful talks. Thank you all. Secondly, I thank Dr. Hamid R. Badiei and Dr. Vassili Karanassios in the Department of Chemistry for collaborations on metal analyses using atomic emission spectrometry. Thirdly, thanks for my roommates Zhirong Li and Wei Zhou for their kindness and care. In addition, I am grateful of encouragements from Catherine Lee, a friend in China.

Lastly, I am grateful of my family, dad, mom, sisters and brother. Thanks for your love, understanding, patience and support. I love you all. It is you who make me to face challenges with ease and confidence.

Dedication

It is dedicated to Hao Du.

Table of Contents

List of Figures

List of Tables

List of Abbreviations

ADH	Alcohol dehydrogenase
ALDC	α-Acetolactate decarboxylase
ALDH	CoA-dependent aldehdye dehydrogenase
ALS	α-Acetolactate synthase
CAPS	3-(Cyclohexylamino)-1-propanesulfonic acid
CbADH	*Clostridium beijerinckii* alcohol dehydrogenase
COG	Clusters of orthologous groups of proteins
DTT	Dithiothreitol
EDTA	Ethylenediaminetetraacetic acid
ee	Enantiomeric excess
EPPS	N-(2-hydroxyethyl)-piperazine-N'-(3-propanedulfonic acid)
ES1ADH	Alcohol dehydrogenase from *Thermococcus* strain ES1
FDH	Formate dehydrogenase
Fe	Iron
FID	Flame ionization detector
FPLC	Fast Protein Liquid Chromatography
GC	Gas chromatography
GDH	Glucose dehydrogenase
G6PDH	Glucose-6-phosphate dehydrogenase
HEPES	4-(2-Hydroxyethyl)-1-piperazineethanesulfonic acid
ICP-MS	Inductively coupled plasma-mass spectrometry
ITV-ICP-AES	In-torch vaporization-inductively coupled plasma-atomic emission Spectrometry
MCO	Metal-catalyzed oxidation
MS	Mass spectrometry
NAD(H)	Nicotinamide adenine dinucleotide (reduced)
NADP(H)	Nicotinamide adenine dinucleotide phosphate (reduced)
PCR	Polymerase chain reaction

PDC	Pyruvate decarboxylase
PIPES	1, 4-Piperazine-bis-(ethanesulfonic acid)
POR	Pyruvate-ferredoxin oxidoreductase
PVDF	Polyvinylidene difluoride
SDS-PAGE	Sodium dodecyl sulfate-polyacrylamide gel electrophoresis
SDT	Sodium dithionite
TbADH	*Thermoanaerobacter brockii* alcohol dehydrogenase
TeADH	*Thermoanaerobacter ethanolicus* alcohol dehydrogenase
TgADH	*Thermococcus guaymasensis* alcohol dehydrogenase
ThADH	*Thermotoga hypogea* alcohol dehydrogenase
Tris	2-Amino-2-hydroxymethyl-1,3-propanediol
Zn	Zinc

Chapter 1 General Introduction

1.1 HYPERTHERMOPHILES: LIFE AT HIGH TEMPERATURES

Hyperthermophiles are a group of microorganisms growing optimally at ≥80°C or have a maximal growth temperature of 90°C and above (Kelly and Adams 1994; Robb and Maeder 1998; Stetter 1989). In general, they are unable to grow below 60°C (Blöchl et al. 1995). Although thermophiles such as some of *Sulfolobus* species have been known for a longer time, the first member of hyperthermophiles, *Methanothermus fervidus*, was isolated from an Icelandic hot spring in 1981 (Brock et al. 1972; Stetter 1981; Stetter 2006). This methanogen exhibited the fastest growth at 82°C and the maximal growth temperature of 97°C (Stetter 1981). Over the last two decades, many hyperthermophiles have been isolated from various geothermal areas (Miroshnichenko and Bonch-Osmolovskaya 2006). The most heat-resistant hyperthermophiles are the anaerobic archaea, including members of the genera *Methanopyrus*, *Pyrolobus*, *Pyrodictium*, and *Pyrococcus* (Huber et al. 1989). The hyperthermophile *Pyrolobus fumarii* isolated from a hydrothermally heated black smoker wall can even grow at 113°C and survive one hour autoclaving at 121°C (Blöchil et al. 1997). The record of the upper temperature limit is currently held by an archaeon known as Strain 121 which can not only grow at 121°C but also survive after 2 hour incubation at 130°C (Kashefi and Lovley 2003).

Hyperthermophiles are present in marine and terrestrial hot environments (Stetter et al. 1990). However, the majority of known hyperthermophiles are isolated from marine thermal areas including shallow or abyssal thermal vents and sediments. The terrestrial biotopes for hyperthermophiles are mainly hot springs and solfataric fields in the volcanic areas. In consistence with their inhabiting environments, terrestrial hyperthermophiles usually adapt to lower salinity and marine ones require higher salinity for growth. Besides natural ecosystems associated with active volcanism, nonvolcanically heated geothermal environments such as oil fields are also a source of hyperthermophiles (Stetter et al. 1993).

Despite the diversity of natural biotopes, hyperthermophiles are primitive in the view of evolution. It has been well known that hyperthermophiles belong to either *Archaea* or

Bacteria domain (Stetter 1996). Hyperthermophiles are generally located near the root of the rRNA-based universal phylogenetic tree. Up to date, the domains of *Archaea* are phylogenetically divided into four kingdoms: *Crenarchaeota*, *Euryarchaeota*, *Korarchaeota* (Barns et al. 1996) and *Nanoarchaeota* (Huber et al. 2002). Except *Korarchaeota* demonstrated by environmental rRNA sequences of uncultivated microorganisms from a hot spring, hyperthermophiles are diversely distributed in other three kingdoms. In contrast to archaeal hyperthermophiles, the bacterial ones are represented as members of *Thermotoga* and *Aquifex* species.

1.1.1 Heterotrophic hyperthermophiles

The domain *Archaea* comprises both autotrophile and heterotrophile (Schönheit and Schäer 1995). Differing from those mesophilic counterparts in *Archaea* domain, most of hyperthermophiles are heterotrophs that grow well on polypeptides as carbon and energy sources. Many species of archaea and *Thermotoga* utilize carbohydrates as substrates. Those saccharolytic hyperthermophiles, in particularly *Thermotoga* species, grow efficiently on various poly-, oligo- and mono-saccharides (**Table 1-1**). A lot of effort has been made to understand saccharolytic pathways by studying the utilization of glucose *in vivo*. Previously, the approaches commonly used include identification of fermentation end products (Kengen et al. 1994) and intermediates of sugar metabolism following the conversion of ^{13}C- or ^{14}C-labelled glucose (Selig et al. 1997; Siebers and Hensel 1993), enzyme-activity measurements in cell extracts (Schäfer and Schönheit 1992), and characterization of purified enzymes (Kengen et al. 1995). During the past decade, the emergence of genomics and proteomics has provided more powerful approaches by analyzing genomic, proteomic, transcriptomic and biochemical data functionally (Ahmed et al. 2005; Dandekar et al. 1999; Ronimus and Morgan 2003; Snijders et al. 2006).

The current views on sugar metabolisms in hyperthermophiles are getting clearer due to the great efforts of several research groups (Ahmed et al. 2005; Kengen et al. 1996; Selig et al. 1997). In hyperthermophilic bacteria, two major pathways are known to be involved

Table 1-1 Carbohydrate-polymer utilization in hyperthermophilic archaea and bacteria

Organism	T_{opt} (°C)	Metabolism	Carbohydrate	Ref.[d]
Archaea[a]				
Archaeoglobus fulgidus[b]	83	Anaerobic	Starch, lactate, pyruvate, valerate	1
Desulfurococcus amylolyticus	90	Anaerobic	Starch, glycogen	2
Pyrobaculum aerophilum[b]	100	Aerobic	Acetate, propionate	3
Pyrococcus furiosus[b]	100	Anaerobic	Starch, pulluanan, glycogen, maltose, cellobiose, glucose, lactose, melibiose, pyruvate	4
Pyrococcus abyssi[b]	96	Anaerobic	Pyruvate, maltose, starch	5
Sulfolobus solfataricus[b]	80	Aerobic	Starch, dextrin, xyloglucan, maltose, sucrose, lactose, glucose, xylose	6
Sulfolobus acidocaldarius[b]	80	Aerobic	D-fucose, D-glucose, sucrose, maltotriose, dextrin, starch	7
Thermoproteus tenax	88	Anaerobic	Starch, glycogen, glucose	8
Thermococcus kodakaraensis[b]	85	Anaerobic	Starch, maltooligosaccharides, cyclodextrins, pyruvate	9
Bacteria				
Thermotoga maritima[b]	80	Anaerobic	Ribose, xylose, glucose, sucrose, maltose, lactose, galactose, starch, glycogen, cellulose, xylan	10
Thermotoga petrophila[b]	80	Anaerobic	Glucose, galactose, fructose, ribose, arabinose, sucrose,	11

			lactose, maltose, starch, cellulose	
Thermotoga naphthophila	80	Anaerobic	Glucose, galactose, fructose, ribose, arabinose, sucrose, lactose, maltose, starch	11
Thermotoga hypogea	70[c]	Anaerobic	Glucose, fructose, galactose, lactose, maltose, mannose, sucrose, xylose, xylan	12
Thermotoga neapolitana	80	Anaerobic	Ribose, xylose, glucose, sucrose, maltose, lactose, galactose, starch, maltodextrin, glycogen	13

T_{opt}, optimal growth temperature.

[a] In archaeal hyperthermophiles, only one representative carbohydrate-utilizing organism of each genus was listed, except those with available genomic sequences.

[b] The organism which genome sequence is available.

[c] *T. hypogea* has the maximal growth temperature of 90°C.

[d] References: 1, Beeder et al. 1994; Labes and Schönheit 2001; 2, Kengen et al. 1996; Selig et al, 1997; 3, Völkl et al. 1993; 4, Driskill et al. 1999; 5, Erauso et al. 1993; González et al. 1998; 6, Moracci et al. 2000; 7, Chen et al. 2005; Grogan 1989; 8, Kengen et al. 1996; 9, Atomi et al. 2004; 10, Nelson et al. 1999; 11, Takahata et al. 2001; 12, Fardeau et al. 1997; 13, Berezina et al. 2003; Jannasch et al. 1988.

in the degradation of glucose to pyruvate, Embden-Meyerhof (EM) and Entner-Doudoroff (ED) pathways, which are different from the classical EM and ED pathways in the key enzymes acting on glucose or glucose-6-phosphate, the first two steps of glycolysis. *T. maritima*, the best-characterized bacterial hyperthermophile, shows a conventional ED pathway as well as a classical EM pathway (Kengen et al. 1996). Both conventional pathways seem to be restricted to bacterial hyperthermophiles. The metabolic conversion of glucose in archaea appears more versatile due to the existence of modifications of either EM or ED pathways (**Fig. 1-1)**. In the hyperthermophilic aerobic archaea such as *T. acidophilum* and *S. solfataricus,* glucose is metabolized *via* the modified ED pathway, whereas the hyperthermophilic fermentative anaerobes including *P. furiosus*, *Thermococcus* species, *D. amylolyticus*, *A. fulgidus* and the microaerophile *P. aerophilum*, use modified EM pathways (**Fig. 1-1**). To date, the only archaeon known to use both modified EM and ED pathways during glucose degradation is *T. tenax*, a hyperthermophilic sulfur-dependent anaerobe (Selig et al. 1997). In particular, the existence of both the semi-phosphorylative and the non-phosphorylative ED pathway in *T. tenax* and *S. solfataricus* has been proved recently (Ahmed et al. 2005).

1.1.2 The genus *Thermococcus*

The euryarchaeal order *Thermococcales* is represented by three genera: *Thermococcus* and *Pyrococcus* which are the best-studied hyperthermophiles (Huber and Stetter 2001; Itoh 2003), and the newly described genus *Paleococcus* (Takai et al. 2000). The genera *Pyrococcus* and *Thermococcus*, have fascinated many microbiological researchers and often been used as the source organism for both fundamental and application-based aspects of research. The complete genome analyses of three *Pyrococcus* species and one *Thermococcus* species have been performed, which are *Pyrococcus horikoshii* (Kawarabayasi et al. 1998), *P. furiosus* (Robb et al. 2001), *P. abyssi* (Cohen et al. 2003) and *T. kodakaraensis* (Fukui et al. 2005).

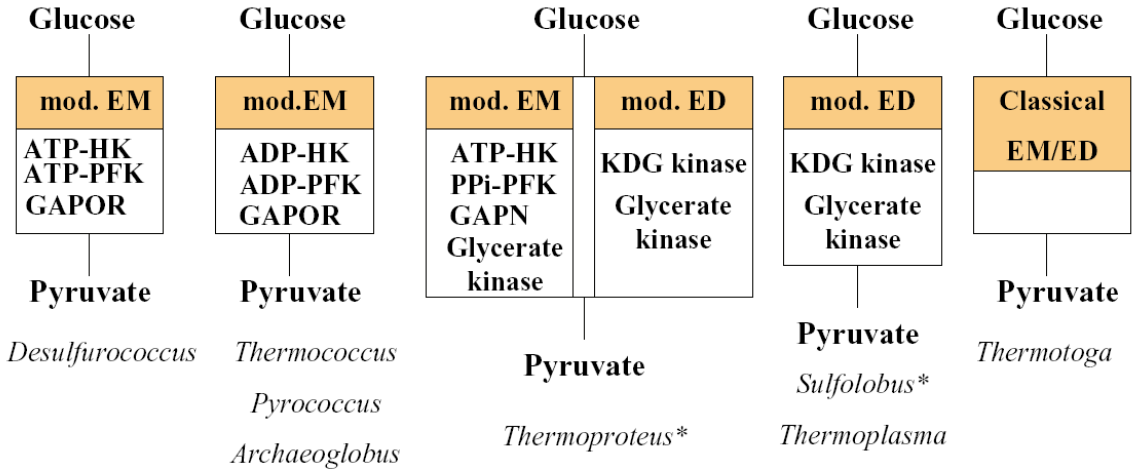

Figure 1-1 Pathways from glucose to pyruvate in hyperthermophiles (summarized from Ahmed et al. 2005; Selig et al. 1997; Siebers and Schönheit 2005; Verhees et al. 2003).

* *T. tenax* and *S. solfataricus* use a non- and semi-phosphorylative ED modification.

The enzymes compared to those in classical EM/ED pathways are in box (white). Abbreviations used: ATP, ADP and PPi, the phosphoryl-donor specificities; ED, Entner-Doudoroff; EM, Embden-Meyerhof; PFK, phosphofructokinase; GAPN, NAD^+-dependent glyceraldehydes-3-phosphate dehydrogenase; GAPOR, glyceraldehydes-3-phosphate ferredoxin oxidoreductase; HK, hexokinase; KDG, 2-keto-3-deoxygluconate.

The genus *Thermococcus* contains the biggest number of characterized isolates among *Archaea*. Deposited in German Collection of Microorganisms and Cell Cultures (Deutsche Sammlung von Mikroorganismen und Zellkulturen, DSMZ), this group contains 27 members (**Fig. 1-2**). Except *Thermococcus sibiricus* (Miroshnichenko et al. 2001), *Thermococcus celer* (Zillig et al. 1983) and *Thermococcus stetteri* (Miroshnichenko et al. 1989), most of *Thermococcus* species are hyperthermophiles, which are usually spherical and obligately anaerobic. Their common ecological habitats are submarine hot vents of both shallow water (Kostyukova et al. 1999) and deep sea areas (Prieur et al. 1995). Two species, *Thermococcus zilligii* (Ronimus et al. 1997) and *Thermococcus waiotapuensis* (Gonzáles et al. 1999) were isolated from terrestrial hot springs in New Zealand and require a lower concentration of salt than marine species. Some *Thermococcus* species were isolated from continental oil wells (Grassia et al. 1996; Orphan et al. 2000; Stetter et al. 1993; Takahata et al. 2000) and the Paris Basin (L'Haridon et al. 1995).

All *Thermococcus* species are chemo-organotrophs and grow on peptide-containing substrates such as yeast extract, peptone and tryptone (Pikuta et al. 2007). Some of them are able to grow on starch as the carbon source, including: *Thermococcus aegaeicus* (Arab et al. 2000), *T. stetteri* (Miroshnichenko et al. 1989), *T. profundus* (Kobayashi et al. 1994), *T. pacificus* (Miroshnichenko et al. 1998), *T. guaymasiensis* (Canganella et al. 1998), *Thermococcus atlanticus* (Cambon-Bonavita et al. 2003), *T. kodakaraensis* KOD1 (Atomi et al. 2004; Fukui et al. 2005), *T. waiotapuensis* (González et al. 1999). Those starch-degrading species are of great interest in biotechnology as the source of thermostable amylolytic enzymes such as α-amylase, pullulanase and α-glucosidase (Legin et al. 1998). It has been established in *Thermococcus litoralis* that glycolysis appears to occur *via* a modified EM pathway containing ADP-dependent hexose kinase and phosphofructokinase, and a tungsten-containing glyceraldehyde-3-phosphate: ferredoxin oxidoreductase (GAPOR) replacing glyceraldehyde-3-phosphate dehydrogenase (GAPDH) and phosphoglycerate kinase in classical EM pathway (**Fig. 1-3**). In addition, all members of the genus *Thermococcus* produce hydrogen as a fermentative means of

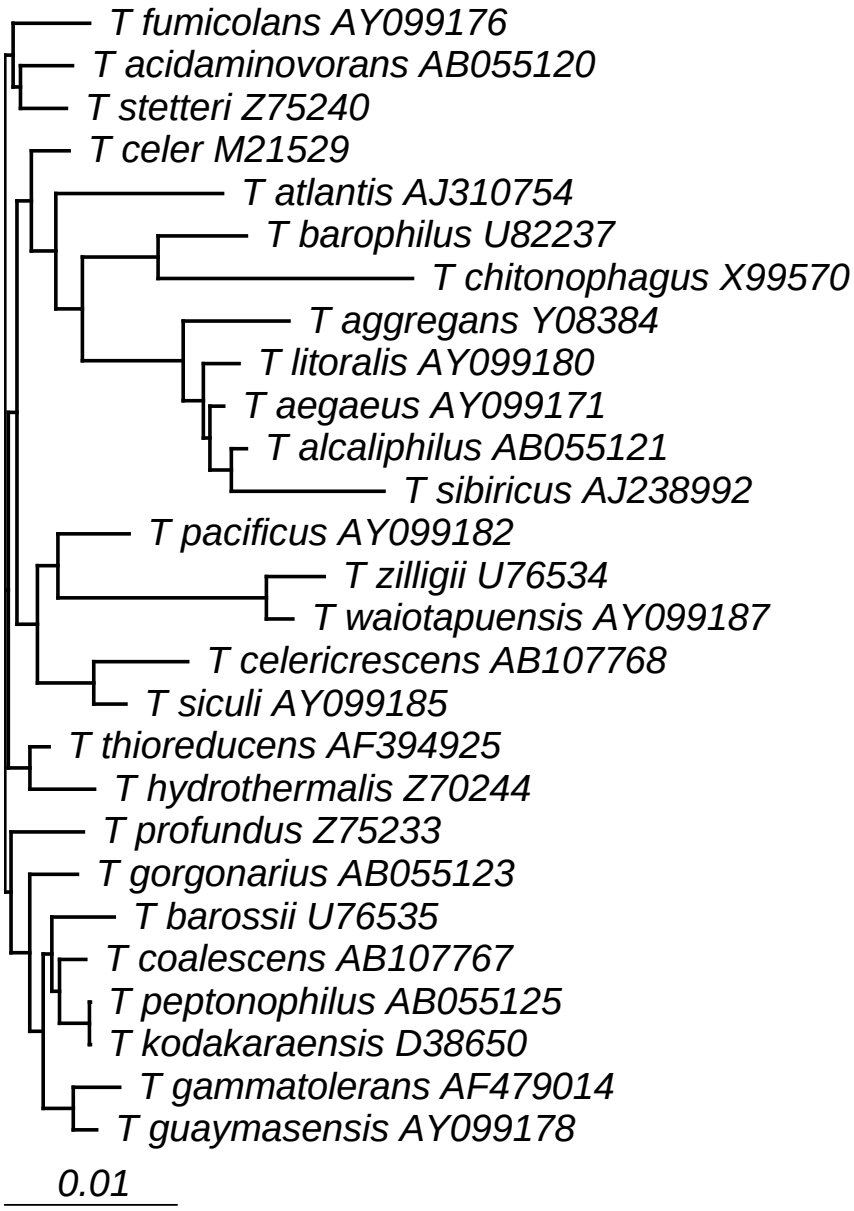
T fumicolans AY099176
T acidaminovorans AB055120
T stetteri Z75240
T celer M21529
T atlantis AJ310754
T barophilus U82237
T chitonophagus X99570
T aggregans Y08384
T litoralis AY099180
T aegaeus AY099171
T alcaliphilus AB055121
T sibiricus AJ238992
T pacificus AY099182
T zilligii U76534
T waiotapuensis AY099187
T celericrescens AB107768
T siculi AY099185
T thioreducens AF394925
T hydrothermalis Z70244
T profundus Z75233
T gorgonarius AB055123
T barossii U76535
T coalescens AB107767
T peptonophilus AB055125
T kodakaraensis D38650
T gammatolerans AF479014
T guaymasensis AY099178
0.01

Figure 1-2 Phylogenetic tree of *Thermococcus* species based on 16S rRNA sequences.

The sequences were aligned using Clustal W and a phylogenetic tree was constructed (Thompson et al. 1994). 16S rRNA gene sequences were all obtained from GenBank. The accession numbers for the organisms used in the analyses are indicated on the figure. Scale bar indicates 0.01 substitutions per sequence position. All characterized 27 species were used and 1,231 sites have been retained for the analyses considering some sequences were reported partly.

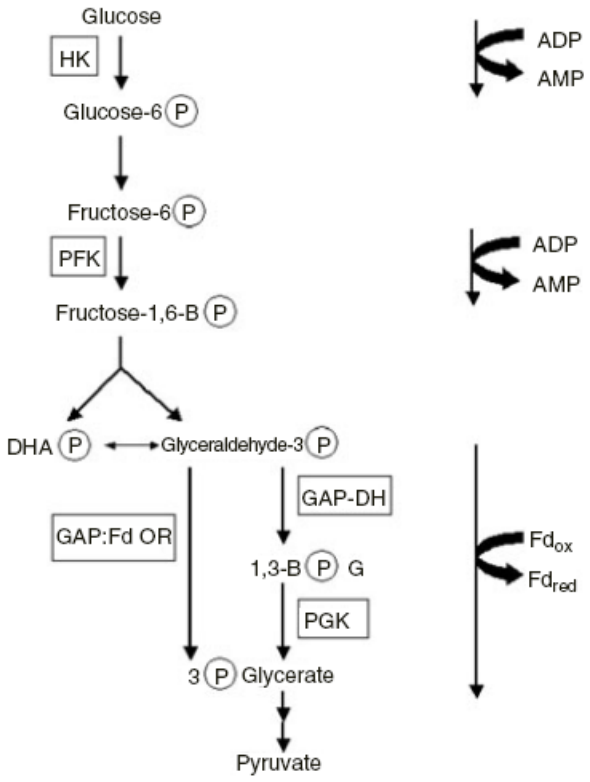

Figure 1-3 Modified Embden-Meyerhof glycolytic pathway in the genus *Thermococcus* (adapted from Bertoldo and Antranikian 2006).

The steps different from those in classical EM pathway are indicated by the solid arrows (on the right side). Abbreviations used: 1, 3-BPG, 1, 3-biphosphoglycerate; DHA-P, dihydroxyacetonephosphate; Fd_{ox}, oxidized ferredoxin; Fd_{red}, reduced ferredoxin; GAP: FdOR, glyceraldehyde-3-phosphate: ferredoxin oxidoreductase; GAP-DH, glyceraldehyde-3-phosphate dehydrogenase; HK, hexokinase; PGK, phosphoglycerate kinase.

disposing excess reducing equivalents. Those carbohydrate-degrading *Thermococcus* species have strikingly high potentials as H_2 producers (Kanai et al. 2005).

In contrast to *Thermococcus* species, the genus *Pyrococcus* contains only 6 members known (Barbier et al. 1999; Erauso et al. 1993; Fiala and Stetter 1986; González et al. 1998; Holden and Baross 1993; Zillig et al. 1987). Members of the genus *Pyrococcus* grow optimally at the range of 95-103°C while those of the genus *Thermococcus* have the optimal growth temperature at the range of 75-93°C. Both *Pyrococcus* and *Thermococcus* species are either sulfur-requried or sulfur-stimulated. *Pyrococcus* strains have been isolated only from marine hydrothermal vents, which appear to be less diverse that *Thermococcus* species (Bertoldo and Antranikian 2006). Thus, *Thermococcus* species possess similar properties to *Pyrococcus* species but provide more options as the source organism for versatile studies such as cultivation, physiology and metabolism.

1.1.3 The genus *Thermotoga*

Along with the *Aquificales*, species in *Thermotogae* have the highest growth temperatures in bacteria. They comprise of obligately organotrophic, strictly anaerobic, moderately thermophilic to hyperthermophilic microorganisms with rodshaped cells surrounded by a sheath known as "Toga", including the genera *Thermotoga*, *Fervidobacterium*, *Thermosipho*, *Geotoga*, *Petrotoga* and *Marinitoga*. The genus *Thermotoga* consists of 9 members (**Fig. 1-4**): *T. maritima* (Huber et al. 1986), *T. neapolitana* (Jannasch et al. 1988), *Thermotoga thermarum* (Windberger et al. 1989), *Thermotoga subterranean* (Jeanthon et al. 1995), *Thermotoga elfii* (Rovot et al. 1995), *T. hypogea* (Fardeau et al. 1997), *T. petrophila* and *T. naphthophila* (Takahata et al. 2001), and *Thermotoga lettingae* (Balk et al. 2002). *T. petrophila, T. naphthophila, T. maritima* and *T. neapolitana* grow optimally at 80 °C while *T. maritima, T. neapolitana* and *T. hypogea* have a maximal growth temperature of 90°C. The genome sequence of *T. maritima* has 24% of its genes homologous to archaeal genes, suggesting the evidence of lateral gene transfer between

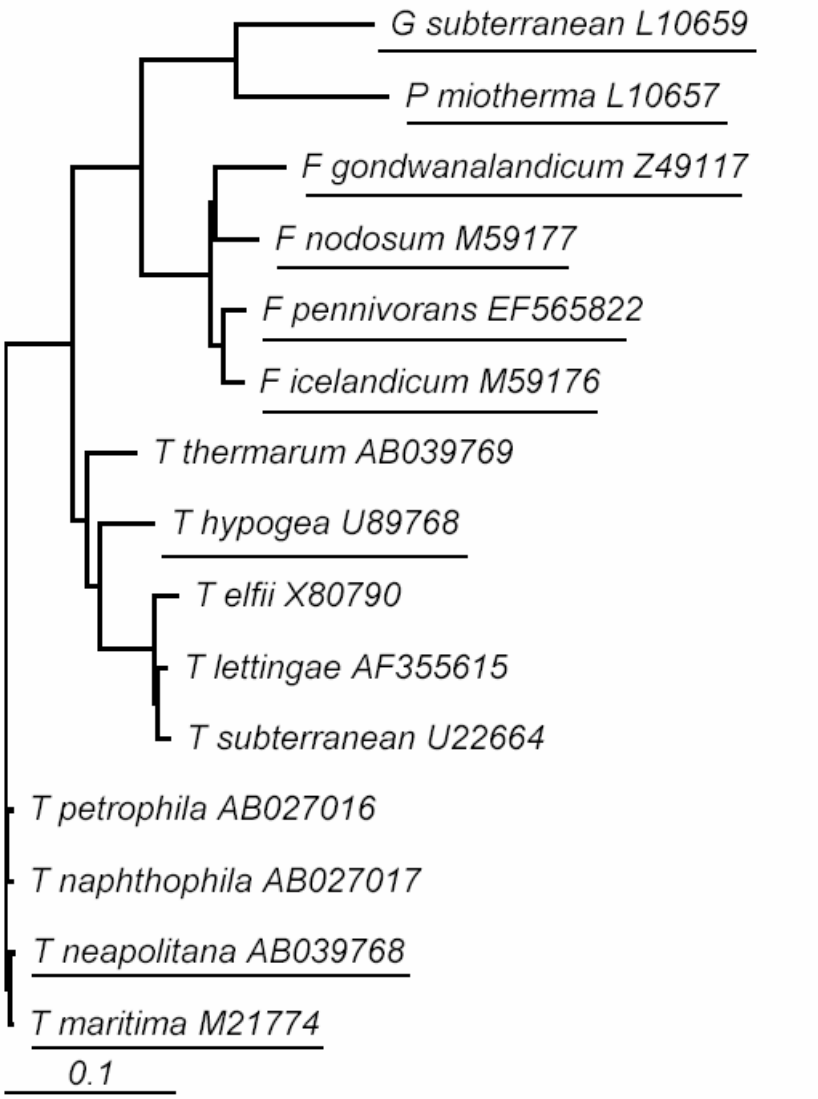
G subterranean L10659
P miotherma L10657
F gondwanalandicum Z49117
F nodosum M59177
F pennivorans EF565822
F icelandicum M59176
T thermarum AB039769
T hypogea U89768
T elfii X80790
T lettingae AF355615
T subterranean U22664
T petrophila AB027016
T naphthophila AB027017
T neapolitana AB039768
T maritima M21774
0.1

Figure 1-4 Phylogenetic tree of *Thermotoga* species and ethanol-producing members in *Thermotogales*.

The sequences were aligned using Clustal W and subsequently a phylogenetic tree was constructed (Thompson et al. 1994). 16S rRNA gene sequences were all obtained from GenBank. The accession numbers for the organisms used in the analyses are indicated on the figure. Scale bar indicates 0.1 substitutions per sequence position. The capital initials denote genera *Fervidobacterium* (F), *Geotoga* (G), *Petrotoga* (P) and *Thermotoga* (T). Among them, ethanol producers were underlined.

thermophilic eubacteria and archaea. This feature makes *T. maritima* an appealing candidate for studying the evolution of metabolic pathways of hyperthermophilic microorganisms, and for investigation of enzyme families (Nelson et al. 1999).

Thermotoga species have been found in diverse locations, volcanic origin as well as nonvolcanically heated geothermal sites such as oil fields (Balk et al. 2002; Fardeau et al. 1997; Huber et al. 1986; Jannasch et al. 1988; Jeanthon et al. 1995; Ravot et al. 1995; Takahata et al. 2001). As an adaptation to environments, *Thermotoga* isolates from oil fields including *T. elfii* and *T. hypogea*, utilize thiosulfate but not sulfur as an electron acceptor. In contrast, all isolates from volcanic hot springs utilize thiosulfate or sulfur except *Thermotoga thermarum*, which has not been reported to use sulfur compounds as electron acceptors (Lowe et al. 1993). The addition of thiosulfate to the carbohydrate-containing growth medium is known to improve the growth rate and cell yield of the tested *Thermotogales* (Ravot et al. 1995).

The adaption to versatile environments also results in the presence of abundant enzymes for diverse carbohydrate utilization (Conners et al. 2006). During glucose fermentation, *Thermotoga* species produce acetate, lactate, CO_2, $_L$-alanine and H_2 as fermentation end products (Ravot et al. 1996). *Thermotoga* species are used as model organisms for research because of their ability to catalyze simple and complex carbohydrates such as glucose, sucrose, starch, cellulose and xylan, which intrigues the consideration for the application in producing renewable energy resources (van Ooteghem et al. 2002; van Ooteghem et al. 2004). Among them, *T. maritima* is the first species whose genome has been sequenced, of which 7% of *T. maritima* genes are predicted to be involved in carbohydrate utilization (Nelson et al. 1999). *T. maritima* appears to possess the enzymatic capability to metabolize a variety of polysaccharides including carboxymethyl cellulose, barley glucan, starch, galactomannan, xylan and thus capable of adapting to a variety of growth environments containing carbohydrate substrates (Bronnenmeier et al. 1995; Chhabra et al. 2002; Chhabra et al. 2006).

1.1.4 Fermentation at elevated temperatures

Thermophilic fermentation has gained great interest since the discovery of thermophiles and hyperthermophiles (Bustard et al. 2000). The advantages of fermentation at elevated temperatures are quite obvious: reduced costs of cooling during large-scale thermophilic fermentations, lower viscosity of media and hence higher efficiency of mixing and harvesting rate *via* centrifugation, increased solubility of reactants allowing the use of less soluble components with higher concentration, easier prevention from undesired microbial contamination. In addition, volatile end products may be removed through application of a mild vacuum, which can prevent from the accumulation of inhibitory byproducts. Particularly, decreased solubility of oxygen benefits the cultivation of anaerobic organisms (Bustard et al. 2000). Despite the aroused interest in hyper/thermophiles, their potential within the biotechnology industry has not been fully explored to date (Karakashev et al. 2007). Although plenty of research has focused on the purification and characterization of thermostable enzymes (Atomi 2005), whole cell applications are relatively rare, which has been hampered by difficulties in large-scale cultivation of hyperthermophiles (Bustard et al. 2000). Most studies aim to understand the nutritional requirements, optimize growth conditions, develop sulfur-free defined media and design new bioreactors for continuous culture at high temperature (Postec et al. 2005; Rinker et al. 1999; Watrin et al. 1995; Worthington et al. 2003). Hyperthermophiles studied for large scale cultivation are mainly from the genera *Pyrococcus*, *Thermococcus* and *Thermotoga*, including: *P. abyssi* (Godfroy et al. 2000; Watrin et al. 1995), *P. furiosus* (Raven et al. 1992; Raven et al. 1997), *T. litoralis* (Rinker and Kelly 1996), *T. maritima* (Rinker and Kelly 2000), and *Thermococcus hydrothermalis* (Postec et al. 2005). In recent years, the hydrogen-producing potential of anaerobic hyperthermophiles has attracted attention as a clean, non-polluting fuel (Kanai et al. 2005; van Ooteghem et al. 2002; van Ooteghem et al. 2004). As an example, hydrogen productivity of *T. kodakaraensis* is as comparably high as those of *Enterobacter* species, well-studied mesophilic hydrogen producers (Kanai et al. 2005).

1.1.5 Thermophiles and hyperthermophiles producing alcohols

Microbial fuel ethanol production using renewable raw materials has attracted great interest due to growing demands for environment-friendly sustainable energy sources (Cook and Beyea 2000; Demain et al. 2005; Dien et al. 2003; Doi 2003; Galbe and Zacchi 2002; Olsson and Hahn-Hagerdal 1996; Ward and Singh 2002; Wheals et al. 1999; Wyman 1999; Zaldivar et al. 2001). Moreover, elevated temperature fermentation for ethanol production has been evaluated in recent years due to the potential use of thermophilic microorganisms as biocatalysts (Banat and Marchant 1995; Banat et al. 1998; Edwards 1990; Klapatch et al. 1994; Sommer et al. 2004). Renewable raw materials such as lignocellulosic biomass are composed of cellulose (40-60%), hemicellulose (20-40%) and lignin (10-25%) (Hamelinck et al. 2005). Except for lignin, the components of lignocellulosic materials can be converted to hexose and pentose sugars *via* pretreatment and enzymatic hydrolysis (Gong et al. 1999; Ingram et al. 1999; Kuhad and Singh 1993; Lynd 1990). Thermophiles capable of utilizing lignocellulosic materials could make bioethanol more competitive to fossil fuel (Larsen et al. 1997; Olsson and Hahn-Hagerdal 1996).

Various thermophilic microorganisms capable of producing lower amounts of ethanol have been isolated and characterized in the past two decades from different environments. These bacteria mainly represent as *Thermoanaerobacter* and *Clostridium* species including *Thermoanaerobacter ethanolicus* (Kannan and Mutharasan 1985; Wiegel and Ljungdahl 1986), *Thermoanaerobacter thermohydrosulfuricus* (Wiegel et al. 1979), *Thermoanaerobacter mathranii* (Larsen et al. 1997), *Thermoanaerobacter brockii* (Lamed and Zeikus 1980a; Sonnleitner et al. 1984; Zeikus et al. 1979), *Geobacillus thermoglucosidasius* (Fong et al. 2006) and *C. thermocellum* (Herrero and Gomez 1980; Lamed and Zeikus 1980b; Ng et al. 1981).

In contrast to thermophiles, the alcohol formation in hyperthermophiles is not the center of attention yet. Their potential as an alcohol producer has been rarely investigated or

reported so far. In archaeal hyperthermophiles, *Stetteria hydrogenophila* DSM11227 belonging to the family of *Desulfurococcaceae*, was isolated from the sediment of a marine hydrothermal system at Paleohori Bay in Milos, Greece. H_2S, CO_2, acetate and ethanol (0.11 mM) were identified as products of metabolism (Jochimsen et al. 1997). *P. furiosus*, one of best studied sugar-utilizing hyperthermophiles, shows growth on starch, cellobiose, and laminarin and produces ethanol (Kengen et al. 1994). *Thermococcus* strain ES1 was observed to form ethanol/butanol under elemental sulfur-limiting growth conditions (Ma et al. 1995). *Hyperthermus butylicus* was reported to produce butanol (Zillig et al. 1990). In contrast, hypertherphilic ethanol producers in the domain *Bacteria* belong to the members of the genus *Thermotoga*. *T. maritima*, *T. neapolitana* and *T. hypogea* produced low amount of ethanol (Ma et al. 2005). Their relatives (**Fig. 1-4**) including *Fervidobacterium islandicum*, *Fervidobacterium nodosum*, *Fervidobacterium gondwanense*, *Fervidobacterium pennavorans* (Andrews and Patel 1996; Friedrich and Antranikian 1999; Huber et al. 1990; Patel et al. 1985), *Geotoga subterranean* and *Petrotoga miotherma* (Davey et al. 1993) were reported to produce ethanol.

1.2 ALCOHOL DEHYDROGENASES

Alcohol dehdyrogenases are a group of oxidoreductases which catalyze interconversion between alcohols and corresponding aldehydes or ketones. Based on the coenzyme specificity, they can be divided into 3 types: $NAD(P)^+$-dependent, FAD-dependent, and pyrro-quinoline quinine (Duine 1991), haem or coenzyme F_{420}. Most known ADHs from thermophiles are $NAD(P)^+$-dependent (Radianingtyas and Wright 2003). One exception is *Methanoculleus thermophilicus* ADH that uses coenzyme F_{420} (Widdel and Wolfe 1989). Those $NADP^+$-dependent ADHs can be further classified into 3 groups based on the metal content: short chain ADHs independent of zinc, zinc-containing medium chain ADHs, and iron-containing or activated ADHs usually with long chains. The availability of isoenzymes utilizing different metals may provide nutritional flexibility for the maintenance of this essential activity under conditions of metal limitation (Mackenzie et al. 1989).

It is known that there are multiple ADHs in thermophiles or hyperthermophiles (**Table 1-2**). In *S. solfataricus*, a thermo-acidophilic crenarchaeon, there are 13 genes annotated as zinc-containing ADHs including the gene encoding $_{L}$-threonine dehydrogenase from its genomic sequence (She et al. 2001). To date, only ADH-10 (SSO2536) and ADH-4 (SSO1300) from *S. solfataricus* have been characterized as an NAD^{+}-dependent ADH and a $_{D}$-arabinose 1-dehydrogenase, respectively (Ammendola et al. 1992; Brouns et al. 2006). In most cases, multiple ADHs from one organism belong to different types. Several types of ADHs from *P. furiosus* have been characterized including an oxygen-sensitive iron- and zinc-containing long-chain ADH, a short chain AdhA and an iron-containing AdhB encoded by the *lamA* operon (Ma and Adams 1999; van der Oost et al. 2001). The recent analyses of *P. furiosus* genome resulted in the identification of 16 additional putative genes encoding ADHs (Machielsen and van der Oost 2006). Two of newly identified genes, *PF0991* and *PF1960*, have been expressed and characterized as a medium chain zinc-containing threonine dehydrogenase and an alcohol dehydrogenase belonging to alde-keto reductase family, respectively (Machielsen and van der Oost 2006; Machielsen et al. 2006). In addition, ADHs commonly have broader substrate specificity with substrate preference. Zinc-containing ADHs mostly are primary-secondary ADHs and prefer to use secondary alcohols and corresponding ketones. In contrast, iron-containing ADHs show higher catalytic activities on primary alcohols and corresponding aldehydes.

The multiplicity and multifunctionality of ADHs increase the difficulties to disentangle their physiological roles in metabolism and regulation. The combination of genomic and proteomic analyses may be an efficient approach to gain a global view of their roles. In *S. solfataricus* which contains 13 putative ADH genes, some of the expression levels of these ADHs do not correlate well with the transcript level when alcohols or ketones are added into the media (Chong et al. 2004). Firstly, the protein level of ADH-10 is up-regulated in ethanol and *n*-propanol cultures without significant change observed on its transcription. In contrast, no significant change on protein regulation of ADH-10 is observed while its transcription level is up-regulated in acetone and phenol cultures. Secondly, the protein

Table 1-2 Abundance of genes encoding ADHs in completed genome sequences

Organism	Lineage	Phynotype[b]	Genes[c]	SDR[d]	Zn[e]	Fe[f]	Ref.[g]
Hyperthermophile[a]							
A. pernix	Crenarchaeota	Ae	1700		2	1	1
Archaeoglobus fulgidus	Euryarchaeota	An	2486		1	3	2
Hyperthermus butylicus	Crenarchaeota	An	1672	3	1		3
Pyrobaculum aerophilum	Crenarchaeota	Fac Ae	2706	2	6		4
Pyrobaculum calidifontis	Crenarchaeota	Fac Ae	2200	5	4		5
Pyrobaculum islandicum	Crenarchaeota	An	2062	3	5	1	6
P. furiosus[h]	Euryarchaeota	An	2125	1		2	7
Pyrococcus abyssi	Euryarchaeota	An	1993	1	1	1	8
P. horikoshii	Euryarchaeota	An	2005	1	1	1	9
Staphylothermus marinus	Crenarchaeota	An	1646	2	2	1	10
Sulfolobus acidocaldarius	Crenarchaeota	Ae	2329	6	10	1	11
S. solfataricus	Crenarchaeota	Ae	2977		13		12
Sulfolobus tokodaoii	Crenarchaeota	Ae	2874		11		13
T. kodakaraensis	Euryarchaeota	An	2306	3	1	2	14
Thermofilum pendens	Crenarchaeota	An	1879	2	2	1	15
T. maritima	Bacteria	An	1858	1	3	2	16
T. petrophila	Bacteria	An	1864	5	3	5	17
Thermophile							
Thermoanaerobacter	Bacteria	An	2270	2	3	6	18

ethanolicus							
Thermoanaerobacter tengcongensis	Bacteria	An	2721	3	3	2	19
Mesophile							
E. coli	Bacteria	Fac An	4131		4	4	20
Z. mobilis	Bacteria	Fac An	1998	1	1	1	21

[a] Heterotrophic or facultatively heterotropic hyperthermophiles

[b] Ae, strict aerobe; An, strict anaerobe; Fac Ae, facultative aerobe; Fac An, facultative anaerobe

[c] total number of genes

[d] SDR, predicted short-chain dehydrogenase/reductase

[e] Zn, predicted zinc-containing ADH including glycerol dehydrogenase or threonine dehydrogenase

[f] Fe, predicted iron-containing ADH

[g] References: 1, Kawarabayasi et al. 1999; 2, Klenk et al. 1997; 3, Brügger et al. 2007; 4, Fitz-Gibbon et al. 2002; 5, Copeland et al. 2007d; 6, Copeland et al. 2006a; 7, Robb et al. 2001; 8, Cohen et al. 2003; 9, Kawarabayasi et al. 1998; 10, Copeland et al. 2007c; 11, Chen et al. 2005; 12, She et al. 2001; 13, Kawarabayasi et al. 2001; 14, Fukui et al. 2005; 15, Copeland et al. 2006b; 16, Nelson et al. 1999; 17, Copeland et al. 2007a; 18, Copelend et al. 2006c; 19, Bao et al. 2002; 20, Blatter et al. 1997; 21, Seo et al. 2005.

[h] Sixteen additional putative genes encoding ADHs have been identified recently in *P. furiosus* genome sequence (Machielsen and van der Oost 2006)

expression of ADH-2 is only up-regulated in the phenol culture, whereas the gene transcript shows up-regulation in both ethanol and iso-propanol cultures. Thirdly, the only change of ADH-5 is the up-regulation of its expression level in the ethanol culture. In addition, although the protein level of ADH-6 is up-regulated in the ethanol and acetone cultures, its transcription level is down-regulated (Chong et al. 2004). The inconsistency between the protein and transcription levels in various cultures implies that factors other than the level of mRNA may be also important.

1.2.1 Iron-containing ADHs

Known iron-containing ADHs contain one iron central for the activity. However, no structural iron has been reported yet. Some of the members of this type of ADHs are iron-dependent, and termed as iron-activated enzymes because their lost activities due to the lack of iron could be re-gained after the iron was re-introduced (Scopes 1983). These $NAD(P)^+$-dependent enzymes usually are homotetramer in archaea, or homodimer in bacteria. The size of their subunits usually ranges from 382 to 406 amino acid residues belonging to long chain ADHs. However, smaller or bigger ones have been noted already, including a putative ADH in *T. maritima* (TM0920) and AdhE in *E. coli* with 359 and 896 amino acid residues, respectively (Goodlove et al. 1989; Nelson et al. 1999). In terms of their physiological role, iron-containing ADHs catalyze anaerobically in the ethanogenic direction in mesophilic facultative anaerobes (Chen and Lin 1991; Leonardo et al. 1993; Membrillo-Hernández and Lin 1999; Mikulskis et al. 1997). Similarly, the role of iron-containing ADHs from hyperthermophilic anaerobes has been proposed to be responsible for alcohol formation *in vivo* (Antoine et al. 1999; Li and Stevenson 1997; Ma et al. 1994; Ma et al. 1995; Ma and Adams 1999).

1.2.1.1 Structural characteristics of iron-containing ADHs

The increasing availability of three-dimension (3-D) structures sheds light on the understanding of iron-containing ADHs. The first structure among the family of iron-

containing bacterial dehydrogenases is $_L$-1, 2-propanediol dehydrogenase from *E. coli* determined experimentally to contain iron, which catalyzes the interconversion between $_L$-lactaldehyde and $_L$-1, 2-propanediol (Montella et al. 2005). The enzyme forms a dimer, in which each monomer folds into an α/β dinucleotide-binding N-terminal domain and an all-α-helix C-terminal domain that are separated by a deep cleft. The binding site for Fe^{2+} is located at the face of the cleft formed by the C-terminal domain, where the metal ion is tetrahedrally coordinated by an aspartate residue (Asp196) and three histidine residues (His200, His263, and His277, numbering in *E. coli*). The glycine-rich turn formed by residues 96 to 98 and the following α -helix is part of the NAD^+ recognition site common in dehydrogenases. The results of site-directed mutageneses indicate that the essential His267 residue does not interact with the metal ion and Asp39 appears to be the key residue for discriminating against $NADP^+$. Among hyperthermophilic counterparts, the crystal structure of the predicted 1, 3-propanediol dehydrogenase from *T. maritima* (TM0920) is currently available (Schwarzenbacher et al. 2004). Different from $_L$-1, 2-propanediol dehydrogenase in *E. coli*, TM0920 is a $NADP^+$-dependent homodimer (Schwarzenbacher et al. 2004). The structure of TM0920 represents a dehydroquinate synthase-like fold and is the third member of the glycerol dehydrogenase-like structural family (Brinen et al. 2002; Ceccarelli et al. 2004). Each monomer also has two distinct domains, N-terminal and C-terminal domains, separated by a deep cleft. The Fe^{2+} ion is deeply located in the catalytic cleft and has a square pyramidal coordination with Asp189, His193, His256, and His270 (numbering in *T. maritima*), all of which are situated in C-terminal domain.

1.2.1.2 Regulation of iron-containing ADHs and their oxygen inactivation

Iron-containing ADHs from either hyperthermophiles or mesophiles have been reported to be sensitive to oxidation. Among the representatives in mesophilic facultative anaerobes, ADHs from *Z. mobilis* and *E. coli* might be the best characterized. Expression of the gene *adhE* in *E. coli* is regulated at both the transcriptional and translational levels. When *E. coli* cells are shifted from anaerobic to aerobic conditions, the transcription of the *adhE*

gene is reduced but maintained at a relatively low level under aerobiosis (Chen and Lin 1991; Leonardo et al. 1993; Membrillo-Hernández and Lin 1999; Mikulskis et al. 1997). Translation of the *adhE* gene is also regulated and requires RNase III. The RNase III might cleave the secondary structure of the transcript and expose the ribosome binding site concealed by base pairing (Aristarkhov et al. 1996; Membrillo-Hernández and Lin 1999). In addition, *adhE* is regulated posttranslationally. In the presence of oxygen, they are irreversibly inactivated by metal-catalyzed oxidation (MCO) (Stadtman 1993; Tamarit et al. 1997). MCO is a site-specific free radical mechanism in which a highly reactive HO (hydroxyl radical) can be generated and covalently attacks amino acid residues such as Arg, Pro, His, and Lys. It has been proposed that one of conserved histidine residues (His277, numbering in *Z. mobilis*) in the iron-binding motif HX_3HX_9H is the target of oxidation by a MCO system (Cabiscol et al. 1994). Accordingly, the Zn^{2+} enzyme resistant to MCO damage plays the major role in aerobic ethanologenesis and the Fe^{2+} enzyme susceptible to MCO damage, in anaerobic ethanologenesis. In addition, when the *adhE* structural gene was cloned into expression vectors under the contol of *lacZ* and *trpC* promoters, the AdhE protein produced at high level under aerobic conditions was inactive. Surprisingly, a single substitution Glu568Lys in AdhE led to active enzyme even under aerobic conditions. Further experiments on site-directed mutageneses showed that virtually any amino acid substitution for Glu568 produced AdhE that was active under both aerobic and anaerobic conditions (Holland-Staley et al. 2000).

The regulation of iron-containing ADHs from hyperthermophilic anaerobes is still obscure. The pioneering work on *Thermococcus* strain ES1 indicated that its iron-containing ADH activity was up-regulated in cells grown under S^0 limiting conditions (Ma et al. 1995). The biochemical data of iron-containing ADHs from hyperthermophilic archaea implied they were involved in alcohol formation other than alcohol oxidation *in vivo* (Antoine et al. 1999; Li and Stevenson 1997; Ma et al. 1994; Ma et al. 1995; Ma and Adams 1999).

1.2.1.3 Inhibition of iron-containing ADHs by zinc

Activity of iron-containing ADHs from either mesophiles or hyper/thermophiles, is inhibited by zinc. The structure of the enzymes in this family makes it possible to bind zinc because zinc-containing glycerol dehydrogenase has highly conserved structural pattern for catalytic metal, which will be described in **Section 1.2.2.3**. Therefore, zinc can replace iron easily *in vitro*. Although zinc ion abolishes the activity of iron-containing ADHs, it could lead to interesting applications. In *E. coli*, treatment of $ZnSO_4$ inactivates AdhE and zinc-treated *E. coli* cells are more susceptible to oxidative stress, thus suggesting a possible way to inhibit pathogenic microorganisms with AdhE homologues (Echave et al. 2003). In *Z. mobilis*, one interesting approach has been proposed to regain the enzyme activity abolished by zinc occupancy. When the zinc bound to enzyme is removed by using *o*-phenanthroline and iron is re-introduced with iron, up to 70% of the initial activity can be restored after 90 min incubation (Tamarit et al. 1997).

Fe^{2+}-containing ADHs commonly function in anaerobiosis and such enzymes have been proposed to evolve earlier than Zn^{2+}-containing ADHs (Lu et al. 1998). When the global environment was highly reducing, the supply of ferrous iron was abundant. Later, iron became mostly sequestered in the Fe^{3+}-containing compounds when oxygen accumulated. It is thus logical to speculate that Fe^{2+}-containing ADHs were gradually supplanted by more oxygen-resistant Zn^{2+}-containing ones. Fe^{2+}-containing ADHs persist either because there is no selective pressure such as environments lacking of oxygen or because they play a role in the shift from anaerobic to aerobic metabolism (Lu et al. 1998).

1.2.2 Zinc-containing ADHs

In terms of quaternary structure, zinc-containing ADHs are either dimers found in higher plants and mammals (Yokoyama et al. 1990), or tetramers in archaea, bacteria and yeast (**Table 1-3**). One of the exceptions is the (*2R*, *3R*)-(-)-2, 3-butanediol dehydrogenase from *Saccharomyces cerevisiae* which is a zinc-contaning homodimer (González et al. 2000).

Table 1-3 Crystal structures of zinc-containing ADHs from hyperthermophiles and related mesophiles or thermophiles

Organism	Phynotype	Coenzyme	Structure	Ref.[a]
One catalytic zinc and one structural zinc				
TDH from *P. horikoshii*	Anaerobic hyperthermophile	NAD^+	homotetramer	1
ADH from *A. pernix*	Aerobic hyperthermophile	NAD^+	homotetramer	2
ADH from *S. solfataricus*	Aerobic hyperthermophile	NAD^+	homotetramer	3
TDH from *from B. stearothermophilus*	Anaerobic thermophile	NAD^+	homotertramer	4
One catalytic zinc only				
ADH from *C. beijerinckii*	Anaerobic Mesophile	$NADP^+$	homotetramer	5
ADH from *T. brockii*	Anaerobic thermophile	$NADP^+$	homotetramer	5
Zinc-containing ADHs structurally similar to iron-containing ADHs				
GDH from *T. maritima*	Anaerobic hyperthermophile	NAD^+	homotetramer	6
GDH from *B. stearothermophilus*	Anaerobic thermophile	NAD^+	homotetramer	7
YqhD from *E. coli*	Facultatively anaerobic mesophile	$NADP^+$	homotetramer	8

Abbreviations: ADH, alcohol dehydrogenase; GDH, glycerol dehydrogenase; TDH, threonine dehydrogenase.

[a] Reference: 1, Ishikawa et al. 2007; 2, Guy et al. 2003; 3, Esposito et al. 2002; 4, Ceccarelli et al. 2004; 5, Korkhin et al. 1998; 6, Brinen et al. 2002; 7, Ruzheinikov et al. 2001; 8, Sulzenbacher et al. 2004.

Zinc is essential for the activity; however, several zinc-containing ADHs contain structural zinc. The accumulation of structure data about zinc-containing ADHs leads to further classification based on its structure and the role of zinc: ADHs with both catalytic zinc and structural zinc; ADHs with only catalytic zinc; zinc-containing ADHs structurally close to iron-containing ADHs (**Table 1-3**). The role of both catalytic zinc and structural zinc in yeast alcohol dehydrogenase has been well investigated. The enzyme contains two zinc ions per subunit. Partial chelation using dithiothreitol to chelate the structural zinc atom had no effect on the zinc located in the active site. Despite no effect on enzyme activity, the enzyme became very sensitive to heat denaturation, revealing that structural zinc plays a role on stabilizing the tertiary structure of yeast alcohol dehydrogenase (Magonet et al. 1992).

1.2.2.1 ADHs with both catalytic zinc and structural zinc

To date, this family of enzymes is the best known, the representatives of which were found in horse liver, yeast, bacteria and archaea. The typical example from hyperthermophilic archaea is the alcohol dehydrogenase from the archaeon *S. solfataricus* (SsADH) which is a thermostable NAD^+-dependent enzyme (Ammendola et al. 1992). The archaeal ADH contains two zinc atoms per subunit. The catalytic zinc is bound to Cys38, His68, Cys154, and a water molecule. This common coordination of the catalytic zinc atom is the same as that observed in ADH from horse liver (In yellow, **Fig. 1-5**). Cys154 is replaced by aspartate in ADHs from *C. beijerinckii* and *T. brockii* (In yellow, **Fig. 1-6**). In zinc-containing ADHs from *E. coli*, *S. solfataricus*, *C. beijerinckii*, and *T. brockii*, a glutamate residue can serve as the fourth zinc ligand, displacing a water molecule normally present in coenzyme-free enzyme subunits (Karlsson et al. 2003). The structural zinc of SsADH interacts with Glu98 and three Cys residues at positions 101, 104, and 112 (Ammendola et al. 1992). However, SsADH is an exception. The structural zinc atom among this family of zinc-containing ADHs usually shows the tetrahedral coordination by four cysteine residues (In blue, **Fig. 1-5**). Despite structural variations, all of these residues are located within typical sequence motifs of all zinc-containing ADHs (Vallee and Auld 1990).

Figure 1-5 Alignment of representative zinc-containing ADHs with catalytic and structural zincs.

The sequences were aligned using Clustal W (Thompson et al. 1994). BsADH, ADH from *B. stearothermophilus*; EcADH, ADH from *E. coli*; SsADH, ADH from *S. solfartaricus*; HlADH, ADH from horse liver. Highlights in yellow, catalytic zinc binding site;

highlights in blue, structural zinc binding site; highlights in green, coenzyme binding site. The letters in red denote the key residues involving in the binding of catalytic zinc, structural zinc, or NAD^+. ‘‘*’’, residues or nucleotides that are identical in all sequences in the alignment; ‘‘:’’, conserved substitutions; ‘‘.’’, semi-conserved substitutions; “-”, no corresponding amino acid.

```
TbADH     1 MKGFAMLSIGKVGWIEKEKPAPGPFDAIVRPLAVAPCTSDIHTVFEGAIGERHNMILGHE
CbADH     1 MKGFAMLGINKLGWIEKERPVAGSYDAIVRPLAVSPCTSDIHTVFEGALGDRKNMILGHE

TbADH    61 AVGEVVEVGSEVKDFKPGDRVVVPAITPDWRTSEVQRGYHQHSGGMLAGWKFSNVKDGVF
CbADH    61 AVGEVVEVGSEVKDFKPGDRVIVPCTTPDWRSLEVQAGFQQHSNGMLAGWKFSNFKDGVF

TbADH   121 GEFFHVNDADMNLAHLPKEIPLEAAVMIPDMMTTGFHGAELADIELGATVAVLGIGPVGL
CbADH   121 GEYFHVNDADMNLAILPKDMPLENAVMITDMMTTGFHGAELADIQMGSSVVVIGIGAVGL

TbADH   181 MAVAGAKLRGAGRIIAVGSRPVCVDAAKYYGATDIVNYKDGPIESQIMNLTEGKGVDAAI
CbADH   181 MGIAGAKLRGAGRIIGVGSRPICVEAAKFYGATDILNYKNGHIVDQVMKLTNGKGVDRVI

TbADH   241 IAGGNADIMATAVKIVKPGGTIANVNYFGEGEVLPVPRLEWGCGMAHKTIKGGLCPGGRL
CbADH   241 MAGGGSETLSQAVSMVKPGGIISNINYHGSGDALLIPRVEWGCGMAHKTIKGGLCPGGRL

TbADH   321 RMERLIDLVFYKRVDPSKLVTHVFRGFDNIEKAFMLMKDKPKDLIKPVVILA
CbADH   321 RAEMLRDMVVYNRVDLSKLVTHVYHGFDHIEEALLLMKDKPKDLIKAVVIL-
```

Figure 1-6 Sequence alignment of TbADH and CbADH with catalytic zinc only.

The sequences were aligned using Clustal W (Thompson et al. 1994). TbADH, ADH from *T. brockii*; CbADH, ADH from *C. berjerinckii*. Highlights in yellow, catalytic zinc binding site; highlights in green, coenzyme binding site. The letters in red denote the key residues involving in the binding of either zinc or $NADP^+$.

The other example from hyperthermophiles is the recently-reported L-threonine dehydrogenase (TDH) from *P. horikoshii* involving in the oxidation of L-threonine to 2-amino-3-ketobutyrate (Ishikawa et al. 2007). This recombinant L-threonine dehydrogenase is an NAD^+-dependent homotetramer containing one catalytic zinc and one structural zinc of each subunit. The structural zinc ion exhibits coordination with four cysteine ligands conserved throughout the structural zinc-containing ADHs and TDHs. The residues coordinating the catalytic zinc are Cys38, His68, Glu69 and Cys154 (numbering in *P. horikoshii*), conserved to the active site of apo-SsADH. However, the catalytic zinc ion has a larger interdomain cleft and is not coordinated at the bottom of the cleft in the crystal of *P. horikoshii* TDH, which is a significant difference in the orientation of the catalytic domain (Ishikawa et al. 2007).

1.2.2.2 ADHs with only one catalytic zinc

The first members of this family were found in thermophiles such as *T. brockii* and *T. ethanolicus*, and mesophiles such as *C. beijerinckii*. The enzyme from *T. brockii* is commercially available. Distinct from most zinc-containing ADHs, all three enzymes are $NADP^+$-dependent. They are medium chain homotetramer containing one zinc ion per subunit (Burdette et al. 1996; Peretz and Burstein 1989). The single catalytic zinc is coordinated by Cys37, His59 and Asp150 (**Figure 1-6**, numbering in *T. brockii*; Bogin et al. 1997). The ADH from *T. brockii* has four cysteines, of which Cys37 the only cysteine residue that is preserved in all the zinc-containing ADHs (Sun and Plapp 1992).

The characterized ADHs from *T. brockii* and *C. beijerinckii* have 75% sequence identity while amino acid sequences of ADHs from *T. brockii* and *T. ethanolicus* are fully identical after correcting early sequencing results recently (Burdette et al. 1996; Ziegelmann-Fjeld et al. 2007). The structures of NADP(H)-dependent ADHs from *T. brockii* and *C. beijerinckii* have been determined (Korkhin et al. 1998), both of which have very similar three-dimensional structures. The monomers are composed of two domains, a coenzyme-binding domain and a catalytic domain, separated by a deep cleft at the bottom of which a

single zinc atom is bound in the catalytic site. The tetramers are composed of two dimers, each structurally homologous to the dimer of alcohol dehydrogenases of vertebrates. A molecule of NADP(H) binds in the interdomain cleft to the coenzyme binding domain of each monomer. In apo-CbADH, the catalytic zinc is tetracoordinated by side chains of residues Cys37, His59, Asp150 and Glu60; in holo-CbADH, Glu60 is retracted from zinc in three of the four monomers. In holo-TbADH, Glu60 does not participate in Zn coordination. In both holo-enzymes, but not in the apo-enzyme, residues Ser39 and Ser113 are in the second coordination sphere of the catalytic zinc. The carboxyl group of Asp150 is oriented with respect to the active carbon of NADP(H) so as to form hydrogen bonds with both *pro-S* and *pro-R* hydrogen atoms.

1.2.2.3 Zinc-containing ADHs structurally similar to iron-containing ADHs

Structures of this family of enzymes are the least characterized. The earlier example is ADH4 from *S. cerevisiae* (Williamson and Paquin 1987). The biochemical data clearly point to an activity dependency on Zn^{2+} rather Fe^{2+}; however, sequence alignment reveals that they possess the sequence pattern conserved within iron-containing ADHs. These enzymes usually are termed as glycerol dehydrogenases, which have been isolated from a number of organisms including bacteria and yeast. Under anaerobic conditions, microorganisms utilize glycerol as a source of carbon through coupled oxidative and reductive pathways. Glycerol dehydrogenase catalyzes the utilization of glycerol to the formation of dihydroxyacetone with concomitant reduction of NAD^+ to NADH. Crystal structures of glycerol dehydrogenases from hyperthermophile *T. maritima* and thermophile *B. stearothermophilus* are available now (Brinen et al. 2002; Ruzheinikov et al. 2001). The glycerol dehydrogenase from *B. stearothermophilus* consists of one Zn^{2+} per subunit (Spencer et al. 1989). One *adh* gene of *T. maritima* (TM0423) is predicted as a zinc-containing glycerol dehydrogenase with a molecular weight of 39.7 kDa (Brinen et al. 2002). Both enzymes have the structural homology. The Zn^{2+} ion is located deep in the catalytic cleft and is coordinated by residues His252, His269, and Asp169 (numbering in *T. maritima*). In contrast, the differences observed between the structures and sequences of

both glycerol dehydrogenases may be valuable. *B. stearothermophilus* is a thermophilic bacterium whose optimal growth temperature is 55°C while *T. maritima* is a hyperthermophilic bacterium which optimal and maximal growth temperatures are 80 and 90°C, respectively. The detailed interpretation of structures could yield insights into the determinants for thermal stability in this protein family.

1.2.2.4 Zinc-containing ADHs as biocatalysts

The interconversion of a ketone to the corresponding alcohol and *vice versa* represents one of the most common redox-reactions in organic chemistry (Kroutil et al. 2004a; Kroutil et al. 2004b). The interest in the reduction of ketones is substantially increasing due to the production of chiral alcohols from prochiral ketones. Reduction of prochiral ketones can be catalyzed by either whole cells or enzymes. However, the use of enzymes offers some advantages including environmentally friendly and simplified reaction systems, high enantioselectivity and higher concentrations of substrates and organic solvents (Hummel et al. 2003). Examples of enzymes used for the biocatalytic production of chiral alcohols are widely described as medium chain ADHs, short chain ADHs and aldo-keto reductases (Ehrensberger and Wilson 2004). It is rarely reported as long-chain iron-containing ADHs. It is known that the iron-activated ADH from *Z. mobilis* transfers the *pro-R* hydrogen of NADH to acetaldehyde (Clasfeld and Benner 1989). An NAD^+-dependent ADH from the sulfate-reducing bacterium *Desulfovibrio* strain HDv shows a preference for (*S*)-1, 2-propanediol over (*R*)-1, 2-propanediol, which N-terminus indicates similarity to iron-containing ADHs (Hensgens et al. 1995). To our knowledge, the only example from hyperthermophiles is an iron-containing ADH from *T. hydrothermalis* which is stereospecific for monoterpenes (Antoine et al. 1999).

The family of zinc-containing ADHs have been widely used in the preparation of chiral alcohols with NAD^+-dependent alcohol dehydrogenases (ADHs) from horse liver (Adolph et al. 1991), yeast (Weinhold et al. 1991) and *S. solfataricus* (Raia et al. 2001), and with $NADP^+$-dependent ADHs from *T. brockii* (Keinan et al. 1986) and *T. ethanolicus* (Bryant

et al. 1988; Pham et al. 1989). They can be used for substrates with different structures. For example, the ADH from horse liver catalyzes the reduction of a variety of cyclic ketones and 2- or 3-keto esters while the ADH from *T. brockii* efficiently catalyzes the asymmetric reduction of aliphatic acyclic ketones (C_4-C_{10} substrates) (Keinan et al. 1986).

In the viewpoint of application, there is a strong demand for improving existing enzymes or finding new ones. The potential useful substrates in industry are usually the ketones with bulky side chains such as acetophenone or pincoline. Moreover, most of them are almost insoluble in water (Hummel 1999). In addition, the stereoselectivity of ADHs is commonly substrate-related. The demerits of ADHs can be summarized as narrow substrate specificity, insufficient stereospecificity and sensitivity to organic solvents. As compared to those from mesophiles, ADHs from thermophiles or hyperthermophiles have attracted increasing biotechnological interest, particularly due to their high thermostability and solvent tolerance (Olofsson et al. 2005; Zhu et al. 2006). When investigated for the enantioselective reduction of 2-pentanone to (*R*)- and (*S*)-2-pentanol, ADH from *T. brockii* retained significant enzymatic activity in mixtures of water and water-miscible organic solvents up to 87% methanol, ethanol and acetonitrile (Olofsson et al. 2005). In order to expand the range of useful enzyme stereoselectivity, it is valuable and necessary to know the factors affecting the stereoselectivity of ADHs. ADH from *T. ethanolicus* has been well characterized and showed substrate structure, temperature and coenzyme dependencies in the reduction of 2-butanone or 2-pentanone, and oxidation of enantiomers of 2-butanol or 2-pentanol (Zheng et al. 1994). The reduction of 2-pentanone and longer chain ketones gives (*S*)-2-pentanol, and (*R*)-stereoselectivity is observed in the case of smaller substrates (2-butanone, 3-methyl-2-butanone, or methyl cyclopropyl ketone) at 37°C. Moreover, on the oxidation of alcohols, (*S*)-2-butanol is the preferred substrate below 26°C, while at temperatures above 26°C, (*R*)-2-butanol is preferred. In addition, the optical purity of (*S*)-2-pentanol diminishes as the temperature of the reaction mixture for 2-pentanone reduction is increased (Pham et al. 1989; Pham and Phillips 1990). ADH from *A. pernix* preferably reduces aliphatic ketone to (*S*)-alcohol. The enantioselectivity

increases with the increase of chain length and showes the highest on 2-nonanone as aliphatic ketones (C_5-C_{10}) were tested (Hirakawa et al. 2004).

Although those observations are not unique, it is still too early to conclude that they are universal rules for all ADHs from thermophiles or hyperthermophiles. For example, ADH from hyperthermophilic archaeon *P. furiosus* efficiently reduces aromatic ketones and aromatic ketoesters to the optically pure alcohols and retains low enantioselectivities using aliphatic compounds. Higher reaction temperatures increase the enzyme activity but exert no effect on the enantioselectivity (Zhu et al. 2006). It seems that the subtle structure of each enzyme is the central determinant of stereoselectivity as proposed for those ADHs from *S. solfotaricus* and *T. brockii*, which shed light on protein engineering by site-directed mutageneses (Esposito et al. 2002; Korkhin et al. 1998; Ziegelmann-Fjeld et al. 2007). Those resolved structures have resulted in an achievement to expand the substrate specificity of ADH in *T. ethanolicus*. As an example, a catalytic site point mutation Trp110Ala makes *T. ethanolicus* ADH active on benzylacetone and phenylacetone, in which the latter is reduced to produce (*S*)-1-phenyl-2-propanol (Ziegelmann-Fjeld et al. 2007).

As for the bioreduction, it is necessary for coenzyme regeneration [NAD(P)H or $NAD(P)^+$] *in situ* to render the process economical (Hummel, 1999). The strategies of NAD(P)H regeneration are either enzyme-coupled or substrate-coupled (**Fig. 1-7**). Among enzyme-coupled systems, a widespread NADPH regeneration system is the oxidation of formate to carbon dioxide by formate dehydrogenase (FDH) (Hummel and Kula 1989; Seelbach et al. 1996; Tishkov et al. 1999). Advantages are inertness, readily removal of the coproduct CO_2 and thereby a favorable thermodynamic equilibrium, good availability, low cost of the FDH, and the cheap co-substrate formate.

However, most of the FDHs are NADH-dependent, while many ADHs are NADPH-dependent. Thus, an alternative approach to overcome this drawback is the use of glucose

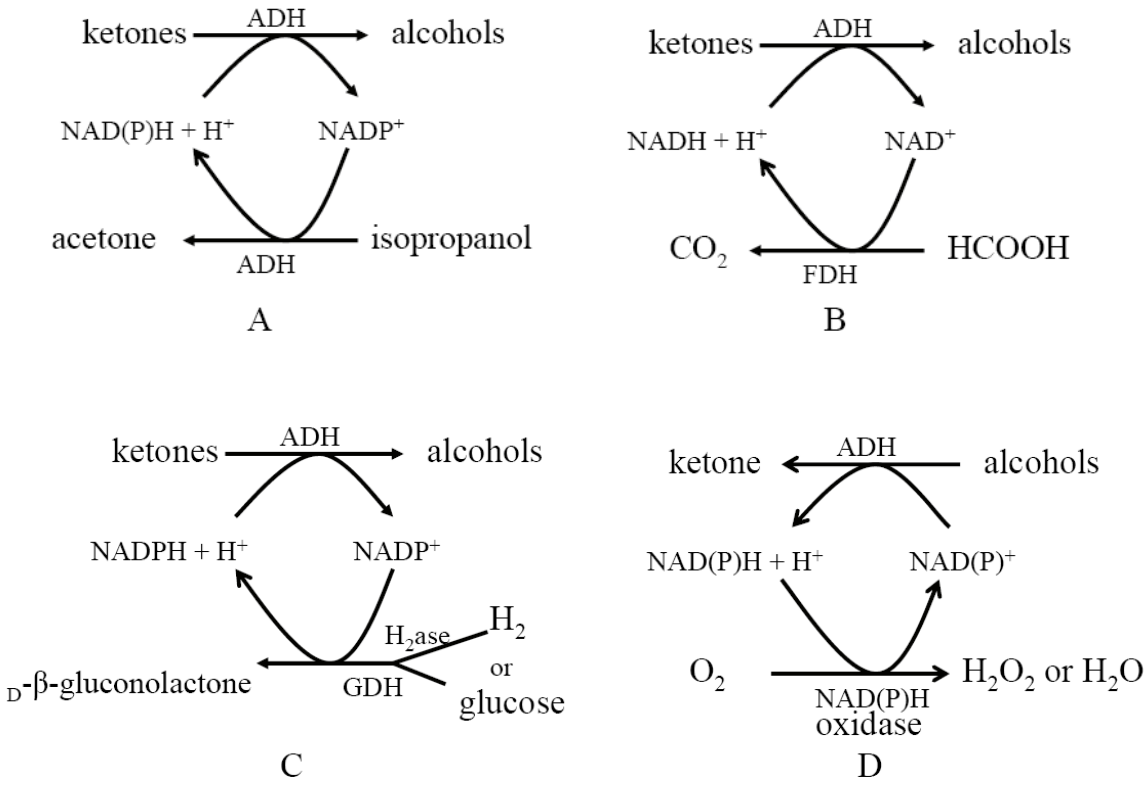

Figure 1-7 Coenzyme regeneration systems.

A, substrate-coupled NADPH regeneration using isopropanol; B, enzyme-coupled NADPH regeneration using formate dehydrogenase; C, enzyme-coupled NADPH regeneration using hydrogenase or glucose dehydrogenase; D, enzyme-coupled $NAD(P)^+$ regeneration using $NAD(P)^+$ oxidase.

dehydrogenase (GDH) or glucose-6-phosphate dehydrogenase (G6PDH) which reaction is $NADP^+$-dependent and nearly irreversible. The GDH or G6PDH oxidizes the co-substrates glucose or glucose-6-phosphate, respectively, and is suited for the regeneration of NADPH (Kizaki et al. 2001; Weckbecker and Hummel 2005). Both enzymes are rather inexpensive, highly active, and stable. A drawback of using G6PDH is the high cost of glucose-6-phosphate (Kataoka et al. 1998; Makino et al. 1989). Recently, a novel regeneration system making use of soluble hydrogenase was reported to regenerate NADPH. Coupled with NADPH regeneration using hydrogenase I from *P. furiosus*, two prochiral substrates, acetophenone and (*2S*)-hydroxy-1-phenyl-propanone, were reduced by an $NADP^+$-dependent ADH from a *Thermoanaerobium* species to the corresponding (*S*)-alcohol and (*1R*, *2S*)-diol (Mertens et al. 2003). Despite the oxygen-sensitivity of hydrogenase, application of hydrogenase I from *P. furiosus* is of great interest, as it uses cheap molecular hydrogen and produce protons as the only by-product (Mentens et al. 2003; Mertens and Liese 2004).

From the viewpoint of NAD(P)H regeneration, the substrate-coupled system using 2-propanol is simpler. This approach only uses a single enzyme, which simultaneously transforms substrate plus the low-cost co-substrate isopropanol. An additional benefit of the coupled-substrate system is that it may be used in the oxidation and reduction mode, whereas separate coenzyme-recycling systems are required for the coupled-enzyme approach. However, excess amount of the second substrate must be applied to drive the equilibrium into the desired direction. As a consequence, these systems are commonly impeded by co-substrate inhibition. The precondition for efficient, large scale coupled-substrate systems is the availability of solvent-tolerant dehydrogenases in order to push the limit of substrate-coupled systems further.

1.2.2.5 Oxidation reactions using dehydrogenases

Although reduction reactions of prochiral compounds represent the most important applications of dehydrogenases, oxidation is also advantageous in some cases (Kroutil et al.

2004a; Kroutil et al. 2004b). First of all, keto compounds, for example, can be prepared by the enzymatic oxidation of alcohols when they are difficult to prepare chemically. Secondly, the preparation of enantiomerically pure compounds can also be achieved by resolving a racemic mixture if both (*S*)- and (*R*)-specific enzymes are available. For example, in order to obtain *R*-phenylpropanol from racemate, the first *S*-specific ADH oxidizes (*S*)-phenylpropanol and the subsequent phenylacetone is reduced to *R*-phenylpropanol using *R*-specific ADHs. It is theoretically possible to use this type of system to achieve 100% enantiomeric excess and 100% yield. In addition, for special substrate structures, ADHs could produce optically pure isomers by oxidation of alcohols such as 2, 3-butanediol. (*2R*, *3R*)-2, 3-butanediol dehydrogenase from *S. cerevisiae* is NAD^+-dependent homotetramer containing zinc and unable to oxidize acetoin to diacetyl. The enzyme catalyze the stereospecific oxidation of (*2R*, *3R*)-2, 3-butanediol and *meso*-butanediol to (*3R*)-acetoin and (*3S*)-acetoin, respectively (González et al. 2000).

The application of alcohol oxidation is currently circumvented by the availability of coenzyme regeneration system. The regeneration of $NAD(P)^+$ could be achieved by using a single ADH together with a ketone (e.g. acetone) as the hydrogen acceptor; however, this approach was not feasible on a preparative scale because of the acetone instability of ADHs. Alternatively, another approach developed recently makes use of enzyme-coupled alcohol oxidation employing nicotinamide oxidases (NADH- and NADPH-oxidases) for coenzyme regeneration (Geueke et al. 2002; Riebel et al. 2003). NADH or NADPH is oxidized at the expense of molecular oxygen by producing hydrogen peroxide or H_2O as by-product. Water-forming oxidases are preferable (Riebel et al. 2002) because the yielding H_2O_2 frequently causes enzyme deactivation even at low concentrations. Therefore, H_2O_2-forming oxidases may have to couple with peroxide-destroying catalase in order to avoid the damage from generated peroxide.

1.3 AIMS OF THE PRESENT STUDY

Among hyperthermophilic heterotrophs, carbohydrate-degrading anaerobes are especially attractive for their potential applications in biotechnology as well as fundamental studies. Hyperthermophilic members of genera *Thermococcus* and *Thermotoga* are obligate chemo-organotrophs growing well on peptide-rich substrates such as yeast extract and tryptone. A large number of them can utilize various carbohydrate polymers including starch, chitin, and xylan. In the genus *Thermococcus*, *T. kodakaraensis*, the genome sequence of which is now available, harbors intriguing proteins including a variety of sugar degradation enzymes (Fukui et al. 2005). In the genus *Thermotoga*, the genome analyses of *T. maritima* and *T. petrophila* revealed the high abundance of enzymes involved in the degradation of sugars and plant polysaccharides (Nelson et al. 1999). Hydrogen is commonly found as one of the end products and a few of hyperthermophiles produce ethanol at a relative low level, implying that these hyperthermophiles have potentials for direct conversion of biomass to renewable fuels (hydrogen and ethanol) at elevated temperatures. However, alcohol metabolism in hyperthermophiles has been relatively overlooked, partially because of low production of alcohols such as ethanol. This prompts us to study the characteristics of alcohol dehydrogenases, one of the key enzymes in alcohol metabolism.

The study of ADHs is important to expand not only the understandings of hyperthmophilic physiology but also their potentials as potent biocatalysts in industry. In general, heat stable enzymes from hyperthermophiles (e.g., amylases, lipases and proteases) are of increasing interest for industrial applications and research. In particular, ADHs from hyperthermophiles are highly attractive due to high stereoselectivity, high solvent tolerance as well as thermostability. Despite the increased rate of discovery of novel ADHs from hyperthermophiles, their potential in biotechnology has not been fully realized. Therefore, their physiological and biochemical characterization pose an interesting set of objectives for enzymology, physiology or biotechnological potentials.

The study aimed to better characterize alcohol dehydrogenases from anaerobic hyperthermophiles, including archaea *T. guaymasensis* and *Thermococcus* strain ES1 as well as a bacterium *T. hypogea*. *T. guaymasensis* is a starch-degrading archaeon growing optimally at 88°C and produces hydrogen (Canganella et al. 1998) while *Thermococcus* strain ES1 grows at temperatures up to 91°C (Pledger and Baross 1989), ADH activities of which are up-regulated under S^0-limiting conditions. In contrast, the xylanolytic bacterium *T. hypogea* has the maximal grow temperature of 90°C and ferments simple and complex carbohydrate substrates (Fardeau et al. 1997).

This work mainly focused on an iron-containing ADH from the bacterium *T. hypogea* and a zinc-containing ADH from *T. guaymasensis*. Both *T. guaymasensis* and *T. hypogea* grew well in a large scale in our lab, which is the solid base of this study. First of all, the ADH activities were detected in the cell-free extract and those native enzymes with dominant activities were purified to homogeneity through a series of liquid chromatographic steps. After that, biophysical and biochemical properties had been extensively examined and their physiological functions were proposed. Studies on iron-containing ADH were highly hampered by their oxygen sensitivity and thus oxygen viability and the role of iron were particularly characterized in *T. hypogea* ADH. Moreover, zinc-containing ADHs are commonly oxygen-resistant secondary ADHs and well known for their stereoselectivity. Accordingly, the studies on *T. guaymasensis* ADH emphasized the exploration of its physiological role and potential applications in biotechnology. In addition, efforts were made to sequence the genes encoding those ADHs, and molecular characterization was carried out by thorough sequence analyses using a variety of databases. Finally, iron-containing ADH from *Thermococcus* strain ES1 and its recombinant version from *E. coli* were purified and characterized. It is intriguing to know whether both native and recombinant enzymes possess identical properties.

Chapter 2 Purification and Characterization of an Iron-containing Alcohol Dehydrogenase in Extremely Thermophilic Bacterium *Thermotoga hypogea*

2.1 ABSTRACT

Thermotoga hypogea is an extremely thermophilic anaerobic bacterium capable of growing at 90°C. $NADP^+$-dependent ADH activities were found to be present in the soluble fraction of *T. hypogea*. The alcohol dehydrogenase was purified to homogeneity, which appeared to be a homodimer with a subunit molecular mass of 40 ± 1 kDa as revealed by SDS-PAGE analyses. The analyses of partial amino acid sequence showed high similary to iron-containing ADHs in hyperthermophilic relatives within the genus *Thermotoga*, revealing putative conserved domains denoting uncharacterized iron-containing ADHs. The metal content of *T. hypogea* ADH was determined by in-torch vaporization-inductively coupled plasma-atomic emission spectrometry and showed that the fully active enzyme contained iron of 1.02 ± 0.06 g-atoms/subunit. The enzyme was oxygen sensitive; however, loss of enzyme activity by exposure to oxygen could be recovered by incubation with dithiothreitol and Fe^{2+}. When cations were added into the assay mixture, the enzyme activity was stimulated by Fe^{2+}, Co^{2+}, Ni^{2+} and Mn^{2+} but inhibited by Zn^{2+} and Cu^{2+}. The enzyme was thermostable with a half-life of about 10 h at 70°C, and its catalytic activity increased along with the rise of temperature up to 95°C. Optimal pH values for production and oxidation of alcohol were 8.0 and 11.0, respectively. The enzyme had a broad specificity to use primary alcohols and aldehydes as substrates. Apparent *K*m values for ethanol and 1-butanol were much higher than that of acetaldehyde and butyraldehyde. The enzyme is the first iron-containing ADH characterized from hyperthermophilic bacteria, and its physiological role was proposed to catalyze the reduction of aldehydes to alcohols *in vivo*.

2.2 INTRODUCTION

Hyperthermophiles are a group of microorganisms that grow optimally at temperatures of ≥80°C (Stetter 1989) or are capable of growing at 90°C or above (Kelly and Adams 1994; Robb and Maeder 1998). They are classified as members of the domains *Archaea* and *Bacteria* (Stetter 1996). The majority of them are anaerobic organisms and many of them have a fermentative metabolism *via* modified Embden-Meyerhof-Parnas and Entner-Doudoroff pathways (Sakuraba et al. 2004; Schönheit and Schäfer 1995; Selig et al. 1997; Siebers and Schönheit 2005; Verhees et al. 2003; de Vos et al. 1998), by which the important intermediate metabolite pyruvate is produced. Pyruvate serves as a precursor for the biosynthesis of amino acids and production of acetate and ethanol (Ingram et al. 1999). A relatively small number of hyperthermophiles including species of *Pyrococcus*, *Thermococcus* and *Thermotoga* can produce ethanol, one of the most desirable renewable energy sources, as the end product (Fardeau et al. 1997; Jochimsen et al. 1997; Kengen et al. 1994; Ma et al. 1995; Sheehan 1994). However, the metabolic pathway for its production in this group of organisms is still not fully elucidated. It has been proposed that enzymes responsible for alcohol production are pyruvate decarboxylase and alcohol dehydrogenase (ADH) (Ma et al. 1997).

ADHs (EC 1.1.1.1) are a family of oxidoreductases that catalyze the interconversion between alcohols and the corresponding aldehydes or ketones, and they are widely distributed in all three domains of life (Reid and Fewson, 1994). They can be classified into the following categories: short-chain ADHs (lack of metal ions), zinc-containing ADHs and Fe-dependent ADHs (Reid and Fewson, 1994). Zinc ions have catalytic or structural functions in several enzymes including hyperthermophilic zinc-containing ADHs (Brinen et al. 2002; Esposito et al. 2002; Guy et al. 2003; Littlechild et al. 2004). However, only a few iron-dependent ADHs are known, of which four are purified from hyperthermophiles (Radianingtyas and Wright 2003). So far, the iron-dependent ADHs that still contain iron after purification are found only in hyperthermophilic archaea. The importance and catalytic mechanism of iron in such enzymes are not well understood.

Furthermore, there has been great interest in studying ADHs in hyper/thermophilic microorganisms (Radianingtyas and Wright 2003) because of their thermostability, broad range of substrate specificity and high tolerance to solvents, which are competitive features for use in the synthesis of various alcohols (Hirakawa et al. 2004; Ma et al. 1994; Ma et al. 1995; Ma and Adams 1999).

Thermotoga hypogea is an anaerobic, extremely thermophilic bacterium that can grow at 90°C (Fardeau et al. 1997). It can utilize carbohydrates including xylan as carbon and energy sources and can produce acetate, CO_2 and hydrogen as the major end products. Ethanol is also produced as an end product of glucose/xylose fermentation (Fardeau et al. 1997). Therefore, *T. hypogea* may have potential application in biomass conversion to ethanol and hydrogen, which are alternative sources of fuel. It was intriguing to study properties of all essential enzymes such as ADH involved in alcohol fermentation in *T. hypogea*. Particularly, the type and metabolic function of the ADH in this extremely thermophilic bacterium warrant further investigation. In this work, we report the properties of the ADH in *T. hypogea*, the first iron-containing ADH purified from the hyperthermophilic bacteria. Its proposed physiological role is to catalyze the reduction of aldehydes to alcohols.[1]

[1] The majority of the work described in this chapter was published in Archives of Microbiology (Ying et al. 2007, Arch Microbiol 187: 499-510).

2.3 MATERIALS AND METHODS

2.3.1 Materials and chemicals

Chromatography columns and protein molecular mass calibration kits were purchased from Amersham Biotech (QC, Canada). Ultrafiltration membranes and Amicon microcentrifuge tubes were from Millipore (MA, USA). All chemicals used with high purities were commercially available products, unless specified. Taq DNA polymerase and DNA ladder were purchased from Fermentas Canada Inc. (Burlington, ON, Canada). KOD Hot Start DNA polymerase and T4 DNA ligase were purchased from Invitrogen and Stratagene (La Jolla, CA, USA), respectively.

2.3.2 Organism and growth conditions

T. hypogea (DSM 11164) was obtained from the Deutsche Sammlung von Mikroorganismen und Zellkulturen, Germany. *T. hypogea* was grown in a medium as described previously (Fardeau et al. 1997; Yang and Ma 2005) and was routinely cultured in a 20-l glass carboy at 70°C. The cells were harvested by centrifugation at 13,000 x *g*. The resulting cell pellet was frozen in liquid nitrogen immediately and stored at -80°C until use.

2.3.3 Determination of ethanol by gas chromatography

Ethanol formation in cultures was determined by Shimadzu GC-14A equipped with a FID detector and an integrator (Shimadzu Corporation, Kyoto, Japan). GC conditions included: column, MXT-624 (0.53mm ID×30m length, Restek, Bellefonte, PA, USA); detector, flame ionization detector (FID); FID sensitivity range, 10^2; detector temperature, 250°C; injector temperature, 200°C; Carrier gas, Helium; linear velocity of Helium, 80cm/s. The temperature program included: initial isotherm at 80°C for 1 min; ramp rate, 30°C/min; final isotherm at 140°C for 1 min. To generate the standard calibration curve, various

concentrations of ethanol (0.86, 1.71, 3.42, 6.84, 10.30, 13.68 and 17.10 mM) were analyzed in the same way. 1 ml culture was transferred into 1.5 ml Eppendorf tube and centrifuged for 8,000 x *g* for 5 min in order to spin down the cells and particles. The resulting supernatant (1 µl) after centrifugation was applied onto the injector (200°C) for GC analyses.

2.3.4 Preparation of cell-free extracts and investigation of oxidoreductase activities

All procedures for the preparation of cell-free extracts were carried out anaerobically. The frozen cells (50 g) of *T. hypogea* were re-suspended in 200 ml of 50 mM Tris–HCl buffer (pH 7.8) containing 2 mM dithiothreitol, 2 mM sodium dithionite and 5% (v/v) glycerol. Subsequently, lysozyme (0.1 mg ml^{-1}) and DNase I (0.01 mg ml^{-1}) were added to the cell suspension. The suspension was incubated at 37°C for 2 h. After centrifugation at 10,000 × *g* for 30 min, the supernatant was collected as cell-free extract for further use.

CoA-dependent aldehdye dehydrogenase activity (ALDH) was measured anaerobically in the CoA-dependent oxidation of butyraldehyde (Yan and Chen 1990). The assay mixture (2 ml) contained 100 mM CAPS buffer (pH 10.0), 2 mM DTT, 0.2 mM CoA, 0.2 mM $NADP^+$, and 60 mM butyraldehyde. Glutamate dehydrogenase was assayed in the direction of $NADP^+$-dependent glutamate oxidation as described previously (Ma et al. 1994; Robb et al. 2001). ADH activities were determined by replacing coenzymes or alcohols as described in **Section 2.3.6**.

2.3.5 Localization of alcohol dehydrogenase in *T. hypogea*

Fractionation of cell-free extract of *T. hypogea* was achieved by centrifugation at various *g* values. After each centrifugation, the supernatant and the pellet were separated in an anaerobic chamber (MBraun, Stratham, NH, USA), and the pellet was re-suspended to its original volume (6 ml). The cell-crude extract of *T. hypogea* (6 ml) was centrifuged at 20,000 × *g* for 30 min at 8°C. The supernatant was the cell-free extract that was then used

for further centrifugation at 30,000 × *g* for 1 h at 10°C. Finally, the supernatant obtained was centrifuged at 115, 000 × *g* for 1 h at 10°C. ADH activity was measured using the method described below and the glutamate dehydrogenase activity was measured as described previously (Kort et al. 1997).

2.3.6 Enzyme assay and protein determination

The catalytic activity of *T. hypogea* ADH was measured anaerobically at 80°C by monitoring the substrate-dependent absorbance change of NADP(H) at 340 nm (ε_{340} = 6.3 $mM^{-1}cm^{-1}$, Ziegenhorn et al. 1976). Unless otherwise specified, the enzyme assay was done in duplicate using the assay mixture (2 ml) for the oxidation of alcohol that contained 20 mM 1-butanol and 0.2 mM $NADP^+$ in 100 mM 3-(cyclohexylamino)-1-propanesulfonic acid (CAPS) buffer (pH 11.0). The assay mixture (2 ml) used for the reduction of aldehyde contained 22 mM butyraldehyde and 0.1 mM NADPH in 100 mM 4-(2-hydroxyethyl)-1-piperazineethanesulfonic acid (HEPES) buffer (pH 8.0). One unit of the activity is defined as 1 μmol NADPH formation or oxidation per min. For determining enzyme kinetic parameters, various substrate concentrations (0 to ≥10 × apparent *K*m unless specified) for NADPH (0, 0.007, 0.014, 0.026, 0.037, 0.050 and 0.092 mM), butyraldehyde (0, 0.05, 0.23, 0.45, 1.10, 2.30, 5.60 and 22.00 mM), acetaldehyde (0, 1.0, 2.2, 4.3, 11.0 and 42.0 mM), $NADP^+$ (0, 0.009, 0.024, 0.047, 0.095 and 0.380 mM), butanol (0, 1.0, 2.1, 5.2, 10.0 and 20.0 mM) and ethanol (0, 4, 6, 10, 20, 40, 60 and 120 mM) were used for the determination of corresponding activities at 80°C, while concentrations of the corresponding co-substrates were kept not only constant, but also higher than 10 × apparent *K*m. Apparent values of *K*m and *V*max were calculated from their Lineweaver-Burk plots. For determining pH optimum of the enzyme activity, 100 mM buffer of 1, 4-piperazine-bis-(ethanesulfonic acid) (PIPES, pH 6.0, 6.5, 7.0), HEPES (7.0, 7.5, 8.0), Tris/HCl (8.0, 8.5, 9.0), glycine (9.0, 9.5, 10.0), CAPS (10.0, 10.5, 11.0, 11.5) and phosphate (12) were used and the assays were performed at 80°C. The protein concentrations of all samples were determined using the Bradford method and bovine serum albumin served as the standard protein (Bradford 1976).

2.3.7 Enzyme purification

The cell-free extract of *T. hypogea* was applied to a DEAE-sepharose column (5 × 10 cm) that was equilibrated with buffer A [50 mM Tris–HCl buffer containing 5% (v/v) glycerol, 2 mM dithiothreitol, 2 mM sodium dithionite, pH 7.8]. After eluting the column using 150 ml buffer A, a gradient (0-0.5 M NaCl) was applied at a flow rate of 3 ml min^{-1}. ADH was eluted while buffer A was applied. Fractions containing enzyme activity were then pooled and loaded onto a Hydroxyapatite column (2.6 × 15 cm) at a flow rate of 2 ml min^{-1}. The column was applied with a gradient (0-0.5 M potassium phosphate in buffer A) and ADH started to elute from the column at the concentration of 0.05 M potassium phosphate. Fractions containing enzyme activity were pooled and applied to a phenylsepharose column (5 × 10 cm) equilibrated with 0.8 M $(NH_4)_2SO_4$ in buffer A at a flow rate of 2 ml min^{-1}. A linear gradient [0.82-0 M $(NH_4)_2SO_4$ in buffer A] was applied and the ADH started to elute at a concentration of 0.64 M $(NH_4)_2SO_4$. Fractions containing ADH activity were pooled and concentrated by ultrafiltration using PM-30 membrane. The concentrated sample was applied to a gel filtration column (Superdex 200, 2.6 × 60 cm) equilibrated with buffer A containing 100 mM KCl at a flow rate of 2 ml min^{-1}. The purity of the fractions containing ADH activity was verified using sodium dodecyl sulfate-polyacrylamide gel electrophoresis (SDS-PAGE) as described by Laemmli (1970). The purified enzyme sample was sent to the Molecular Biology Core Facilities at Dana-Farber Cancer Institute (Boston, MA, USA) for N-terminal sequence determination (Deutscher 1990).

2.3.8 Activation of oxygen-inactivated ADH

Dithiothreitol and sodium dithionite present in the purified enzyme sample (0.08 mg ml^{-1}) were first removed using a Microcon YM-30 (Millipore, MA, USA) with aerobic 50 mM Tris/HCl buffer (pH 7.8) containing 5% (w/v) glycerol at the room temperature, which took approximately 30 min. The enzyme sample without dithiothreitol and sodium

dithionite was adjusted to its original volume, and an aliquot of the oxygen-inactivated sample was added into different stoppered vials. Each vial was then immediately degassed for approximately 5 min before the addition of the following compounds (final concentration): 1 mM dithiothreitol, 1 mM sodium dithionite, 0.1 mM $FeCl_2$, or 1 mM dithiothreitol plus 0.1 mM $FeCl_2$. Each vial was then incubated at room temperature and the ADH activities were assayed at different intervals as specified. To determine if the length of the enzyme exposure to air would affect the activity recoverability by incubating dithiothreitol and Fe^{2+} under anaerobic conditions, the sample solutions were vortexed well in the air. At each specified length of exposure time (0.5, 5 and 24 h), the oxygen-inactivated sample was transferred to a stoppered vial that was then degassed and filled with oxygen-free nitrogen gas. Both dithiothreitol and Fe^{2+} were added to a final concentration of 1 mM and 0.1 mM, respectively. At different intervals of the incubation at room temperature, ADH activities were determined using an aliquot (0.5 μg) of each sample at 80°C, as described above.

2.3.9 Determination of metal contents in the purified ADH

The iron (Fe) and zinc (Zn) contents of the purified enzyme were determined using in-torch vaporization inductively coupled plasma atomic emission spectrometry (ITV-ICP-AES) as described previously (Badiei et al. 2002). The remarkable aspect of the ITV-ICP-AES system used for elemental determinations is that it can provide accurate, precise and simultaneous multi-element determinations from microliter volumes (e.g., 1-3 μl) of metal-containing enzymes (with an absolute weight of the metal content in the picogram range). In general, ITV can be used with micro- to nano-amounts of liquids or solids by employing interchangeable rhenium (Re) coiled filaments or Re cups (Badiei et al. 2002). Prior to the determination, the enzyme samples were washed ten times with ultra pure buffer (10 mM Tris-HCl prepared with 18.2 MΩ cm deionized water) in the anaerobic chamber to remove Na^+ and unbound ions by using YM-30 Amicon microcentrifuge tubes. Due to the difficulty in obtaining fully active enzyme after such filtration procedures, 2 mM dithiothreitol was added to the ultra pure buffer, which resulted in fully active ADH

samples after completing the washing procedures. Aerobically prepared enzyme samples were obtained by exposure to the air after removing dithiothreitol. To construct calibration curves, standard solutions containing Fe and Zn with concentrations of 10, 30, 100 and 300 ng ml^{-1} (for each element) were prepared via serial dilution using 18.2 MΩ cm distilled, de-ionized water and 1,000 μg ml^{-1} stock solutions (SCP Science, Quebec, Canada). The stock solutions of Fe and Zn were in 4% (v/v) HNO_3 and 2% (v/v) HCl, respectively. Throughout this work, 3 μl aliquots were used for ITV-ICP-AES experiments.

2.3.10 Determination of molecular mass and effects of metal ions

The molecular mass of the enzyme subunit was determined using SDS-PAGE (Laemmli 1970) and a calibration curve was obtained using the low molecular mass standard from Bio-Rad (14-97 kDa, Bio-Rad Laboratories, ON, Canada). The native molecular mass of the purified enzyme was estimated by gel filtration on the Superdex 200 column (2.6 × 60 cm). The column was equilibrated with buffer A containing 100 mM KCl at a flow rate of 2 ml min^{-1} before applying standard samples of protein kits (Pharmacia, NJ, USA) that contained blue dextran (molecular mass, Da, 2,000,000), thyroglobulin (669,000), ferritin (440,000), catalase (232,000), aldolase (158,000), bovine serum albumin (67,000), ovalbumin (43,000), chymotrysinogen A (25,000) and ribonuclease A (13,700). In order to determine the effect of the metal ions, the chelator and the reducing agents on the enzyme activity, the enzyme activity was assayed using an NADPH dependent reduction of butyraldehyde in 100 mM PIPES at pH 7.0 to obtain improved solubility of cations over those at alkaline pHs. Each or combination of the following compounds (1 mM unless specified) - $FeCl_2$, $ZnCl_2$, $CoCl_2$, $NiCl_2$, $MgCl_2$, $CuCl_2$, $MnCl_2$, $CaCl_2$, $CdCl_2$, ethylenediaminetetraacetic acid (EDTA), dithiothreitol (2 mM) and mercaptoethanol (2 mM) was added into the anaerobic ADH assay mixture containing 100 mM PIPES buffer (pH 7.0), 22 mM butyraldehyde and 0.1 mM NADPH. The enzymatic reaction was started by the addition of the purified enzyme (0.9 μg). The assay control did not contain any of the compounds listed above. For the pre-incubated enzyme samples (0.045 mg protein per ml) with these compounds (1 mM) and $HgCl_2$ (1 mM) for either 1 h at 4°C or

10 min at 70°C, the activities were measured using the assay mixture that did not contain any of the compounds, and the enzyme sample without any treatment was used as an assay control.

2.3.11 Determination of amino-terminal sequence

The purified enzyme (1 μg) was run on 12.5% SDS-PAGE and electrophoretically blotted onto a polyvinylidene difluoride (PVDF) membrane by using Mini Trans-Blot Electrophoretic Transfer cell (Bio-Rad Laboratories, Hercules, CA, USA). The PVDF membrane was wet in 100% methanol for 1 min right before use. The transferring buffer [25 mM Tris/HCl containing 192 mM glycine and 15% (v/v) methanol] was pre-cooled at 4°C and one cooling unit was put inside the transfer cell to maintain the low temperature. Blotting was run for one and half hours at 110V and 230 mA. After that, the PVDF membrane was stained for 3 min by 0.1% (w/v) Coomassie Blue R-250 in 10% (v/v) methanol solution and subsequently destained by a solution containing 45% (v/v) methanol and 10% (v/v) acetic acid. After destaining, the PVDF membrane was washing with Millipore-grade water (18.2 MΩ·cm) for 2 days. The bands on the PVDF membrane were cut in a flow hood by using a surgical cutter. The cut samples were transferred into clean Eppendorf tubes and stored at -20°C freezer. The samples were sequenced by Edman degradation (Molecular Biology Core Facility, Dana Farber Cancer Institute, Boston, MA, USA).

2.3.12 Identification of *T. hypogea* ADH internal sequences by mass spectrometry

The purified enzyme was run in a 12.5% SDS-PAGE, and the band of *T. hypogea* ADH was cut from the SDS-PAGE and sent for mass spectrometry analyses (Custom Biologics, Toronto, ON, Canada).

2.3.13 Gene cloning of *T. hypogea* ADH

The genomic DNA used as the template of PCR was extracted using the solution of phenol, chloroform and isoamyl alcohol (25: 24: 1). DNA concentrations of samples were quantified using NanoDrop Spectrophotometer (NanoDrop Technologies, Wilmington, DE, USA). On the basis of N-terminal (MENFVFHNPTKLIFG) and internal sequence (LMLYGGGSI), two oligonucleotides naming as THADHNF and THADHIR (**Table 2-1**), were synthesized and used as forward and reverse PCR primers, respectively. A PCR was performed by a thermal cycler TC-312 (Techne incorporated, NJ, USA) with 15 pmol of each primer against 100 ng of genomic DNA isolated from *T. hypogea* cells. After preheating at 94°C for 4 min, the thermal program consisted of 36 cycles of denaturation at 94°C for 30 seconds, annealing at 55°C for 45 seconds, and extension at 72°C for 30 seconds. The PCR products were run on a 2% agarose gel and visualized and graphed by FluorChem 8000 Chemiluminescence and Visible Imaging System (Alpha Innotech Corporation, San Leandro, CA, USA). The resulting 130 bp PCR product was sequenced by the dye-termination method (Molecular Biology Core Facility, University of Waterloo, ON, Canada). DNA and protein sequencing were analyzed with Gene Runner and compared to the GenBank database by BLAST (Altschul et al. 1997). The BLAST search of 130 bp indicated the highest similarity to the iron-containing ADH from *T. maritima* (TM0820). Thus, the new forward and reverse primers THAUNF and THAUIR01 were designed based on the nucleotide sequence of TM0820. Following the above PCR conditions, 1.3 kb PCR product was obtained and its primary sequencing results also indicated highest similarity to TM0820. Three new primers THADHIR, THADHIF1 and THADHIF2 were designed based on that preliminary sequencing results of *T. hypogea* ADH and eventually led to a sequence of 1074 bp encoding 358 amino acid residues.

2.3.14 Data mining

Gene sequences of *T. hypogea* ADH were identified by performing BLAST searches with

Table 2-1 Primers designed for sequencing the gene encoding *T. hypogea* ADH

Name	Primers[a] (5'-3')
THADHNF	ATGGAGAACTTCGTCTTCCACAATCC
THADHIR	TATCGATCCACCACCGTATAGCATCAG
THAUNF	AACTTCGTCTTCCACAATCC
THAUIR01	TCATCTCCGTTCCTGTCG
THADHYIR	GTGTGTGCTATTGCGTCG
THADHYIF1	ACTGAGATGAACGGAAACG
THADHYIF2	GCGACGATAGCCCTGAAC

[a] Pirmer properties like melting temperature (Tm), GC content (mol% G+C), primer loops and primer dimers were evaluated by a DNA analysis tool Gene Runner (Hastings Research, Inc., Las Vegas, USA).

sequences from iron-containing ADHs (Altschul et al. 1997). Conserved domains (CDs) were analyzed with CD search (Marchler-Bauer et al. 2005) and Motif Search (http://www.genome.jp/kegg/ssdb/ and http://www.expasy.org/prosite/) (Kanehisa et al. 2002). Alignment of *T. hypogea* ADH against close homologues of iron-containing families was performed using Clustal W (http://align.genome.jp/) (Thompson et al. 1994). The secondary structure was predicted by using SSpro (Cheng et al. 2005; Pollastri et al. 2002). The tertiary structure of ThADH monomer was predicted by using the SWISS-MODEL server (Guex and Peitsch 1997; Kopp and Schwede 2004; Peitsch 1995; Schwede et al. 2003) and subsequently the PDB file was analyzed and visualized by the software PyMOL (Delano, 2002).

2.4 RESULTS

2.4.1 Growth, ethanol production and ADH activities

T. hypogea is a glucose-utilizing anaerobe and grew both in the presence and absence of sodium thiosulfate, which serves as electron acceptor (**Figure 2-1**). The addition of sodium thiosulfate increased the growth as well as ethanol formation determined by cell counting and gas chromatography, respectively. Although the ethanol concentration was lower than 1 mM under all tested conditions, the ethanol formation of *T. hypogea* appeared to correlate to its growth.

T. hypogea grew well in a 15-liter scale and approximately 2 g cells (wet weight) per liter were obtained. It was intriguing to know properties of its alcohol dehydrogenase, one of the key enzymes in alcohol formation. When various alcohols were used as substrates to determine the type of ADH activities, only $NADP^+$ specific ADH activities were found to be present in the cell-free extract of *T. hypogea* (**Table 2-2**). The activities on butanol and 1, 4-butanediol as the substrate were 0.38 and 0.15 U mg^{-1}, respectively, suggesting that the dominant ADHs catalyze the oxidation of primary alcohols. ADH activities on butanol oxidation were almost constant in cell-free extract prepared from cells of mid-log, late-log and stationary growth phases. The ADH was located in the soluble fractions of the cell of *T. hypogea* because more than 95% of the ADH activity was present in the supernatant fraction after ultracentrifugation (115,000 × *g*, 1 h) of the cell-free extract. This supernatant fraction also contained more than 90% of the glutamate dehydrogenase activity, a known cytoplasmic enzyme (Ma et al. 1994; Robb et al. 2001). Surprisingly, CoA-dependent aldehyde dehydrogenase activities were not measurable under assay conditions.

2.4.2 Purification and physical properties of *T. hypogea* ADH

The cell-free extract showed the highest activity using 1-butanol as substrate; hence,

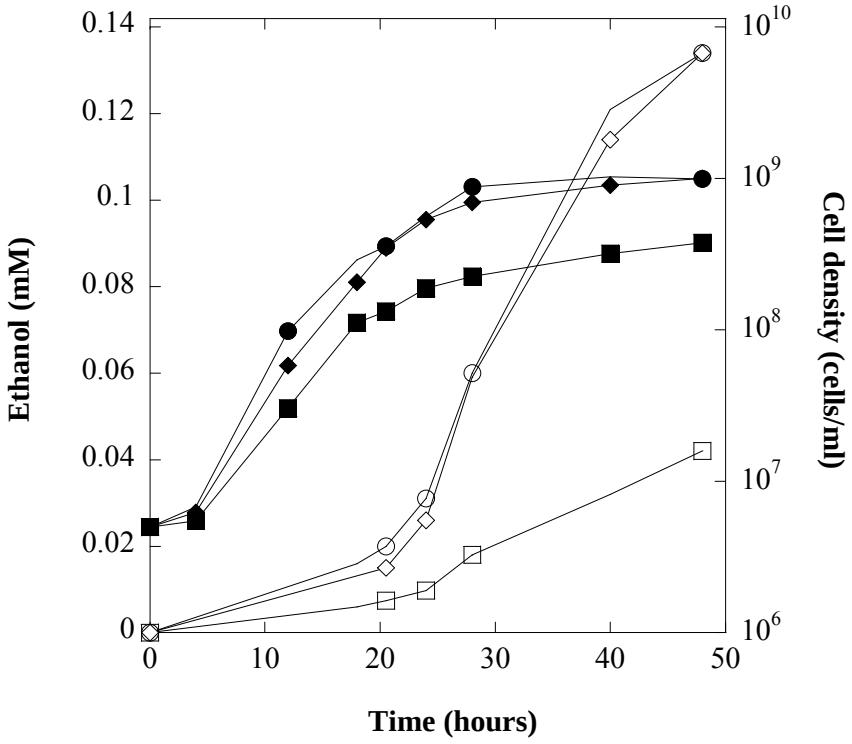

Figure 2-1 Growth and ethanol production of *T. hypogea*.

Solid symbols represent cell density while open symbols represent ethanol production. was *T. hypogea* was cultured anaerobically at 70°C. Media used: squares, 0.3%(w/v) glucose and 0.5%(w/v) NaCl; diamonds, 0.3%(w/v) glucose and 0.5%(w/v) sodium thiosulfate; circles, 0.3%(w/v) xylose and 0.5%(w/v) sodium thiosulfate.

Table 2-2 ADH activities in *T. hypogea* cell-free extract

Substrate	Actvitiy using $NADP^+$ as coenzyme (U mg^{-1})
1-butanol	0.38
2-butanol	*ND*
2,3-butanol	*ND*
1,4-butanediol	0.15
Glycerol	*ND*

Activities were not detectable when NAD^+ was used as coenzyme.

ND stands for no detectable activity.

1-butanol was used to trace the ADH activities during purification steps. ADH was partially eluted during the loading of the sample on to the DEAE-sepharose column and completely eluted once buffer A was applied. This implied that ADH did not bind to the column well and its separation from the majority of other proteins in the cell-free extract was achieved. The ADH was eluted out as a predominant single peak in all subsequent purification steps. The final purification step using the gel-filtration chromatography resulted in a preparation of ADH with a specific activity of 57 U mg^{-1} (**Table 2-3**). Its purity was determined by SDS-PAGE, which showed a single type of subunit with a molecular mass of 40 ± 1 kDa (**Fig. 2-2**). A single protein peak corresponding to the ADH activity was eluted from the gel-filtration column Superdex 200, which had a molecular mass of 70 ± 5 kDa, indicating that the purified ADH was a homodimer enzyme.

Amino-terminal sequence (15 amino acids) was determined to be MetGluAsnPheValPheHisAsnProThrLysLeuIlePheGly by using Edman degradation. Five internal sequences (**Table 2-4**) were obtained by mass spectrometry, two of which were aligned and revealed to be parts of an iron-containing ADH from *T. maritima* (TM0820). Referring to the nucleotide sequence of TM0820, the non-degenerate primers were designed and amplifications using the genomic DNA as template led to PCR products with approximately 130 bp and 1400 bp, respectively (**Fig. 2-3**). The sequencing results indicated the shorter PCR product was a part of the longer one. Finally, a 1074-bp nucleotide sequence was obtained, and it encoded 358 amino acids including the initiating methionine (**Fig. 2-4**). The BLASTP search of the deduced amino acid sequence showed extremely low identity (<30%) to iron-containing ADHs in hyperthermophilic archaea (Antoine et al. 1999; Li and Stevenson 1997), but shows high sequence identity (58-76%) to the enzymes in *Thermotogales* such as *Thermotoga maritima* (Nelson et al. 1999), *Thermotoga petrophila* (Copeland et al. 2007a), *Fervidobacterium nodosum* Rt17-B1 (Copeland et al. 2007b) and *Thermosipho melanesiensis* (Copeland et al. 2007e), moderately high identity (46-58%) to those enzymes in other thermophilic bacteria such as *Symbiobacterium thermophilum* (Ueda et al. 2004) and *Thermoanaerobacter ethanolicus*

Table 2-3 Purification of ADH from *T. hypogea*

Purification steps	Total proteins (mg)	Total activity[a] (U)	Specific activity (U mg^{-1})	Purification-fold	Yield (%)
Cell-free extract	721	127	0.2	1	100
DEAE-Sepharose	57	112	2.0	10	88
Hydroxyapatite	29	75	2.5	13	59
Phenyl-Sepharose	3.5	49	14	70	39
Gel filtration	0.7	40	57	285	31

[a] ADH activities were determined using the method described in "Materials and Methods", except the CAPS buffer at pH 10.5.

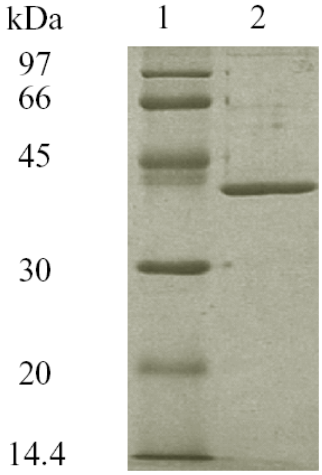

Figure 2-2 SDS-PAGE (12.5%) analyses of ADH purified from *T. hypogea*.

Lane 1, molecular mass markers (6 μg) (Bio-Rad Laboratories, ON, Canada); Lane 2, 1.5 μg of ADH;

Table 2-4 N-terminal and internal sequences of *T. hypogea* ADH

Location	Sequences
N-terminal	MENFVFHNPTKLIFG
Internal 1	LPLLLHLE(L)[a]
Internal 2	RAPVSL
Internal 3	LMLYGGGSI
Internal 4	PRSLSLR(A)[a]
Internal 5	LILAS

[a] Parentheses indicate less certainty

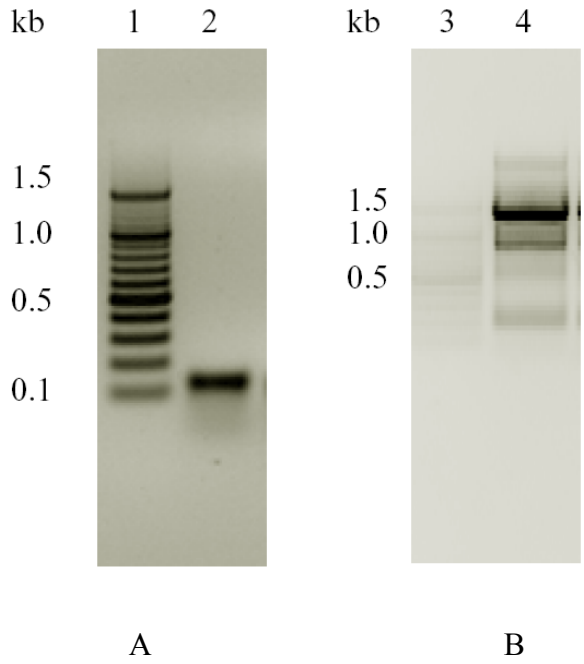

Figure 2-3 PCR products of 130 bp (A) and 1400 bp (B).

A, amplification using primers THADHNF and THADHIR; B, amplification using primers THAUNF and THAUIR1 as described in **Table 2-1**. Lane 1 and 3, 100 bp DNA ladders; Lane 2 and 4, PCR products.

```
1          ATGGAGAACTTCGTCTTCCACAATCCCACCAAGTTGATATTCGGTAAAGGAACCATTCCA
1           M  E  N  F  V  F  H  N  P  T  K  L  I  F  G  K  G  T  I  P

61         AAGATAGGCGAGGAGATCAAATCTTTCGGGATCAAAAAGGTTTTGATGCTCTACGGCGGT
21          K  I  G  E  E  I  K  S  F  G  I  K  K  V  L  M  L  Y  G  G

121        GGTTCGATAAAGAAGAACGGTGTCTACGATCAGGTCGTGGAATCTTTGAAAAGAAACGGC
41          G  S  I  K  K  N  G  V  Y  D  Q  V  V  E  S  L  K  R  N  G

181        ATCGAGTGGGTTGAGGTTTCTGGCGTCAAACCCAATCCAGTGCTCTCGAAGGTCCACGAG
61          I  E  W  V  E  V  S  G  V  K  P  N  P  V  L  S  K  V  H  E

241        GCTATAGAAGTTTGCAGAAAAGAGAACGTGGAGGCTGTTCTGGGCGTCGGTGGTGGAAGT
81          A  I  E  V  C  R  K  E  N  V  E  A  V  L  G  V  G  G  G  S

301        GTTATCGATTCAGCTAAAGCGATCGCAGCCGGTGTTCTCTACGAAGGAGACATTTGGGAC
101         V  I  D  S  A  K  A  I  A  A  G  V  L  Y  E  G  D  I  W  D

361        GCATTCGCCGGAAAGCATAAGATCAACAATGCCTTGCCAGTGTTCGCAATTTTGACCATA
121         A  F  A  G  K  H  K  I  N  N  A  L  P  V  F  A  I  L  T  I

421        TCTGCCACTGGAACTGAGATGAACGGAAACGCCGTGGTCACCAACGAAAAGACCCAGGAA
141         S  A  T  G  T  E  M  N  G  N  A  V  V  T  N  E  K  T  Q  E

481        AAGTGGGCGATCAGTGCAAAGTGTCTTTATCCACGAGTTTCTATAATCGATCCCACCGCA
161         K  W  A  I  S  A  K  C  L  Y  P  R  V  S  I  I  D  P  T  A

541        CAGTTTTCTCTACCGAAGGAGCAGACCGTCTATGGTGCGGTCGACGCAATAGCACACACG
181         Q  F  S  L  P  K  E  Q  T  V  Y  G  A  V  D  A  I  A  H  T

601        CTCGAGTACTACTTCGACGGTTCAGACTCGGACATACAGAACCAGATCAGCGAGTCCATT
201         L  E  Y  Y  F  D  G  S  D  S  D  I  Q  N  Q  I  S  E  S  I

661        ATCAGATCGATAATGAAGTCCACAGAAGTTTTGATAGACAATCCACAAGACTACGAGGCG
221         I  R  S  I  M  K  S  T  E  V  L  I  D  N  P  Q  D  Y  E  A

721        AGGGCGAACTTCGCCTGGTGTGCGACGATAGCCCTGAACGGTCTGACCGCCGCAGGTAGG
241         R  A  N  F  A  W  C  A  T  I  A  L  N  G  L  T  A  A  G  R

781        AAAGGTGGGGATTGGTCCTGTCACAAGATAGAGCATTCTCTCAGCGCGCTCTACGACATT
261         K  G  G  D  W  S  C  H  K  I  E  H  S  L  S  A  L  Y  D  I

841        GCTCACGGTGCAGGACTTGCGATCGTTTTCCCCGCGTGGATGAGATACGTCTATAAACAA
281         A  H  G  A  G  L  A  I  V  F  P  A  W  M  R  Y  V  Y  K  Q

901        AAACCACAGCAGTTCGAGAGGTTCGCGAAGCACGTTTTCTCGATCGATGCCGTGGGAGAA
301         K  P  Q  Q  F  E  R  F  A  K  H  V  F  S  I  D  A  V  G  E

961        GAAGCGATCTTGAAAGGTATAGACGCTTTCAAAGCTTGGCTCAGGAAGGTCGGTGCTCCC
321         E  A  I  L  K  G  I  D  A  F  K  A  W  L  R  K  V  G  A  P

1021       GTTTCGTTGAGAGACGTTGGTATACCAGCACAGGACATCGACAGGAACGGAGATGA
341         V  S  L  R  D  V  G  I  P  A  Q  D  I  D  R  N  G  D
```

Figure 2-4 Partial nucleotide and deduced amino acid sequences of *T. hypogea* ADH.

The amino acid sequence was deduced using the program DNAMAN (Lynnon Corporation ,Vaudreuil-Dorion, Quebec, Canada). The nucleotide sequence corresponding to N-terminus (5'-ATGGAGAACTTCGTCTTCCACAATCC) was from the designed primer THADHNF (**Table 2-1**).

X514 (Copeland et al. 2006c). Genes encoding these enzymes are annotated as either iron-containing ADH or NADH-dependent butanol dehydrogenase. The conserved domain search indicated the enzyme belonged to a family of uncharacterized, iron-containing ADHs (**Fig. 2-5**). However, none of them has been purified and characterized, indicating that *T. hypogea* ADH is the first one purified from this uncharacterized type of hyper/thermophilic bacterial ADHs.

Amino-terminus of *T. hypogea* ADH contained a GGGS motif (residues 39-42) which was well accepted to be involved in the interactions of the pyrophosphate groups of $NADP^+$ (Sulzenbacher et al. 2004). Moreover, *T. hypogea* ADH shared 76% identity to iron-containing ADH from *T. maritima* (TM0820) and harbored most of amino acid residues observed in the crystal structure of TM0820 in response of $NADP^+$ binding **(Fig. 2-6**). The putative iron-binding sites ($Asp_{195}His_{199}His_{268}His_{282}$) were highly conserved motifs among iron-containing ADHs (**Fig. 2-6**). The 3-D modeling of *T. hypogea* ADH showed that the enzyme folded into two structural domains separating with a deep cleft (**Fig. 2-7**). Like other iron-containing ADHs, the N-terminal domain was formed by an α/β region containing the dinucleotide-binding fold, whereas the C-terminal part was an all-helical domain responsible for the iron binding.

Both Fe and Zn were detected from the *T. hypogea* ADH using ITV-ICP-AES analysis which is a newly developed method to determine pico-gram level elements (**Fig. 2-8**). Prior to both Fe and Zn signals, a decrease in plasma background levels was observed, which was attributed to a pressure pulse. This pulse is due to a momentary increase in the carrier gas flow rate, which, in turn, is due to a gas expansion in the chamber by the rapidly heated rhenium coil. For plasma background levels in UV range, the pressure pulse typically becomes more pronounced with the wavelength of a spectral line (e.g., Fe II 259.940 nm vs. Zn I 213.856 nm). Fe and Zn contents of the fully active enzyme were found to be 1.02 ± 0.06 *g*-atoms per subunit and 0.08 ± 0.01 *g*-atoms per subunit, respectively, indicating that *T. hypogea* ADH is an iron-containing enzyme and that the

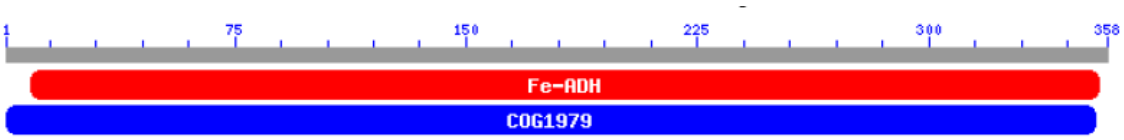

Figure 2-5 Putative conserved domains of *T. hypogea* ADH against its homologues.

Fe-ADH (Pfam 00465) denotes Fe-dependent alcohol dehydrogenase family in Pfam protein family database; COG1979 denotes uncharacterized oxidoreductases, Fe-dependent alcohol dehydrogenase family in the database of Clusters of Orthologous Groups of proteins (COG).

```
THADH       MENFVFHNPTKLIFGKGTIPKIGEEIKSFGIKKVLMLYGGGSIKKNGVYDQVVESLKRNG
TM0820      MENFVFHNPTKIVFGRGTIPKIGEEIKNAGIRKVLFLYGGGSIKKNGVYDQVVDSLKKHG
            ***********:**:**********. **:***:****************:***::*

THADH       IEWVEVSGVKPNPVLSKVHEAIEVCRKENVEAVLGVGGGSVIDSAKAIAAGVLYEGDIWD
TM0820      IEWVEVSGVKPNPVLSKVHEAVEVAKKEKVEAVLGVGGGSVVDSAKAVAAGALYEGDIWD
            **********************:**.:**:***********:*****:***.********

THADH       AFAGKHKINNALPVFAILTISATGTEMNGNAVVTNEKTQEKWAISAKCLYPRVSIIDPTA
TM0820      AFIGKYQIEKALPIFDVLTISATGTEMNGNAVITNEKTKEKYGVSSKALYPKVSIIDPSV
            ** **:*::***:* :***************:*****:**:.:*:*.***:******:.

THADH       QFSLPKEQTVYGAVDAIAHTLEYYFDGSDSDIQNQISESIIRSIMKSTEVLIDNPQDYEA
TM0820      QFTLPKEQTVYGAVDAISHILEYYFDGSSPEISNEIAEGTIRTIMKMTERLIEKPDDYEA
            **:***************:* ********.:*.*:*:*. **:*** ** **::*:****

THADH       RANFAWCATIALNGLTAAGRKGGDWSCHKIEHSLSALYDIAHGAGLAIVFPAWMRYVYKQ
TM0820      RANLAWSATIALNGTMAVGRRGGEWACHRIEHSLSALYDIAHGAGLAIVFPAWMKYVYRK
            ***:**.*******  *.**:**:*:**:*************************:***::

THADH       KPQQFERFAKHVFSIDAVGEEAILKGIDAFKAWLRKVGAPVSLRDVGIPAQDIDRNGD--
TM0820      NPAQFERFAKKIFGFEGEGEELILKGIEAFKNWLKKVGAPVSLKDAGIPEEDIDKIVDNV
            :* *******::*.::. *** *****:*** **:********:*.*** :***:  *

THADH       ----------------------------------
TM0820      MLLVEKNLKPKGASLGRIMVLEREDVREILKLAAK
```

Figure 2-6 Sequence alignment of *T. hypogea* ADH and ADH from *T. maritima* (TM0820).

The sequences were aligned using Clustal W and a phylogenetic tree was constructed (Thompson et al. 1994). Highlight in yellow, ion-containing alcohol dehydrogenases signatures (residue 174-202 and 265-285); highlights in green, ligands for $NADP^+$ binding. The role of residues in red has been interpreted in the crystal structure of TM0820. ‘‘*’’: residues or nucleotides that are identical in all sequences in the alignment; ‘‘:’’, conserved substitutions; ‘‘.’’, semi-conserved substitutions. The amino acid sequence of *T. hypogea* ADH is partially determined; the symbol “-” indicates unidentified amino acid residues.

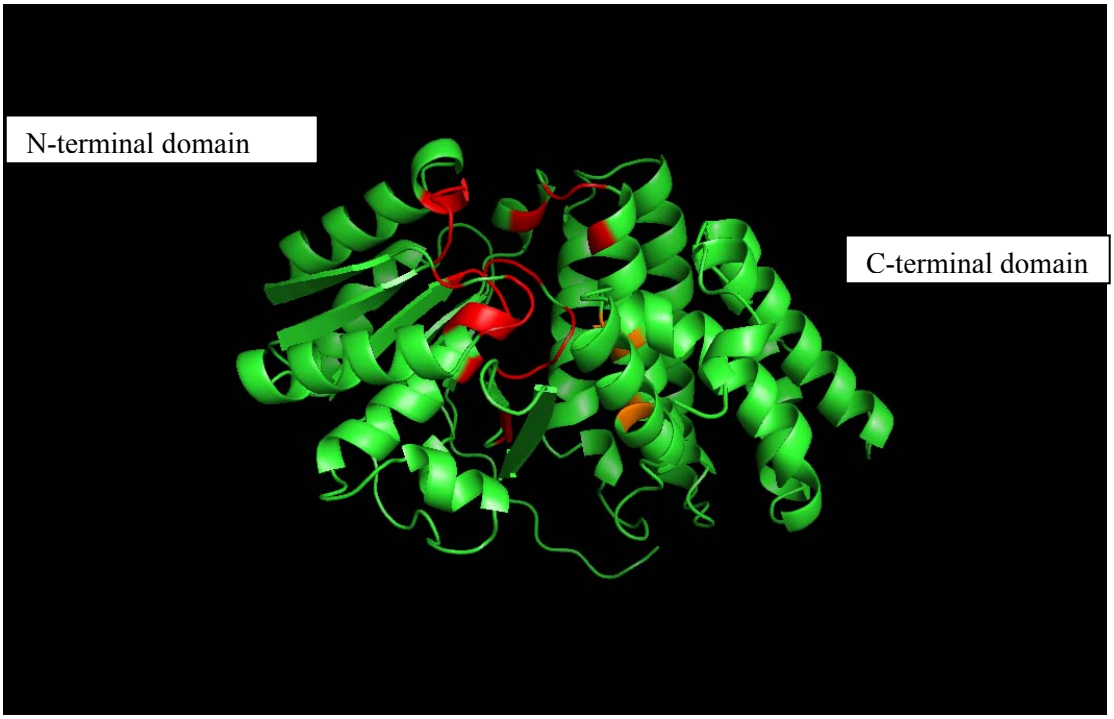

Figure 2-7 Predicted tertiary structure of *T. hypogea* ADH monomer.

The structure modeling was run on the Swiss-Model server using an iron-containing ADH in *T. maritima* (TM0820; PDB number: 1vljB) as the template. The structure figure was constructed using the software PyMOL (Delano 2002). Residues in red, the putative $NADP^+$-binding site; residues in orange, the putative iron-binding site.

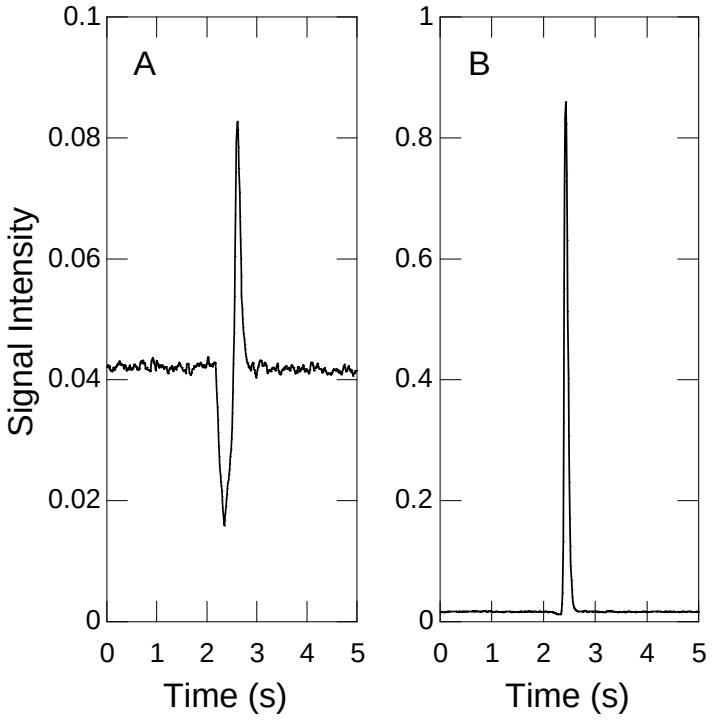

Fig. 2-8A

Fig. 2-8B

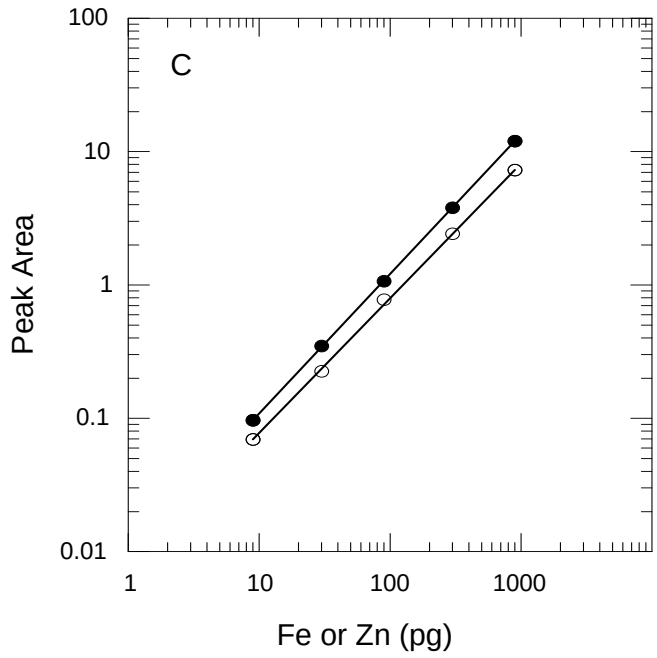

Fig. 2-8C

Figure 2-8 Determination of Fe and Zn in the ADH purified from *T. hypogea* using ITV-CP-AES.

A, representative Fe signal detected at 259.940 nm; B, representative Zn signal detected at 213.856 nm; C, standard curves for the determination of Fe (open circles) and Zn (filled circles) using the ITV-ICP-AES system.

trace amount of Zn detected may come from the non-specific binding.

The activity of the purified ADH increased along with the rise of assay temperature up to 95°C (**Fig. 2-9**). However, the enzyme activities were not measured at temperatures above 95°C because of the instability of NADPH at such high temperatures (Robb et al. 1992). An Arrhenius plot showed no obvious transition point between 30 and 95°C. Thermostability of *T. hypogea* ADH was determined by monitoring its temperature-dependent change of enzyme activity. The time required for a 50% loss of activity ($t_{1/2}$) in the presence of dithiothreitol was approximately 10 and 2 h at 70 and 90°C, respectively (**Fig. 2-10**). There was a decrease in $t_{1/2}$ values in the absence of dithiothreitol ($t_{1/2}$ = 6 h at 70°C and $t_{1/2}$ = 1 h at 90°C).

2.4.3 Catalytical properties of the purified *T. hypogea* ADH

The optimal pH for alcohol oxidation was determined to be 11, while that of the aldehyde reduction was about 8 (**Fig. 2-11**), which is similar to the common feature of pH preference of many ADHs (Antoine et al. 1999; Guagliardi et al. 1996; Hirakawa et al. 2004; Ma et al. 1994; Rella et al. 1987; van der Oost et al. 2001). It showed that the aldehyde reduction activity was about 17 times higher than that of the alcohol oxidation at pH 8.0, indicating that this enzyme is more efficient for catalyzing the aldehyde reduction in the cell where approximately neutral pH is maintained.

T. hypogea ADH was able to transform a broad range of primary alcohols and diols, but secondary alcohols such as 2-propanol, 2-butanol and polyols such as glycerol were not oxidized, and acetone was not reduced (**Table 2-5**). Therefore, this enzyme can be classified as a primary ADH. The purified *T. hypogea* ADH was NADP(H) specific, a characteristic of iron-containing ADHs in other hyperthermophiles (Radianingtyas and Wright 2003). The apparent *K*m value for NADPH was more than three times lower than that of the $NADP^+$ (**Table 2-6**). Furthermore, the apparent *K*m values for ethanol and 1-butanol were approximately three to four times higher than those for acetaldehyde and

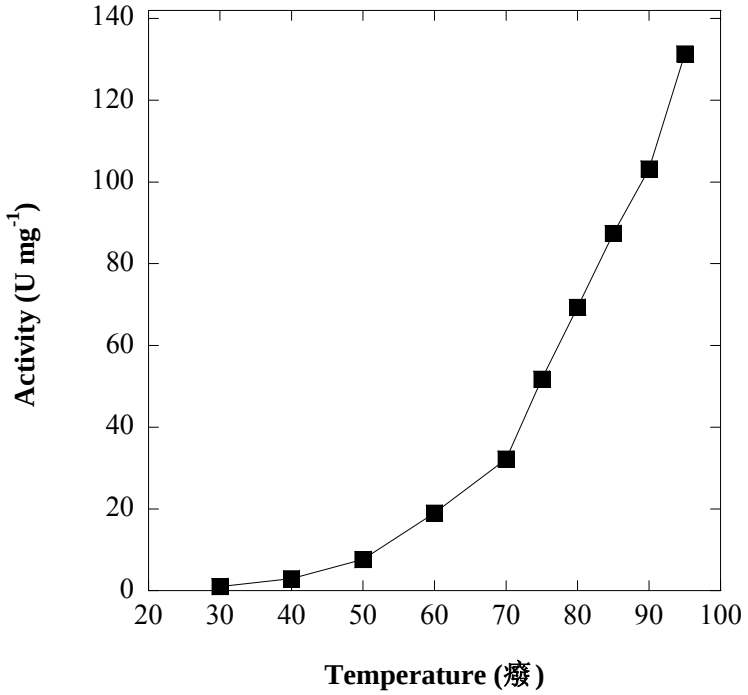

Figure 2-9 Temperature dependence of the purified ADH from *T. hypogea*.

The assay was performed in the standard assay conditions except varying assay temperatures from 30 to 95°C.

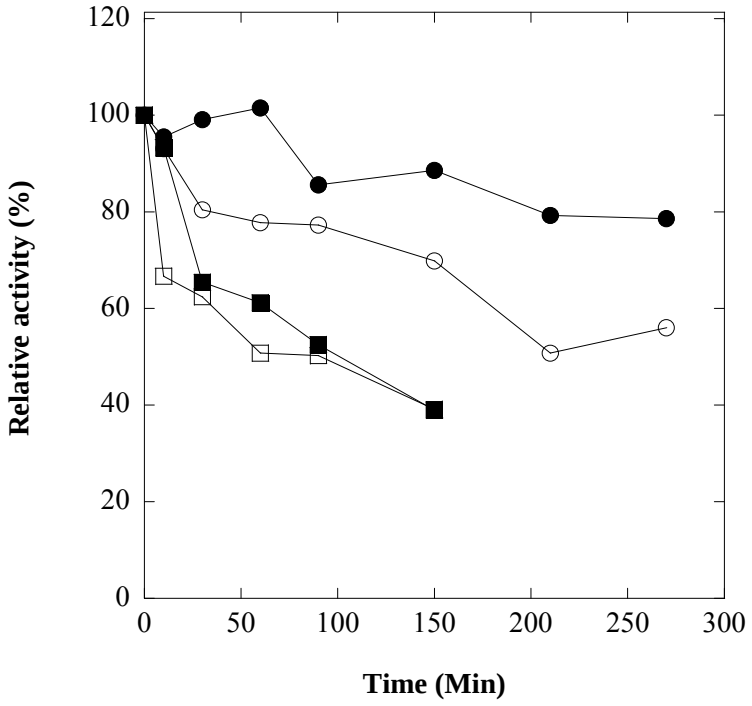

Figure 2-10 Thermostability of the purified ADH from *T. hypogea*.

The enzyme activity was determined by following 1-butanol oxidation in the CAPS buffer (pH 11.0) at 80°C, unless stated otherwise. Filled circles, in the presence of 2 mM DTT at 70°C; open circles, in the absence of DTT at 70°C; filled squares, in the presence of 2 mM DTT at 90°C; open squares, in the absence of DTT at 90°C.

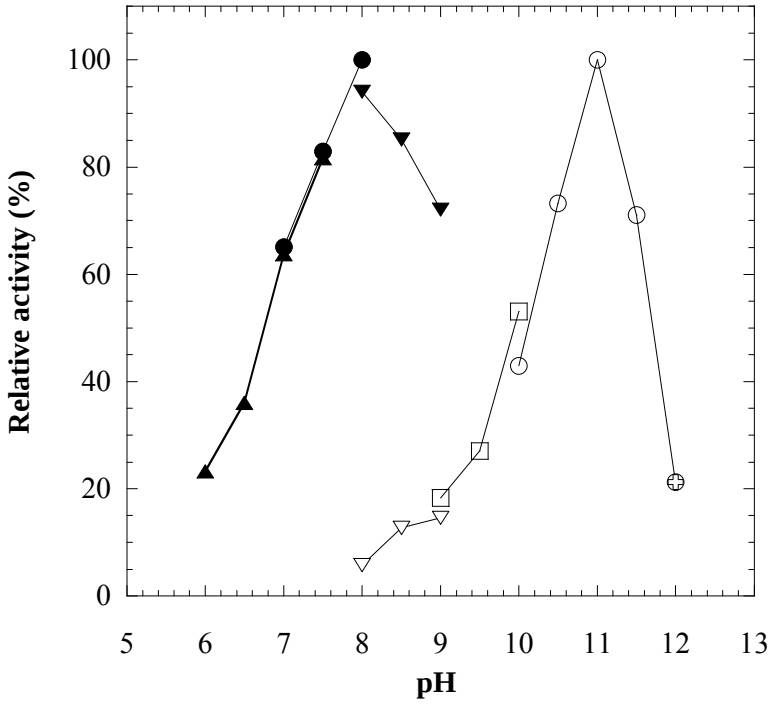

Figure 2-11 pH dependence of *T. hypogea* ADH on the alcohol oxidation and aldehyde reduction.

Filled symbols represent the reduction of butyraldehyde; open symbols represent the oxidation of 1-butanol. Buffers used (100 mM) were PIPES (pH 6.0, 6.5, 7.0 and 7.5; filled triangle), HEPES (pH 7.0, 7.5 and 8.0; filled circle), Tris/HCl (pH 8.0, 8.5 and 9.0; both filled and open inverted triangle), glycine (pH 9.0, 9.5 and 10.0; open square), CAPS (pH 10.0, 10.5, 11.0 and 11.5; open circle), and phosphate (pH 12.0; open plus mark). The relative activity of 100% equals to 69 and 71 U mg^{-1} for the oxidation of 1-butanol and the reduction of butyraldehyde, respectively.

Table 2-5 Substrate specificity of the purified ADH from *T. hypogea*

Substrates[a]	Relative activity (%)
Alcohols	
Methanol	0
Ethanol	100 ± 3
1-Propanol	298 ± 6
1-Butanol	400 ± 47
1-Pentanol	287 ± 3
Hexyl alcohol	245 ± 3
1-Heptanol	210 ± 19
1-Octanol	190 ± 3
2-Propanol	0
2-Butanol	0
2-Phenylethanol	132 ± 10
1,3-Propanediol	63 ± 5
1,4-Butanediol	91 ± 7
1,5-Pentanediol	147 ± 4
Aldehydes or ketones	
Acetaldehyde	100 ± 6
Methylglyoxal	307 ± 7
Acetone	0
Butyraldehyde	362 ± 12

[a] The concentration of substrates used was 60 mM. The relative activity of 100% corresponds to 17.3 ± 0.5 U mg^{-1} for alcohol oxidation at pH 11.0 and 19.7 ± 1.1 U mg^{-1} for aldehyde reduction at pH 8.0, respectively.

Table 2-6 Kinetic parameters of *T. hypogea* ADH

Substrate (mM)	Co-substrate (mM)	Apparent *K*m (mM)	Apparent *V*max (U mg^{-1})	*k*cat (s^{-1})	*k*cat/*K*m ($s^{-1}M^{-1}$)
NADPH (0.007-0.092)[a]	Butyraldehyde (22)	0.006 ± 0.001	75.8 ± 2.2	52	8,500,000
Butyraldehyde (0.05-22)[a]	NADPH (0.1)	0.45 ± 0.06	73.1 ± 2.1	48	110,000
Acetaldehyde (1-42)[a]	NADPH (0.1)	3.10 ± 0.04	21.8 ± 1.5	15	5,000
NADP (0.009-0.380)[b]	Butanol (20)	0.020 ± 0.002	75.8 ± 3.1	50	2,500,000
Butanol (1-20)[b]	NADP (0.2)	1.90 ± 0.05	73.5 ± 2.6	48	27,000
Ethanol (4-120)[b]	NADP (0.2)	9.7 ± 0.1	21.5 ± 1.7	14	1,500

[a] Assays were performed at pH 8.0.

[b] Assays were performed at pH 11.0.

butyraldehyde (**Table 2-6**). The specificity constant *k*cat/*K*m for aldehyde reduction using NADPH as electron donor (8.5×10^6 s^{-1} M^{-1}) was also more than three times higher than that of alcohol oxidation using NADP as electron acceptor (2.5×10^6 s^{-1} M^{-1}). These catalytic properties suggest that the enzyme can play an important role in the reduction of aldehydes, rather than the *in vivo* oxidation of alcohols.

2.4.4 Effects of metal ions and thiol reagents on the *T. hypogea* ADH activity

It was observed that less iron and more zinc present in the purified sample correlated to lower specific activity, and the lowest iron content and the highest zinc content resulted from the aerobically prepared samples (**Table 2-7**), indicating that iron was lost more readily in the presence of oxygen and so was the activity. The enzyme activities increased when the iron content was higher in the samples up to 1 atom per subunit. In contrast, an increase in zinc content in the enzyme (up to 0.5 *g* atoms/subunit or Zn/Fe ratio >5) was at the expense of a decrease in its iron content and, hence, its activity. This suggests that the extraneous zinc can substitute iron that may be dissociated after reaction with oxygen. The decrease of iron content in the enzyme sample prepared anaerobically in the presence of 2 mM dithiothreitol and 1 mM EDTA (**Table 2-7**) suggests that iron-enzyme binding affinity is only strong enough to survive the purification procedures.

When pre-incubated with the enzyme, EDTA, $ZnCl_2$, $CuCl_2$, $CdCl_2$ and $HgCl_2$ inhibited the activity by 80-100%, but dithiothreitol, mercaptoethanol and $FeCl_2$ stimulated the activity by 10-15%, while $CaCl_2$ did not have any effect on the activity. When added to the enzyme assay mixture, $ZnCl_2$ and $ZnSO_4$ inhibited the activity completely; however, such inhibition was reduced to about 20% when dithiothreitol was also present in the assay mixture, which was similar to an inhibitory effect achieved by $ZnCl_2$ alone at a much lower concentration (0.02 mM); EDTA, $CuCl_2$ (0.02 mM) and $CdCl_2$ inhibited enzyme activity by 20–60%, and $FeCl_2$, $CoCl_2$, $NiCl_2$, $MnCl_2$ stimulated the enzyme activity by 20–40%, while dithiothreitol, mercaptoethanol, $MgCl_2$ and $CaCl_2$ showed almost no effect on the activity (**Table 2-8**). These results indicate that Fe^{2+} is a required metal ion for the

Table 2-7 Metal contents and activities of the purified ADH from *T. hypogea*

Treatment of samples	Protein concentration (mg ml^{-1})	Specific activity (U mg^{-1})[a]	Metals (g-atoms/subunit)	
			Iron	Zinc
Anaerobic	0.100 ± 0.005[b]	70.4 ± 2.1	1.02 ± 0.06	0.08 ± 0.02
	0.060 ± 0.002[c]	59.1 ± 1.9	0.60 ± 0.02	0.02 ± 0.01
	0.040 ± 0.002	53.7 ± 1.5	0.76 ± 0.03	0.11 ± 0.02
	0.045 ± 0.001	31.6 ± 0.2	0.28 ± 0.04	0.31 ± 0.11
	0.080 ± 0.003	20.3 ± 0.6	0.21 ± 0.03	0.34 ± 0.16
	0.040 ± 0.001	18.1 ± 0.5	0.12 ± 0.01	0.46 ± 0.06
Aerobic	0.057 ± 0.002	3.6 ± 0.2	0.18 ± 0.01	0.47 ± 0.09
	0.210 ± 0.005	3.1 ± 0.1	0.09 ± 0.01	0.49 ± 0.06

[a] The purified ADH had a specific activity of 68.0 ± 2.2 U mg^{-1} , which was kept in 50 mM Tris/HCl, pH 7.8, containing 2 mM dithiothreitol, 2 mM sodium dithionite and 5% (w/v) glycerol; however, the values in the table were determined from samples that were washed ten times using ultra-pure buffer without any reducing reagent (10 mM Tris/HCl, pH 7.8 unless otherwise specified) under anaerobic (in the anaerobic chamber) and aerobic (in the air) conditions, respectively.

[b] The washing buffer contained 10 mM Tris/HCl (pH 7.8) and 2 mM dithiothreitol.

[c] The enzyme sample was incubated with buffer containing 50 mM Tris/HCl (pH 7.8), 5% (w/v) glycerol, 2 mM sodium dithionite, 2 mM dithiothreitol and 1 mM EDTA at room temperature for 1 h before washing using anaerobic buffer containing 10 mM Tris/HCl (pH 7.8) and 2 mM dithiothreitol.

Table 2-8 Effects of metal ions and thio-reducing agents on *T. hypogea* ADH activity

Chemicals added the assay mixture (mM)	Relative activity (%)[a]
No	100 ± 3
DTT (2)	100 ± 3
DTT (2) + $FeCl_2$ (1)	140 ± 4
DTT (2) + $ZnCl_2$ (1)	84 ± 3
Mercaptoethanol (2)	110 ± 6
Mercaptoethanol (2) + $FeCl_2$ (1)	120 ± 5
Mercaptoethanol (2) + $ZnCl_2$ (1)	0
$FeCl_2$ (1)	140 ± 4
$ZnCl_2$ (1)	0
$ZnCl_2$ (0.02)	71 ± 5
$ZnSO_4$ (1)	0
EDTA (1)	54 ± 3
$CoCl_2$ (1)	140 ± 3
$NiCl_2$ (1)	120 ± 3
$MgCl_2$	100 ± 6
$CuCl_2$ (0.02)	32 ± 3
$MnCl_2$ (1)	120 ± 5
$CaCl_2$ (1)	95 ± 5
$CdCl_2$ (1)	84 ± 3

[a] Enzyme activities were measured when the chemicals were added in the assay mixture. 100% activity is equal to 35.0 ± 0.9 U mg^{-1}.

enzyme activity, while Zn^{2+} inhibits the catalytic activity. The effects of both thiol reagents, dithiothreitol and mercaptoethanol, could be seen only when they were incubated with the enzyme for a period of time (10-60 min) before the assay, and the Zn^{2+} inhibition could be reduced by dithiothreitol, indicating that thiol reagents may have a role in decreasing interaction of toxic metal ions such as Zn^{2+} with the enzyme.

2.4.5 Oxygen sensitivity and recoverability of the oxygen-inactivated *T. hypogea* ADH

The purified enzyme lost about 80% of its activity within the first 0.5 and 3 h of exposure to air in the absence and presence of dithiothreitol and sodium dithionite, respectively (**Fig. 2-12**). This suggests that the enzyme is very oxygen sensitive and that the reducing agents can slow down such oxidation processes. The lost activity of oxygen-inactivated *T. hypogea* ADH could not be recovered merely by removing oxygen from the environment. But, the lost activity was partially recovered by adding either dithiothreitol or Fe^{2+} and fully recovered by adding both dithiothreitol and Fe^{2+} under anaerobic conditions for about 1 h (**Fig. 2-13**). Addition of sodium dithionite did not result in any recovery of the lost enzyme activity. This may further indicate that Fe^{2+} is the required metal ion for the catalytic activity and dithiothreitol may help complete a full binding of Fe^{2+} by not only providing the reducing equivalents that are required, but also decreasing the possible inhibitory effect of other metal ions such as Zn^{2+}.

The recoverability and rate of recovery of the oxygen-inactivated enzyme were dependent on the duration of enzyme exposure to air (**Fig. 2-14**). The lost activity of the enzyme exposed to air for 0.5 and 5 h could be recovered within 20 and 120 min, respectively. It appeared that the shorter the time of exposure to air, the faster the rate of recovery. However, only 50% of the lost activity of the enzyme exposed to air for 24 h could be recovered, even with an extended incubation time to 5 h. It was also observed that the recovery rate for the 66 h exposure to air at 4°C was faster than that of the 24 h exposure to air at room temperature, which might be caused by the slow oxidation of ferrous iron at

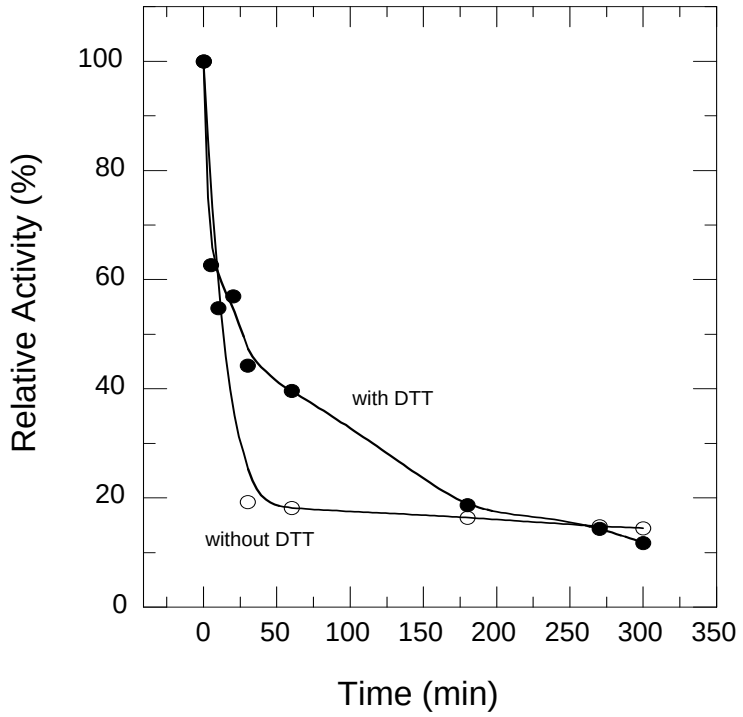

Figure 2-12 Oxygen sensitivity of the purified ADH from *T. hypogea.*

Filled circles, in the presence of 2 mM DTT and 2 mM SDT; open circles, in the absence of 2 mM DTT and 2 mM SDT. The relative activity of 100% equals to the ADH activity prior to exposure to air (58 U mg^{-1}).

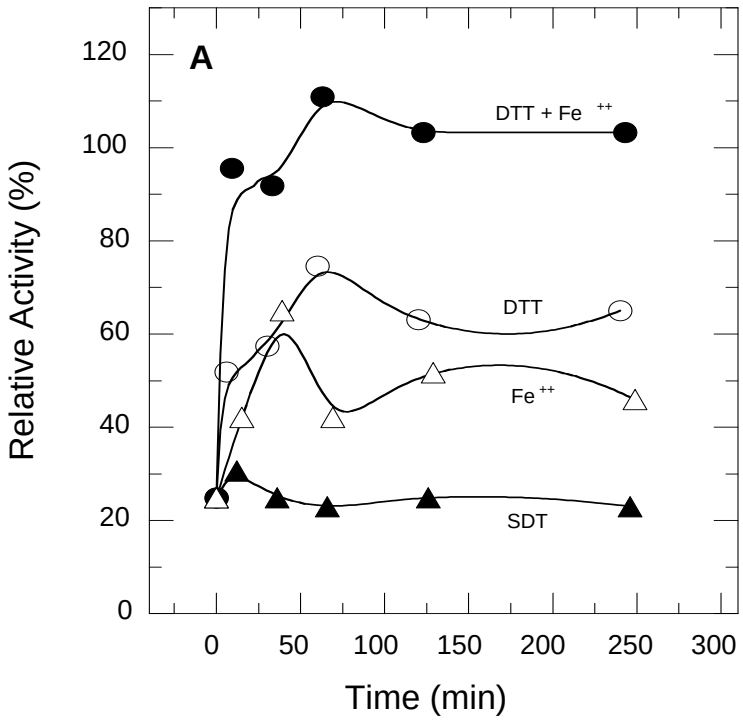

Figure 2-13 Reactivation of *T. hypogea* ADH inactivated by exposure to air.

Activity recovery of inactivated ADH (exposure to air for one half hour) by incubation with different reagents: combination of 1 mM DTT and 0.1 mM Fe^{2+} (filled circles), 1 mM DTT (open circles), 0.1 mM Fe^{2+} (open triangles), 1 mM SDT (filled triangles). The relative activity of 100% equals to the ADH activity prior to exposure to air (58 U mg^{-1}).

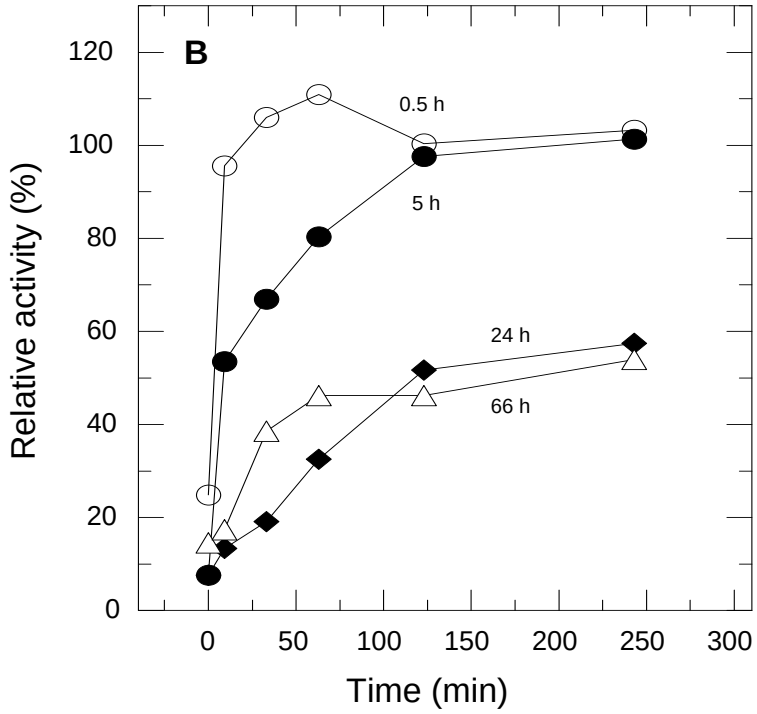

Figure 2-14 Reactivation of *T. hypogea* ADH inactivated by various exposures to air.

The activity recovery of samples that were exposed to air for different periods of time at room temperature unless specified. Inactivation time by exposure to air: 0.5 hour (open circles), 5 hours (filled circles), 24 hours (filled diamonds), and 66 hours at 4°C (open triangles). All samples were incubated with 1 mM DTT and 0.1 mM Fe^{2+} under anaerobic conditions for their activation.

low temperatures. Obviously, the precise mechanism of oxygen inactivation and reactivation is not known, which warrants further investigation.

2.5 DISCUSSION

ADHs are present in all three domains of life, and they can be classified into three groups based on their molecular properties and metal content (Reid and Fewson 1994). Group I contains long-chain ADHs whose size varies from approximately 350 to 900 amino acid residues and zinc is at their catalytic site and, sometimes, the enzyme also has structural zinc (Littlechild et al. 2004). Group II contains short-chain ADHs with approximately 250 amino acid residues and lacks metals (Reid and Fewson 1994). Group III consists only of a small number of iron-dependent ADHs including examples of mesophilic iron-activated ADH2 from *Zymomonas mobilis* (Scopes 1983) and hyperthermophilic iron-containing ADH from *Thermococcus* strain ES-1 (Ma et al. 1995). All groups of ADHs are found to be present in hyperthermophiles (Radianingtyas and Wright, 2003). Apparently, group III has a dominant number of iron-containing ADHs in hyperthermophilic archaea (**Table 2-9**). *T. hypogea* ADH represents the first hyperthermophilic bacterial ADH that contains iron with full activity after purification, whose catalytic properties show similarities to the enzyme in archaea (Ma et al. 1995). The bacterial *T. hypogea* ADH is one of the most thermostable iron-containing ADHs known (**Table 2-9**). The homologues of *T. hypogea* ADH seem abundant in bacteria but not archaea (**Fig. 2-15**). The partial sequence (358 aa) of *T. hypogea* ADH has high similarity to those within *Thermotoga* species, moderately high similarty to those in other bacterial thermophiles, and extremely low similarity to ADHs from archaeal hyperthermophiles, an indication of the divergence of iron-containing ADHs from hyper/thermophiles. The sequencing of the entire encoding gene is in progress in our lab, which will yield valuable insights on understanding the evolutionary relationship between the bacterial iron-containing ADH and the archaeal ADHs.

The inhibition of *T. hypogea* ADH activity by zinc is similar to a sulfur-regulated iron-containing ADH in *Thermococcus* strain ES-1 and iron-activated ADH II from *Z. mobilis*

Table 2-9 Comparison of iron-containing ADHs from hyperthermophilic microorganisms

Properties	*T. hypogea*	*T. hydrothermalis*	*Thermococcus* strain ES-1	*T. litoralis*	*P. furiosus*
Subunit (Structure, kDa)	40 (α_2)	45 (α_4 or α_2)	46 (α_4)	48 (α_4)	48 (α_6)
Metal (g-atoms/subunit)	Fe (1.0)	Fe (0.5)	Fe (0.95)	Fe (0.45)	Fe (0.9), Zn (0.8)
Co-enzyme	NADPH	NADPH	NADPH	NADPH	NADPH
App. *K*m (alcohol, mM)	1.9 (1-butanol) 9.7 (Ethanol)	2.0 (Benzylalcohol)	8.0 (Ethanol)	11.0 (Ethanol)	29.4 (Ethanol)
App. *K*m (aldehyde, mM)	0.45 (Butyraldehyde) 3.1 (acetyraldehyde)	0.01 (Benzaldehyde)	0.25 (acetaldehyde)	0.4 (Acetaldehyde)	0.17 (Acetaldehyde)
App. *k*cat (s^{-1})	48 (Butanol) 14 (ethanol) 48 (Butyraldehyde) 15 (Acetaldehyde)	23 (Benzyladcohol) 2.1 (Benzaldehyde)	48 (Ethanol) 19 (Acetaldehyde)	26 (Ethanol)	19 (Ethanol) 5.5 (Acetaldehyde)
App. *K*cat/App. *K*m ($s^{-1}M^{-1}$)	2.7×10^4 (1-butanol) 1.1×10^5 (butyraldehyde) 1.5×10^3 (Ethanol) 5.0×10^3 (Acetaldehyde)	1.2×10^4 (Benzyl alcohol) 2.1×10^5 (Benzyaldehyde)	6.0×10^3 (Ethanol) 7.6×10^4 (Acetaldehyde)	2.3×10^3 (Ethanol) 1.1×10^5 (Acetaldehyde)	6.5×10^2 (Ethanol) 3.2×10^4 (Acetaldehyde)
Optimal pH (alcohol oxidation)	11.0	10.5	8.8-10.4	8.8	9.4-10.2
Optimal pH (aldehyde reduction)	8.0	7.5	ND	ND	ND

Optimal temperature	>95°C	80°C	>95°C	85°C	>95°C
Stability ($t_{1/2}$, h)	10 (70°C) 2 (90°C)	0.25 (80°C)	35 (85°C), 4 (95°C)	5 (85°C) 0.3 (96°C)	160 (85°C) 7 (95°C)
Reference(s)	This work	Antoine et al. 1999	Ma et al. 1995	Ma et al. 1994	Ma and Adams 1999

A recombinant 1, 3-propanediol dehydrogenase in *T. maritima* was reported to contain iron by X-ray crystallography analyses, but no further catalytical properties are available (Schwarzenbacher et al. 2004)

ND, not determined

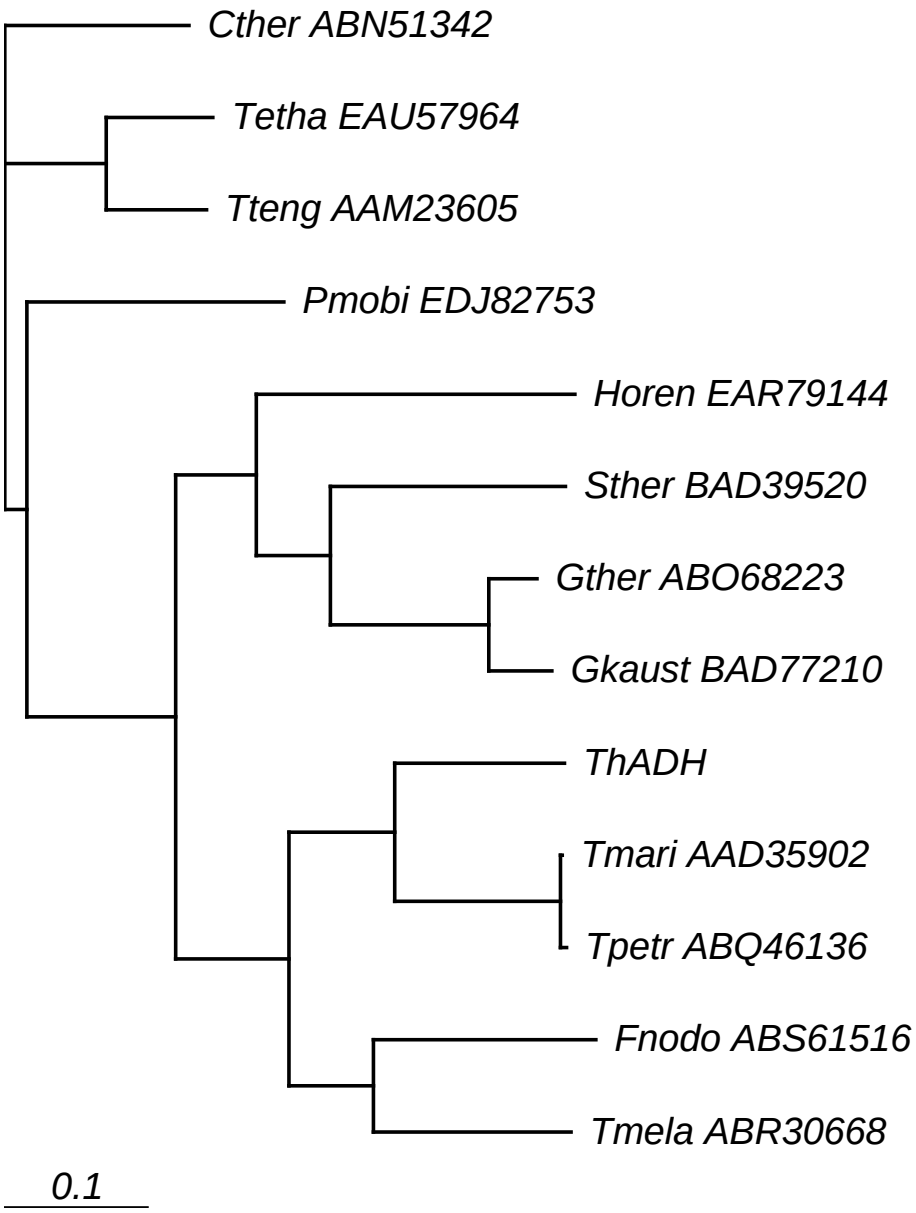
Cther ABN51342
Tetha EAU57964
Tteng AAM23605
Pmobi EDJ82753
Horen EAR79144
Sther BAD39520
Gther ABO68223
Gkaust BAD77210
ThADH
Tmari AAD35902
Tpetr ABQ46136
Fnodo ABS61516
Tmela ABR30668
0.1

Figure 2-15 Phylogenetic relationships between *T. hypogea* ADH and related iron-containing ADHs from bacterial hyperthermophiles or thermophiles.

The sequences were aligned using Clustal W and a subsequent phylogenetic tree was constructed (Thompson et al. 1994). The accession numbers for the genes encoding ADHs used in the analyses are indicated on the figure. Scale bar indicates 0.1 substitutions per sequence position. The sequences equivalent to 358 aa ThADH were used for the alignment. Abbreviations used: Tetha, *Thermoanaerobacter ethanolicus* X514; Tteng, *Thermoanaerobacter tengcongensis* MB4; Cther, *Clostridium thermocellum* ATCC 27405; Pmobi, *Petrotoga mobilis* SJ95; Gther, *Geobacillus thermodenitrificans* NG80-2; Gkaust, *Geobacillus kaustophilus* HTA426; Sther, *Symbiobacterium thermophilum* IAM 14863; Horen, *Halothermothrix orenii* H 168; Tmari, *Thermotoga maritima*; Tpetr, *Thermotoga petrophila*; ThADH, ADH from *T. hypogea*; Fnodo, *Fervidobacterium nodosum* Rt17-B1; Tmela, *Thermosipho melanesiensis* BI429.

(Ma et al. 1995). It was noted that zinc replaced iron at the metal-binding site but abolish the activity in *Z. mobilis* ADH II (Tamarit et al. 1997). Moreover, glycerol dehydrogenase-type ADHs from thermophile *Bacillus stearothermophilus* and mesophile *E. coli*, show a strict dependence on zinc for activitiy but their crystal structures are highly silimilar to those of iron-containing ADH family, suggesting that zinc might occupy on the metal-binding site. But, the mechanism of zinc inhibition in hyperthermophilic enzymes is not yet understood. It seems that iron in the bacterial *T. hypogea* enzyme is more easily lost in the absence of reducing reagent dithiothreitol, and iron substitution by zinc is also high under aerobic conditions (**Table 2-7**). It is plausible to speculate that the loss of activity could be partially attributed to oxidation of Fe^{2+} to Fe^{3+} in the absence of the reducing agents, and Fe^{3+} may have less affinity to the iron-binding site of the enzyme, so that zinc may substitute the Fe^{3+} at a greater rate under aerobic conditions.

The iron-containing enzyme can be reactivated by incubation with ferrous iron, for example, fumarase in *Bacteroides thetaiotaomicron* was restored to its full activity by ferrous ion and aconitase in the same organism was recovered by the treatment of iron and dithiothreitol (Pan and Imlay 2001). Both enzymes contain iron-sulfur clusters, which are vulnerable to oxygen stress. It is unlikely that the purified *T. hypogea* enzyme contains any iron-sulfur cluster because of the low content of iron present in the enzyme (1.02×0.06 *g*-atoms/subunit). Different from fumarase in *B. thetaiotaomicron*, the activity of oxygen-inactivated *T. hypogea* ADH was partly restored by the incubation with ferrous ion alone. It was also suggested that dithiothreitol was required for restoring the full activity (Scopes 1983), implying that thio groups might be important for maintaining the correct conformation of iron binding.

When various cations were tested by adding in the assay mixture, the addition of Fe^{2+} increased the activity up to 40% higher than the control, implying that Fe^{2+} was easily lost at high temperatures such as 80°C and the loss was compensated by the supplement of abundant added Fe^{2+}. Co^{2+} showed identical effect on the activity of *T. hypogea*, which

seemed a promising candidate substituting iron at the active site and thus changing the oxygen viability of the enzyme. The alternative substitution to change enzyme viability was anaerobic replacement with zinc since zinc-containing ADHs are more oxygen-resistant. The inability of activity by zinc could be restored by re-introducing ferrous ion after chelating zinc with *o*-phenanthroline (Tamarit et al. 1997).

Iron-containing ADHs prefer to use NADPH as a coenzyme, which is similar to other ADHs characterized from *Pyrococcus furiosus* and *Thermococcus* spp. (**Table 2-9**), although it is contrary to the usual use of NAD(H) in catabolic pathways. These ADHs have a very broad substrate specificity to utilize a series of aliphatic primary alcohols (C_2–C_8), diols (C_3–C_5) and aromatic primary alcohol (2-phenylethanol), except for secondary alcohols. The ADHs have much lower apparent *K*m values for aldehydes. All organisms that possess such ADH produce ethanol as an end product (Kengen et al. 1994; Ma et al. 1995). This is despite the fact that *T. hypogea* ADH has a relatively high value of *k*cat/*K*m for butanol, while archaeal ones show preference for benzyl alcohol or ethanol (**Table 2-9**). It has been proposed that these ADHs are responsible for the alcohol formation using the excess of reducing equivalents generated during their growth (Ma et al. 1995), which can also be supported by the optimal pH for aldehyde reduction of 8.0 that is closer to the pH values in the cells. This is true for *T. hypogea* ADH that catalyzes the aldehyde reduction much faster than the alcohol oxidation at pH 8.0. Among the organisms that have ADHs with very high sequence similarity to *T. hypogea* ADH, *F. nodosum* (Patel et al. 1985), *T. ethanolicus* (Wiegel and Ljungdahl 1981) and *T. maritima* (Ma et al. 2005) produce ethanol. It is plausible to predict that *S. thermophilum* and *T. petrophila* can produce ethanol because they may have the same type of ADH, and *Thermotoga lettingae* may have a similar type of ADH because it produces ethanol and is a member of *Thermotoga* (Balk et al. 2002). Such speculation needs to be proved experimentally in the future.

The content of *T.hypogea* ADH was estimated to be 0.3% of proteins in the cell-free extract and its activity was relatively high. However, the level of ethanol formation in *T.*

hypogea was relatively low under tested conditions. The pathways of alcohol formation from pyruvate in bacteria are divergent: either a three-enzyme step catalyzed by pyruvate ferredoxin oxidoreductase, CoA-dependent aldehyde dehydrogenase and alcohol dehydrogenase, or a two-enzyme step driven by pyruvate decarboxylase and alcohol dehydrogenase (**Fig. 2-16**). The pyruvate: ferredoxin oxidoreducase from *T. hypogea* has been purified with a specific activity of 140 U mg^{-1} (Yang and Ma, unpublished results). However, the CoA-dependent aldehyde dehydrogenase activity was not detectable in the cell-free extract of *T. hypogea*, suggesting the possibility of the alternative metabolic step using pyruvate decarboxylase.

In addition to its principal role in alcohol production, the activity of iron-containing ADHs is found to be associated with other physiological processes. In hyperthermophiles, the production of the ADH in *Thermococcus* strain ES-1 is regulated by the concentration of elemental sulfur in the medium, and the ADH activity is much higher when S^0 concentration is as low as 1 g l^{-1} (Ma et al. 1995). The regulation of the hyperthermophilic bacterial *T. hypogea* ADH production is not known and needs to be further investigated.

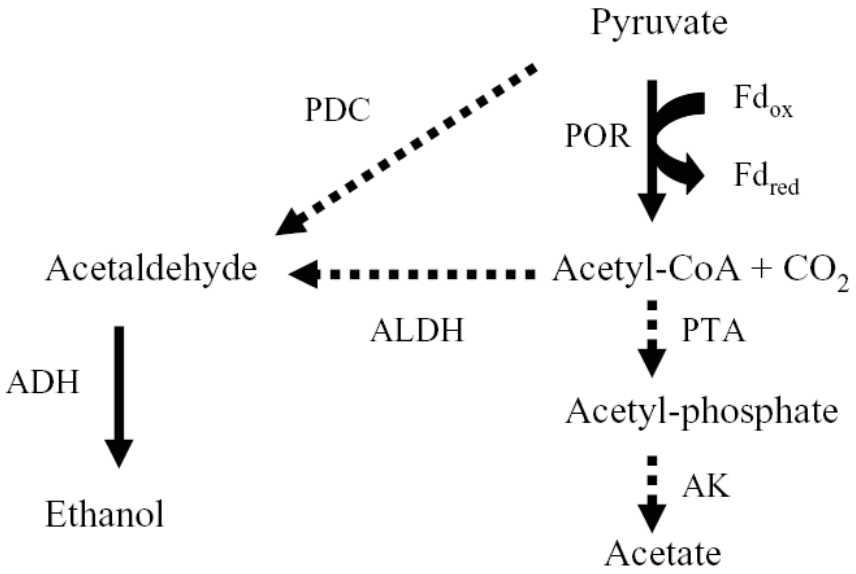

Figure 2-16 Schematic pathway of alcohol formation in *T. hypogea*.

ADH, alcohol dehydrogenase; AK, acetate kinase; ALDH, CoA-dependent aldehdye dehydrogenase; PDC, pyruvate decarboxylase; POR, pyruvate: ferredoxin oxidoreductase; PTA, phosphotransacetylase. Dashed arrows represent speculated steps.

Chapter 3 A Zinc-containing Alcohol Dehydrogenase from Anaerobic Hyperthermophilic Archaeon *Thermococcus guaymasensis*: Purification, Characterization and Gene Cloning

3.1 ABSTRACT

Thermococcus guaymasensis is a hyperthermophilic starch-degrading archaeon producing acetate, CO_2, H_2, ethanol and acetoin as end products. The cell-free extract harbored $NADP^+$-dependent primay, secondary alcohol and glycerol dehydrogenase activities. An alcohol dehydrogenase (ADH) from *T. guaymasensis* was purified to homogeneity, and the purified enzyme was a homotetramer with a subunit size of 40 ± 1 kDa. The enzyme was a primary-secondary ADH and exhibited substrate preference for secondary alcohols and corresponding ketones. The enzyme had no stereoselectivity on interconversion between 2-butanol and butanone but between 2, 3-buanediol and acetoin. The enzyme showed higher activity on (*2R*, *3R*)-(-)-2, 3-butanediol and *meso*-2, 3-butanediol than (*2S*, *3S*)-(+)-2, 3-butanediol while the reduction of racemic (*R*/*S*)-acetoin produced (*2R*, *3R*)-2, 3-butanediol and *meso*-2, 3-butanediol, respectively. The optimal pHs for the oxidation and formation of alcohols were pH 10.5 and pH 7.5, respectively. The enzyme activity increased as the temperature was elevated up to 95°C, and it was highly stable with a half-life of 24 hours at 95°C. The enzyme could retain 50% of full activity when methanol concentration was 24% (v/v) in the assay mixture. The reduction of ketones underwent high efficiency by coupling with excess isopropanol to regenerate NADPH. Thus, the enzyme could be a potent biocatalyst for asymmetric synthesis due to its high thermoactivity, thermostability, stereoselectivity, broad substrate specificity and solvent tolerance.

The purified enzyme reduced diacetyl and acetoin to 2, 3-butanediol *in vitro*. However, it catalyzed the oxidation of 2, 3-butanediol to acetoin but no further oxidation to diacetyl. Acetoin but not 2, 3-butanediol, was detected in *T. guaymasensis* cultures. The kinetic parameters of the enzyme showed slightly lower *K*m-values for ketones than corresponding alcohols but the *K*m-values and catalytic efficiency for NADPH was 40 times lower and 5 times higher respectively than those for $NADP^+$. Ethanol was also one of the end products, the formation of which was proportional to the growth of *T. guaymasensis*. In addition, the enzyme could not catalyze the oxidation of either L-

threonine or $_{L}$-serine. Thus, the physiological roles of the purified enzyme were suggested to favor the NADPH oxidation in the formation of alcohols such as ethanol or acetoin.

The gene encoding the enzyme was cloned by combining the use of conventional and inverse PCRs, the codon usage pattern of which seemed to be different from that of *E. coli*. The deduced amino acid sequence had a total of 364 amino acids with a calculated molecular mass of 39.4 kDa. The alignment of the deduced amino acid sequence showed high similarity to zinc-containing ADHs from *Thermoanaerobacter* species. There was a conserved domain that belongs to either zinc-containing ADHs or $_{L}$-threonine dehydrogenase. The enzyme contained 0.9±0.03 *g* atom zinc per subunit analyzed by inductively coupled plasma-mass spectrometry, thus belonging to the family of zinc-containing ADHs with catalytic zinc only. It was verified by motif searches that the enzyme had motifs of catalytic zinc only ($GHEX_2GX_5GX_2V$, residues 62-76) and $NADP^+$ ($GXGX_2G$, residues 183-188). The tertiary structural modeling showed two typical domains, one catalytic domain close to amino-terminal and one coenzyme-binding domain close to C-terminal end. However, the enzyme had distinct features from other zinc-containing ADHs known. The enzyme activity was almost fully inhibited in the presence of 100 μM Zn^{2+} in the assay mixture and it was sensitive to oxygen.

3.2 INTRODUCTION

Alcohol dehydrogenases are ubiquitous in three life domains and a family of oxidoreductases that catalyze the NAD(P)H-dependent interconversion between alcohols and the corresponding aldehydes or ketones (Reid and Fewson 1994). Among them, the medium chain ADHs have been studied extensively, which usually contain zinc. Zinc-containing ADHs constitute a big protein family with various enzyme activities, including alcohol dehydrogenase, polyol dehydrogenase and cinnamyl alcohol dehydrognease activities (Larroy et al. 2002). A big number of zinc-containing ADHs including those from hyperthermophiles *Pyrococcus horikoshii*, *Aeropyrum pernix* and *Sulfolobus solfarticus*, contain one catalytic zinc and one structural zinc (Esposito et al. 2002; Guy et al. 2003; Ishikawa et al. 2007). The zinc-containing ADHs from mesophile *Clostridium beijerinckii*, and thermophiles *Thermoanaerobacter brockii* and *Thermoanaerobacter ethanolicus* contain only catalytic zinc (Korkhin et al. 1998).

Hyperthermophiles are a group of microorganisms growing optimally at ≥80°C, of which anaerobic heterotrophs have attracted increasingly attention for the use of fermentation at the elevated temperatures (Karakashev et al. 2007). All members of genus *Thermococcus* are chemo-organotrophs which can grow on peptide-containing substrates (Bertoldo and Antranikian 2006; Pikuta et al. 2007). Interestingly, some of them are able to grow on carbohydrate substrates including starch and chitin as the carbon source (Bertoldo and Antranikian 2006). It is demonstrated that glycolysis from glucose to pyruvate in *Thermococcus celer* and *Thermococcus litoralis*, appears to occur *via* a modified EM pathway containing ADP-dependent hexose kinase and phosphofructokinase, and a tungsten-containing glyceraldehyde-3-phosphate: ferredoxin oxidoreductase (Selig et al. 1997). Among *Thermococcus* species, *Thermococcus* strain ES1 was firstly reported to produce ethanol under S^0-limiting conditions (Ma et al. 1995). Moreover, other ADHs have been purified and characterized, all of which are iron-containing (Antoine et al. 1999; Li and Stevenson 1997; Ma et al. 1994; Ma et al. 1995; Ronimus et al. 1997).

Besides the interest on their physiologically alcohol-forming roles, zinc-containing ADHs from hyperthermophiles are highly desired as promising catalysts in industry because of the features such as solvent tolerance, high stereoselectivity as well as thermostability. In hyperthermophilic archaea, the zinc-containing ADHs from aerobic archaea *S. solfataricus* and *A. pernix* have been extensively studied in terms of structure, catalysis, function or regulation (Ammendola et al. 1992; Chong et al. 2007; Esposito et al. 2003a; Fiorentino et al. 2003; Guy et al. 2003; Hirakawa et al. 2004; Raia et al. 2001). It is known that a zinc-containing ADH from anaerobic archaeon *Pyrococcus furiosus* underwent asymmetric ketone reduction to the corresponding chiral alcohols (Machielsen et al. 2006; Zhu et al. 2006). The crystal structure of a zinc-containing ADH from *P. horikoshii* has been resolved recently. However, no zinc-containing ADHs from *Thermococcus* species have been characterized yet.

Thermococcus guaymasensis is a hyperthermophilic starch-utilizing archaeon, producing products such as acetate, propionate, isobutyrate, isovalerate, CO_2 and H_2S if sulfur is present in growth medium (Canganella et al. 1998). Here, we report the production of ethanol and acetoin by *T. guaymasensis* during glucose fermentation and the properties of ADH from this hyperthermophile. Moreover, the purified ADH from *T. guaymasensis* is the first zinc-containing ADH characterized from *Thermococcus* species, which is thermostable, and has a broad substrate specificity and high stereoselectivity.

3.3 MATERIALS AND METHODS

3.3.1 Chemicals and organisms

All chemicals were commercially available. The restriction enzymes were obtained from Invitrogen (Carlsbad, CA, USA). (*R*)-(-)-2-butanol, (*S*)-(+)-2-butanol, (*2R, 3R*)-(-)-2,3-butanediol, (*2S, 3S*)-(+)-2, 3-butanediol and *meso*-2, 3-butanediol were purchased from Sigma-Aldrich Canada (Oakville, ON, Canada). *T. guaymasensis* DSM 11113^T was obtained from DSMZ- Deutsche Sammlung von Mikroorganismen und Zellkulturen, Braunschweig, Germany. KOD Hot Start DNA polymerase and T4 DNA ligase were purchased from Invitrogen and Stratagene (La Jolla, CA, USA), respectively. DNA ladder and restriction enzymes were purchased from Fermentas Canada Inc. (Burlington, ON, Canada). The pGEM-T easy vector (Promega, Madison, WI, USA) was used for the cloning of PCR products. *E. coli* DH5α was used for a host for cloning and grown under standard conditions following the instructions of the manufacturers.

3.3.2 Growth conditions

T. guaymasensis was cultured in the medium as described previously (Canganella et al. 1998) with modifications. The medium at pH 7.0 contained chemicals (g/l) in a small scale: KCl, 0.33; $MgCl_2$▪ $2H_2O$, 2.7; $MgSO_4$▪$7H_2O$, 3.4; NH_4Cl, 0.25; $CaCl_2$▪$2H_2O$, 0.14; K_2HPO_4, 0.14; Na_2SeO_3, 0.01 mg; $NiCl_2$▪$6H_2O$, 0.01 mg; $NaHCO_3$, 1.0; NaCl, 18; resazurin, 0.001; cysteine▪HCl▪H_2O, 0.5; Na_2S▪$9H_2O$, 0.5; bacto-yeast extract, 10; trypticase soy broth, 10; elemental sulfur, 10; dextrose, 5; HEPES, 5.2; trace mineral solution, 10 ml; vitamin solution, 10ml. The preparation of trace mineral and vitamin solutions was described as previously (Balch et al. 1979). In a large scale cultivation of Dr. Ma's lab, it was routinely cultured in a 20-l glass carboy at 88°C in which elemental sulfur and HEPES were omitted. The incubation time was about 18-20 hours. The resulting cell pellet after centrifugation was frozen in liquid nitrogen immediately and stored at -80°C until use.

3.3.3 Preparation of cell-free extract

The frozen cells (50 g) of *T. guaymasensis* were re-suspended in 450 ml of 10 mM Tris-HCl anaerobic buffer (pH 7.8) containing 2 mM dithiothreitol (DTT), 2 mM sodium dithionite (SDT) and 5% (v/v) glycerol. The suspension was incubated at 37°C for 2 h under stirring. The supernatant was collected as the cell-free extract after 30 min centrifugation at 10,000 x *g*.

3.3.4 Purification of *T. guaymasensis* ADH

All the purification steps were carried out anaerobically at room temperature. The cell-free extract of *T. guaymasensis* was loaded onto a DEAE-Sepharose column (5 × 10 cm) that was equilibrated with buffer A [50 mM Tris/HCl (pH 7.8) buffer containing 5% (v/v) glycerol, 2 mM DTT, 2 mM SDT]. *T. guaymasensis* ADH bound weakly to the column was eluted while buffer A was running at a flow rate of 3 ml min^{-1}. A linear gradient (0-0.5 M NaCl) was run further in order to concurrently purify other enzymes. Fractions containing ADH activity were then pooled and loaded onto a Hydroxyapatite column (2.6 × 15 cm) at a flow rate of 2 ml min^{-1}. The column was applied with a gradient (0-0.5 M potassium phosphate in buffer A) and ADH started to elute from the column at a concentration of 0.25 M potassium phosphate. Fractions containing enzyme activity were pooled and applied to a Phenyl-Sepharose column (2.6 × 10 cm) equilibrated with 0.8 M ammonia sulfate in buffer A. A linear gradient (0.82-0 M ammonia sulfate in buffer A) was applied at a flow rate of 2 ml min^{-1} and the ADH started to elute at a concentration of 0.4 M ammonia sulfate. Fractions containing ADH activity were desalted and concentrated by ultrafiltration using 44.5 mm YM-10 membranes (Millipore Corporation, Bedford, MA, USA). The concentrated samples were applied to a Superdex-200 gel filtration column (2.6 × 60 cm) equilibrated with buffer A containing 100 mM KCl at a flow rate of 2.5 ml min^{-1}. The purity of the fractions containing ADH activity was verified using sodium dodecyl

sulfate-polyacrylamide gel electrophoresis (SDS-PAGE) as described previously (Laemmli 1970).

3.3.5 Enzyme assay and protein determination

The catalytic activity of *T. guaymasensis* ADH was measured at 80°C by using Genesys 10UV-Vis spectrophotometer (Thermo Fisher Scientific, Waltham, MA, USA) and monitoring the substrate-dependent absorbance change of NADP(H) at 340 nm (ε_{340}=6.3 $mM^{-1}cm^{-1}$, Ziegenhorn et al. 1976). Unless otherwise specified, the enzyme assay was carried out in duplicate using the assay mixture (2 ml) for the oxidation that contained 50 mM 2-butanol and 0.4 mM $NADP^+$ in 100 mM CAPS buffer (pH 10.5). The assay mixture (2 ml) for the reduction of ketone/aldehyde contained 6 mM 2-butanone and 0.2 mM NADPH in 100 mM HEPES (pH 7.5). The purified enzyme (0.25 μg) initiated the enzyme assay. One unit of the activity is defined as 1 μmol NADPH formation or oxidation per min. The protein concentrations of all samples were determined using the Bradford method and bovine serum albumin served as the standard protein (Bradford 1976).

3.3.6 Determination of catalytic properties

The effect of pH on the enzyme activities was determined over a range of pH 5.5-11.4. The buffers at the concentration of 100 mM used included: phosphate (pH 5.5-8.0), EPPS (8.0-9.0), glycylglycine (9.0-9.7), and CAPS (9.7-11.4). The effect of the temperature on the enzyme activity was examined in the temperature range from 30 to 95°C. The assay was carried out under standard assay conditions except the reaction temperature. Enzyme thermostability was determined by incubating the enzyme in sealed serum bottles at 80°C and 95°C, respectively. Residual activity was assayed at various time intervals under the standard assay conditions. Substrate specificity was tested by transforming 50 mM alcohols including primary, secondary, diols and polyols, or 6 mM aldehydes and ketones under standard assay conditions. The effect of cations, ethylenediaminetetraacetic acid (EDTA) or DTT on enzyme activities was carried out by measuring the reduction of 2-

butanone in 100 mM HEPES buffer (pH 7.0) considering low solubility of cations at alkaline pHs. Unless specified, chemical was added at a final concentration of 1 mM into the enzyme assay mixture.

3.3.7 Kinetic measurements

Kinetic parameters were determined for the enzyme using different substrates and coenzymes ($NADP^+$ or NADPH). For determining enzyme kinetic parameters, various substrate concentrations (0 to ≥ 10 × apparent *K*m unless specified) for NADPH (0, 0.0095, 0.019, 0.075, 0.094, 0.11, 0.17 and 0.24 mM), *sec*-butanol (0, 2.9, 5.8, 11.6, 23.0, 34.2, 45.2, and 55.9 mM), $NADP^+$ (0, 0.047, 0.094, 0.14, 0.19, 0.28, 0.37, and 0.91 mM), 2-butanone (0, 0.14, 0.27, 0.41, 0.55, 0.68, 0.82, 0.95, 1.08 , 1.62, 3.1 and 5.5 mM) were used for the determination of corresponding activities at 80°C, while concentrations of the corresponding co-substrates were kept constant and higher than 10 × apparent *K*m. Apparent values of *K*m and *V*max were calculated from their Lineweaver-Burk plots.

3.3.8 Determination of amino-terminal sequence

The purified enzyme (1 μg) was separated on 12.5% SDS-PAGE and electro-blotted onto polyvinylidene difluoride (PVDF) membrane by using Mini Trans-Blot Eelectrophoretic Transfer cell (Bio-Rad Laboratories, Hercules, CA, USA). The PVDF membrane was wet in 100% methanol for 1 min right piror to use. The transferring buffer [25 mM Tris/HCl buffer containing 192 mM glycine and 15% (v/v) methanol] was pre-cooled at 4°C and one cooling unit was put inside the transfer cell to maintain the low temperature. Blotting was run for one and half hours at 110 V and 230 mA. After that, the PVDF membrane was stained for 3 min by 0.1% (w/v) Coomassie blue R-250 in 10% (v/v) methanol solution and subsequently destained by a solution containing 45% (v/v) methanol and 10% (v/v) acetic acid. After destaining, the PVDF membrane was washed with Millipore-grade water (18.2 MΩ·cm) for 2 days. The bands on the PVDF membrane were cut in a flow hood by using a surgical cutter. The samples were transferred into clean Eppendorf tubes and stored

at -20°C freezer for further analyses. The amino-terminal sequence was determined by Edman degradation (Molecular Biology Core Facility, Dana Farber Cancer Institute Boston, MA, USA).

3.3.9 Metal analyses

The metal contents of *T. guaymasensis* ADH were determined by using inductively coupled plasma mass spectrometry (VG Elemental PlasmQuad 3 ICP-MS at the Chemical Analysis Laboratory, University of Georgia, USA). The purified enzyme was pretreated to wash off non-binding metals in the anaerobic chamber where the oxygen level was kept below 1 ppm. The washing buffer used was 10 mM Tris/HCl containing 2 mM DTT (pH 7.8). The washing procedure was carried out by using the YM-10 Amicon centrifuge tubes, including 7 cycles of centrifugation (concentration and refilling of buffers). The passthrough solution was collected as its control.

3.3.10 Ketone reduction coupled with regeneration of NADPH

The reaction mixture (2 ml) contained 100 mM HEPES buffer (anaerobic, pH 7.5), 50 mM 2-butanone or 2-pentanone, 25 μg *T. guaymasensis* ADH, 500 mM isopropanol and 1 mM NADPH. The reaction was carried out at 30°C for 24 hours unless specified. The reactants (butanone/2-butanol and 2-pentanone/2-pentanol) were determined in a Shimadzu GC-14A gas chromatography (GC) equipped with a flame ionization detector (FID, 250°C) and an integrator Shimadzu CR601 (Shimadzu Corporation, Kyoto, Japan). The GC analyses were performed under the following conditions: column, MXT-624 (0.53 mm ID×30 m length, Restek, Bellefonte, PA, USA); FID sensitivity range, 10^2; Carrier gas, helium at a linear velocity of 80 cm s^{-1}. For the 2-pentenone/2-pentanol determination, the following temperature program was used: isotherm at 60°C for 3 min, 30°C/min ramp to 110°C, and isotherm at 110°C for 2 min. For the 2-butanone/2-butanol determination, the following temperature program was used: isotherm at 40°C for 3 min, 30°C/min ramp to 100°C, and isotherm at 100°C for 2 min. The reaction mixture (1 μl) was directly applied onto the

injector (200°C) for GC analyses. The peak areas were quantitated by using specific external standards.

3.3.11 GC analyses of fermentation products

The possible fermentation products such as ethanol, acetoin and 2, 3-butanediol, were measured by using the above-mentioned GC systems with modifications. The temperature program was modified at the FID sensitivity range of 10: isotherm at 80°C for 3 min, 10°C /min ramp to 150°C, and isotherm at 150°C. The peak areas were quantitated by using specific external standards. Prior to the analyses, the culture medium was centrifuged at 10,000 × *g* for 5 min and the supernatant was filtered to remove the residual cells by using nylon syring filters (National Scientific Company, Rockwood, TN, USA).

3.3.12 Stereoselective conversion between acetoin and 2, 3-butanediol

The reaction mixture (2 ml) of 2, 3-butanediol oxidation contained 100 mM CAPS buffer (anaerobic, pH 10.5), 50 mM (*2R*, *3R*)-(-)-2, 3-butanediol or *meso*-2, 3-butanediol, 25 μg *T. guaymasensis* ADH, 500 mM acetone and 1 mM $NADP^+$. The reaction mixture (2 ml) of acetoin reduction contained 100 mM HEPES buffer (anaerobic, pH 7.5), 50 mM racemic *R*/*S*-acetoin, 25 μg *T. guaymasensis* ADH, 500 mM isopropanol and 1 mM NADPH. All the reactions were carried out at 30°C for 24 hours unless specified. After that, the reaction mixture (1 ml) was extracted with 1 ml ethyl acetate or dichloride methane with shaking on a Gyrotory water bath shaker model G76 (New Brunswick Scientific Co., INC., NJ, USA) at 350 rpm for 30 min (room temperature). The stereoselectivity of the purified enzyme was determined by the Shimadzu GC-14A gas chromatography equipped with a CP-Chirasil-Dex CB column (0.25 mm ID × 25 m length, Varian Inc., Palo Alto, CA, USA). The following GC operating conditions included the FID detector (250°C) at a sensitivity range of 10 and helium as the carrier gas at a linear velocity of 40 cm s^{-1}. The temperature program for *R*/*S*-acetoin, (*2R*, *3R*)-(-)-2, 3-butanediol, (*2S*, *3S*)-(+)-2, 3-butanediol and *meso*-2, 3-butanediol was listed as the following: isotherm at 60°C for 5

min, 30°C/min ramp to 90°C, isotherm at 90°C for 6 min. The reaction mixture after extraction (0.5 µl) was directly applied onto the injector (200°C) for each assay. The peak areas were quantitated by using specific external standards. In order to identify if *T. guaymasensis* ADH catalyzed asymmetric reduction of 2-butanone to chiral 2-butanols, *R*-2-butanol or *S*-2-butanol formation was verified by using GC operating conditions described in this section except that the temperature program was set isothermally at 45°C for 10 min.

3.3.13 Mass spectrometry for identification of the internal sequences of *T. guaymasensis* ADH

The purified enzyme was separated in 12.5% SDS-PAGE and subjected to in-gel trypsin digestion. The resulting peptides were extracted and cleaned with the procedures described previously (Shevchenko et al. 1996). The resulting samples were applied for mass spectrometry analyses on a Waters Micromass Q-TOF Ultima using nano-spray injection as the sample delivery method (Mass Spectrometry Facility, University of Waterloo, Waterloo, ON, Canada). The PEAKS software (BSI, Waterloo, ON, Canada) was used for MS/MS profiling.

3.3.14 Gene cloning of *T. guaymasensis* ADH

The genomic DNA used as the template of PCR was extracted using the solution of phenol, chloroform and isoamyl alcohol (25: 24: 1). DNA concentrations of samples were quantified using NanoDrop Spectrophotometer (NanoDrop Technologies, Wilmington, DE, USA). On the basis of amino-terminal and internal sequences, two oligonucleotides TGADHNF and TGADHIR (**Table 3-1**) were synthesized and used as forward and reverse PCR primers, respectively. A PCR was performed using a thermal cycler TC-312 (Techne incorporated, NJ, USA) with 15 pmol of each primer against 100 ng of genomic DNA isolated from *T. guaymasensis* cells. Unless otherwise stated, PCR was performed using Hot Start KOD polymerase according to the standard conditions

Table 3-1 Primers designed for sequencing the gene encoding *T. guaymasensis* ADH

Name	Primers[a] (5'-3')
TGADHNF	AARATGMGNGGTTTTGCAATG
TGADHIR	GGAGTGCTGGTGATATCC
TGMAYN01	TCTCCTTCTCAATCCACTCG
TGMAYC02	GCAATAACTCCCGACTGG
TGMAY28C01	TGCCGAAGTAGTTGATGTTG
TGMAY28C02	GAGGTCAAGCAGGCGNTC
TGJL1N1	ATGTCNAAGGATGCGCGGT
TGJL1N2	ATGAGYAAGGATGCGCGGT

[a] Pirmer properties like melting temperature (Tm), G+C content (mol% G+C), primer loops and primer dimmers were evaluated by a DNA analysis tool Gene Runner (Hastings Research, Inc., Las Vegas, USA).

recommended by the suppliers. The thermal program consisted of 40 cycles of denaturation at 95°C for 20 seconds, annealing at 56°C for 20 seconds, and extension at 70°C for 30 seconds. The generated DNA fragment was modified using the procedure of addition of 3'-A overhangs (A-tailing) and ligated into the pGEM-T easy vector (Kobs 1997). *E. coli* DH5α was transformed with this construct. After the blue/white screening, the recombinant plasmid was extracted, purified (Sambrook et al. 1989) and sent for sequencing (Core Molecular Biology and DNA Sequencing Facility, York University, ON, Canada). The inverse PCR was design for obtaining the flanking sequences by using two primers: TGMAYN01 and TGMAY28C02 (**Table 3-1**). The genomic DNA was digested by the restriction enzyme *Hind* III for 6 hours at 37°C. After that, the sample was incubated at 65°C for half an hour to denature the enzyme *Hind* III. Then, the digested product was ligated to circle DNA by using T4 DNA ligase overnight at room temperature, which was used as the template in inverse PCRs (Triglia et al. 1988). After preheating to 94°C for 5 min, 36 cycles were performed, consisting of denaturation at 95°C for 20 seconds, primer annealing at 58°C for 20 seconds, and elongation at 70°C for 1 min. The resulting 1.4 kb product of inverse PCRs was sequenced by the dye-termination method using several primers designed on raw sequence information (Molecular Biology Core Facility, University of Waterloo, ON, Canada). The nucleotide sequences were analyzed with the program GeneRunner and its deduced amino acid sequence was compared to the GenBank Data Base by BLASTP (Altschul et al. 1997).

3.3.15 Data mining

The homologues of *T. guaymasensis* ADH were identified by performing BLASTP searches (Altschul et al. 1997). Conserved domains were analyzed with CD-search and Motif Search (Kanehisa et al. 2002). Phylogenetic analyses were performed by aligning *T. guaymasensis* ADH and close homologues of zinc-containing families using the program Clustal W (Thompson et al. 1994). The codon usage of the enzyme was calculated using the program Sequence Manipulation Suite (Stothard, 2002; http://www.bioinformatics.org/sms2/about.html). The primary structure analyses including

the amino acid composition, theoretical molecular weight and isoelectric point (pI) was estimated using the program ProtParam on the ExPASy server (Gasteiger et al. 2005). The secondary and tertiary structure prediction was performed using the SWISS-MODEL server (Guex and Peitsch 1997; Kopp and Schwede 2004; Peitsch 1995; Schwede et al. 2003). The software PyMOL was used to analyze and visualize the tertiary structure of *T. guaymasensis* ADH monomer (Delano 2002).

3.4 RESULTS

3.4.1 Growth and alcohol formation of *T. guaymasensis*

T. guaymasensis is a heterotrophic archaeon and could grow in the absence of sulfur during glucose fermentation while the supplement of elemental sulfur (greater than 0.5% w/v) almost resulted in doubling the cell density after 10 hours incubation at 88°C. Ethanol as one of end products was found in the tested culture, and its production appeared to correlate with the growth (**Fig. 3-1**). Whether *T. guaymasensis* was cultured in the presence of 20 mM HEPES buffer and 0.5% sulfur or not, the final pH of the media after 48 hours growth was around 6.0. Acetoin was detected as a metabolite in the spent medium with a relatively higher level (2-3 mM), which was a possible response to environmental changes, such as oxygen concentration, low pH, or pyruvate excess in different bacteria (Collins 1972; McFall and Montville 1989; Starrenburg and Hugenholtz 1991). The acetoin formation of *T. guaymasensis* was detectable after 2 hours in incubation and accumulated as the cell density increased under all tested conditions (**Fig. 3-2**), implying that its production might not be as a response to the pH change. 2, 3-butanediol could not be detected in the fermentation culture yet, which warrants further investigations.

3.4.2 ADH activities in the cell-free extract of *T. guaymasensis*

The production of ethanol and acetoin indicated that *T. guaymasensis* might harbor multiple ADHs or one dominant ADH with multifunctions. The cell-free extract was prepared to investigate the ADH activities. Alcohols such as glycerol, 1-butanol, 2-butanol, 2, 3-butanediol and 1, 4-butanediol, were used to differentiate the possible types of ADHs such as polyol, primary-alcohol, secondary-alcohol, diol dehydrogenase activies. The results (**Table 3-2**) showed that all ADH activities in the cell-free extract of *T. guaymasensis* were $NADP^+$-dependent. The types of ADH activities were diverse and the activities were detectable over all the alcohols mentioned above. The highest ADH

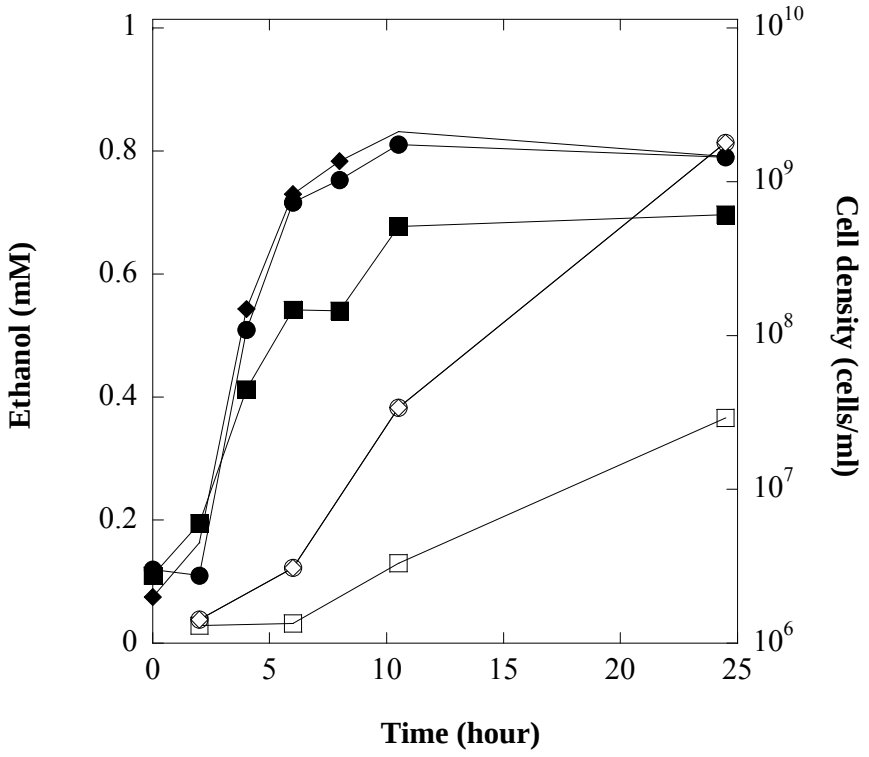

Figure 3-1 Growth and ethanol production of *T. guaymasensis*.

T. guaymasensis was cultured under different sulfur concentrations: 0% (squares), 0.5% (circles) and 2% sulfur (diamonds). The cell density (filled symbols) and ethanol production (open symbols) were determined using direct cell counting and gas chromatography, respectively.

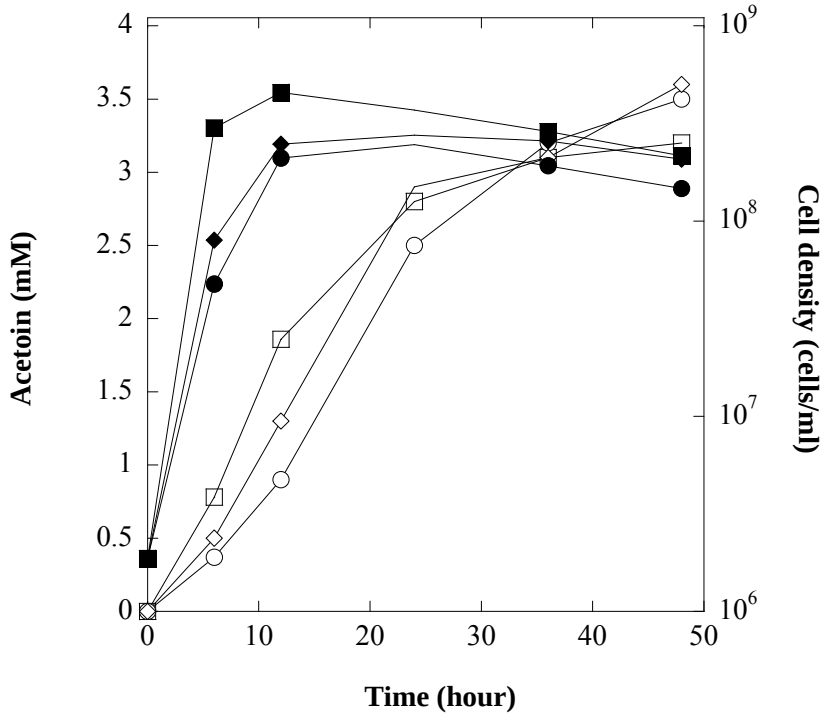

Figure 3-2 Growth and acetoin production of *T. guaymasensis*.

T. guaymasensis was cultured under different conditions: 0.5% w/v elemental sulfur with 20 mM HEPES buffer (squares), no sulfur and no buffer (circles), and 20 mM HEPES buffer but no sulfur (diamonds). The cell density (filled symbols) and acetoin production (open symbols) were determined using direct cell counting and gas chromatography as described in Materials and Methods, respectively.

Table 3-2 ADH activities in cell-free extract of *T. guaymasensis*

Substate	Actvity using $NADP^+$ as coenzyme (U mg^{-1})
1-Butanol	1.21
2-Butanol	18.9
2, 3-Butanediol	11.3
1, 4-Butanediol	0.14
Glycerol	0.17

Activities were not detectable when NAD^+ was used as coenzyme.

activity (18.9 U mg^{-1}) showed on the 2-butanol as the substrate.

3.4.3 Purification of *T. guaymasensis* ADH

Considering the possibility of multiple ADHs in the cell-free extract, the ADH activities were traced by using 2-butanol, 1-butanol and glycerol as substrates during the purification procedure. ADH activities showed on a single peak from all liquid chromatographys and the ratio of ADH activities on 2-butanol, 1-butanol and glycerol (200: 10: 0.5-1) was almost constant till the enzyme was purified to homogeneity by a four-step procedure using fast protein liquid chromatography (FPLC). Similar to *T. hypogea* ADH, the ADH in *T. guaymasensis* was partially eluted during the loading of the sample on to the DEAE-Sepharose column, suggesting the enzyme might have higher isoelectric point (pI) value which was confirmed later by theoretical pI calculated from the deduced amino acid sequence. The enzyme could be completely eluted by using buffer A, and such property significantly facilitated the separation from other proteins in the cell-free extract. Subsequently, the ADH activity was eluted out as a predominant single peak in the following chromatographys. The purified ADH after the gel-filtration chromatography had a specific activity of 1149 U mg^{-1} with the yield of 17% (**Table 3-3**). The native molecular mass was determined using gel filtration to be 135 ± 5 kDa. The SDS-PAGE analyses of the purified enzyme yielded a single band with a molecular weight of 40 ± 1 kDa (**Fig. 3-3**). Thus, the purified ADH could be a homotetramer. The ADH content was estimated to be about 3% of proteins in the cell-free extract.

3.4.4 Catalytical and biophysical properties of the purified *T. guaymasensis* ADH

T. guaymasensis ADH was $NADP^+$-dependent and could not use NAD^+ as coenzyme. The optimal pHs of the enzyme were tested for the oxidation and formation of 2-butanol using various buffers at a concentration of 100 mM. The enzyme had an optimal pH of 10.5 for the 2-butanol oxidation and 7.5 for the 2-butanone reduction, respectively (**Fig. 3-4**). The purified enzyme from *T. guaymasensis* was thermophilic and its activity increased along

Table 3-3 Purification of ADH from *T. guaymasensis*

Purification Steps	Total protein (mg)	Total activity (U)	Specific activity (U mg^{-1})	Purification fold	Yield (%)
Cell-free extract	3718.5	1.2×10^5	33.7	1	100
DEAE-Sepharose	446.8	6.3×10^4	142	4.2	52
Hydroxyapatite	58.7	5.7×10^4	970	28.8	47
Phenyl-Sepharose	30.7	3.4×10^4	1099	32.6	28
Gel filtration	17.4	2.0×10^4	1149	34.1	17

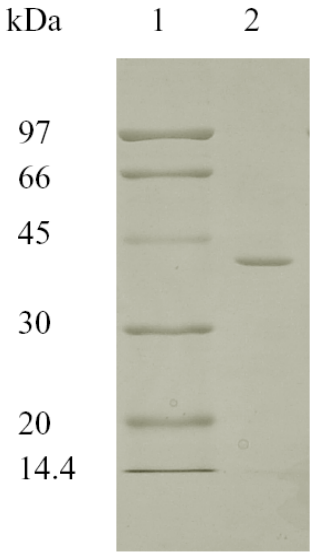

Figure 3-3 SDS-PAGE (12.5%) of the purified ADH from *T. guaymasensis.*

Lane 1, molecular markers; lane 2, 1.5 μg purified *T. guaymasensis* ADH.

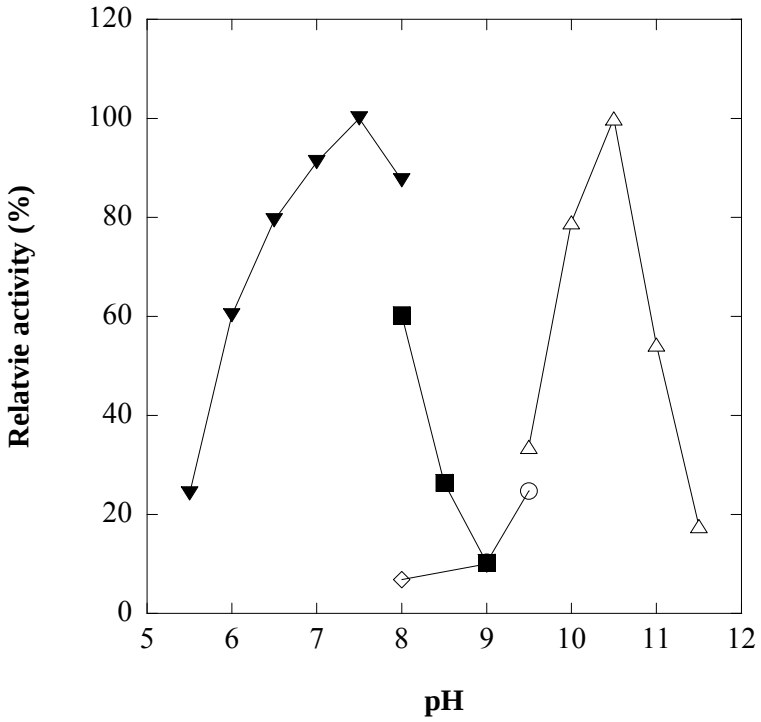

Figure 3-4 pH dependence of the purified ADH from *T. guaymasensis*.

Optimal pHs for alcohol oxidation and formation were determined by measuring the activities on the oxidation of *sec*-butanol (open symbols) and the reduction of 2-butanone (filled symbols), respectively. The buffers (100 mM) used were phosphate (inverted triangles), EPPS (squares), Tris (diamonds), glycylglycine (circles), and CAPS (vertical triangle).

with the elevated temperatures up to 95°C (**Fig. 3-5**). The oxygen sensitivity of the enzyme was monitored by the residual activity after exposure to the air at room temperature. It was unexpected that the enzyme was oxygen sensitive although it was more resistant to oxidation than that of iron-containing ADHs. The time required to decrease 50% of the full activity upon exposure to the air ($t_{1/2}$) was about 4 hours, and such inactivation was slightly decreased in the presence of 2 mM dithiothreitol (**Fig. 3-6**). The thermostability of the purified enzyme was investigated by determining its residual activities when the enzyme samples were incubated at 80 and 95°C, respectively. The $t_{1/2}$ values at 95 and 80°C were determined to be 24 and 70 hours, respectively (**Fig. 3-7**), revealing its hyperstable feature.

The substrate specificity of the purified enzyme was tested with a set of alcohols, aldehydes and ketones (**Table 3-4**). In the oxidation reactions, *T. guaymasensis* ADH was able to transform a broad range of primary alcohols but not oxidize methanol. Moreover, the purified enzyme showed higher activities using secondary alcohols such as 2-butanol and 2-pentanol as substrates, suggesting that the enzyme is a primary-secondary ADH. The enzyme could oxidize diols but not primary diols such as ethanediol, 1, 4-butanediol and 1, 5- pentanediol as tested. The enzyme exhibited very low activity towards polyols such as glycerol and had no activity on $_{L}$-serine and $_{L}$-threonine. In the reduction reactions, the enzyme exhibited the ability of reducing various aldehydes and ketones. In particular, the purified enzyme from *T. guaymasensis* could not oxidize acetoin to diacetyl, indicating the reduction of diacetyl to acetoin is irreversible.

The apparent *K*m value for the coenzyme NADPH was more than forty times lower than that for the coenzyme $NADP^+$ (**Table 3-5**). The specificity constant *k*cat/*K*m for NADPH as election donor in the ketone reduction (14,363,000 $s^{-1}M^{-1}$) was 4-5 times higher than that of $NADP^+$ electron acceptor in the oxidation of corresponding alcohol (3,333,000 $s^{-1}M^{-1}$). These catalytic properties suggest that the enzyme could play an important role in the oxidation of NADPH rather than the reduction of $NADP^+$ *in vivo*. However, apparent

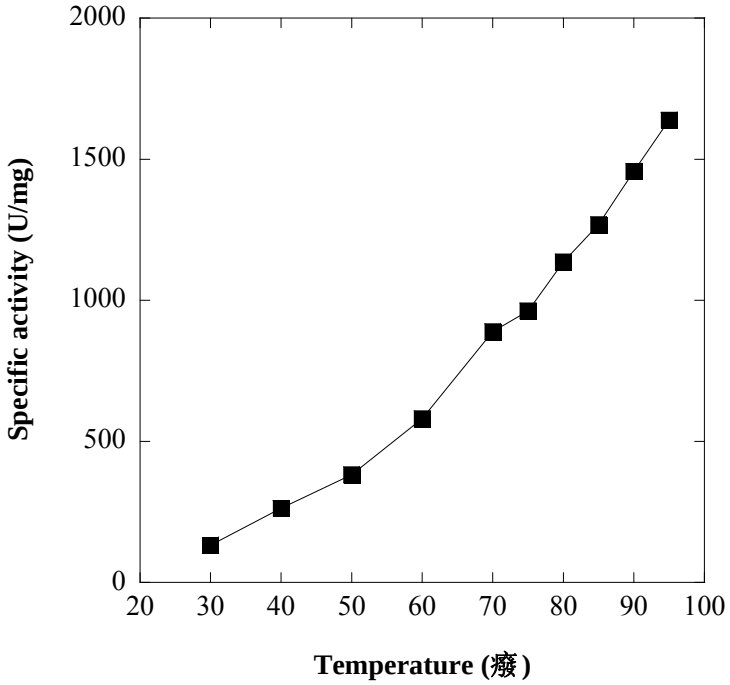

Figure 3-5 Temperature dependence of the purified ADH from *T. guaymasensis*.

The activities were measured in the standard assay conditions except varying assay temperatures from 30 to 95°C.

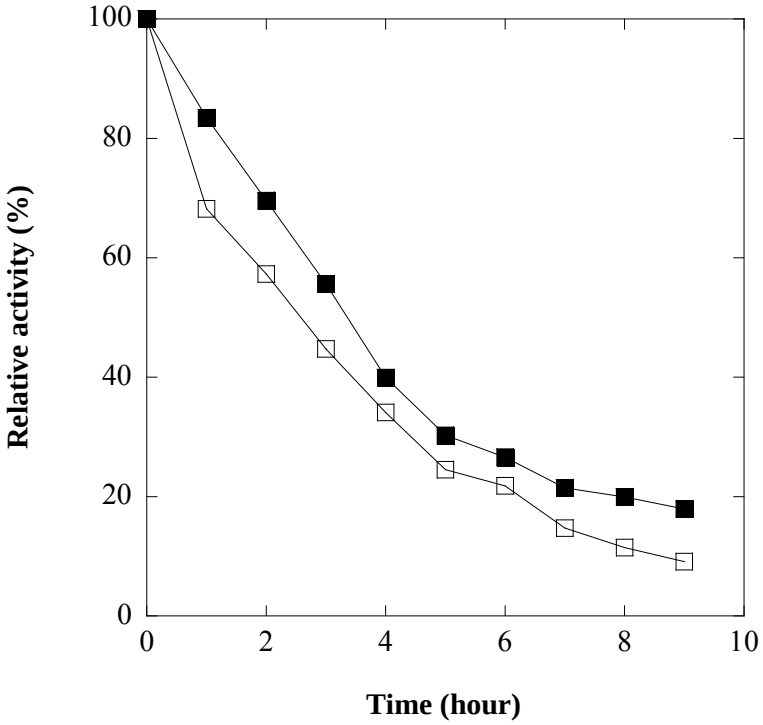

Figure 3-6 Oxygen sensitivity of the purified ADH from *T. guaymasensis*.

Filled squares, in the presence of SDT and DTT; open squares, in the absence of SDT and DTT. The relative activity of 100% equals to the ADH activity prior to exposure to air (1148 U mg^{-1}).

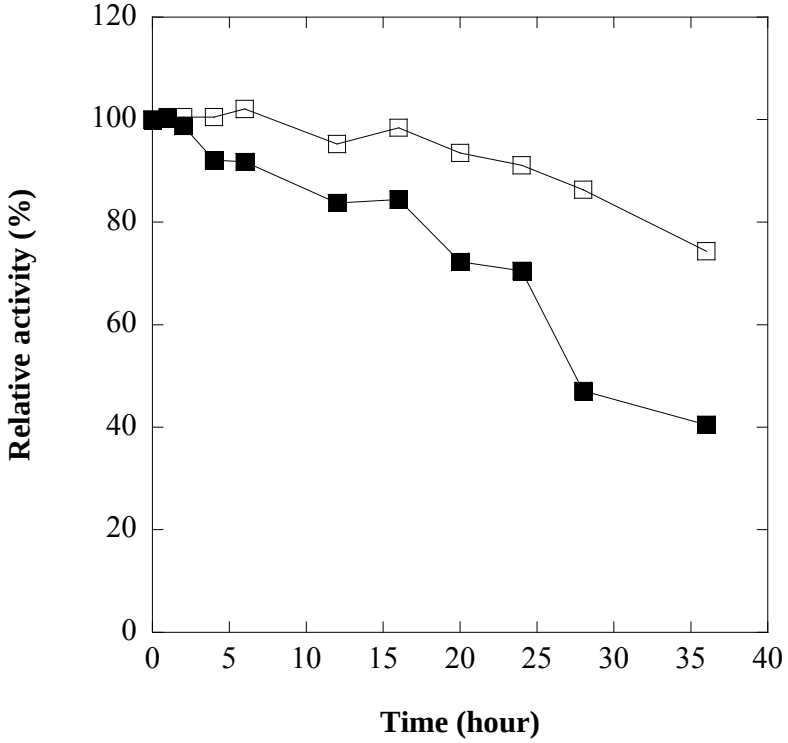

Figure 3-7 Thermostability of the purified ADH from *T. guaymasensis*.

Open squares, incubation at 80°C; filled squares, incubation at 95°C. The relative activity of 100% equals to the ADH activity without the heat treatment.

Table 3-4 Substrate specificity of *T. guaymasensis* ADH

Alcohols (50 mM)	Relative activity (%)	Aldehydes or ketones (6 mM)	Relative activity (%)
Methanol	0	Acetone	149.4 ± 2.8
Ethanol	5.7 ± 0.3	2-Butanone	100 ± 3.4[b]
1-Propanol	15.1 ± 0.3	2-Pentanone	86.2 ± 3.1
1-Butanol	5.1 ± 0.2	Acetoin	93 ± 3.2
1-Pentanol	0.8 ± 0.2	Diacetyl	134.8 ± 5.9
Glycerol	0.2 ± 0.1	Acetaldehyde	36 ± 4.2
2-Propanol	88 ± 1.1	Butyraldehyde	112.4 ± 11.9
2-Butanol	100 ± 2.2[a]		
2-Pentanol	66.3 ±		
1, 2-Butanediol	25.6 ± 2.3		
1, 3-Butanediol	35.4 ± 1.1		
1, 4-Butanediol	0		
2, 3-Butanediol	78.7 ± 3.4		
1, 2-Pentanediol	4.7 ± 0.3		
1, 5-Pentanediol	0		
2, 4-Pentanediol	9.2 ± 0.1		
Ethanediol	0		
Phenylethanol	0		
L-Serine	0		
L-Threonine	0		
Acetoin	0		

[a] The relative activity of 100% in alcohol oxidation means 1144 ± 24 U mg^{-1}.

[b] The relative activity of 100% in aldehyde/ketone reduction means 223 ± 7.6 U mg^{-1}.

Table 3-5 Kinetic parameters of *T. guaymasensis* ADH

Substrate (mM)	Co-substrate (mM)	Apparent *K*m (mM)	Apparent *V*max (U mg^{-1})	*k*cat (s^{-1})	*k*cat/*K*m ($s^{-1}M^{-1}$)
2-butanol	$NADP^+$ (0.4)	0.38	1250	833	2,192,000
(*2R*, *3R*)-(-)-2,3-butanediol[a]	$NADP^+$ (0.4)	15.2	1111	740	49,000
(*2S*, *3S*)-(+)-2,3-butanediol[a]	$NADP^+$ (0.4)	246	769	512	2082
meso-2,3-butanediol[a]	$NADP^+$ (0.4)	19.3	1428	952	49,000
$NADP^+$	2-butanol (11)	0.4	2000	1333	3,333,000
2-butanone	NADPH (0.2)	0.31	285	190	613,000
R/*S*-acetoin	NADPH (0.2)	0.32	213	142	444,000
Diacetyl	NADPH (0.2)	0.21	303	202	962,000
NADPH	2-butanone (3)	0.011	237	158	14,363,000

[a] Various concentrations for (*2R*, *3R*)-(-)-2, 3-butanediol (0, 2.7, 5.4, 8.1, 10.7, 16, 21.2, 26.5 and 51.7 mM), (*2S*, *3S*)-(+)-2, 3-butanediol (0, 11, 22, 27.5, 44, 55, 82.5 and 110 mM) and *meso*-2, 3- butanediol (0, 2.7, 5.4, 8.1, 10.7, 16, 21.2, 26.5 and 51.7 mM) were used for the determination of kinetic parameters.

*K*m value for 2-butanone (0.31 mM) was close to that of 2-butanol (0.38 mM) and the specificity constant *k*cat/*K*m for 2-butanone (613,000 s^{-1} M^{-1}) was about one third of that for 2-butanol (2,192,000 s^{-1} M^{-1}). Towards substrates of the reduction from diacetyl to 2, 3-butanediol *via* acetoin, the enzyme showed the highest and lowest affinity/catalytic efficiency on diacetyl and 2, 3-butanediol, respectively, suggesting its possible roles involving in the reduction of diacetyl to acetoin or 2, 3-butanediol (**Table 3-5**).

3.4.5 Effect of metals on the activity of *T. guaymasensis* ADH and its metal content

Since the enzyme was a medium-chain ADH rather than short-chain ADH lacking of metal, it was speculated that the enzyme could contain either zinc or iron. The metal content of the enzyme was measured by using inductively coupled plasma-mass spectrometry (ICP-MS). The data from the ICP-MS analyses indicated that the purified enzyme contained 0.9±0.03 *g* atom zinc per subunit. Therefore, each subunit of the enzyme could contain 1 *g* zinc per subunit. In addition, the enzyme contained trace amount of nickel (<0.01 *g* atom per subunit) and 0.1 *g* iron atom per subunit, which could be exogenous. Thus, the enzyme from *T. guaymasensis* was the first purified zinc-containing ADH from *Thermococcus* species.

The effect of various cations on the enzyme activity was examined by adding selected chemical (1 mM) into each enzyme assay mixture. EDTA slightly reduced the enzyme activity, indicating zinc was resistant to the chelation of EDTA. The cations such as Ni^{2+} and Fe^{2+} decreased the enzyme activity by 10-20% while Co^{2+}, Ca^{2+}, Mg^{2+} and Mn^{2+} slightly increased the activity (no more than 15% increase). The enzyme was completely inhibited by 1 mM Zn^{2+}, Cu^{2+}, Hg^{2+} and Cd^{2+} in assay mixtures (**Table 3-6**). It was unexpected that the zinc-containing ADH was inhibited by zinc ion. Thus, the inhibiton by zinc was further confirmed by reducing the concentration of zinc in the assay mixture. When the zinc concentration was 10, 25 and 100 μM in the assay mixtures, the corresponding activity was approximately 90%, 85% and 3% of the full actvity, respectively (**Fig. 3-8**).

Table 3-6 Effect of divalent metal ions or DTT on the activity of *T. guaymasensis* ADH

Chemicals (mM)	Relative activity[a] (%)
None	100 ± 2.2
EDTA (1)	96.2 ± 1.0
$NiCl_2$ (1)	93.7 ± 3.3
$CoCl_2$ (1)	104.4 ± 3.3
$ZnCl_2$ (1)	0
$FeCl_2$ (1)	80.4 ± 2.8
$CaCl_2$ (1)	113.3 ± 4.5
$MgCl_2$ (1)	107.6 ± 5.0
$MnCl_2$ (1)	111.4 ± 3.6
$CuCl_2$ (1)	0
$HgCl_2$ (1)	0
$CdCl_2$ (1)	0
DTT (2)	98.1 ± 1.1

[a] The activity was examined on the reduction of 2-butanone in the HEPES buffer (100 mM, pH 7.0). Divalent metal ion or DTT was added into the assay mixtures. The relative activity of 100% equals to 208 ± 4.5 U mg^{-1}.

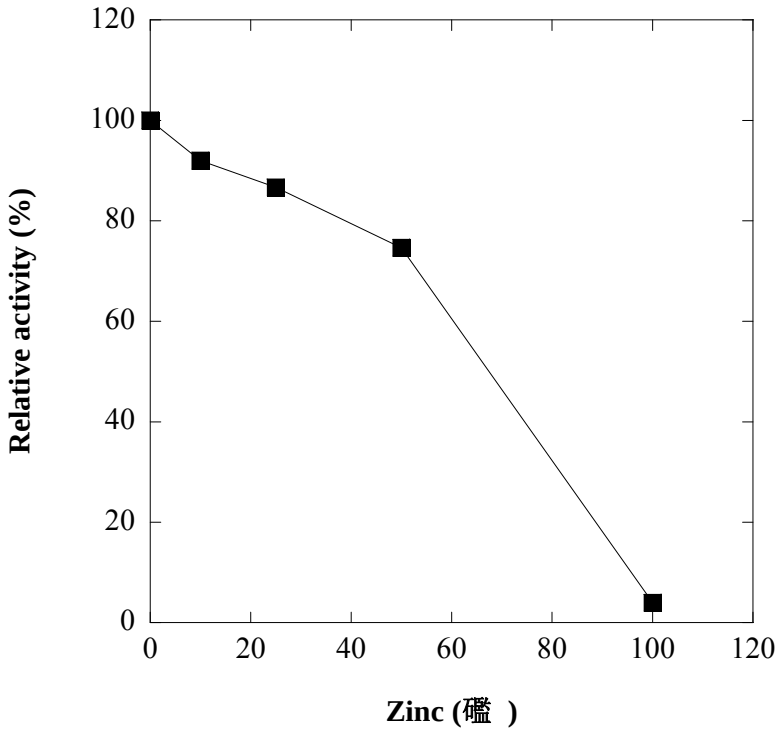

Figure 3-8 Effect of zinc on activity of *T. guaymasensis* ADH.

0.25 μg *T. guaymasensis* ADH was used for each assay.

3.4.6 Reduction of 2-butanone coupled with NADPH regeneration

Enzymes resistant to solvent inactivation are of great interest from scientific and practical points of view. The solvent tolerance of *T. guaymasensis* ADH was examined on the oxidation of 2-butanol and the reduction of 2-butanone by adding methanol in the assay mixtures. The purified enzyme did not oxidize methanol. The enzyme retained almost its full activity when the concentration of methanol was up to 5% (v/v) (**Fig. 3-9**). When the concentration of methanol was 30% (v/v) in the assay mixture, the enzyme activity remained about 40% of full activity on both oxidation and reduction, indicating that the enzyme had the outstanding solvent tolerance.

T. guaymasensis ADH was solvent tolerant, which made it feasible to regenerate the coenzyme NADPH using the co-substrate isopropanol in excess amount (500 mM). A gas chromatography method was developed to determine the reactants which had the following retention times: 1.33 min for isopropanol, 2.26 min for 2-butanone, 2.51 min for 2-butanol (**Fig. 3-10**). Driven by isopropanol (500 mM), the addition of 50 mM 2-butanone could result in the production of 45.6 mM 2-butanol, while the control without the addition of isopropanol produced 2-butanol in a low concentration of coenzyme as that coenzyme added (1 mM). The transfer yield was about 91%. Similar results were also obtained when 2-pentanone was used to replace 2-butanone using the same reaction system (**Table 3-7**).

3.4.7 Stereoselectivity of *T. guaymasensis* ADH

In order to investigate the stereoselectivity of *T. guaymasensis* ADH, two GC-based methods equipped with a chiral column were developed to efficiently separate substrates and products of the reactions, transformations between acetoin and 2, 3-butanediol or between 2-butanone and 2-butanol. In the interconversion between acetoin and

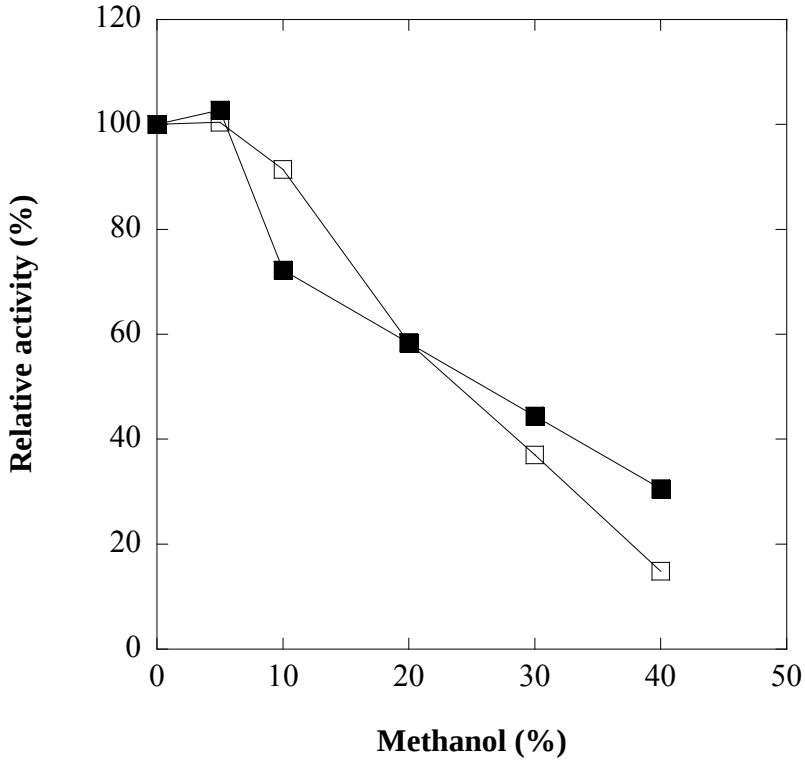

Figure 3-9 Effect of methanol on the activity of the purified ADH *T. guaymasensis*.

The solvent tolerance of the enzyme was examined by measuring the oxidation of 2-butanol (filled squares) and the reduction of 2-butanone (open squares).

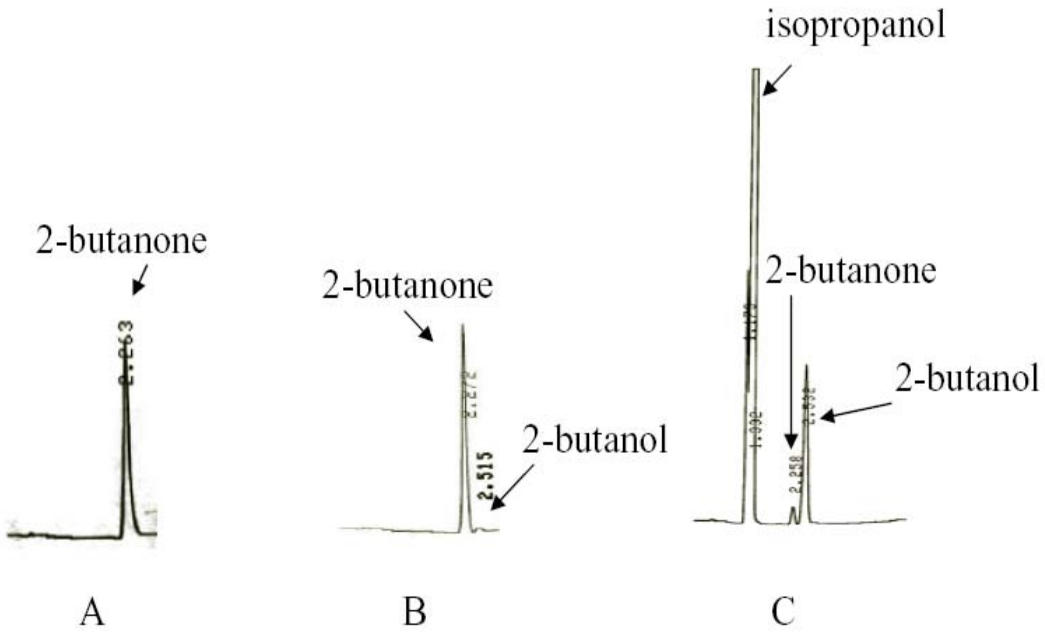

Figure 3-10 GC analyses of the substrates and products of 2-butanone reduction catalyzed by *T. guaymasensis* ADH.

A, no *T. guaymasensis* ADH and no isopropanol; B, no isopropanol; C, NADPH regeneration coupled with co-substrate isopropanol. The graphs were recorded on plain thermal sensitive roll paper (Mandel Scientific Company Inc., Guelph, ON, Canada) and scanned using a photo scanner ScanJet 5300C (Hewlett-Packard Canada Co., Mississauga, ON, Canada).

Table 3-7 Ketone reduction catalyzed by *T. guaymasensis* ADH

Parameters	Control[a]	Isopropanol used for NADPH regeneration
2-butanone as substrate (mM)	50	50
2-butanol produced (mM)	0.96 ± 0.1	45.6 ± 1.2
Transfer rate[b] (%)	1.9	91
2-pentanone as substrate (mM)	50	50
2-pentanol produced (mM)	0.95 ± 0.1	44.5 ± 1.5
Transfer rate[b] (%)	1.9	89
Extraction rate of ethyl acetate	*ND*	78 ± 3.0

[a] The control means no addition of 500 mM isopropanol.

[b] The transfer rate means the final concentration of 2-butanol divided by the initial concentration of 2-butanone in the reaction mixture.

ND, not determined

2,3-butanediol, the retention times of their isomers were 3.6 min for (*3R*)-acetoin, 4.2 min for (*3S*)-acetoin, 9.1 min for (*2S*, *3S*)-(+)-2, 3-butanediol, 9.4 min for (*2R*, *3R*)-(-)-2, 3-butanediol, and 10.2 min for *meso*-2, 3-butanediol (**Fig. 3-11**). The enzyme showed higher oxidation activities on the (*2R*, *3R*)-(-)-2, 3-butanediol and *meso*-2, 3-butanediol than on the (*2S*, *3S*)-(+)-2, 3-butanediol, indicating the enzyme predominantly oxidized *R*-hydroxyl group of 2, 3-butanediol and minorly functioned on *S*-hydroxyl group. When *meso*-2, 3-butanediol was oxidized, (*3S*)-acetoin was the predominant product with the enantiomeric excess (ee) of 88%, while oxidation of (*2R*, *3R*)-2, 3-butanediol resulted in the production of (*3R*)-acetoin with extremely high specificity (94% enantiomeric excess) (**Table 3-8**). With respect to the reduction reaction, the racemic *R*/*S*-acetoin was used since either *R*- or *S*-acetoin was not commercially available. Consistently, the reduction of racemic *R*/*S*-acetoin formed (*2R*, *3R*)-2, 3-butanediol (presumely from *R*-acetoin) and *meso*-2, 3-butanediol (presumely from *S*-acetoin) with extremely high specificity [>99% enantiomeric excess over (*2S*, *3S*)-(+)-2, 3-butanediol]. In addition, the kinetic parameters also confirmed that the enzyme had higher *K*m value for (*2S*, *3S*)-(+)-2, 3-butanediol than (*2R*, *3R*)-(-)-2, 3-butanediol or *meso*-2, 3-butanediol (**Table 3-5**).

With respect to the reduction of 2-butanone to 2-butanol, the retention times of products on gas chromatography profiles were 6.5 min for *R*-2-butanol and 6.85 min for *S*-2-butanol. The products from reduction of 2-butanone showed the equal composition of *R*-2-butanol and *S*-2-butanol (**Fig. 3-12**) whereas *T. guaymasensis* ADH showed almost identical activity on the oxidation of *R*-2-butanol and *S*-2-butanol, indicating the enzyme does not possess stereoselectivity on the 2-butanol or 2-butanone as the substrates. It was previously observed that stereoselectivity varied at different reaction temperatures. However, it seems not a general rule because *T. guaymasensis* ADH showed no stereoselectivity when it was examined on the reduction of 2-butanone at different reaction temperatures: 30, 50 and 80°C (**Table 3-9**).

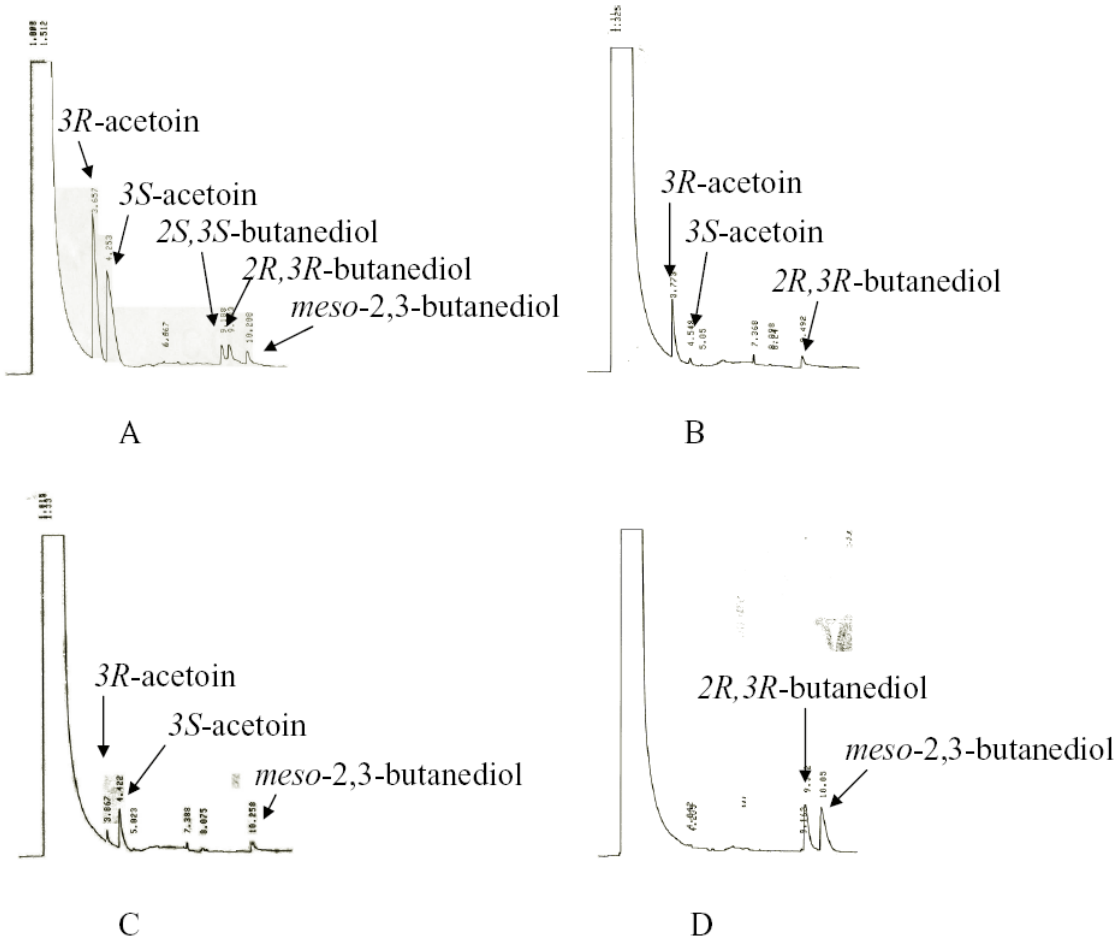

Figure 3-11 Analyses of the chirality of substrates and products in the reaction mixtures catalyzed by *T. guaymasensis* ADH.

The initial mixtures: A, 50 mM (*2R*, *3R*)-(-)-2,3-butanediol, 1 mM $NADP^+$ and 500 mM acetone in 100 mM CAPS buffer (pH 10.5); B, 50 mM *meso*-2,3-butanediol, 1 mM $NADP^+$ and 500 mM acetone in 100 mM CAPS buffer (pH 10.5); C, 50 mM (*3R*/*3S*)-acetoin, 1 mM NADPH and 500 mM isopropanol in 100 mM HEPES buffer (pH 7.5); D, a standard mixture of 50 mM (*3R*/*3S*)-acetoin, 25 mM (*2S*, *3S*)-(+)-2, 3-butanediol, 25 mM (*2R*, *3R*)-(-)-2,3-butanediol, and 25 mM *meso*-2, 3-butanediol in 100 mM HEPES buffer (pH 7.5). All reactions were performed for 24 h at 30°C. The final mixtures were extracted with ethyl acetate and analyzed by GC as described in Materials and Methods. Small peaks other than those labeled in the figures were presumably from the acceptable baseline shift

instability. The graphs were recorded on plain thermal sensitive roll paper (Mandel Scientific Company Inc., Guelph, ON, Canada) and scanned using a photo scanner ScanJet 5300C (Hewlett-Packard Canada Co., Mississauga, ON, Canada).

Table 3-8 Enantiomeric excess (ee) for oxidation of 2, 3-butanediol stereoisomers

Substrate	Specific activity ($U\ mg^{-1}$)	product	Stereoselectivity (ee, %)
meso-2, 3-butanediol	926 ± 25	*3S*- acetoin	84 ± 3
(*2R*, *3R*)-(-)-2, 3-butanediol	905 ± 30	*3R*- acetoin	94 ± 3
(*2S*, *3S*)-(+)-2, 3-butanediol	158 ± 5	*ND*	*ND*

ND, not determined

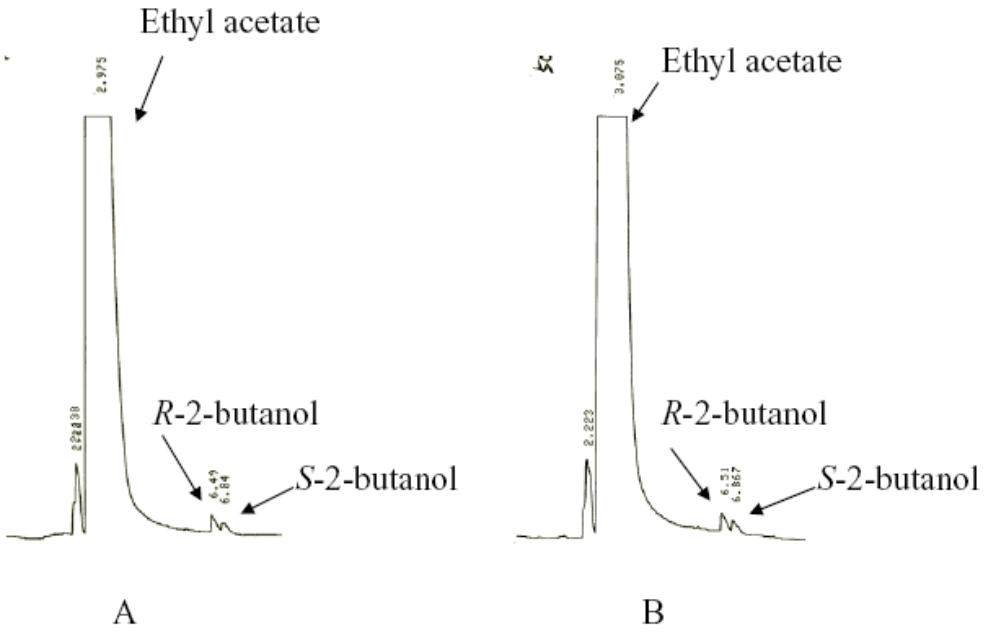

Figure 3-12 Analyses of the chirality of the products of 2-butanone reduction catalyzed by *T. guaymasensis* ADH.

A, racemic standards of *R*/*S*-2-butanol; B, a representative profile of products after reactions at 30, 50, or 80°C. The GC graphs were recorded on plain thermal sensitive roll paper (Mandel Scientific Company Inc., Guelph, ON, Canada) and scanned using a photo scanner ScanJet 5300C (Hewlett-Packard Canada Co., Mississauga, ON, Canada).

Table 3-9 Reduction of 2-butanone at different temperatures[a]

Parameters	30°C	50°C	80°C
Transfer rate (%)	91	83	70
Ratio of *R*-2-butanol/*S*-2-butanol	1:1	1:1	1:1

[a] The reaction mixtures were described in Materials and Methods except the different reaction temperatures.

3.4.8 Sequencing the encoding gene of *T. guaymasensis* ADH

In order to sequence the encoding gene, the amino-terminal (N-terminal) sequence was determined first using the Edman degradation. The N-terminal sequence of mature enzyme (SKMRGFAMVDF) started from S (serine), indicating the presence of N-terminal methionine excision after translation. Three internal sequences were successfully identified using the mass spectrometry (**Table 3-10**). Those amino acid sequences were aligned to determine conserved regions where the primers fitted in. One degenerate primer was designed based on its N-terminal amino acid sequence considering the codon bias of *Thermococcus kodakaraensis* KOD1 while the other non-degenerate primer was designed based on one of the internal sequences (GYHQHSGGMLAGW) and its corresponding nucleotide sequence in the gene encoding the ADH in *T. brockii*. The results of PCR showed a single band with the size of approximately 300 bp (**Fig. 3-13a**). The deduced amino acid sequence of the PCR product contained other internal sequences from mass spectrometry as listed in **Table 3-10**. In order to explore the flanking sequences of that fragment, the inverse PCR was applied. The genomic DNA of *T. guaymasensis* was digested by using the *Hind* III restriction enzyme, and then ligated by the T4 DNA ligase. Those treated DNA samples were used as PCR templates and then a 1.4 kb PCR product was obtained using the primers TGMAYN01 and TGMAYC02 (**Fig. 3-13b**). After a few steps of sequencing, 1.4 kb PCR product was fully sequenced but no expected restriction site of the *Hind* III enzyme. The alignment of deduced amino acid sequence revealed the obtained 1.4 kb sequence is situated downstream of the first 300 bp fragment, suggesting that the primer TGMAYN01 might anneal somewhere rather than the designed site.

The structural gene encoding *T. guaymasensis* ADH consisted of 1092 bp including the unknown codon of its putative penultimate amino acid (serine) (**Fig. 3-14**). The encoding nucleotide sequence ended at two consecutive stop codons (TGA TAA) and one putative archaeal terminator sequence, TTTTTCT, was found beginning 24 bases downstream of

Table 3-10 N-terminal and internal sequences of *T. guaymasensis* ADH

Location	Sequences
N-terminal[a]	SKMRGFAMVDF
Internal 1[b]	DFKPGDR
Internal 2[b]	VVVPAITPDWR
Internal 3[b]	GYHQHSGGMLAGW

[a] Amino-terminal sequence was determined by using Edman-degradation.

[b] Internal sequences were determined by using mass spectrometry as described in Materials and Methods. The listed internal sequences showed high identities to corresponding sequences of *T. brockii* ADH (A32973), threonine dehydrogenase from *Thermoanaerobacter tengcongensis* (Q8RBW3) and *T. ethanolicus* ADH (S71131).

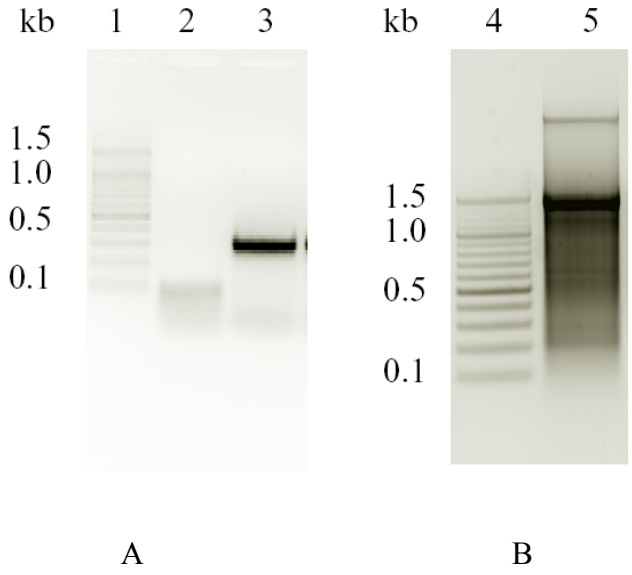

Figure 3-13 Amplification of the gene encoding *T. guaymasensis* ADH.

A represents the PCR reaction using primers TGADHNF and TGADHIR. B represents the inverse PCR reaction using primers TGMAYN01 and TGMAYC02. Lane 1 and 4, 100 bp DNA ladders (Fermentas Canada Inc., Burlington, ON); lane 2, negative control (no DNA template); lane 3 and 5, PCR products of 300 bp and 1400 bp, respectively.

```
1          NNNAAGATGCGCGGTTTTGCAATGGTGGACTTCGGCAAGGCCGAGTGGATTGAGAAGGAG
1           S  K  M  R  G  F  A  M  V  D  F  G  K  A  E  W  I  E  K  E

61         AGGCCGAAGCCCGGGCCGTACGATGCAATCGTCAAGCCCATTGCAGTCGCCCCATGCACC
21          R  P  K  P  G  P  Y  D  A  I  V  K  P  I  A  V  A  P  C  T

121        TCGGACATCCACACGGTCTTTGAGGCAGCGTTTCCCAGGGAGATGTGTGAGTTCCCGCGC
41          S  D  I  H  T  V  F  E  A  A  F  P  R  E  M  C  E  F  P  R

181        ATACTGGGTCACGAAGCAGTCGGAGAGGTAGTCGAGGTCGGAAGCCACGTCAAGGACTTC
61          I  L  G  H  E  A  V  G  E  V  V  E  V  G  S  H  V  K  D  F

241        AAGCCCGGGGACAGGGTTGTTGTCCCGGCAATAACTCCCGACTGGAGGACCCTTGACGTT
81          K  P  G  D  R  V  V  V  P  A  I  T  P  D  W  R  T  L  D  V

301        CAGAGGGGCTACCACCAGCACTCCGGTGGAATGCTCGCCGGATGGAAGTTCAGCAACCCC
101         Q  R  G  Y  H  Q  H  S  G  G  M  L  A  G  W  K  F  S  N  P

361        CTCAAGGAGGGCGGTAAGGACGGTGTGTTTGCAGAATACTTCCACGTCAACGACGCTGAC
121         L  K  E  G  G  K  D  G  V  F  A  E  Y  F  H  V  N  D  A  D

421        ATGAACCTGGCACACCTTCCGGACGAAATCAAGCCGGAAGTCGCTGTCATGGCCACCGAC
141         M  N  L  A  H  L  P  D  E  I  K  P  E  V  A  V  M  A  T  D

481        ATGATGACCACGGGATTCCACGGCGCCGAGCTCGCCGACATTCCGCTCGGAGGAACAGTC
161         M  M  T  T  G  F  H  G  A  E  L  A  D  I  P  L  G  G  T  V

541        GCCGTCATTGGAATTGGACCGGTCGGCCTGATGGCGGTTGCCGGGGCAAGACTGCTCGGT
181         A  V  I  G  I  G  P  V  G  L  M  A  V  A  G  A  R  L  L  G

601        GCCGGAAGGATCATCGCGGTCGGCAGCAGGCCGGTGTGCGTTGAGGCCGCTAAGTACTAC
201         A  G  R  I  I  A  V  G  S  R  P  V  C  V  E  A  A  K  Y  Y

661        GGAGCCACCGACATAGTCAACCGCAGGGAGCACCCGGACATCGCCGGAAGGATCCTGGAG
221         G  A  T  D  I  V  N  R  R  E  H  P  D  I  A  G  R  I  L  E

721        CTGACCGGTGGAGAGGGTGTTGATTCGGTGATAATCGCCGGCGGAAACGTTGACGTAATG
241         L  T  G  G  E  G  V  D  S  V  I  I  A  G  G  N  V  D  V  M

781        AAGACCGCGGTGAAGATAGTCAAGCCCGGAGGAACGGTGGCCAACATCAACTACTTCGGC
261         K  T  A  V  K  I  V  K  P  G  G  T  V  A  N  I  N  Y  F  G

841        AGCGGTGACTACCTCCCGATCCCGAGGATTGAGTGGGGCCAGGGAATGGCCCACAAGACC
281         S  G  D  Y  L  P  I  P  R  I  E  W  G  Q  G  M  A  H  K  T

901        ATCAAGGGAGGGCTCTGCCCAGGCGGACGCCTGAGGATGGAGCGCCTGCTTGACCTCATC
301         I  K  G  G  L  C  P  G  G  R  L  R  M  E  R  L  L  D  L  I

961        AAGTACGGCAGGGTTGACCCGTCAAGGCTCATAACCCACAAGTTCAAGGGATTCGATAAG
321         K  Y  G  R  V  D  P  S  R  L  I  T  H  K  F  K  G  F  D  K

1021       ATACCAGAAGCCCTCTACCTGATGAAGGACAAGCCCAAAGACCTGATAAAGCCCGTGGTC
341         I  P  E  A  L  Y  L  M  K  D  K  P  K  D  L  I  K  P  V  V
```

```
1081       ATCATAGAGGAGTGATAAAGCTCTGCCCTCGCTATTCTTTTTTCTTCAACAGGCAATATC
361         I  I  E  E  *  *

1141       ATATCCCGTTCTAAACCTTTAGTTCAAAAAACGCTTTTATCGTGCGTTTCGAACTCAAAA
1201       ATGGAGTGAAAAGCGGAGGTGAAGGCTTTGGGCGAGGTAACCCTCGACAAGGTTTGCAGG
1261       ATTGCAGGTGAGGCCAAGCTCATCCTGTACGAGGAAGACGGAACCGTTCAAGATGCCCTC

1321       TTCATAGCGACGGCTCCGGTGAGGGGTTTCGAGAAGATGGNGGTCGGAAAGAACCCCCTC
                                                 M  X  V  G  K  N  P  L

1381       TTTGCGGTCGAGGCTGTTATGAGGATATGCGGTCTCTGCCACGCCTCCCACGGCATAGCG
            F  A  V  E  A  V  M  R  I  C  G  L  C  H  A  S  H  G  I  A

1441       GCGAGCGAGGCCATAGAGCACGCCATAGGCATTGCCCCCCCGAGGAACGGAAGGCTCATG
            A  S  E  A  I  E  H  A  I  G  I  A  P  P  R  N  G  R  L  M

1501       CGGGAAGCCCTCGGCCTGATAAACAGGGCCCAGAGCCACGCACTGCTCTTCCTGATGGTC
            R  E  A  L  G  L  I  N  R  A  Q  S  H  A  L  L  F  L  M  V

1561       GCGGGCGACCTGATTAAGGAGGAAAAGAGGGACGAGGTGCTCTTCAAGCTCATGGACTTC
            A  G  D  L  I  K  E  E  K  R  D  E  V  L  F  K  L  M  D  F

1621       CACGCGAAGATCAGCGACTACCTGCTAAAGCTCGGTGGCGCTGCGACACATCCACCGAAC
            H  A  K  I  S  D  Y  L  L  K  L  G  G  A  A  T  H  P  P  N

1681       CTGACGATAGGTGGCATGCTCTCCGTTCCAAAGTGGAGCGTCTTCAACAACCTGAAGGCG
            L  T  I  G  G  M  L  S  V  P  K  W  S  V  F  N  N  L  K  A

1741       AGGTTCAAAGACCTCGCCGCAAGCTGGGAGGCCGCTGAGGAGCTTTTAATTGATGAGGAT
            R  F  K  D  L  A  A  S  W  E  A  A  E  E  L  L  I  D  E  D

1801       ATCCAGACCGAGATTGCGGATGAGCTTAGAGAGGCCAAAAGGCCCTTCAAGTACCTCGCG
            I  Q  T  E  I  A  D  E  L  R  E  A  K  R  P  F  K  Y  L  A

1861       AGCGGCTTCTTCTACGGGGACAGGTACAACATCGAGTGGATTGAGAAGGAGAA
621         S  G  F  F  Y  G  D  R  Y  N  I  E  W  I  E  K  E
```

Figure 3-14 Nucleotide and deduced amino acid sequences of *T. guaymasensis* ADH.

The amino acid sequence was deduced using the program DNAMAN (Lynnon Corporation,Vaudreuil-Dorion, Quebec, Canada). The stop codon is marked with an asterisk and the possible terminator sequence in the 3'-untranslated region is underlined. The partial gene encoding a nickel-containing hydrogenase is highlighted in grey. N in the nucleotide sequence represents either A, T, C or G while X in the deduced amino acid sequence represents unknown amino acid residue. The nucleotide sequence corresponding to N-terminus (5'-AAGATGCGCGGTTTTGCAATG) was from the designed primer TGADHNF (**Table 3-1**). The codon for the initial serine was unknown.

the stop codon of TGA (Reiter et al. 1988). The downstream of the structural gene of *T. guaymasensis* ADH was deduced and appeared a part of putative gene encoding archaeal hydrogenase. In addition, the codon usage pattern for the *adh* genes from *T. guaymasensis* seemed biased (**Table 3-11**). Of the 61 sense codons, thirteen were not used in the gene encoding *T. guaymasensis* ADH. However, the 14 most frequently used codons (greater than 2.7%) accounted for 58% of the amino acid residues, reflecting the abundant tRNA species in *T. guaymasensis* (Peretz et al. 1997).

3.4.9 Structural analyses of *T. guaymasensis* ADH

The deduced amino acid sequence of *T. guaymasensis* ADH contained 364 amino acid residues corresponding to a calculated size of 39.4 kDa. The primary structural analyses revealed that the enzyme had higher ratio (molar fraction, >0.8% increase) for Ala, Arg, Glu, Lys and Pro but lower ratio (molar fraction, >0.8% decrease) for Asn, Gln, Leu, Ser and Met as compared to the ADH from the mesophile *C. beijerinckii* (**Table 3-12**). In particular, the amino acid composition of *T. guaymasensis* ADH had higher ratio (molar fraction, >0.8% increase) for Arg, Pro and Tyr but lower ratio (molar fraction, >0.8% decrease) for Ala, Asn and Val than that of the ADH from the thermophile *T. brockii*. Moreover, the negatively charged amino acid resides were almost equal to the positively charged residues, which could contribute to more ion pairs. The deduced amino acid sequence of *T. guaymasensis* ADH showed high overall identities to threonine dehydrogenase or zinc-containing ADHs from thermophilic bacteria, e.g., ADHs from *T. tengcongensis* MB4 (77% identity, AAM23957), *T. brockii* (77% identity, CAA46053), *T. ethanolicus* ATCC 33223(77% identity, EAO63648), *T. ethanolicus* X514(76% identity, EAU57308), *Thermosinus carboxydivorans* Nor1 (72% identity, EAX46383) and the mesophile *C. beijerinckii* (67% identity, EAX46383). The N-terminal region of the sequence showed homology to ADH_N while the C-terminal region showed ADH_zinc_N (**Fig. 3-15**). The central region spanning the majority of peptides showed homology to the domain of TDH. All three domains are classified as zinc-related.

Table 3-11 Codon usage of the gene encoding *T. guaymasensis* ADH

triplet	aa	No.[a]	triplet	aa	No.[a]	triplet	aa	No.[a]	triplet	aa	No.[a]
UUU	F	4	UCU	S	0	UAU	Y	0	UGU	C	1
UUC	F	9	UCC	S	1	UAC	Y	9	UGC	C	3
UUA	L	0	UCA	S	1	UAA	*	0	UGA	*	1
UUG	L	0	UCG	S	2	UAG	*	0	UGG	W	4
CUU	L	3	CCU	P	0	CAU	H	0	CGU	R	0
CUC	L	10	CCC	P	9	CAC	H	11	CGC	R	5
CUA	L	0	CCA	P	3	CAA	Q	0	CGA	R	0
CUG	L	10	CCG	P	13	CAG	Q	3	CGG	R	0
AUU	I	6	ACU	T	1	AAU	N	0	AGU	S	0
AUC	I	13	ACC	T	9	AAC	N	7	AGC	S	4
AUA	I	9	ACA	T	1	AAA	K	1	AGA	R	1
AUG	M	13	ACG	T	3	AAG	K	24	AGG	R	13
GUU	V	8	GCU	A	3	GAU	D	3	GGU	G	9
GUC	V	18	GCC	A	16	GAC	D	20	GGC	G	11
GUA	V	2	GCA	A	9	GAA	E	5	GGA	G	20
GUG	V	7	GCG	A	4	GAG	E	18	GGG	G	4

[a] The number of each codon (No.) was calculated by using Sequence Manipulation Suite (Stothard, 2000) .

"*", stop codons.

Abbreviations for amino acid (aa): A, alanine; R, arginine; N, asparagine; D, aspartic acid; C, cysteine; E, glutamic acid; Q, glutamine; G, glycine; H, histidine; I, isoleucine; L, leucine; K, lysine; M, methionine; F, phenylalanine; P, proline; S, serine; T, threonine; W, tryptophan; Y, tyrosine; V, valine.

Table 3-12 Amino acid compositions of TgADH, TbADH and CbADH

Amino acid	TgADH[a]	TbADH[a]	CbADH[a]
Ala (A)	32 (8.8)	35 (9.9)	27 (7.7)
Arg (R)	19 (5.2)	14 (4.0)	14 (4.0)
Asn (N)	7 (1.9)	10 (2.8)	13 (3.7)
Asp (D)	23 (6.3)	20 (5.7)	21 (6.0)
Cys (C)	4 (1.1)	4 (1.1)	5 (1.4)
Gln (Q)	3 (0.8)	3 (0.9)	6 (1.7)
Glu (E)	23 (6.3)	21 (6.0)	18 (5.1)
Gly (G)	44 (12.1)	43 (12.2)	45 (12.8)
His (H)	11 (3.0)	10 (2.8)	11 (3.1)
Ile (I)	28 (7.7)	26 (7.4)	26 (7.4)
Leu (L)	23 (6.3)	23 (6.5)	28 (8.0)
Lys (K)	25 (6.8)	24 (6.8)	21 (6.0)
Met (M)	14 (3.8)	15 (4.3)	18 (5.1)
Phe (F)	13 (3.6)	14 (4.0)	11 (3.1)
Pro (P)	25 (6.8)	21 (6.0)	13 (3.7)
Ser (S)	9 (2.5)	9 (2.6)	17 (4.8)
Thr (T)	14 (3.8)	13 (3.7)	11 (3.1)
Trp (W)	4 (1.1)	4 (1.1)	4 (1.1)
Tyr (Y)	9 (2.5)	6 (1.7)	7 (2.0)
Val (V)	35 (9.6)	37 (10.5)	35 (10)

[a] The number in parenthesis means the molar fraction of amino acid. As compared to the composition of *C. beijerinckii* ADH (CbADH), the values for *T. guaymasensis* ADH (TgADH) and *T. brockii* ADH (TbADH) are highlighted in yellow to indicate amino acid residues with molar fraction increase (>0.8%) and in grey to indicated those with molar fraction decrease (>0.8%), respectively.

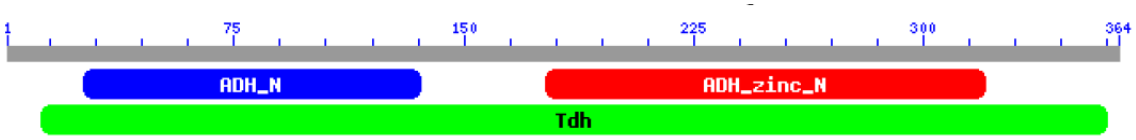

Figure 3-15 Putative conserved domains of *T. guaymasensis* ADH.

ADH_N, alcohol dehydrogenase GroES-like domain; ADH_zinc_N, zinc-binding dehydrogenase; Tdh, L-threonine dehydrogenase

GroES is an oligomeric molecular chaperone and folds as a partly opened beta-barrel (Ranford et al. 2000; Walter 2002).

T. guaymasensis ADH and its homologues harbored the highly conserved amino acid residues (**Fig. 3-16**). The putative active site and $NADP^+$ binding motifs were identified to be $G_{62}H_{63}E_{64}X_2G_{67}X_5G_{73}X_2V_{76}$ and $G_{183}XG_{185}XXG_{188}$, respectively. Consistent with metal analyses, no structural zinc-binding motif was observed. On the 3-D modeling of the structure (**Fig. 3-17**), the monomer of *T. guaymasensis* ADH folded into two domains, one catalytic domain closing to amino-terminal end and one $NADP^+$-binding domain closing to C-terminal end. Both domains were separated by the cleft where the active site of the enzyme might be situated.

Figure 3-16 Alignment of sequence of *T. guaymasensis* ADH and other related zinc-containing ADHs.

The sequences were aligned using Clustal W (Thompson et al. 1994). Highlights in yellow, putative binding sites of catalytic zinc; highlights in purple, putative motif of coenzyme binding. TgADH, *T. guaymasensis* ADH; TbADH, *T. brockii* ADH; CbADH, *C. beijerinckii* ADH. ‘‘*’’: residues or nucleotides that are identical in all sequences in the alignment; ‘‘:’’, conserved substitutions; ‘‘.’’, semi-conserved substitutions; “-”, no corresponding amino acid.

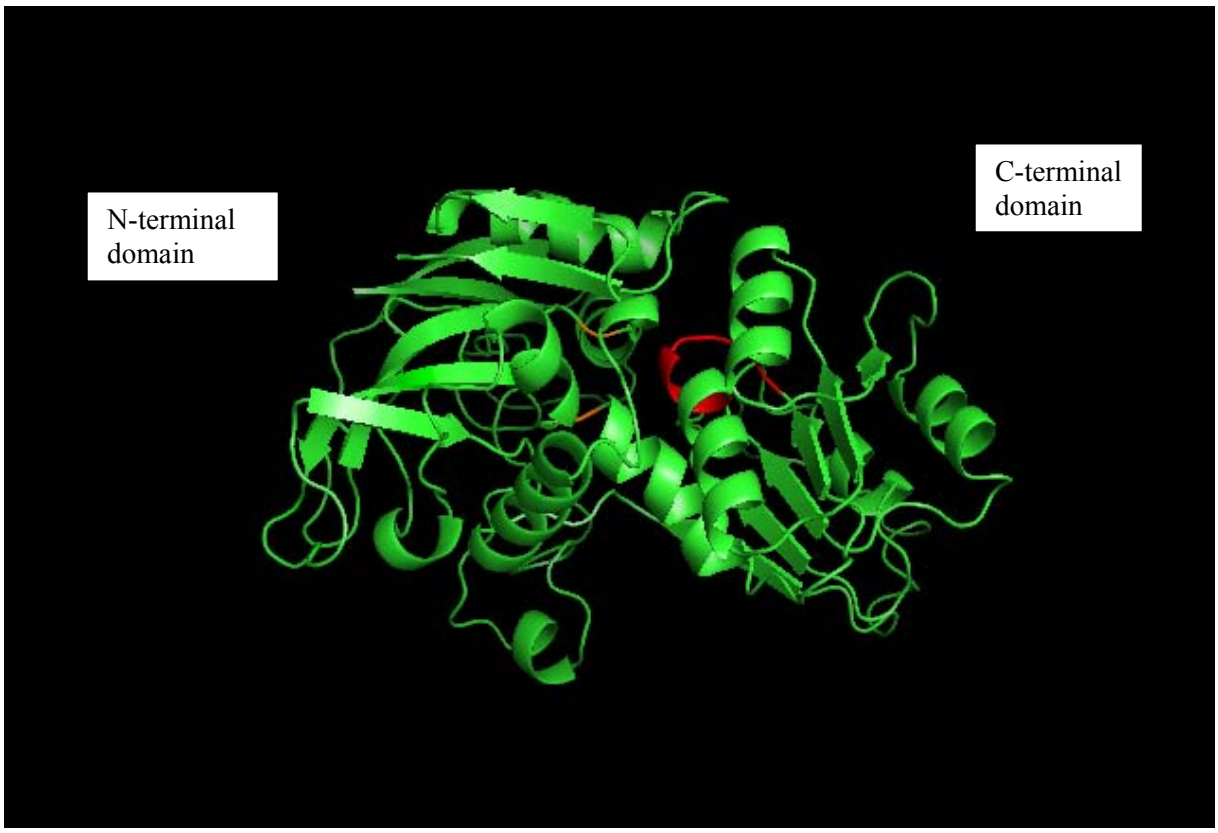

Figure 3-17 Predicted tertiary structure of *T. guaymasensis* ADH monomer.

The structure modeling was run on the Swiss-Model server using *T. brockii* ADH (PDB entry: 1ykf) as template. The structure figure was constructed using the software PyMOL (Delano 2002). Residues in orange, the putative zinc-binding site; residues in red, the putative $NADP^+$-binding site.

3.5 DISCUSSION

In hyperthermophilic archaea, a few zinc-containing ADHs have been recently purified and characterized. They are either ADHs from aerobic hyperthermophilic archaea *S. solfataricus* and *A. pernix* or TDHs from anaerobic hyperthermophiles *P. furiosus* and *Pyrococcus horikoshii* (**Table 3-13**). Similar to other zinc-containing ADHs or TDHs, ADH from the anaerobic hyperthermophile *T. guaymasensis* contained 364 amino acid residues and thereby was a member of medium-chain ADHs. The native *T. guaymasensis* ADH was in the ternary structure of homotetramer, which is a usual structural characteristic of zinc-containing ADHs in archaea and bacteria. The hyperthermophilic ADHs including *T. guaymasensis* ADH showed that the optimum pH for the oxidation reaction was more alkaline than that for the reduction reaction. In contrast, those hyperthermophilic TDHs tended to optimally oxidize $_{L}$-threonine at pHs close to the neutral pH.

T. guaymasensis ADH was specific for $NADP^+$ as coenzyme, whereas other hyperthermophilic zinc-containing ADHs or TDHs preferred to NAD^+ as coenzyme. The momoner of zinc-containing ADHs from hyperthermophiles contained catalytic and structural zinc atoms except that *T. guaymasensis* showed 1 *g* atom zinc per subunit. Its amino acid sequence possessed the binding motif of catalytic zinc and lack of the binding motif of structural zinc, thus indicating that its zinc atom was highly likely to play a catalytic role. Its sequence alignment also showed high similarities to those $NADP^+$-dependent ADHs containing catalytic zinc atom only, e.g., ADHs from *T. brockii* and *T. ethanolicus*, other than those containing both catalytic and structural zinc atoms (**Fig. 3-18**)

The enzyme from *T. guaymasensis* possesses several outstanding features to be a competitive biocatalyst. The enzyme was active within a broad temperature range from 30 to 95°C as tested while the optimal temperature was over 95°C, which feature is common for ADHs originating from hyperthermophiles. The thermo activity with 1149 Umg^{-1} at 80°C was remarkably higher than other zinc-containing ADHs characterized except the

Table 3-13 Properties of zinc-containing ADHs from hyperthermophilic archaea

Properties	*T. guaymasensis*	*S. solfataricus*	*A. pernix*	*P. furiosus*	*P. horikoshii*
Enzyme Structure	ADH homotetramer	ADH homotetramer[a]	ADH homotetramer	TDH homotetramer	TDH homotetramer[a]
Polypeptide (aa)	364	347	359	348	348
Coenzyme	$NADP^+$	NAD^+	NAD^+	NAD^+	NAD^+
Specific activity (U mg^{-1})	1149	5.3	1.1	10.3	1750[b]
Optimal temperature (°C)	>95	>95	>95	>100	NA
Optimal pHs	10.5/7.5	9.0/5.5	10.5/8.0	6.6	7.5
Types of zinc	Putative catalytic	Catalytic and structural	Catalytic and structural	Putative catalytic and structural	Catalytic and structural
Reference[c]	1	2	3	4	5

[a] The information refers to the recent crystal structures (Esposito et al. 2002; Esposito et al. 2003b).

[b] The maximal activity using NAD^+ as the coenzyme.

[c] Reference: 1, this work; 2, Ammendola et al. 1992; Rella et al. 1987; 3, Guy et al. 2003; Hirakawa et al. 2004; 4, Machielsen and van der Oost 2006; 5, Higashi et al. 2005; Ishikawa et al. 2007.

NA, not available.

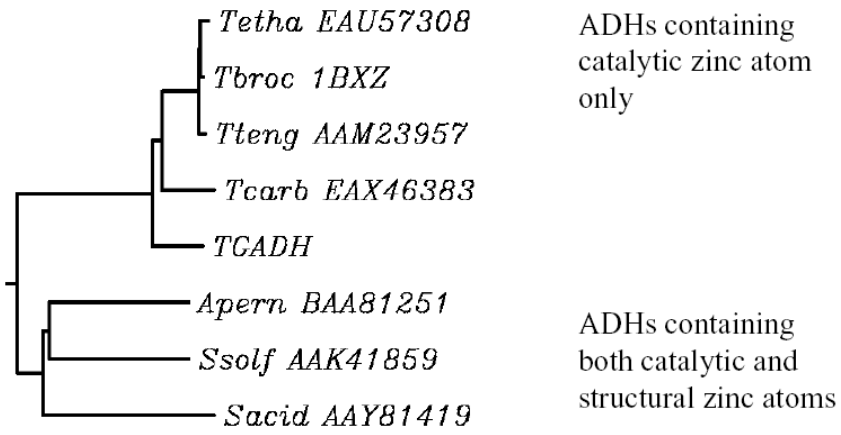

Figure 3-18 Phylogenetic relationships between *T. guaymasensis* ADH and related zinc-containing ADHs from hyperthermophiles or thermophiles.

The sequences were aligned using Clustal W and a subsequent phylogenetic tree was constructed (Thompson et al. 1994). The accession numbers for the organisms used in the analyses are indicated on the figure. Abbreviations used: Tetha, *T. ethanolicus*; Tbroc, *T. brockii*; Tteng, *T. tengcongnesis*; Tcarb, *Thermosinus carboxydivorans*; TGADH, *T. guaymasensis* ADH; Apern, *Aeropyrum pernix*; Ssolf, *S. solfataricus*; Sacid, *Sulfolobus acidocaldarius*.

TDH from *P. horikoshii* (**Table 3-13**). The activity of the butanediol dehydrogenase from *S. cerevisiae* was reported to be 968 U mg^{-1} (González et al. 2000) and obviously not as thermostable as *T. guaymasensis* ADH. The enzyme was hyper thermostable and its $t_{1/2}$ at 95°C was about 24 hours, which is the most thermostable one among the family of zinc-containing ADHs. The enzyme had broad substrate specificity. In the oxidation direction, the enzyme transformed various alcohols including primary and secondary, poly and di-ols while it reduced various aldehydes and ketones in the reduction direction. When the methanol was used to test the solvent tolerance, the methanol concentration at which half of full activity remained was about 24%. Therefore, high activity, outstanding thermostability and solvent tolerance make it a good candidate for chemical synthesis.

Aiming at the practical synthesis in industry, the coenzyme regeneration is necessary due to its high cost. To date, the coenzyme regeneration in the synthesis catalyzed by hypertherphilic ADHs follows the enzyme-coupled or substrate-coupled strategy (**Table 3-14**). The solvent tolerance of *T. guaymasensis* ADH is of great interest by offering an option to regenerate NADPH with the cheaper co-substrate isopropanol instead of enzymes such as formate dehydrogenase or glucose dehydrogenase. It has been pointed out that the 2-propanol concentration usually was in excess amount, which was not only crucial to shift the equilibrium in the reduction direction, but also possible to enhance the solubility of hydrophobic substrates in the aqueous reaction medium. The NADPH regeneration system led to produce 45.6 mM by using only 1 mM NADPH with a transfer yield up to 92%, indicating it is a successful example on the NADPH regeneration.

Coupled to the NADPH regeneration using isopropanol, the enzyme showed the asymmetric reduction of racemic acetoin, in which only (*2R*, *3R*)-2, 3-butanediol and *meso*-butanediol were produced. The enzyme also showed the asymmetric oxidation of 2, 3-butanediol isomers, in which it had much lower specificity constant on (*2S*, *3S*)-(+)-2, 3-butanediol than (*2R*, *3R*)-2, 3-butanediol and *meso*-2, 3-butanediol. Regarding the stereoselectivity of *T. guaymasensis* ADH, the highly similar example was the butanediol

Table 3-14 Substrate- or enzyme-coupled coenzyme regeneration for ADHs from hyperthermophilic archaea

Parameter	TgADH[a]	ApADH[a]	PfADH[a]
Substrate (mM)	2-butanone (50)	ketone (10)	2-pentanone (250)
Enzyme (nmol)	0.16	0.6	4
Coenzyme (mM)	NADPH (1)	NADH (0.02)	NADH (1)
Co-substrate (mM)	Isopropanol (500)	Cyclohexanol (100)	Glucose (300)
Aid-enzyme (U)	None	None	Glucose dehydrogenase (10)
Yield (%)	92	*NA*	*NA*
Extraction	Ethyl acetate or CH_2Cl_2	CH_2Cl_2	Chloroform
Reference[b]	1	2	3

[a] Abbreviations used: TgADH, *T. guaymasensis* ADH; ApADH, ADH from *Aeropyrum pernix*; PfADH, ADH from *Pyrococcus furiosus*.

[b] Reference: 1, this work; 2, Hirakawa et al. 2004; 3, Machielsen et al. 2006.

NA, not available

dehydrogenase from *S. cerevisiae* (González et al. 2000). Obeying anti-prelog's rule, *T. guaymasensis* ADH might undergo transferring a hydride ion from an *R*-configured alcohol to the *pro-R* face of $NADP^+$ or transferring a hydride ion from the *pro-R* face of NADPH to the *si* face of a carbonyl group of a ketone (Prelog 1964). The anti-Prelog ADHs were of greater interest since they are not only as abundant as Prelog ADHs like those in horse liver, *T. brockii*, *P. furiosus* and *S. solfataricus* which transfer *pro*-R hydrogen atom of the coenzyme onto the *re*-face of the substrate ketone thus forming (*S*)-alcohol (**Table 3-15**).

Since *T. guaymasensis* ADH shared high similarity to the ADHs from *T. brockii* and *T. ethanolicus*, it was not expected that the enzyme had no stereoselectivity on the reduction of 2-butanone, which has been well characterized in ADHs from *T. brockii* and *T. ethanolicus* (Keinan et al. 1986; Zheng et al. 1992). The equal amount of *R*-2-butanol and *S*-2-butanol resulting from the 2-butanone reduction were verified by a chiral gas chromatography. Moreover, the enzyme had almost identical oxidation activity on *R*-2-butanol and *S*-2-butanol. In addition, the enzyme could not catalyze the $_L$-threonine and $_L$-serine. It was recently noted that the ADH from *P. furiosus* showed higher enantioselectivity on phenyl-substituted ketoesters than the substrates lacking phenyl groups (Zhu et al. 2006). Similarly, the stereoselectivity of enzyme appeared relying strictly on side groups of carbonyl group, in particular, the larger side group (**Table 3-16**).

N-terminal methione was excised in the mature enzyme of *T. guaymasensis* ADH, which is governed by the side-chain length of the penultimate amino acid (Hirel et al. 1989). Although the nucleotide sequence encoding N-termius was from the designed primer, the N-terminal amino acid sequence determined by Edman degradation indicated that serine was the initial amino acid of mature *T. guaymasensis* ADH and possibly its penultimate amino acid. As observed in bacteria and yeasts, N-terminal methionine excision of an enzyme could be critical for its function and stability (Eichler and Adams 2005) but its role for achaeal enzymes is not clear yet. Amino acid composition and its substitution

Table 3-15 Characterization of thermostable ADHs with stereoselectivity

	T. guaymasensis ADH	*T. brockii* ADH	*P. furiossi* ADH
classification	zinc-containing	zinc-containing	alde-keto family
Required coenzyme	NADPH	NADPH	NADH and NADPH
Preferred substrates	Ketones	Ketones	Ketones
Specific activity (U mg^{-1})	1149[a]	30-90[b]	32.4[c]
Stereoselectivity	*R*- configured	*S*-configured	*S*-configured
Thermo-stability ($t_{1/2}$)	24 hour at 95°C	60 min at 93.8°C	130 min at 100°C
Solvent tolerance	24 % methanol[d]	64% isopropanol[d]	Active in 30% isopropanol
Reference[e]	1	2	3

[a] The activity was assayed on the oxidation of 2-butanol.

[b] The activity was assayed on the oxidation of isopropanol.

[c] The activity was assayed on the oxidation of 2, 3-butanediol.

[d] The solvent concentration at which half of the full activity remains.

[e] Reference: 1, this work; 2, Bogin et al. 2002; Olofsson et al. 2005 3, Machielsen et al. 2006; Zhu et al. 2006.

Table 3-16 Correlation between the substrate structure and the activity of *T. guaymasensis* ADH

Name	R groups[a] [R'-CH(OH)-R"]	Specific activity (U mg^{-1})	Stereoselectivity
L-threonine	CH_3-CH(OH)-$CH(NH_2)COOH$	0	
2-butanol	CH_3-CH(OH)-CH_2CH_3	1149 ± 24	No
2, 3-butanediol	CH_3-CH(OH)-$CH(OH)CH_3$	896 ± 30[b]	Yes

[a] R', smaller side group (methyl group, in red); R", larger side group (in blue).

[b] The data was from the oxidation of (*2R*, *3R*)-(-)-2, 3-butanediol.

patterns between mesophilic and hyperthermophilic proteins shed light on the understanding of common features of thermostability (Robb and Clark 1999; Sælensminde et al. 2007; Sterner and Liebl 2001). *T. guaymasensis* ADH showed 77% identity to *T. brockii* ADH and 65% identity to *C. beijerinckii* ADH (**Fig. 3-19**), suggesting that gains in stabilization might be achieved in regions that are less conserved (Kumar et al. 2000). The uncharged polar residues Gln, Asn, Ser decreased in *T. guaymasensis* ADH, in which the first two are prone to deamidation and known to be the most temperature sensitive (Cambillau and Claverie 2000; Wright 1991). In contrast, hyperthermophilic and thermophilic proteins showed an increase of charged amino acid residues, especially Arg, Glu. The equal increase of oppositely charged residues (Arg and Glu) in hyperthermophiles most likely led to the increased amount of ion pairs observed already on their proteins (Cambillau and Claverie 2000). As the best helix-forming residue, alanine increased, similarly to previous observations (Vieille et al. 2001). Proline, on the other side, prevents the formation of hydrogen bonds to the main chain nitrogen atom. Proline composition increased significantly, which might be the structural base of rigidity of hyperthermophilic enzymes. The difference between hyperthmophilic and mesophilic proteins/enzymes would provide thoughts to increase thermal stability of mesophilic enzymes (**Fig. 3-19**). Referring to the information from *T. brockii* ADH, several mutants of *C. beijerinckii* ADH with site-directed substitution were successfully constructed and characterized showing enhanced thermal stability (**Table 3-17**). The comparison among ADHs from *T. guaymasensis*, *T. brockii* and *C. beijerinckii* will provide useful guidance for the future improvements of thermal stability.

It was unexpected that the enzyme was oxygen sensitive. The reports of ADH oxygen inactivation were usually associated with iron-containing ADHs. The oxygen inactivation of zinc-containing ADHs has been scarcely reported. The well known example is the zinc-containing ADH from mesophilic *S. cerevisiae* whose inactivation was due to oxidation of SH group (Bühner and Sund 1969). Since zinc cannot be oxidized further, the inactivation of the enzyme may also be a consequence of the damage of amino acid residues such as

Figure 3-19 Amino acid sequence alignment of alcohol dehydrogenases from *T. guaymasensis* (TgADH), *T. brockii* (TbADH), and *C. beijerinckii* (CbADH).

The sequences were aligned using Clustal W (Thompson et al. 1994) with subsequent manual adjustments. Amino acid residues of TgADH are in the one-letter code. The red letters highlighted in yellow represent those amino acid residues which site-directed mutageneses have been performed (Bogin et al. 1998; Bogin et al. 2002; Goihberg et al. 2007; Musa et al. 2007; Phillips 2002). Symbols used: "*", residues or nucleotides that are identical in all sequences in the alignment; ":", conserved substitutions; "." , semi-conserved substitutions; "-", identical amino acid; blank, no corresponding amino acid.

Table 3-17 Protein engineering of zinc-containing ADHs

Origin	Substitution	Characteristics[a]	Ref. [b]
C. beijerinckii	L316P, S24P	Increase thermal stability from $T_{1/2}^{60min}$ of 63.8°C to 68.2°C (L316P) and 66.0°C (S24P), respectively	1
	V224E/S254K Q165E/M304R	Increase thermal stability from $T_{1/2}^{60min}$ of 63.8°C to 69.2°C (V224E/S254K) and 68.4°C (Q165E/M304R), respectively	2
	Q100P	Increase thermal stability from $T_{1/2}^{60min}$ of 63.8°C to 72.5°C	3
S. solfataricus	N249Y	Increase thermal stability from Tm of 90 to 93°C; increase activity from *k*cat of 3.6 s^{-1} to 21.7 s^{-1} as measured at 65°C with benzyl alcohol as the substrate	4
T. ethanolicus	S39T C295A	Change substrate specificity; change stereospecificity from *R*-configured to *S*-configured	5
	W110A	Expand range of catalyzing substrates including phenyl ring-containing substrates	6
E. coli	H90R H90N H90A	Change substrate specificity for threonine amide, threonine methyl ester, threonine, 2-Amino-3-hydroxypentanoate and threonine hydroxamate	7

Abbreviations for amino acids (aa): A, alanine; R, arginine; N, Asparagine; C, cysteine; E, glutamic acid; Q, glutamine; H, histidine; L, leucine; K, lysine; M, methionine; P, proline; S, serine; T, threonine; W, tryptophan; Y, tyrosine; V, valine.

[a] $T_{1/2}^{60min}$ is the temperature at which 50% of the enzymatic activity is lost after 1-h incubation. Tm is the temperature at which the protein denatures.

[b] References: 1, Bogin et al. 1998; 2, Bogin et al. 2002; 3, Goihberg et al. 2007; 4, Esposito et al. 2003; Giordano et al. 1999; Giordano et al. 2005; 5, Phillips 2002; 6, Musa et al. 2007; 7, Johnson and Dekker 1998.

cysteine residues. The enzyme of *T. guaymasensis* ADH had 4 cysteine residues per subunit (Cys38, Cys55, Cys212 and Cys305). Except Cys55, all the other three were conserved to *T. brockii* ADH. Cys38 was highly conserved in zinc-containing ADHs and a putative active site residue, which has been proved to coordinate the binding of catalytic zinc in *T. brockii* ADH.

The potential role of *T. guaymasensis* ADH is not easy to ascertain although the conserved domain search indicated homology to threonine dehydrogenase. *T. guaymasensis* ADH did not catalyze the oxidation of threonine as tested at different pHs (pH 7.5, 8.8 and 10.5). Meanwhile, the possible physiological role for *T. guaymasensis* ADH might arise from its ability of interconversion between alcohols and corresponding ketone or aldehydes. *T. guaymasensis* ADH reversibly catalyzed the oxidation of 2, 3-butanediol to acetoin, which cannot be oxidized to diacetyl. Regarding this feature, properties of *T. guaymasensis* ADH including its stereoselectivity were highly similar to those observed on the (*2R*, *3R*)-(-)-butanediol dehydrogenase (BDH) from *S. cerevisiae* (González et al. 2000). *S. cerevisiae* can grow on 2, 3-butanediol as the sole carbon and energy source, in which BDH content had over 3 fold increases. The role of BDH from *S. cerevisiae* was suggested to be required for oxidation and formation of 2, 3- butanediol. However, no 2, 3-butanediol production was observed for the present organism *T. guaymasensis*, implying that *T. guaymasensis* ADH might be more likely to be involved the formation of acetoin from diacetyl. In addition, *T. guaymasensis* also produced mM-level of ethanol and the enzyme had higher catalytic efficiency on NADPH over $NADP^+$ as coenzymes, which leads to propose that the enzyme could be concurrently responsible for ethanol and acetoin formation during fermentation (**Fig. 3-20**).

In terms of real or potential industrial applications, catalytic properties of enzymes are usually enhanced by using three approaches, biodiversity prospecting, random mutagenesis and site-directed mutagenesis (Rubin-Pitel and Zhao 2006). The last one is a robust approach widely applied for ADHs from hyperthermophile *S. solfataricus*,

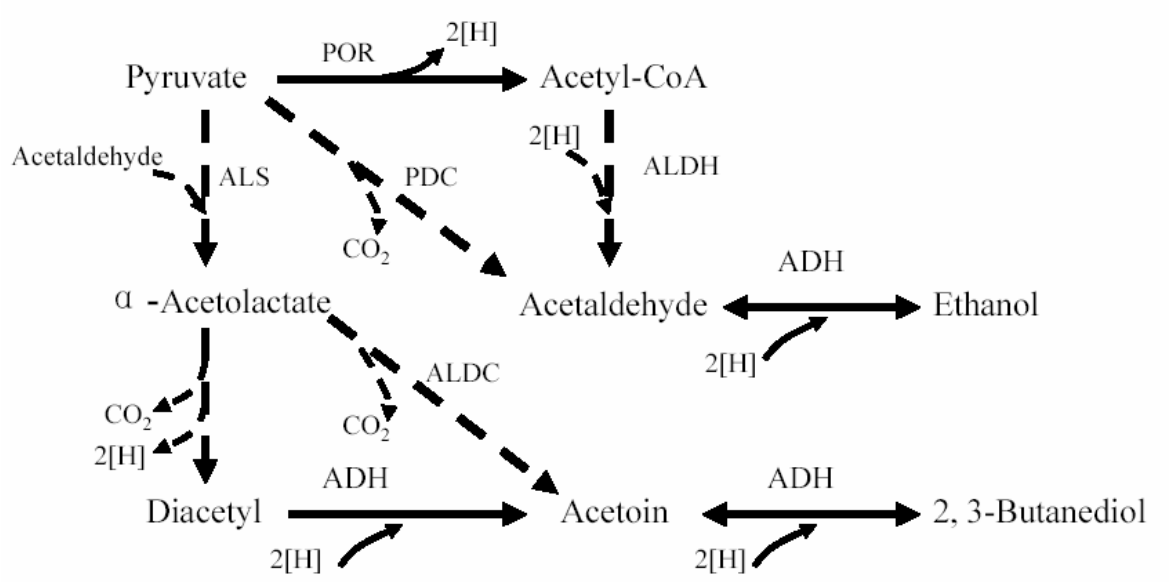

Figure 3-20 Schematic pathways of alcohol formation in *T. guaymasensis*.

ADH, alcohol dehydrogenase (This study); ALDC, α-acetolactate decarboxylase (Blomgvist et al. 1993); ALDH, CoA-dependent aldehyde dehydrogenase (Yan and Chen 1990); ALS, α-acetolactate synthase (Blomgvist et al. 1993); PDC, pyruvate decarboxylase (Ma et al. 1997); POR, pyruvate ferredoxin oxidoreductase (Eram and Ma, unpublished results). The dashed arrows represent speculated steps while the solid arrows represent the steps approved by activities of purified enzymes.

thermophiles *T. brockii* and *T. ethanolicus,* and mesophile *E. coli*. A catalytic site point mutation (Trp110Ala) made *T. ethanolicus* ADH active on phenylacetone to stereoselectively produce phenyl-2-propanol with *S*-configuration and also active on benzyl acetone (Ziegelmann-Fjeld et al. 2007). Mutations Ser39Thr and Cys295Ala in the active site of *T. ethanolicus* ADH shifted enantioselectivity toward (*R*)-alcohols: mutation Ser39Thr decreased the size of the large alkyl-binding pocket and mutation Cys295Ala enlarged the small binding pocket, allowing for longer alkyl chains to fit (Heiss et al. 2001b; Tripp et al. 1998). Those three amino acid residues are conserved in *T. guaymasensis* ADH, which shed light on further protein engineering (**Fig. 3-19**). Other amino acid substitution might be also instructive albert no guarantee for close relevance (**Table 3-17**). The substitution Asn249Tyr at the coenzyme binding domain of *S. solfataricus* ADH decreased the affinity for NAD(H) coenzyme and increased thermophilicity and thermal stability (Esposito et al. 2003a; Giordano et al. 1999). In the $_{L}$-threonine dehydrogenase from *E. coli*, the substitution His90 to Ala, Asp, or Arg by site-directed mutagenesis caused the alternation of substrate specificity (Johnson and Dekker 1998). It is believed that the 3-D structure of *T. guaymasensis* ADH is needed to further clarify amino acid residues critical for catalysis.

Chapter 4 An Iron-containing Alcohol Dehydrogenase from *Thermococcus* strain ES1 and Its Recombinant Form from *Escherichia coli*: Property Comparison and Molecular Characterization

4.1 ABSTRACT

The native ADH from *Thermococcus* strain ES1 was purified to homogeneity using a three-step liquid chromatography while the recombinant enzyme over-expressed in *Escherichia coli* was isolated by a simpler procedure including heat treatment. After purification, the recombinant enzyme exhibited specific activity of 52.8 Umg^{-1} and very close to that of native enzyme (57 U mg^{-1}). Both $NADP^+$-dependent enzymes were homotetramers with the subunit size of 45 ± 1 kDa. The optimal pHs for ethanol oxidation and acetaldehyde reduction were 10.5 and 7.0, respectively. Both enzymes enabled the oxidation of a series of primary alcohols and diols but no activity towards methanol, glycerol and secondary alcohols. The recombinant enzyme contained 1 *g* atom Fe per subunit determined by inductively coupled plasma mass spectrometry, which is consistent with the number reported for the native enzyme. Both enzymes were sensitive to oxygen, and a half life upon exposure to oxygen was about 3-4 min. Both enzymes showed lower *K*m values for acetaldehyde and NADPH than on ethanol and $NADP^+$, indicating the native enzyme could be involved in ethanol formation *in vivo*.

The deduced amino acid sequence was a 406 amino acid polypeptide corresponding to the calculated molecular mass of 44.5 kDa. Its sequence showed the highest identity to ADHs from *Thermococcus zilligii* and *Thermococcus hydrothermalis* (80%) and high degrees of identity (62 to 72%) to iron-containing ADHs from *Thermotoga* and *Thermoanaerobacter* species. The conserved domain search revealed it belonged to the family of iron-containing ADHs. The enzyme had classical catalytic metal and dinucleotide-binding motifs among iron-containing ADHs, $D_{208}H_{212}H_{278}H_{292}$ and $GGGSX_2D$ (residues 109-115), respectively. The 3-D structure modeling of the enzyme further verified two typical domains: the α/β-dinucleotide-binding N-terminal domain and the all-α-helix C-terminal domain.

4.2 INTRODUCTION

Alcohol dehydrogenases are a group of oxidoreductases that catalyze the interconversion between alcohols and corresponding aldehydes or ketones. ADHs are ubiquitous and most of them are either NAD^+-dependent or $NADP^+$-dependent or both. The group of $NAD(P)^+$-dependent ADHs differ in size and metal content. The metal-free and zinc-containing ADHs have the size of ~250 and ~350 amino acids, respectively. The typical representatives of iron-containing ADHs are larger, varying from 382 to 891 amino acids (Reid and Fewson 1994). Iron-containing ADHs share high similarity of structural characteristics. Crystal structures of iron-containing ADHs revealed that iron was coordinated by conserved residues in *T. maritima* (Asp189, His193, His256, and His270) and *Escherichia coli* (Asp196, His200, His263, and His277) (Montella et al. 2005; Schwarzenbacher et al. 2004). Particularly, some zinc-containing ADHs, e.g., glycerol dehydrogenases, share high sequence similarity to this group of iron-containing ADHs (Ruzheinikov et al. 2001; Williamson and Paquin 1987). The physiological role of characterized iron-containing ADHs in mesophiles is involved in the formation of various alcohols such as ethanol, 1, 2-propanediol, 1, 3-propanediol and 1-butanol (Conway and Ingram 1989; Mackenzie et al. 1989; Walter et al. 1992; Zheng et al. 2004). In hyperthermophiles, how ADHs function in alcohol metabolism is not well understood. It was proposed that the iron-containing ADH from *Thermococcus* strain ES1 was in response of disposing of excess reductant to produce alcohols (Ma et al. 1995).

Hyperthermophiles are designated as the organisms growing optimally ≥80°C and belong to the domains of bacteria and archaea. Of ADHs from hyperthmophilic archaea, those from the genus *Thermococcus* are the best characterized. Four iron-containing ADHs have been purified and well characterized from *Thermococcus* species: *Thermococcus litoralis* (Ma et al. 1994), *Thermococcus* strain ES1 (Ma et al. 1995), *Thermococcus zilligii* (Li and Stevenson 1997; Ronimus et al. 1997), and *Thermococcus hydrothermalis* (Antoine et al. 1999). ADHs from hyperthermophiles are usually expressed in *Escherichia coli* (Antonie et al. 1999; Cannio et al. 1996; Hirakawa et al. 2004; Kube et al. 2002; Machielsen et al.

2006; van der Oost et al. 2001). To date, the ADH from *T. hydrothermalis* is the only example of heterotrophic over-expression in *E. coli* among iron-containing ADHs from archaeal hyperthermophiles. Despite the activity discrepancy between native and recombinant ADHs from *T. hydrothermalis*, they possess identical main characteristics (Antonie et al. 1999).

The archaeon *Thermococcus* strain ES1 is an anerobic hetertroph growing up to 91°C (Pledger and Baross 1989). The ADH from *Thermococcus* strain ES1 is iron-containing and up-regulated under S^0-limited conditions (Ma et al. 1995). This report here describes the molecular characterization of ADH from *Thermococcus* strain ES1 and comparison of properties between native enzyme and its recombinant form from *E. coli*.

4.3 MATERIALS AND METHODS

4.3.1 Organisms and chemicals

High-grade chemicals and enzymes (lysozyme and DNase I) were commercially supplied by Sigma-Aldrich (Oakville, ON, Canada). Additional items were purchased from VWR International Canada (Mississauga, ON, Canada), or Fisher Scientific (Ottawa, ON, Canada). All fast protein liquid chromatography (FPLC) materials and columns (DEAE-Sepharose, Hydroxyapatite, Phenyl-Sepharose and Superdex 200 gel filtration columns) used were obtained from Amersham Health (Oakville, ON, Canada). The cells for *Thermococcus* strain ES1 were grown as described previously (Ma et al. 1995) and the recombinant *E. coli* was supplied by collaborators (Grunden and Adams, University of Georgia, GA, USA).

4.3.2 Purification of native ADH

Since iron-containing ADHs are commonly oxygen sensitive, all the purification steps were carried out anaerobically. Frozen cells (15 g) were thawed anaerobically in 75 ml buffer A [10 mM Tris buffer containing 5% (v/v) glycerol, 2 mM dithiothreitol (DTT), 2 mM sodium dithionite (SDT) and 0.01 mg mL^{-1} DNase I, pH 7.8]. The resuspended mixture was incubated under stirring at 37°C for 2 h. The cell extracts were then centrifuged at 10,000× *g* for 30 min at room temperature and the supernatant was collected as the cell-free extract (CFE). The CFE was loaded onto a DEAE-Sepharose column (5 × 10 cm) which had been equilibrated with buffer A. A linear gradient (0-0.35 M NaCl in buffer A) was applied at a flow rate of 3 ml min^{-1} and the ADH was eluted out at a concentration of 0.22 M NaCl in buffer A. The fractions with ADH activity were pooled and loaded onto a pre-equilibrated Hydroxyapatite column (2.6 × 15 cm) at a flow rate of 1.5 ml min^{-1}. A linear gradient (0-0.5 M potassium phosphate in buffer A) was run and the ADH activity was eluted out when the salt concentration was as high as 0.5 M potassium phosphate in buffer A. Lastly, the fractions with ADH activity was desalted and

concentrated by ultrafiltration with YM-10 membrane. The concentrated sample was loaded onto a gel filtration column pre-equilibrated with buffer A containing 150 mM potassium chloride.

4.3.3 Purification of the recombinant ES1ADH from *E. coli*

Frozen cells (10 g) were thawed anaerobically and resuspended in 50 ml buffer A (50 mM Tris/HCl buffer containing 5% (v/v) glycerol, 2 mM DTT, 2 mM SDT, 0.1 mg ml^{-1} lysozyme and 0.01 mg ml^{-1} DNase I, pH 7.8). The mixture incubated at 37°C for 2 hours under stirring. Since the enzyme was thermostable, a step of heat precipitation was applied prior to the purification. The cell extract was incubated at 60°C for 1 hour and the solution turned gel-like. The denatured proteins and cell debris in the cell-crude extract were removed by centrifugation at 10,000 × *g* for 30 min at room temperature. The supernatant was loaded onto a pre-equilibrated DEAE-Sepharose column (5 × 10 cm) with buffer A. A linear gradient (0-0.35 M NaCl in buffer A) was applied at a flow rate of 3 ml min^{-1} and the ADH was eluted out at a concentration of 0.25 M NaCl in buffer A. Although the recombinant ADH was purified after DEAE-Sepharose column, a part of sample was loaded onto the gel filtration column (2.6 × 60 cm) in order to determine the size of its native form.

4.3.4 Determination of molecular mass

The molecular mass of the enzyme subunit was determined using SDS-PAGE (Laemmli 1970) and a calibration curve was obtained using the low molecular mass standard from Bio-Rad (14-97 kDa, Bio-Rad Laboratories, ON, Canada). Alternatively, the subunit size of both native and recombinant ES1ADHs was measured using mass spectrometry. The enzyme (native or recombinant ES1ADH) was dissolved in 18.2 MΩ cm deionized water and sent for positive electrospray ionization-mass spectrometry analyses (Mass Spectrometry Facility, University of Waterloo, Waterloo, ON, Canada). The native molecular mass of the purified enzyme was estimated by the gel filtration chromatography

on the Superdex 200 column (2.6 × 60 cm). The column was equilibrated with buffer A containing 100 mM KCl at a flow rate of 2 ml min^{-1} before applying standard samples of protein kits (Pharmacia, NJ, USA) that contained blue dextran (molecular mass, Da, 2,000,000), thyroglobulin (669,000), ferritin (440,000), catalase (232,000), aldolase (158,000), bovine serum albumin (67,000), ovalbumin (43,000), chymotrysinogen A (25,000) and ribonuclease A (13,700).

4.3.5 Enzyme assay and protein determination

ADH activities were anaerobically determined at 80°C by measuring the ethanol-dependent reduction of $NADP^+$ or the acetaldehyde-dependent oxidation of NADPH at 340nm. Unless specifically stated, the enzyme assay was carried out in duplicate using the standard reaction mixture of ethanol oxidation that contained 100 mM CAPS (pH 10.4), 90 mM ethanol, and 0.4 mM $NADP^+$. The reaction mixture of acetaldehyde reduction composed of 100 mM HEPES buffer, 0.4 mM NADPH and 90 mM acetaldehyde. The reaction was initiated by adding 1.5 μg enzyme. One unit of ADH activity is defined as the formation or oxidation of 1 μmol of NADPH per min. The protein concentrations of all samples were determined using the Bradford method and bovine serum albumin served as the standard protein (Bradford 1976).

4.3.6 Characterization of catalytic properties

The optimal pH of ethanol-dependent oxidation of native and recombinant ES1ADHs was determined at 80°C using a set of 100 mM buffers: HEPES (pH 6.5, 7.0, 7.5 and 8.0), EPPS (pH 8.0, 8.5, 8.8, 9.0), glycine (pH 9.0, 9.5, 10.0) and CAPS (pH 10.0, 10.5, 11.0). The optimal pH of acetaldehyde-dependent reduction of native and recombinant ES1ADH was measured between pH 5.5 and 9.5 using the following buffers (100 mM): citrate (pH 5.5 and 6.0), PIPES (pH 6.0, 6.5 and 7.0), HEPES (pH 7.0, 7.5 and 8.0), EPPS (pH 8.0, 8.5, and 9.0), glycine (pH 9.0 and 9.5). The thermostability was evaluated by incubating the enzyme in sealed serum bottle at 95°C and measuring the residual activities at different

time intervals. The effect of oxygen on enzyme activity was investigated by vortexing the enzyme sample in the air at room temperature and determining the residual activity after oxygen exposure. For the test of substrate specificity, various primary and secondary alcohols were used to replace ethanol in the standard oxidation assay mixture.

Kinetic parameters were determined for the substrates (ethanol or acetaldehyde) and coenzymes ($NADP^+$ or NADPH). For determining enzyme kinetic parameters, various substrate concentrations (0 to ≥ 10 × apparent *K*m unless specified) for NADPH (0, 0.025, 0.05, 0.1, 0.15, 0.2 and 0.4 mM), acetaldehyde (0, 2.3, 4.6, 9.1, 22.3, 27.3, 36.4, 45.5 and 91 mM), $NADP^+$ (0, 0.02, 0.04, 0.08, 0.10, 0.15, 0.2, 0.3 and 0.4 mM), ethanol (0, 4.4, 8.7, 13.0, 17.4, 34.8, 52.2, 70, 87 and 174 mM) were used for the determination of corresponding activities at 80°C, while concentrations of the corresponding co-substrates were kept constant and higher than 10 × apparent *K*m. Apparent values of *K*m and *V*max were calculated from their Lineweaver-Burk plots.

4.3.7 Metal analyses

The metal contents of the homogeneous proteins were determined by inductively coupled plasma mass spectrometry (VG Elemental PlasmQuad 3 ICP-MS at the Chemical Analysis Laboratory, University of Georgia, USA). The enzyme was pretreated to wash off non-binding metals in the anaerobic chamber where the oxygen level was kept below 1 ppm. The buffer used was 10 mM Tris/HCl containing 2 mM DTT (pH 7.8). The washing procedure was carried out by using the YM-10 Amicon centrifuge tubes (Millipore, Billerica, MA, USA). The washing procedures included 7 cycles of centrifugation (concentration and refilling with the washing buffer) and the passthrough was collected as controls.

4.3.8 Data mining

The homologues of the deduced amino acid sequence of ES1ADH were identified by the BLAST program (http://www.ncbi.nlm.nih.gov/BLAST) using the default parameters (Altschul et al. 1997). Additional sequences were retrieved from the Pfam database (Bateman et al. 2002). Sequence alignments and phylogenetic trees were constructed by the neighbor-joining method of Clustal W with default parameters (Thompson et al. 1994). Theoretical isoelectric point and molecular weight were calculated by the ProtParam program at the ExPASy Proteomics Server using standard parameters (Gasteiger et al. 2005). A 3-D structure of ES1ADH monomer was modeled using the Swiss Model server (Guex and Peitsch 1997; Kopp and Schwede 2004; Peitsch 1995; Schwede et al. 2003). PyMOL was used to analyze and visualize the 3-D structure (Delano 2002).

4.4 RESULTS

4.4.1 Purification of native and recombinant ES1ADHs

The ADH from *Thermococcus* strain ES1 was purified through a three-step chromatography using the FPLC system. A major separation was achieved using the DEAE-Sepharose column and the fractions with ADH activity showed only two dominant bands on the SDS-PAGE. The subsequent Hydroxyapatite chromatography successfully separated the ADH and non-target proteins (**Fig. 4-1**). The gel filtration chromatography revealed that the size of the purified native enzyme was 182 ± 4 kDa. The purified ES1 ADH had a specific activity of 57 U mg^{-1} with a yield of 40% (**Table 4-1**). The ADH content was estimated to be about 10% of proteins in the cell-free extract.

The recombinant ADH was purified from *E. coli* using a modified procedure. Prior to liquid chromatography, heat treatment was applied to the cell extract. To access the effect of heat treatment, *E. coli* cell extract was incubated at 60°C and the residual activity was determined at different time intervals. One-hour heating at 60°C caused no loss of enzyme activity but significantly reduced the protein concentration from 13 mg ml^{-1} to 2.9 mg ml^{-1} (**Fig. 4-2**). Subsequently, the recombinant ADH was purified to homogeneity after DEAE-Sepharose column (**Fig. 4-3**). The purified recombinant ES1ADH had a specific activity of 52.8 U mg^{-1} with a higher yield of 75% (**Table 4-2**). The recombinant ES1ADH content in *E. coli* was calculated to be about 13% of proteins in the cell extract. The data from gel filtration showed that the size of the recombinant enzyme was 176 ± 4 kDa. The SDS-PAGE analyses showed that both native and recombinant ES1ADHs had almost identical subunit size of 45 ± 1 kDa, suggesting that both enzymes were homotetramers in the native form (**Fig. 4-4**). Moreover, the data from mass spectrometry indicated that the molecular mass of native and recombinant ES1ADH subunits were 44819 and 44831 Dalton, respectively, both of which were slightly greater than the theoretical molecular weight calculated from the deduced amino acid sequence of ES1ADH (44807 Dalton).

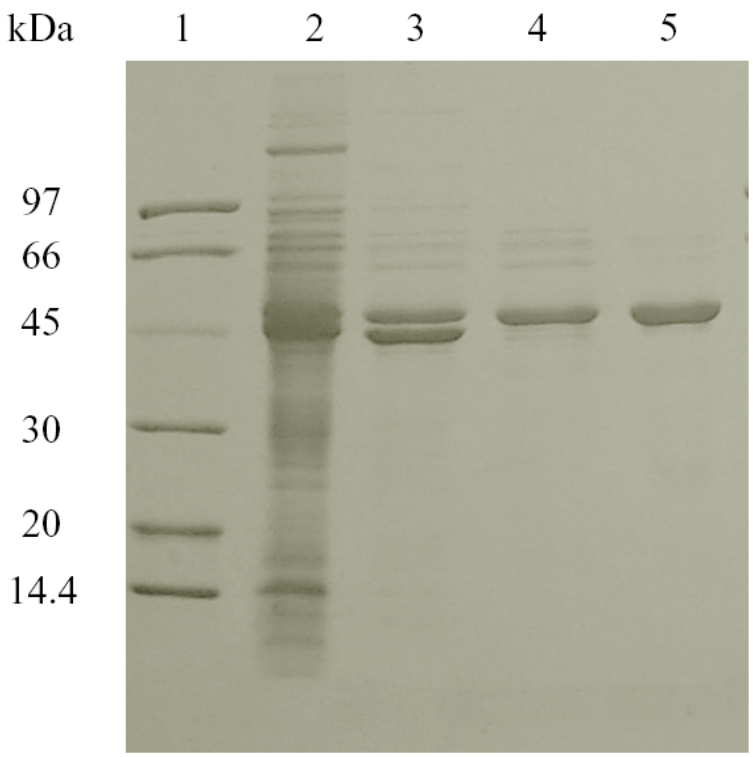

Figure 4-1 SDS-PAGE (12.5%) of the purified ADH from *Thermococcus* strain ES1.

Lane 1, molecular markers; lane 2, cell-free extract; lane 3, DEAE-Sepharose; lane 4, Hydroxyapatite; lane 5, gel filtration. Amongst lanes 2-5, the proteins with equivalent amounts to 2 μg pure ADH was loaded into each lane.

Table 4-1 Purification of the ADH from *Thermococcus* strain ES1

Purification Steps	Total protein (mg)	Total Activity (U)	Specific activity (U mg^{-1})[a]	Purification Fold	Yield (%)
Cell-free extract	154	862	5.6	1	100
DEAE-Sepharose	33.7	797	23.6	4.2	92
Hydroxyapatite	12.9	616	47.8	8.5	71.4
Gel-filtration	6.1	348	57	10.1	40

[a] Enzyme activity was measured in 100 mM EPPS buffer (pH 8.8).

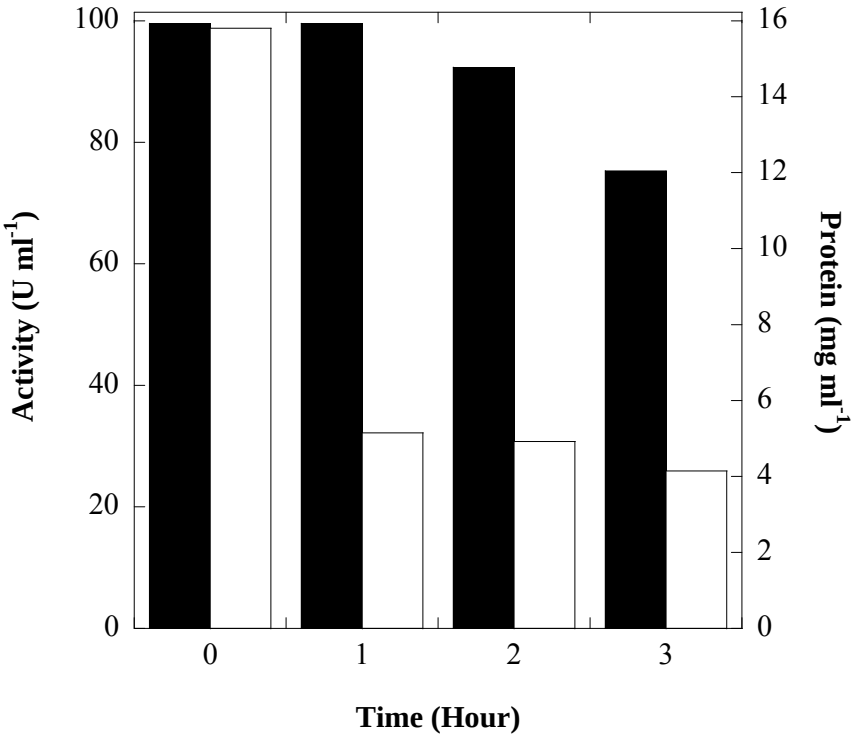

Figure 4-2 Heat treatment of *E. coli* cell extract.

The enzyme activity was assayed in the EPPS buffer (100 mM, pH 8.8). Filled columns stand for enzyme activity. Open columns stand for protein concentration.

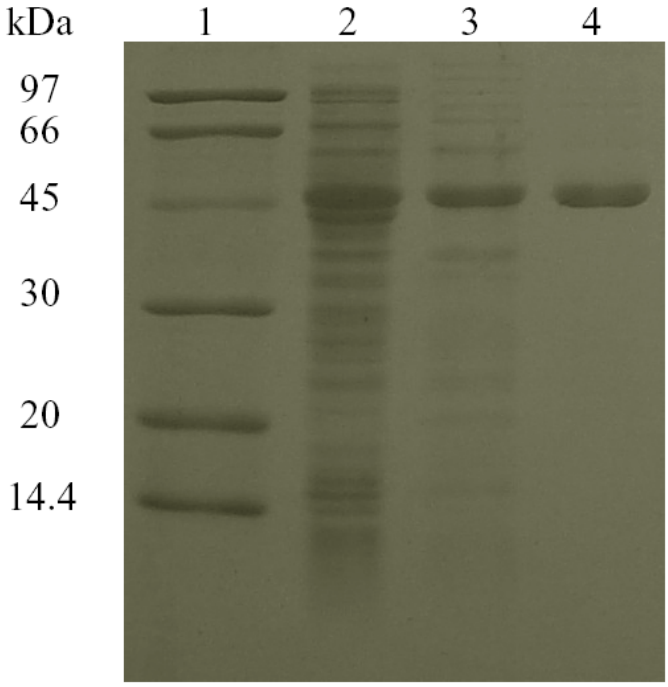

Figure 4-3 SDS-PAGE analyses (12.5%) of ES1ADH from *E. coli*.

Lane 1, molecular markers; lane 2, cell-crude extract; lane 3, heat precipitation; lane 4, DEAE-Sepharose. Amongst lanes 2-4, the proteins with equivalent amounts to 2 μg pure ADH were loaded into each lane.

Table 4-2 Purification of the recombinant ES1ADH from *E. coli*

Purification Steps	Total protein (mg)	Total activity (U)	Specific activity (U mg^{-1})[a]	Purification Fold	Yield (%)
Cell-crude extract	650	4445	6.8	1	100
Heat precipitation	145	3596	24.8	3.6	81
DEAE-Sepharose	63	3326	52.8	7.8	75

[a] Enzyme activity was measured in the 100 mM EPPS buffer (pH 8.8).

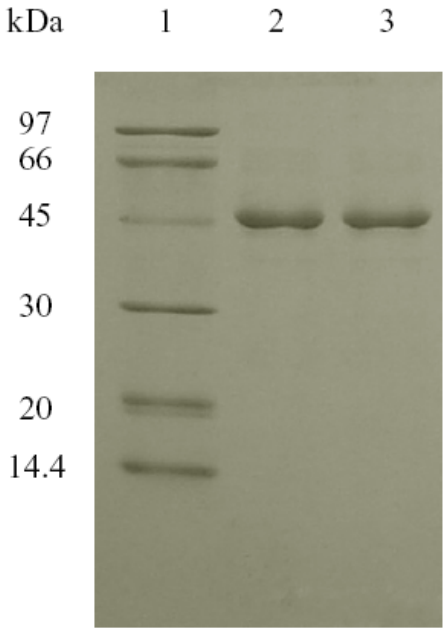

Figure 4-4 SDS-PAGE (12.5%) of native and recombinant ES1ADHs.

Lane 1, molecular markers; lane 2, 1.5 μg native ES1ADH; lane 3, 1.5 μg recombinant ES1ADH.

4.4.2 Comparison of catalytic properties

Both enzymes had very similar catalytic properties. The effect of pH on enzyme activities was investigated with a set of buffers ranging from pH 5.5 to 11.0. The optimal pH for ethanol oxidation was pH 10.3-10.5 (**Fig. 4-5**) and that for acetaldehyde reduction was pH 7.0 (**Fig. 4-6**). When the buffer pH value was higher than 10.5, the activity of ethanol oxidation had a remarkable decrease and no activity was detectable at pH 11.0. Over a temperature range from 30 to 95°C, the activity of both enzymes increased along with the increase of assay temperature (**Fig. 4-7**). When the thermostability was tested at 95°C, the $t_{1/2}$ of both enzymes was calculated to about 4 hours (**Fig. 4-8**).

To investigate the substrate specificity, various primary and secondary alcohols were used in activity assays with $NADP^+$ (**Table 4-3**). No activity on methanol, glycerol and secondary alcohols (2-propanol, 2-butanol and 2-pentanol) was detected. Primary alcohols with C_2–C_8 carbon chains provided 60–180% of the ADH activity compared with ethanol oxidation. Among C_2–C_8 primary alcohols, 1-pentanol gave the highest specific activity of 180 U mg^{-1}. In addition, ADH had the activity of 41 U mg^{-1} toward 2-phenylethanol.

The apparent *K*m and *V*max values for $NADP^+$, ethanol, NADPH and acetaldehyde were determined (**Table 4-4**). The catalytic efficiency (*k*cat/*K*m) of NADPH and acetaldehyde was 2.5-3 folds greater than that of $NADP^+$ and ethanol. Moreover, the *K*m value of NADPH and acetaldehyde was almost 10 times lower than that of $NADP^+$ and ethanol.

The metal content of the recombinant ADH was determined using ICP-MS. The results (**Table 4-5**) indicated the recombinant ADH contained 1 *g* atom iron per subunit, which is consistent with previous observation on the native enzyme (Ma et al. 1995). The recombinant also contained 0.3 *g* zinc atom per subunit and trace amount of nickel (0.03 g atom per subunit). The occupancy of zinc with 0.3 *g* atom per subunit did not appear to

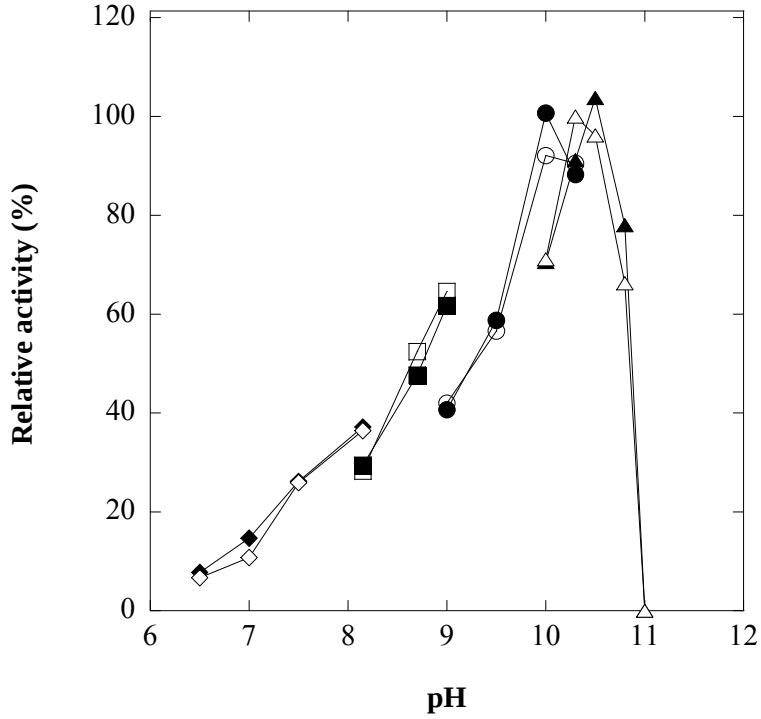

Figure 4-5 pH dependence of ES1ADHs on the ethanol oxidation.

Open symbols represent the ADH from *Thermococcus* strain ES1 and filled symbols represent its recombinant ADH from *E. coli*. The buffers used were HEPES (diamonds), EPPS (squares), glycine (circles) and CAPS (triangles). The relative activity of 100% equals to 105.2 U mg^{-1} on the ethanol oxidation.

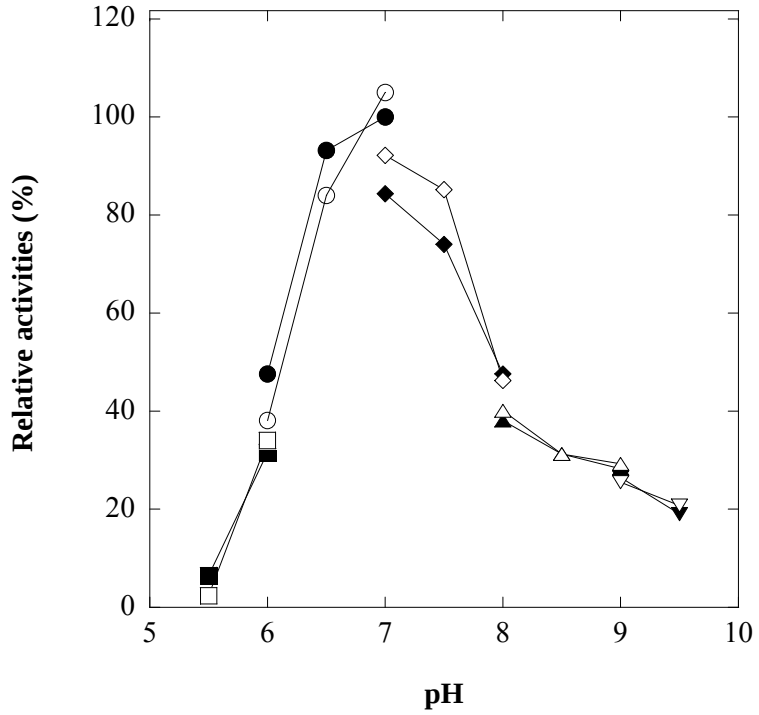

Figure 4-6 pH dependence of ES1ADHs on the acetaldehyde reduction.

Filled symbols represent the native ES1ADH. Open symbols represent the recombinant ES1ADH. The buffers used were sodium citrate (squares), PIPES (circles), HEPES (diamonds), EPPS (vertical triangles), glycine (inverted triangles). The relative activity of 100% means 28.0 U mg^{-1} on the acetaldehyde reduction.

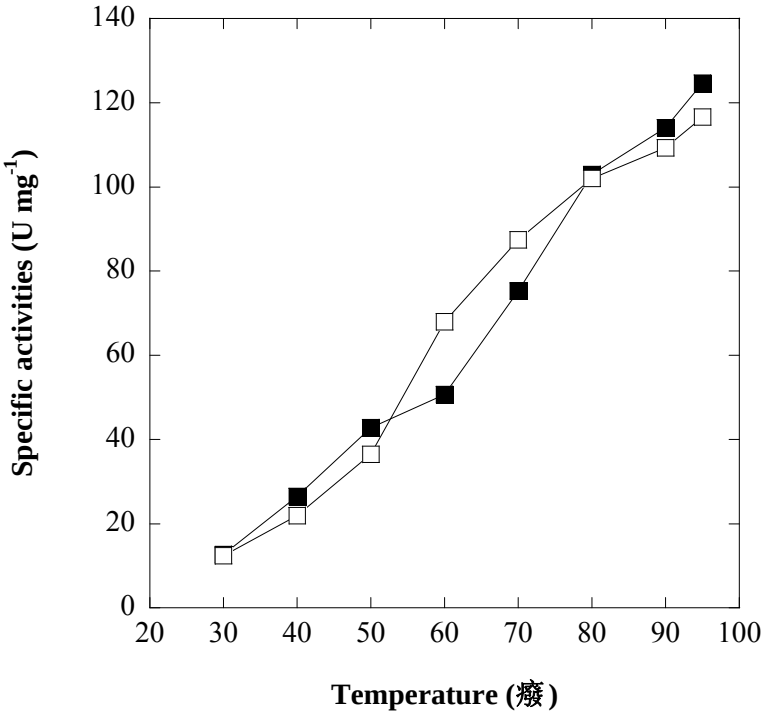

Figure 4-7 Temperature dependence of ES1ADHs.

Filled squares, native ES1ADH; open squares, recombinant ES1ADH.

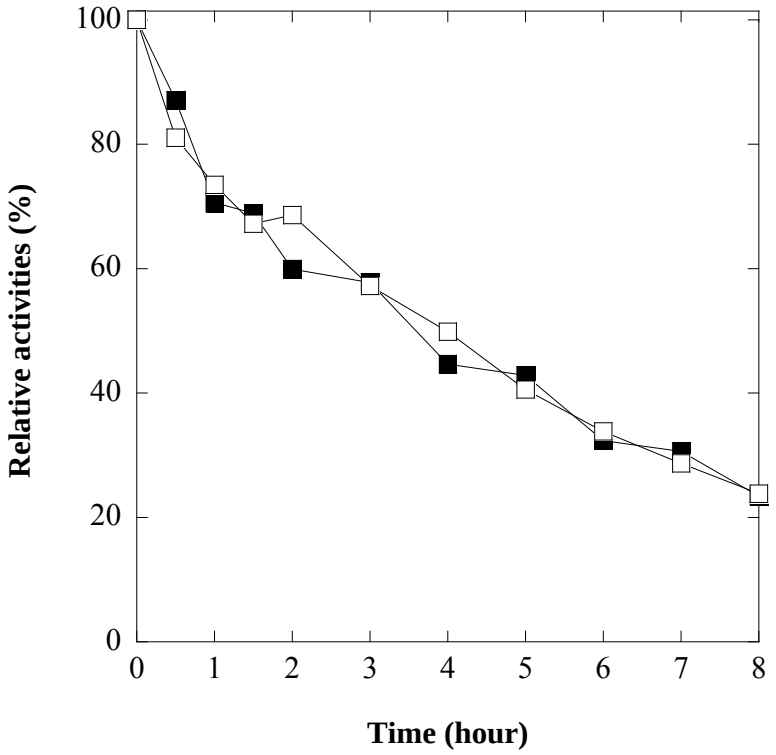

Figure 4-8 Thermostability of native and recombinant enzymes.

The relative activity of 100% means the full activity of both enzymes. Filled squares, the native ES1ADH; open squares, the recombinant ES1ADH.

Table 4-3 Relative activities of native and recombinant ADHs towards alcohol oxidation

Alcohols (90 mM)	Native ES1ADH (%)	Recombinant ES1ADH (%)
Methanol	0	0
Ethanol	100 ± 2.6	91.6 ± 3.0
1-Propanol	120.6 ± 3.2	102.8 ± 2.0
1-Butanol	154.6 ± 5.2	142.6 ± 2.6
1-Pentanol	184 ± 3.2	175.6 ± 5.2
Hexyl alcohol	137.8 ± 4.0	114.4 ± 3.6
1-Heptanol	94 ± 3.6	100.8 ± 4.8
1-Octanol	68.8 ± 2.6	79 ± 1.0
2-Propanol	0	0
2-Butanol	0	0
2-Pentanol	0	0
2-Phenylethanol	40.2 ± 2.0	43 ± 1.5
Glycerol	0	0

Activities were determined using each substrate to replace 90 mM ethanol. The activity of native enzyme on ethanol (110 ± 2.9 U mg^{-1}) was taken as 100%.

Table 4-4 Kinetic parameters of native and recombinant ES1ADHs

Substrate	Co-substrate (mM)	Parameter	Native	Recombinant
$NADP^+$	Ethanol(90)	Apparent *K*m (mM)	0.06	0.058
		Apparent *V*max (U mg^{-1})	120	116
		*k*cat (s^{-1})	90	87
		*k*cat/*K*m ($s^{-1}M^{-1}$)	1,500,000	1,500,000
NADPH	Acetaldehyde (90)	Apparent *K*m (mM)	0.007	0.006
		Apparent *V*max (U mg^{-1})	32	32
		*k*cat (s^{-1})	24	24
		*k*cat/*K*m ($s^{-1}M^{-1}$)	3,692,000	3,871,000
Ethanol	$NADP^+$ (0.4)	Apparent *K*m (mM)	10.4	9.7
		Apparent *V*max (U mg^{-1})	112	108
		*k*cat (s^{-1})	84	81
		*k*cat/*K*m ($s^{-1}M^{-1}$)	8,000	8,000
Acetaldehyde	NADPH(0.4)	Apparent *K*m (mM)	1.0	0.84
		Apparent *V*max (U mg^{-1})	31.4	30.5
		*k*cat (s^{-1})	23.6	22.9
		*k*cat/*K*m ($s^{-1}M^{-1}$)	24,000	27,000

Table 4-5 Metal content of recombinant ES1ADH[a]

Parameter	Iron	Zinc	Nickel
Metal (ppb)	1120	375	37
Metal fraction (mol/mol subunit)	1.0	0.3	0.03

[a] The enzyme used for metal content determinations had the specific activity of 101 U mg^{-1} at a concentration of 0.89 mg ml^{-1}. The enzyme activity was determined in the standard reaction mixture of ethanol oxidation as described in Materials and Methods.

significantly inhibit the enzyme activity. It is well known that iron-containing ADHs are oxygen sensitive. However, it still surprised us that both enzymes lost almost 80% of full activity within 5 min exposure to the air. The oxygen inactivation could not be protected by the presence of dithiothreitol, distinct from the observation on *T. hypogea* ADH (Chapter 2). When both enzymes were exposed to the air, their $t_{1/2}$s were about 3-4 min (**Fig. 4-9**).

4.4.3 Molecular characterization

The deduced sequence was a 406 amino acid polypeptide (Amy Grunden, unpublished results) with a calculated theoretical isoelectric point (pI) and molecular mass of pH 5.5 and 44.8 kDa, respectively. BLASTP searches of the nonredundant database with its amino acid sequence revealed more than 100 hits; all of them were members of ADH family, including iron-containing ADH, 1, 3-propanediol dehydrogenase, or alcohol dehydrogenase IV. The two best scores were obtained with ADHs from *T. zilligii* and *T. hydrothermalis* (80% identity). It showed high degrees of identity (62 to 72%) to iron-containing ADHs from various bacterial thermophiles such as *Thermoanaerobacter* species, and low degrees of identity (30 to 32%) to well-characterized ADHs from *E. coli* and *Klebsiella pneumoniae* (Zheng et al. 2004). In particular, ES1ADH had extremely low sequence identity (<30%) to iron-containing ADHs from *T. maritima*, distinct from *T. hypogea* ADH which had 75% sequence identity to TM0820, an iron-containing ADH in *T. maritima*.

The conserved domain search of the deduced sequence indicated the regions of site 22-372 and site 22-400 were putative domains of iron-containing ADHs and ADHs class IV, respectively (**Fig. 4-10a**). However, the alignment of amino-terminal sequences among known ADHs from *Thermococcus* species indicated the presence of well-conserved residues (**Fig. 4-10b**; Antonie et al. 1999; Li and Stevenson 1997; Ma et al. 1994; Ma et al. 1995; Ronimus et al. 1997). Sequence alignment of iron-containing ADHs from archaea

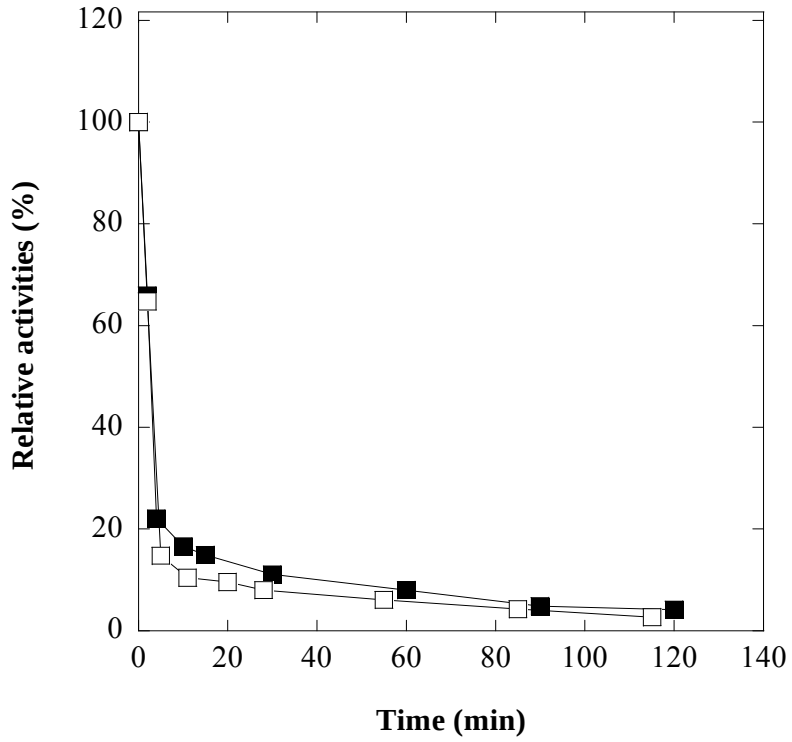

Figure 4-9 Oxygen inactivations of native and recombinant enzymes.

The relative activity of 100% means the full activity of both enzymes. Filled squares, native ES1ADH; open squares, recombinant ES1ADH.

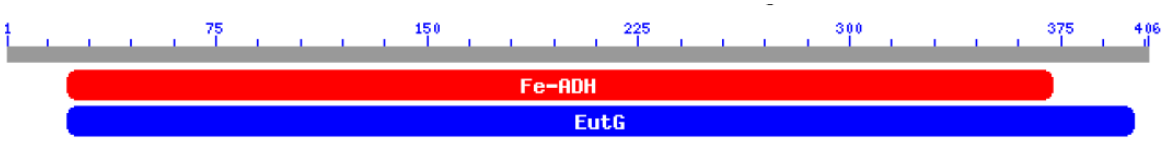

A

B

Figure 4-10 Putative conserved domains of ES1ADH (A) and N-terminal sequence alignment of iron-containing ADH in *Thermococcus* species (B).

Fe-ADH denotes iron-containing ADHs (pfam00465); EutG denotes alcohol dehydrogenase, class IV (COG1454). The letter X in Figure 4-10B represents unknown amino acid residue. The letters shaded in black represent identical amino acid residues among aligned ADHs. ES1ADH, ADH from *Thermococcus* strain ES1; Tlito, *T. litoralis*; Tzill, *T. zilligii*; Thyro, *T. hydrothermalis*.

and bacteria showed that 26 residues were strictly conserved, including conserved amino acid residues on putative iron-binding and coenzyme-binding sites (**Fig. 4-11**). The monomer of ES1ADH, like other proteins in the family, folded into two structural domains that were separated by a deep cleft (**Fig. 4-12**). The N-terminal domain (residues 1 to 182) was formed by an α/β region containing the dinucleotide-binding fold, whereas the C-terminal part (residues 183 to 383) was an all-helical domain.

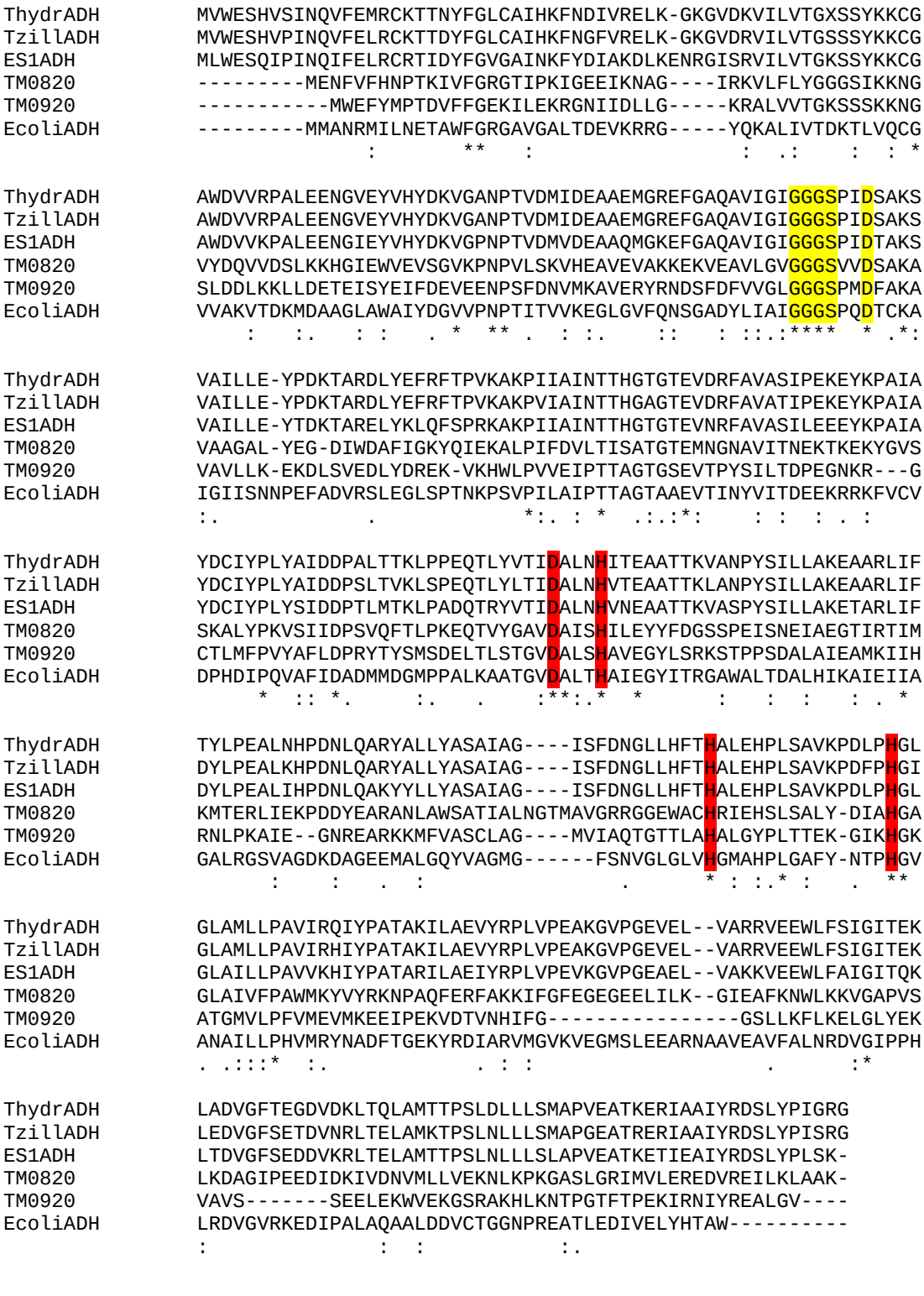
ThydrADH MVWESHVSINQVFEMRCKTTNYFGLCAIHKFNDIVRELK-GKGVDKVILVTGXSSYKKCG
TzillADH MVWESHVPINQVFELRCKTTDYFGLCAIHKFNGFVRELK-GKGVDRVILVTGSSSYKKCG
ES1ADH MLWESQIPINQIFELRCRTIDYFGVGAINKFYDIAKDLKENRGISRVILVTGKSSYKKCG
TM0820 ---------MENFVFHNPTKIVFGRGTIPKIGEEIKNAG----IRKVLFLYGGGSIKKNG
TM0920 -----------MWEFYMPTDVFFGEKILEKRGNIIDLLG-----KRALVVTGKSSSKKNG
EcoliADH ---------MMANRMILNETAWFGRGAVGALTDEVKRRG-----YQKALIVTDKTLVQCG
ThydrADH AWDVVRPALEENGVEYVHYDKVGANPTVDMIDEAAEMGREFGAQAVIGIGGGSPIDSAKS
TzillADH AWDVVRPALEENGVEYVHYDKVGANPTVDMIDEAAEMGREFGAQAVIGIGGGSPIDSAKS
ES1ADH AWDVVKPALEENGIEYVHYDKVGPNPTVDMVDEAAQMGKEFGAQAVIGIGGGSPIDTAKS
TM0820 VYDQVVDSLKKHGIEWVEVSGVKPNPVLSKVHEAVEVAKKEKVEAVLGVGGGSVVDSAKA
TM0920 SLDDLKKLLDETEISYEIFDEVEENPSFDNVMKAVERYRNDSFDFVVGLGGGSPMDFAKA
EcoliADH VVAKVTDKMDAAGLAWAIYDGVVPNPTITVVKEGLGVFQNSGADYLIAIGGGSPQDTCKA
ThydrADH VAILLE-YPDKTARDLYEFRFTPVKAKPIIAINTTHGTGTEVDRFAVASIPEKEYKPAIA
TzillADH VAILLE-YPDKTARDLYEFRFTPVKAKPVIAINTTHGAGTEVDRFAVATIPEKEYKPAIA
ES1ADH VAILLE-YTDKTARELYKLQFSPRKAKPIIAINTTHGTGTEVNRFAVASILEEEYKPAIA
TM0820 VAAGAL-YEG-DIWDAFIGKYQIEKALPIFDVLTISATGTEMNGNAVITNEKTKEKYGVS
TM0920 VAVLLK-EKDLSVEDLYDREK-VKHWLPVVEIPTTAGTGSEVTPYSILTDPEGNKR---G
EcoliADH IGIISNNPEFADVRSLEGLSPTNKPSVPILAIPTTAGTAAEVTINYVITDEEKRRKFVCV
ThydrADH YDCIYPLYAIDDPALTTKLPPEQTLYVTIDALNHITEAATTKVANPYSILLAKEAARLIF
TzillADH YDCIYPLYAIDDPSLTVKLSPEQTLYLTIDALNHVTEAATTKLANPYSILLAKEAARLIF
ES1ADH YDCIYPLYSIDDPTLMTKLPADQTRYVTIDALNHVNEAATTKVASPYSILLAKETARLIF
TM0820 SKALYPKVSIIDPSVQFTLPKEQTVYGAVDAISHILEYYFDGSSPEISNEIAEGTIRTIM
TM0920 CTLMFPVYAFLDPRYTYSMSDELTLSTGVDALSHAVEGYLSRKSTPPSDALAIEAMKIIH
EcoliADH DPHDIPQVAFIDADMMDGMPPALKAATGVDALTHAIEGYITRGAWALTDALHIKAIEIIA
ThydrADH TYLPEALNHPDNLQARYALLYASAIAG----ISFDNGLLHFTHALEHPLSAVKPDLPHGL
TzillADH DYLPEALKHPDNLQARYALLYASAIAG----ISFDNGLLHFTHALEHPLSAVKPDFPHGI
ES1ADH DYLPEALIHPDNLQAKYYLLYASAIAG----ISFDNGLLHFTHALEHPLSAVKPDLPHGL
TM0820 KMTERLIEKPDDYEARANLAWSATIALNGTMAVGRRGGEWACHRIEHSLSALY-DIAHGA
TM0920 RNLPKAIE--GNREARKKMFVASCLAG----MVIAQTGTTLAHALGYPLTTEK-GIKHGK
EcoliADH GALRGSVAGDKDAGEEMALGQYVAGMG------FSNVGLGLVHGMAHPLGAFY-NTPHGV
ThydrADH GLAMLLPAVIRQIYPATAKILAEVYRPLVPEAKGVPGEVEL--VARRVEEWLFSIGITEK
TzillADH GLAMLLPAVIRHIYPATAKILAEVYRPLVPEAKGVPGEVEL--VARRVEEWLFSIGITEK
ES1ADH GLAILLPAVVKHIYPATARILAEIYRPLVPEVKGVPGEAEL--VAKKVEEWLFAIGITQK
TM0820 GLAIVFPAWMKYVYRKNPAQFERFAKKIFGFEGEGEELILK--GIEAFKNWLKKVGAPVS
TM0920 ATGMVLPFVMEVMKEEIPEKVDTVNHIFG----------------GSLLKFLKELGLYEK
EcoliADH ANAILLPHVMRYNADFTGEKYRDIARVMGVKVEGMSLEEARNAAVEAVFALNRDVGIPPH
ThydrADH LADVGFTEGDVDKLTQLAMTTPSLDLLLSMAPVEATKERIAAIYRDSLYPIGRG
TzillADH LEDVGFSETDVNRLTELAMKTPSLNLLLSMAPGEATRERIAAIYRDSLYPISRG
ES1ADH LTDVGFSEDDVKRLTELAMTTPSLNLLLSLAPVEATKETIEAIYRDSLYPLSK-
TM0820 LKDAGIPEEDIDKIVDNVMLLVEKNLKPKGASLGRIMVLEREDVREILKLAAK-
TM0920 VAVS-------SEELEKWVEKGSRAKHLKNTPGTFTPEKIRNIYREALGV----
EcoliADH LRDVGVRKEDIPALAQAALDDVCTGGNPREATLEDIVELYHTAW----------

Figure 4-11 Sequence alignment of ES1ADH and related iron-containing ADHs.

The sequences were aligned using Clustal W (Thompson et al. 1994). Thydr, *T. hydrothermalis*; Tzill, *T. zilligii*; EcoliADH, $_{L}$-1, 2-propanediol dehydrogenase in *E. coli*. TM0820 and TM0920 are iron-containing ADHs in *T. maritima*. The typical coenzyme binding site, GGGSXXD, of iron-containing ADHs is marked in yellow. The conserved iron-binding site is marked in red. ‘‘*’’, residues or nucleotides that are identical in all sequences in the alignment; ‘‘:’’, conserved substitutions; ‘‘.’’: semi-conserved substitutions; “-”, no corresponding amino acid.

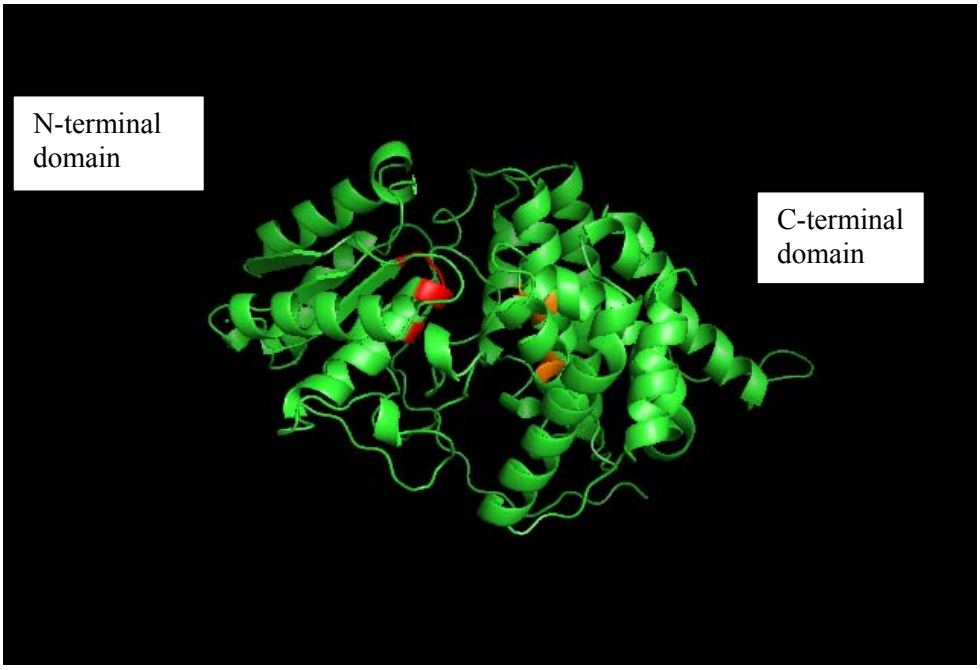

Figure 4-12 Predicted tertiary structure of ES1ADH monomer.

The structure modeling was run on the Swiss Model server using an iron-containing ADH from *T. maritima* (TM0820; PDB number: 1vljB) as the template. The structure figure was constructed using PyMOL (Delano, 2002). Residues in red, the putative $NADP^+$-binding site; Residues in orange, the putative iron-binding site.

4.5 DISCUSSION

Over-expression in mesophilic hosts such as *E. coli* is attractive due to simpler requirement of culture conditions, easier purification steps and higher yields of target thermo/hyperthermophilic protein. The native ES1ADH was abundant in *Thermococcus* strain ES1; however, the recombinant *E. coli* had a much higher yield of ES1ADH (about 6 mg per gram cells) than *Thermococcus* strain ES1 (about 0.4 mg per gram cells). Moreover, the purification of ES1ADH from *E. coli* took a simpler procedure than that for native ES1ADH. The specific step heat treatment was introduced to remove most of proteins from the mesophilic host, which is an outstanding characteristic of thermostable enzymes expressed in mesophilic hosts.

The enzyme activity of ES1ADH from *E. coli* does not require the heat activation prior to enzyme assay. However, heat activation seemed essential for over-expressed iron-containing ADH from *T. hydrothermalis* and 2, 3-butanediol ADH from *P. furiosus* (Antoine et al. 1999; Kube et al. 2006). The activity of *T. hydrothermalis* ADH increased 10-25% after 1 min incubation at 80°C while *P. furiosus* ADH mentioned above showed no activity without heat treatment and the highest activity after 10 min incubation at 100°C. Moreover, the temperature of heat treatment does not contribute to the increase of activity, similar to the observations on an over-expressed short-chain ADH from *P. furiosus* (van der Oost et al. 2001). The recombinant ES1ADH activity was independent of heat activation, which might suggest the enzyme did not require the structural adjustment or rearrangement. In addition, various tests on catalytic properties and kinetic parameters were carried out and all of them showed that both native and recombinant enzymes had almost identical properties, suggesting that this iron-containing ADH was successfully expressed in *E. coli* which could be a good expression system for iron-containing ADHs from hyperthermophilic archaea. However, no general rules for successful overexpression of ADHs from hyperthermophilic archaea could be presented yet (Kube et al. 2006).

ES1ADH had biophysical and biochemical properties highly similar to other characterized ADHs from *Thermococcus* species (**Table 4-6**). Those ADHs from *Thermococcus* species had the homotetrameric structure in the native form and were $NADP^+$-dependent primary ADHs. The polypeptide was 406 aa long with the apparent size of 45 ± 1 kDa on SDS-PAGE.

ES1ADH was one of the most thermostable iron-containing ADHs, and such feature might be partially contributed by their amino acid composition. Sequence analyses indicated that ES1ADH shared high similarity to iron-containing ADHs from *T. ethanlicus* (EAU56972) and *Clostridium cellulolyticum* (EAV69097) with the identity of 69% and 64%, respectively. However, the amino acid composition of three enzymes was quite close except variation of few amino acids (**Table 4-7**). As compared to thermophilic and mesophilic counterparts, the ratio of amino acid residues Arg, Gln, Pro and Tyr increased, whereas Ala, Asn and Val had a lower ratio. The increasing of Gln seemed antiparallel with the decreasing of Asn. It is very likely that other determinants are critical for thermostability, which needs further investigation.

Both native and recombinant ES1ADHs were oxygen sensitive. The loss of activity after exposure to the air, might be due to the oxidation of ferrous to ferric, and/or loss of ferrous ion, and replacement with other metals such as zinc. However, both enzymes could be successfully purified under anaerobic conditions, suggesting the ferrous ion is bound tightly enough for the purification. Both enzymes were oxygen sensitive and had the half life of 3-4 min. The loss of enzyme activity was irreversible, implying that it is likely that oxidation of some amino acids such as cysteine residues results in irreversible structure change and thus inactivation of activity (Neale et al. 1986). It has been pointed out that single amino acid residue is critical for aerobic inactivation of iron-containing ADHs in the facultative anaerobe *E. coli*. Propanediol oxidoreductase (FucO protein) in *E. coli* contains Fe and is sensitive to oxidation (Lu et al. 1998). Mutations (Ile7Leu and Leu8Val)

Table 4-6 Comparison of ADHs from *Thermococcus* species

organism	*Thermococcus* stain ES1	*T. zilligii*	*T. hydrothermalis*	*T. litoralis*
T_{opt} (°C)	91	75-80	85	85
Amino acids (aa or kDa)	406 aa	406 aa	406 aa	48kDa[b]
Estimated ADH content in CFE (%)	10	1.4	1.1	1.3
Type of ADH	Primary	Primary	Primary	Primary
Coenzyme	NADP(H)	NADP(H)	NADP(H)	NADP(H)
Reference[a]	1	2	3	4

T_{opt}, optimal growth temperature

[a] References used: 1, This study; Pledger and Baross, 1989; 2, Klages and Morgan, 1994; Li et al. 1997; Ronimus et al. 1997; 3, Antoine et al. 1999; 4, Ma et al. 1994; Neuner et al. 1989.

[b] molecular mass estimated from SDS-PAGE.

Table 4-7 Amino acid compositions of ES1ADH, TeADH and CcADH

Amino acid	ES1ADH[a]	TeADH	CcADH
Ala (A)	43 (10.6)	46 (11.5)	49 (12.3)
Arg (R)	13 (3.2)	8 (2.0)	8 (2.0)
Asn (N)	12 (3.0)	15 (3.8)	16 (4.0)
Asp (D)	22 (5.4)	18 (4.5)	23 (5.8)
Cys (C)	3 (0.7)	3 (0.8)	1 (0.3)
Gln (Q)	8 (2.0)	3 (0.8)	3 (0.8)
Glu (E)	29 (7.1)	28 (7.0)	26 (6.5)
Gly (G)	23 (5.7)	26 (6.5)	24 (6.0)
His (H)	9 (2.2)	6 (1.5)	8 (2.0)
Ile (I)	34 (8.4)	30 (7.5)	33 (8.3)
Leu (L)	45 (11.1)	41 (10.3)	42 (10.5)
Lys (K)	28 (6.9)	35 (8.8)	27 (6.8)
Met (M)	5 (1.2)	5 (1.3)	5 (1.3)
Phe (F)	11 (2.7)	10 (2.5)	11 (2.8)
Pro (P)	25 (6.2)	24 (6.0)	22 (5.5)
Ser (S)	19 (4.7)	18 (4.5)	20 (5.0)
Thr (T)	26 (6.4)	27 (6.8)	29 (7.3)
Trp (W)	3 (0.7)	3 (0.8)	3 (0.8)
Tyr (Y)	21 (5.2)	19 (4.8)	15 (3.8)
Val (V)	27 (6.7)	34 (8.5)	34 (8.5)

Abbreviations used: ES1ADH, ADH from *Thermococcus* strain ES1; TeADH, ADH from *T. ethanlicus* (EAU56972); CcADH, ADH from *Clostridium cellulolyticum* (EAV69097).

[a] The number in parenthesis means the molar fraction of amino acid. As compared to CcADH, the residues with increased molar fraction (>1% difference, including Pro) are shaded in red and those with decreased molar fraction (>1% difference) are shaded in blue.

increased resistance to oxidative stress but lowered its specific activity, appearing to act *via* changes in protein structure. In contrast, the single substitution of Glu568 in AdhE, another iron-containing ADH in *E.coli*, yielded not only the enzyme activity but also the increased specific activity under aerobic culturing conditions (Holland-Staley et al. 2000). AdhE exists anaerobically in cells as a complex that disassembles upon exposure of the cells to oxygen, resulting in loss of enzyme activity (Kessler et al. 1992). The proposed mechanism was due to the charge repulsion between adjacent acidic residues (e.g., Glu568) at the interface between two monomers of AdhE, which provides a possible explanation for its disassembly. Those observations were based on the activities in *E. coli* cultures. Since *Thermococcus* strain ES1 is strictly anaerobic and lacks of oxygen stress in natural ecosystems, such a mechanism of aerobic inactivation is unlikely involved. How oxygen alters the enzyme structure is not well understood. Iron-sulfur centers are the oxidation-sensitive sites in several proteins (Unden et al. 1994); however, iron in ES1ADH does not appear to be in a Fe-S cluster considering its content of 1 *g* atom iron per subunit.

The ICP-MS analyses of the recombinant ES1ADH showed the presence of 0.3 *g* atom zinc per subunit. It is surprising that the recombinant enzyme still had the closest activity to the native one. This fact implies that zinc might have a non-specific binding site that has no effect on the activity. Compared to the iron-containing ADH from *T. hypogea*, ES1ADH seemed to be more resistant to exogenous zinc inhibition than the hyperthermophilic bacterial ADH (**Table 2-7, Chapter 2**).

The activity of ES1ADH was regulated by the concentration of S^0 when growing on peptide medium (Ma et al. 1995). It is still not known whether posttranslational modification of ES1ADH occurred *in vivo*, which has been well demonstrated for two iron-containing ADHs from the facultatively fermentative *E. coli* (Holland-Staley et al. 2000; Lu et al. 1998). The physiological role was proposed to be responsible for disposing of excess reductant under S^0-limited conditions; however, the ES1ADH content in the cell-free extract of *Thermococcus* strain ES1 was high up to 10% of proteins, which seemed

oversizing the metabolic flux. Whether ES1ADH possessed other physiological roles warrants further investigation.

The amino-terminal sequence of 21 amino acids was highly conserved only within ADHs from *Thermococcus* species, which could act as a unique molecular mark for members of iron-containing ADH from *Thermococcus* species (**Fig. 4-10b**). Moreover, the further analyses of primary structures showed that ES1ADH had structural similarity to other iron-containing ADHs from either hyperthermophiles or mesophiles. ES1ADH had typical iron and coenzyme-binding sites, $Asp_{208}His_{212}His_{278}His_{292}$ and $GlyGlyGlySerX_2Asp$ (residues 109-115), respectively. The structural modeling was based on the crystal structure of a putative iron-containing ADH from *T. maritima* (TM0820) due to the lack of 3-D structures of homologues from hyperthermophilic archaea. The structural modeling clearly showed two typical domains belonging to the family of iron-containing ADHs, the α/β-dinucleotide-binding N-terminal domain and the all-α-helix C-terminal domain separated by a deep cleft (Montella et al. 2005; Schwarzenbacher et al. 2004). Although iron-containing ADHs possessed conserved primary and tertiary structural characteristics, their evolution seems divergent. ES1ADH homologues spanned the domains *Bacteria* and *Archaea* while *T. hypogea* ADH homologues clustered in the domain *Bacteria* (**Fig. 4-13**).

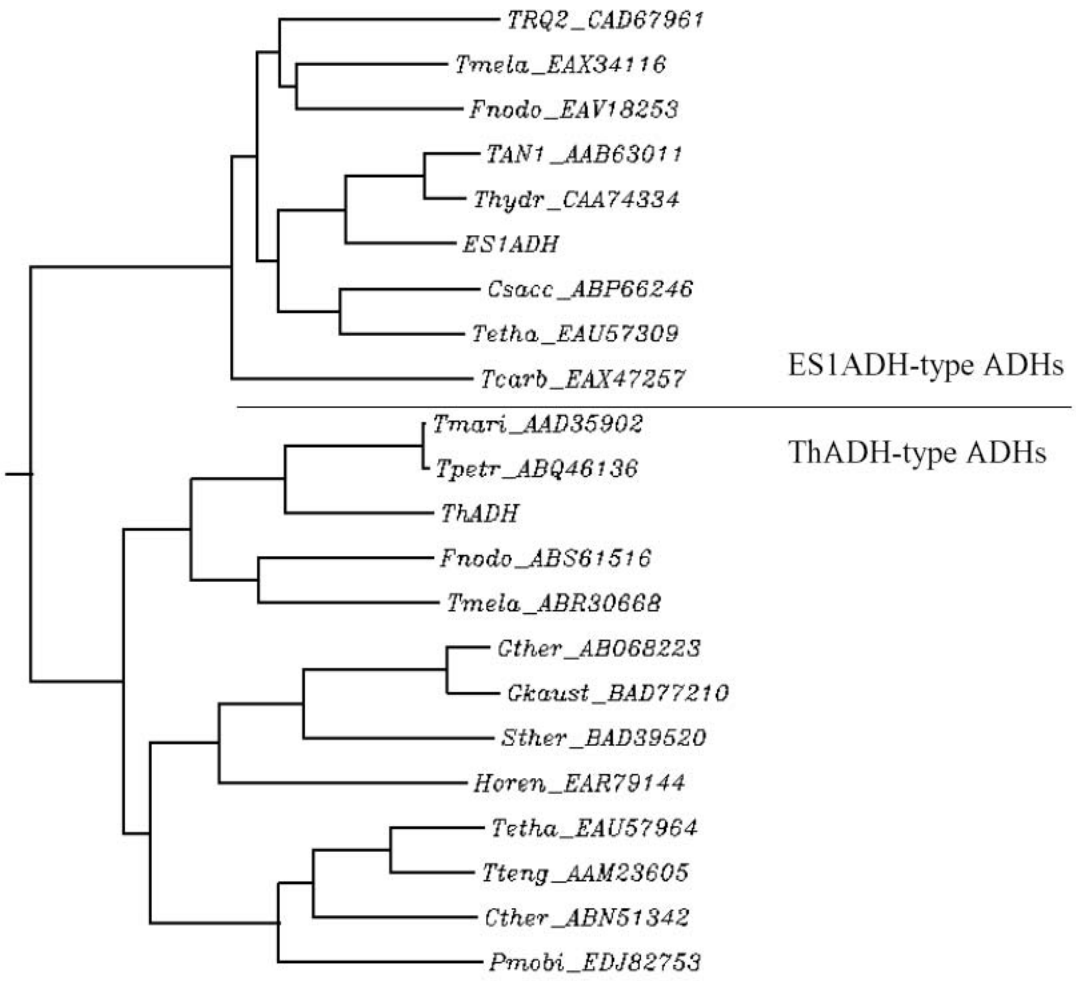

Figure 4-13 Phylogenetic relationship between ES1ADH and related iron-containing ADHs.

The sequences were aligned using Clustal W and subsequently a phylogenetic tree was constructed (Thompson et al. 1994). The accession numbers for the genes encoding ADHs used in the analyses are indicated on the figure. Abbreviations used: TRQ2, *Thermotoga* sp. RQ2; Tmela, *Thermosipho melanesiensis* BI429; Fnodo, *Fervidobacterium nodosum* Rt17-B1; TAN1, *Thermococcus* strain AN1; Thydr, *Thermococcus hydrothermalis*; ES1ADH, ADH from *Thermococcus* strain ES1; Csacc, *Caldicellulosiruptor saccharolyticus* DSM 8903; Tetha, *Thermoanaerobacter ethanolicus* X514; Tcarb,

Thermosinus carboxydivorans Nor1; Tmari, *Thermotoga maritima*; Tpetr, *Thermotoga petrophila*; ThADH, ADH from *T. hypogea*; Gther, *Geobacillus thermodenitrificans* NG80-2; Gkaust, *Geobacillus kaustophilus* HTA426; Sther, *Symbiobacterium thermophilum* IAM 14863; Horen, *Halothermothrix orenii* H 168; Tteng, *Thermoanaerobacter tengcongensis* MB4; Cther, *Clostridium thermocellum* ATCC 27405; Pmobi, *Petrotoga mobilis* SJ95.

Chapter 5 General conclusions

Alcohol dehydrogenases are ubiquitous enzymes catalyzing interconversions between alcohols and corresponding ketones or aldehydes. They are well characterized in mesophiles, particularly for those ADHs from horse liver, yeast and *Escherichia coli*, whereas the information on the characterization of ADHs from hyperthermophiles is still very limited. Hyperthermophiles are a group of microorganisms growing optimally at ≥80°C, belonging to either archaea or bacteria domain. The ADHs from hyperthermophiles are generally thermostable, highly stereoselective and solvent tolerate, thus attract great attention for fundamental studies as well as exploration of their potentials in biotechnological applications. The biochemical and molecular characterizations of ADHs from the selected hyperthermophiles were studied in this report.

5.1 Biophysical properties

All three enzymes ThADH, TgADH and ES1ADH are $NADP^+$-dependent. ThADH and ES1ADH contain 1 *g* atom iron per subunit. The bacterial ThADH is a medium-chain homodimer, whereas archaeal ES1ADH is a long-chain homotetramer in the native form. In contrast, TgADH contains 1 *g* atom Zn per subunit which plays a catalytic role. TgADH monomer is a 364 aa polypeptide. Compared to thermophilic and mesophilic counterparts, TgADH contains more Ala, Arg, Glu, Pro residues and less Asn, Ser, Met and Ile residues, indicating both composition and strengthening ion pairs might be important determinants of thermostability. In addition, the nucleotide sequence analyses of TgADH have showed that the pattern of its codon usage is different from that of *E. coli*.

5.2 Biochemical properties

All the enzymes are thermophilic and have an optimal temperature of over 95°C. Their optimal pHs for the oxidation of alcohols are more alkaline than for the reduction of aldehydes or ketones, which is a common feature among hyperthermophilic ADHs. They are thermostable, of which TgADH has the highest thermostability. The enzymes have broad substrate specificity; however, their substrate preference differs. ThADH and

ES1ADH react with various primary alcohols and corresponding aldehydes while TgADH catalyzes oxidation of both primary and secondary alcohols and reduction of corresponding aldehydes or ketones. In particular, TgADH catalyzes the interconversion between acetoin and 2, 3-butanediol and irreversibly reduce diacetyl to acetoin. However, it does not catalyze the oxidation of $_{L}$-threonine or $_{L}$-serine. All the enzymes are oxygen sensitive and exhibit zinc-inhibition. The oxygen inactivation of ThADH results in the loss of catalytic iron and subsequently occupancy by zinc at the metal-binding site. The oxygen-inactivation mechanism of TgADH is not well understood but may be associated with oxygen damage on amino acid residues.

5.3 Physiological roles

It is well known that iron-containing ADHs are responsible for ethanogenesis in facultative anaerobes. *Thermotoga hypogea* and *Thermococcus* strain ES1 are strict anaerobes and produce ethanol as one of their end products. The physiological role of both ThADH and ES1ADH is proposed to be involved in alcohol formation. In contrast, zinc-containing ADHs could have more diverse roles. *Thermococcus guaymasensis* produces ethanol and acetoin as parts of the end products. The kinetic parameters of TgADH also support its preference to catalyze the oxidation of NADPH. Therefore, TgADH as the dominant ADH activity in the cell-free extract of *T. guaymasensis* is likely responsible for the formation of ethanol and/or acetoin.

5.4 Structural properties

The amino acid sequence of ES1ADH shows the highest similarity to ADHs from *Thermococcus zilligii* and *Thermococcus hydrothermalis* (80% identity) and high degrees of identity (62 to 72%) to iron-containing ADHs from *Thermotoga* and *Thermoanaerobacter* species. The conserved domain search reveals it belongs to the family of iron-containing ADHs. The enzyme has classical catalytic metal and dinucleotide-binding motifs among iron-containing ADHs, $D_{208}H_{212}H_{278}H_{292}$ and

$GGGSX_2D$ (residues 109-115), respectively. The 3-D structural modeling of the enzyme further verified two typical domains: the α/β-dinucleotide-binding N-terminal domain and the all-α-helix C-terminal domain.

The alignment of TgADH deduced amino acid sequences shows high similarity to zinc-containing ADHs from *Thermoanaerobacter* species. The conserved domain analyses have revealed that this enzyme belongs to either zinc-containing ADHs or $_L$-threonine dehydrogenase, but the latter has been excluded by enzyme assays. The motif search verifies that the enzyme has only catalytic zinc ($GHEX_2GX_5GX_2V$, residues 62-76) and $NADP^+$ binding sites ($GXGX_2G$, residues 183-188). The modeling of 3-D structure of TgADH also shows two typical domains, one catalytic domain close to amino-terminal end and one coenzyme-binding domain close to C-terminal end.

5.5 Potentials as a potent biocatalyst

TgADH has the extremely high specific activity of 1149 U mg^{-1} on the oxidation of 2-butanol. Such catalytic properties meet the requirements of good biocatalysts in industry, including high thermoactivity, thermostability, stereoselectivity, broad substrate specificity and solvent tolerance. The simplest NADPH regeneration system is also established for efficient reduction of ketones by using a co-substrate isopropanol. Thus, the enzyme could be used for synthesis of chiral molecules such as 2, 3-butanediol and acetoin.

5.6 Future outlooks

ADHs are important for the fundamentally scientific studies as well as exploration of their potential in biotechnological applications. However, large-scale production of ADHs from hyperthermophiles is still a bottleneck because of very low biomass productivity (Schiralde et al. 2002). Alternatively, heterologous expression in mesophilic hosts is a frequently used approach. The genes encoding ADHs from hyperthermophilic archaea are commonly over-expressed in *E. coli* (Antoine et al. 1999; Cannio et al. 1996; Hirakawa et

al. 2004; Kube et al. 2006; Machielsen and van der Oost 2006; van der Oost et al. 2001). The *E. coli* expression systems have been the most extensively applied as they offer certain advantages: simplicity of purification, high cell density cultivation, convenience for mutation and tag fusion to improve their biochemical properties, the enhanced productivity by using strong promoters or controlling the copy number of plasmids (Marrides 1996). The gene encoding ADH from hyperthermophilic archaeon *T. guaymasensis* harbors codon usage bias and exhibits a high proportion of rare codons, which could highly interfere with its heterologous expression in *E. coli*. This difficulty could be overcome by the recent understanding on the expression of *Thermoplasma acidophilum* $_{D}$-gluconate dehydratase in *E. coli*, which demonstrated the effect of the position and frequency of the rare codons on the expression of the archaeal proteins in heterologous systems (Kim and Lee 2006). In addition, a hydrolase gene from *Thermus thermophilus* HB8, was engineered by introducing several silent mutations downstream of the initial codon, revealing that the expression level of *ndx3* increased in proportion to the AT-content in the third to sixth codons (Nishikubo et al. 2005).

Besides extensive investigations on characterization of ADHs, protein engineering is the powerful approach to alter the properties of enzymes, enabling them to transform new substrates or catalyze exsisting substrates more efficiently. Successful examples have been reported on those representative ADHs from *Yeast* (Murali and Creaser 1986), *Clostridium beijerinckii* (Bogin et al. 2005; Goihberg et al. 2007), *Sulfolobus solfataricus* (Esposito et al. 2003a; Giordano et al. 1999; Giordano et al. 2005). Moreover, site-directed mutagenesis is also widely used for identifying the role of specific amino acid in catalysis. However, the 3-D structural information of enzymes is critical to understand the structure-function relationships for either native or mutant enzymes. In our lab, the work of crystallography is in progress, which will shed light on the design of site-directed mutagenesis.

How ADHs from hyperthermophiles are regulated has been scarcely reported. Moreover, the molecular mechanisms of their gene regulation in specific metabolic pathways are still not completely exploited. To address those questions, some progress has been achieved on understanding the regulation of ADHs from *S. solfataricus* on the translational and transcriptional analyses (Chong et al. 2007; Fiorentino et al. 2003). In addition, the interpretation of cellular metabolic pathways will offer the option to use hyperthermophiles in whole cell catalysis as observed in *S. solfatarticus*, e.g., degradation of alcohols (Chong et al. 2007; Radianingtyas and Wright 2003).

Chapter 6 References

Adolph HW, Maurer P, Schneider-Bernlöhr H, Sartorius C, Zeppezauer (1991) Substrate specificity and stereoselectivity of horse liver alcohol dehydrogenase: kinetic evaluation of binding and activation parameters controlling the catalytic cycles of unbranched, acyclic secondary alcohols and ketones as substrates of the native and active-site-specific Co (II)-substituted enzyme. Eur J Biochem 201: 615-625

Ahmed H, Ettema TJG, Tjaden b, Geerling ACM, van der Oost J, Siebers B (2005) The semi-phosphorylative Entner-Doudoroff pathway in hyperthermophilic archaea: a re-evaluation. Biochem J 390: 529-540

Altschul SF, Madden TL, Schäffer AA, Zhang J, Zhang Z, Miller W, Lipman DJ (1997) Gapped BLAST and PSI-BLAST: a new generation of protein database search programs. Nucl Acids Res 25: 3389-3402

Ammendola S, Raia CA, Caruso C, Camardella L, D'Auria S, De Rosa M, Rossi M (1992) Thermostable NAD^+-dependent alcohol dehydrogenase from *Sulfolobus solfataricus*: gene and protein sequence determination and relationship to other alcohol dehydrogenases. Biochemistry 31: 12514-12523

Andrews KT, Patel BKC (1996) *Fervidobacterium gondwanense* sp. nov., a new thermophilic anaerobic bacterium isolated from nonvolcanically heated geothermal waters of the great artesian basin of Australia. Int J Syst Bacteriol 46: 265-269

Antoine E, Rolland JL, Raffin JP, Dietrich J (1999) Cloning and over-expression in *Escherichia coli* of the gene encoding NADPH group III alcohol dehydrogenase from *Thermococcus hydrothermalis*. Eur J Biochem 264: 880–889

Arab H, Völker H, Thomm M (2000) *Thermococcus aegaeicus* sp. nov. and *Staphylothermus hellenicus* sp. nov., two novel hyperthermophilic archaea isolated from geothermally heated vents off Palaeochori Bay, Milos, Greece. Int J Syst Evol Microbiol 50: 2101-2108

Aristarkhov A, Mikulskis A, Belasco JG, Lin ECC (1996) Translation of the *adhE* transcript to produce ethanol dehydrogenase requires RNase III cleavage in *Escherichia coli*. J Bacteriol 178: 4327-4332

Atomi H (2005) Recent progress towards the application of hyperthermophiles and their enzymes. Curr Opin Chem Biol 9: 166-173

Atomi H, Fukui T, Kanai T, Morikawa M, Imanaka T (2004) Description of *Thermococcus kodakaraensis* sp. nov., a well studied hyperthermophilic archaeon previously reported as *Pyrococcus* sp. KOD1. Archaea 1: 263–267

Badiei HR, Smith AT, Karanassios V (2002) Rhenium-cup, in-torch vaporization (ITV) sample introduction for axially viewed ICP-AES and its application to the analysis of a microscopic, ng-weight solid sample. J Anal At Spectrom 17: 1030–1036

Bairoch A (1991) PROSITE: a dictionary of sites and patterns in proteins. Nucleic Acids Res 19: 2241-2245

Balch WE, Fox GE, Magrum LJ, Woese CR, Wolfe WS (1979) Methanogens: re-evaluation of a unique biological group. Microbiol Rev 43: 260-296

Banat IM, Marchant R (1995) Characterization and potential industrial applications of five novel, thermotolerant, fermentative, yeast strains. World J Microbiol Biotechnol 11: 304–306

Banat IM, Nigam P, Singh D, Marchant R, McHale AP (1998) Review: ethanol production at elevated temperatures and alcohol concentrations: Part I. Yeasts in general. World J Microbiol Biotechnol 14: 809–821

Balk M, Weijma J, Stams AJM (2002) *Thermotoga lettingae* sp. nov., a novel thermophilic, methanol-degrading bacterium isolated from a thermophilic anaerobic reactor. Int J Syst Evol Microbiol 52: 1361–1368

Barbier G, Godfroy A, Meunier JR, Querellou J, Cambon MA, Lesongeur F, Grimont PA, Raguenes G (1999) *Pyrococcus glycovorans* sp. nov., a hyperthermophilic archaeon isolated from the East Pacific Rise. Int J Syst Bacteriol 49 Pt 4: 1829-1837

Barns SM, Delwiche CF, Palmer JD, Pace NR (1996) Perspectives on archaeal diversity, thermophily and monophyly from environmental rRNA sequences. Proc Natl Acad Sci 93: 9188-9193

Bateman A, Birney E, Cerruti L, Durbin R, Etwiller L, Eddy SR, Griffiths-Jones S, Howe KL, Marshall M, Sonnhammer EL (2002) The Pfam protein families database. Nucl Acids Res 30: 276–280.

Beeder J, Nilsen RK, Rosnes JT, Torsvik T, Lien T (1994) *Archaeoglobus fulgidus* isolated from hot North Sea oil field waters. Appl Environ Microbiol 60: 1227–1231

Berezina OV, Lunina NA, Zverlov VV, Naumoff DG, Liebl W, Velikodvorskaya GA (2003) A cluster of *Thermotoga neapolitana* genes involved in the degradation of starch and maltodextrins: the molecular structure of the locus. Mol Biol 37: 678-685 (translated from Molekulyarnaya Biologiya)

Bertoldo C, Antranikian G (2006) The order *Thermococcales*. Prokaryotes 3: 69-81

Betancor L, Berne C, Luckarift HR, Spain JC (2006) Coimmobilization of a redox enzyme and a cofactor regeneration system. Chem Commun 3640-3642

Blattner FR, Plunkett III G, Bloch CA, Perna NT, Burland V, Riley M, Collado-Vides J, Glasner JD, Rode CK, Mayhew GF, Gregor J, Davis NW, Kirkpatrick HA, Goeden MA, Rose DJ, Mau B, Shao Y (1997) The complete genome sequence of *Escherichia coli* K-12. Science 277: 1453-1474

Blöchl E, Burggraf S, Fiala G, Lauerer G, Huber G, Huber R, Rachel R, Segerer A, Stetter KO, Völkl P (1995) Isolation, taxonomy and phylogeny of hyperthermophilic microorganisms. World J Microbiol Biotech 11: 9-18

Blöchl E, Rachel R, Burggraf S, Hafenbradl D, Jannasch HW, Stetter KO (1997) *Pyrolobus fumarii*, gen. and sp. nov., represents a novel group of archaea, extending the upper temperature limit for life to 113°C. Extremophiles 1: 14–21

Blomqvist K, Nikkola M, Lethtovaara P, Suihko M, Airaksinen U, Straby KS, Knowles JKC, Penttila ME (1993) Characterization of the genes of the 2,3-butanediol operons from *Klebsiella terrigena* and *Enterobacter aerogenes*. J Bacteriol 175: 1392-1404

Bogin O, Levin I, Hacham Y, Tel-Or S, Peretz M, Frolow F, Burstein Y (2002) Structural basis for the enhanced thermal stability of alcohol dehydrogenase mutants from the mesophilic bacterium *Clostridium beijerinckii*: contribution of salt bridging. Protein Sci 11: 2561-2574

Bogin O, Peretz M, Hacham Y, Korkhin Y, Frolow F, Kalb AJ, Burstein Y (1998) Enhanced thermal stability of *Clostridium beijerinckii* alcohol dehydrogenase after strategic substitution of amino acid residue with prolines from the homologous thermophilic *Thermoanaerobacter brockii* alcohol dehydrogenase. Protein Sci 7: 1156-1163

Bogin O, Peretz M, Burstein Y (1997) *Thermoanaerobacter brockii* alcohol dehydrogenase: characterization of the active site metal and its ligand amino acids. Protein Sci 6: 450-458

Bradford MM (1976) A rapid and sensitive method for the quantitation of microgram quantities of protein utilizing the principle of protein-dye binding. Anal Biochem 72: 248–254

Brinen LS, Canaves JM, Dai X, Deacon AM, Elsliger MA, Eshaghi S, Floyd R, Godzik A, Grittini C, Grzechnik SK, Guba C, Jaroszewski L, Karlak C, Klock HE, Koesema E, Kovarik JS, Kreusch A, Kuhn P, Lesley SA, McMullan D, McPhillips TM, Miller MA, Miller MD, Morse A, Moy K, Ouyang J, Robb A, Rodrigues K, Selby TL, Spraggon G, Stevens RC, van den Bedem H, Velasquez J, Vincent J, Wang X, West B, Wolf G, Taylor

SS, Hodgson KO, Wooley J, Wilson IA (2003) Crystal structure of a zinc-containing glycerol dehydrogenase (TM0423) from *Thermotoga maritima* at 1.5 Å resolution. Proteins-Structure Function and Genetics 50: 371–374

Brock TD, Brock KM, Belly RT, Weiss RL (1972) *Sulfolobus*: a new genus of sulphur oxidizing bacteria living at low pH and high temperature. Arch Microbiol 84:54–68

Bronnenmeier K, Kern A, Liebl W, Staudenbauer WL (1995) Purification of *Thermotoga maritima* enzymes for the degradation of cellulosic materials. Appl Environ Microbiol 61: 1399-1407

Brouns SJ, Walther J, Snijders AP, van deWerken HJ, Willemen HLDM, Worm P, de Vos MGJ, Andersson A, Lundgren M, Mazon HFM, van den Heuvel RHH, Nilsson P, Salmon L, de Vos WM, Wright PC, Bernander R, van der Oost J (2006) Identification of the missing links in prokaryotic pentose oxidation pathways. J Biol Chem 281: 27378–27388

Brügger K, Chen L, Stark M, Zibat A, Redder P, Ruepp A, Awayez M, She Q, Garrett RA, Klenk HP (2007) The genome of *Hyperthermus butylicus*: a sulfur-reducing, peptide fermenting, neutrophilic Crenarchaeote growing up to 108 degrees C. Archaea 2: 127-135

Bryant FO, Wiegel J, Ljungdahl LG (1988) Purification and properties of primary and secondary alcohol dehydrogenases from *Thermoanaerobacter ethanolicus*. Appl Environ Microbiol 54: 460-465

Bühner M, Sund H (1969) Yeast alcohol dehydrogenase: -SH groups, disulfide groups, quaternary structure, and reactivation by reductive cleavage of disulfide groups. Eur J Biochem 11: 73-79

Burdette DS, Secundo F, Phillips RS, Dong J, Scott RA, Zeikus JG (1997) Biophysical and mutagenic analysis of *Thermoanaerobacter ethanolicus* secondary-alcohol dehydrogenase activity and specificity. Biochem J 326: 717-724

Bustard MT, Burgess JG, Meeyoo V, Wright PC (2000) Novel opportunities for marine hyperthemophiles in emerging biotechnology and engineering industries. J Chem Technol Biotechnol 75: 1095-1109

Cabiscol E, Aguilar J, Ros J (1994) Metal-catalyzed oxidation of Fe^{2+} dehydrogenases. J Biol Chem 269: 6592–6597

Cambillau C, Claverie JM (2000) Structural and genomic correlates of hyperthermostability. J Biol Chem 275: 32383-32386

Cambon-Bonavita M, Lesongeur F, Pignet P, Wery N, Lambert C, Godfroy A, Querellou J, Barbier G (2003) *Thermococcus altanticus* sp. nov., a hyperthermophilic archaeon isolated from a deep-sea hydrothermal vent in the mid-atlantic ridge. Extremophiles 7: 101-109

Canganella F, Jones WJ, Gambacorta A, Antranikian G (1998) *Thermococcus guaymasensis* sp. nov. and *Thermococcus aggregans* sp. nov., two novel thermophilic archaea isolated from the Guaymas Basin hydrothermal vent site. Int J Syst Bacteriol 48: 1181-1185

Cannio R, Fiorentino G, Carpinelli P, Rossi M, Bartolucci S (1996) Cloning and overexpression in *Escherichia coli* of the genes encoding NAD-dependent alcohol dehydrogenase from two *Sulfolobus* species. J Bacteriol 178: 301–305

Ceccarelli C, Liang ZX, Strickler M, Prehna G, Goldstein BM, Klinman JP, Bahnson BJ (2004) Crystal structure and amide H/D exchange of binary complexes of alcohol dehydrogenase from *Bacillus stearothermophilus*: insight into thermostability and cofactor binding. Biochem 43: 5266-5277

Chen L, Brügger K, Skovgaard M, Redder P, She Q, Torarinsson E, Greve B, Awayez M, Zibat A, Klenk HP, Garrett RA (2005) The genome of *Sulfolobus acidocaldarius*, a model organism of the *Crenarchaeota*. J Bacteriol 187: 4992-4999

Chen YM, Lin ECC (1991) Regulation of the *adhE* gene, which encodes ethanol dehydrogenase in *Escherichia coli*. J Bacteriol 173: 8009-8013

Cheng J, Randall A, Sweredoski M, Baldi P (2005) SCRATCH: a protein structure and structural feature prediction server. Nucl Acids Res 33: w72-76

Chhabra SR, Shockley KR, Conners SB, Scott KL, Wolfinger RD, Kelly RM (2003) Carbohydrate-induced differential gene expression patterns in the hyperthermophilic bacterium *Thermotoga maritima*. J Biol Chem 278: 7540-7552

Chhabra SR, Shockley KR, Ward DE, Kelly RM (2002) Regulation of endo-acting glycosyl hydrolases in the hyperthermophilic bacterium *Thermotoga maritima* grown on glucan- and mannan-based polysaccharides. Appl Environ Microbiol 68: 545-554

Chong PK, Burja AM, Radianingtyas H, Fazeli A, Wright PC (2007) Translational and transcriptional analysis of *Sulfolobus solfataricus* P2 to provide insights into alcohol and ketone utilization. Proteomics 7: 424-435

Cohen GN, Barbe V, Flament D, Galperin M, Heilig R, Lecompte O, Poch O, Prieur D, Querellou J, Ripp R, Thierry JC, van der Oost J, Weissenbach J, Zivanovic Y, Forterre P (2003) An integrated analysis of the genome of the hyperthermophilic archaeon *Pyrococcus abyssi*. Mol Microbiol 47: 1495-1512

Collins EB (1972) Biosynthesis of flavor compounds by microorganisms. J Dairy Sci 55: 1022-1028

Conners SB, Mongodin EF, Johnson MR, Montero CI, Nelson KE, Kelly RM (2006) Microbial biochemistry, physiology, and biotechnology of hyperthermophilic *Thermotoga* species. FEMS Microbiol Rev 30: 872-905

Conway T, Ingram LO (1989) Similarity of *Escherichia coli* propanediol oxidoreductase (fucO product) and an unusual alcohol dehydrogenase from *Zymomonas mobilis* and *Saccharomyces cerevisiae*. J Bacteriol 171: 3754-3759

Conway T, Sewell GW, Osman YA, Ingram LO (1987) Cloning and sequencing of the alcohol dehydrogenase II gene from *Zymomonas mobiis*. J Bacteriol 169: 2591-2597

Cook J, Beyea J (2000) Bioenergy in the United States: progress and possibilities. Biomass Bioenerg 18:441-455

Copeland A, Lucas S, Lapidus A, Barry K, Detter JC, Glavina del Rio T, Dalin E, Tice H, Pitluck S, Meincke L, Brettin T, Bruce D, Han C, Tapia R, Gilna P, Schmutz J, Larimer F, Land M, Hauser L, Kyrpides N, Mikhailova N, Lowe T, Richardson P (2006a) Complete sequence of *Pyrobaculum islandicum* DSM 4184. US DOE Joint Genome Institute

Copeland A, Lucas S, Lapidus A, Barry K, Detter JC, Glavina del Rio T, Dalin E, Tice H, Pitluck S, Thompson LS, Brettin T, Bruce D, Han C, Tapia R, Schmutz J, Larimer F, Land M, Hauser L, Kyrpides N, Kim E, Anderson I, Olsen G, Reich C, Woese C, Richardson P (2006b) Complete sequence of chromosome1 of *Thermofilum pendens* Hrk 5. US DOE Joint Genome Institute

Copeland A, Lucas S, Lapidus A, Barry K, Glavina del Rio T, Dalin E, Tice H, Bruce D, Pitluck S, Richardson P (2006c) Sequencing of the draft genome and assembly of *Thermoanaerobacter ethanolicus* X514. US DOE Joint Genome Institute

Copeland A, Lucas S, Lapidus A, Barry K, Glavina del Rio T, Dalin E, Tice H, Bruce D, Pitluck S, Richardson P (2007a) Complete sequence of *Thermotoga petrophila* RKU-1. US DOE Joint Genome Institute

Copeland A, Lucas S, Lapidus A, Barry K, Glavina del Rio T, Dalin E, Tice H, Bruce D, Pitluck S, Richardson P (2007b) Complete sequence of *Fervidobacterium nodosum* Rt17-B1. US DOE Joint Genome Institute

Copeland A, Lucas S, Lapidus A, Barry K, Dalin E, Tice H, Pitluck S, Sun H, Schmutz J, Larimer F, Land M, Hauser L, Kyrpides N, Kim E, Huber H, Woese C, Anderson IJ,

Richardson P (2007c) Complete sequence of *Staphylothermus marinus* F1. US DOE Joint Genome Institute

Copeland A, Lucas S, Lapidus A, Barry K, Glavina del Rio T, Dalin E, Tice H, Pitluck S, Chain P, Malfatti S, Shin M, Vergez L, Schmutz J, Larimer F, Land M, Hauser L, Kyrpides N, Mikhailova N, Cozen AE, Fitz-Gibbon ST, House CH, Saltikov C, Lowe TM, Richardson P (2007d) Complete sequence of *Pyrobaculum calidifontis* JCM 11548. US DOE Joint Genome Institute

Copeland A, Lucas S, Lapidus A, Barry K, Glavina del Rio T, Dalin E, Tice H, Pitluck S, Chertkov O, Brettin T, Bruce D, Detter JC, Han C, Schmutz J, Larimer F, Land M, Hauser L, Kyrpides N, Mikhailova N, Nelson K, Gogarten JP, Noll K, Richardson P (2007e) Complete sequence of *Thermosipho melanesiensis* BI429. US DOE Joint Genome Institute

Dandekar T, Schuster S, Snel B, Huynen M, Bork P (1999) Pathway alignment: application to the comparative analysis of glycolytic enzymes. Biochem J 343: 115-124

Davey ME, Wood WA, Key R, Nakamura K, Stahl DA (1993) Isolation of three species of *Geotoga* and *Petrotoga*: two new genera, representing a new lineage in the bacterial line of descent distantly related to the '*Thermotogales*'. Syst Appl Microbiol 16:191-200

Delano WL (2002) The PyMOL molecular graphics system. Delano Scientific, Palo Alto, CA

Demain AL, Newcomb M, Wu JH (2005) Cellulase, *Clostridia*, and ethanol. Microbiol Mol Biol Rev 69:124-154

Deutscher MP (1990) Guide to protein purification. Methods Enzymol 182: 588-604

Dien BS, Cotta MA, Jeffries TW (2003) Bacteria engineered for fuel ethanol production: current status. Appl Microbiol Biotechnol 63:258-266

Doi RH (2003) Microbial conversion of corn stalks to riches. J Bacteriol 185:701-702

Driskill LE, Kusy K, Bauer MW, Kelly RM (1999) Relationship between glycosyl hydrolase inventory and growth physiology of the hyperthermophile *Pyrococcus furiosus* on carbohydrate-based media. Appl Environ Microbiol 65: 893-897

Echave P, Tamarit J, Cabiscol E, Ros J (2003) Novel antioxidant role of alcohol dehydrogenase E from *Escherichia coli*. J Biol Chem 278: 30193-30198

Edwards C (1990) Thermophiles. In: Edwards C (eds) Microbiology of extreme environments. McGraw-Hill Publishing Co., New York, pp 1-32

Ehrensberger AH, Wilson DK (2004) Structural and catalytic diversity in the two family 11 aldo-keto reductases. J Mol Biol 337: 661-673

Eichler J, Adams MWW (2005) Posttranslational protein modification in *Archaea*. Microbiol Mol Biol Rev 69: 393-425

Erauso G, Reysenbach AL, Godfroy A, Meunier JR, Crump B, Partensky F, Baross JA, Marteinsson V, Barbier G, Pace NR, Prieur D (1993) *Pyrococcus abyssi* sp. nov., a new hyperthermophilic archaeon isolated from a deep-sea hydrothermal vent. Arch Microbiol 160:338–349

Esposito L, Bruno I, Sica F, Raia CA, Giordano A, Rossi M, Mazzarella L, Zagari A (2003a) Sructural study of a single-point mutant of *Sulfolobus solfataricus* alcohol dehydrogenase with enhanced activity. FEBS Lett 539: 14-18

Esposito L, Bruno I, Sica F, Raia CA, Giordano A, Rossi M, Mazzarella L, Zagari A (2003b) Crystal structure of a ternary complex of the alcohol dehydrogenase from *Sulfolobus solfataricus*. Biochemistry 42: 14397-14407

Esposito L, Sica F, Raia CA, Giordano A, Rossi M, Mazzarella L, Zagari A (2002) Crystal structure of the alcohol dehydrogenase from the hyperthermophilic archaeon *Sulfolobus solfataricus* at 1.85 Å resolution. J Mol Biol 318: 463-477

Fardeau ML, Ollivier B, Patel BKC, Magot M, Thomas P, Rimbault A, Rocchiccioli F, Garcia JL (1997) *Thermotoga hypogea* sp. nov., a xylanolytic, thermophilic bacterium from an oil-producing well. Int J Syst Bacteriol 47:1013-1019

Fiala G, Stetter KO (1986) *Pyrococcus furiosus* sp. nov. represents a novel genus of marine heterotrophic archaebacteria growing optimally at 100°C. Arch Microbiol 145: 56-61

Fiorentino G, Cannio R, Rossi M, Bartolucci S (2003) Transcriptional regulation of the gene encoding an alcohol dehydrogenase in the archaeon *Sulfolobus solfataricus* involves multiple factors and control elements. J Bacteriol 185: 3926-3934

Fitz-Gibbon ST, Ladner H, Kim UJ, Stetter KO, Simon MI, Miller JH (2002) Genome sequence of the hyperthermophilic crenarchaeon *Pyrobaculum aerophilum*. Proc Natl Acad Sci 99: 984-989

Fong JCN, Svenson CJ, Nakasugi K, Leong CTC, Bowman JP, Chen B, Glenn DR, Neilan BA, Rogers PL (2006) Isolation and characterization of two novel ethanol-tolerant facultative-anaerobic thermophilic bacteria strains from waste compost. Extremophiles 10: 363-372

Friedrich AB, Antranikian G (1996) Keratin degradation by *Fervidobacterium pennavorans*, a novel thermophilic anaerobic species of the order *Thermotogales*. Appl Environ Microbiol 62: 2875-2882

Fukui T, Atomi H, Kanai T, Matsumi R, Fujiwara S, Imanaka T (2005) Complete genome sequence of the hyperthermophilic archaeon *Thermococcus kodakaraensis* KOD1 and comparison with *Pyrococcus* genomes. Genome Res 15: 352-363

Galbe M, Zacchi G (2002) A review of the production of ethanol from softwood. Appl Microbiol Biotechnol 59: 618-65

Gasteiger E, Hoogland C, Gattiker A, Duvaud S, Wilkins MR, Appel RD, Bairoch A (2005) Protein identification and analysis tools on the ExPASy Server. In: Walker JM (eds) The proteomics protocols handbook. Humana Press, Totowa, NJ, pp: 571-607

Geueke B, Riebel B, Hummel W (2003) NADH oxidase from *Lactobacillus brevis*: a new catalyst for the regeneration of NAD. Enzyme Microb Technol 32: 205-211

Giordano A, Cannio R, La Cara F, Bartolucci S, Rossi M, Raia CA (1999) Asn249Tyr substitution at the coenzyme binding domain activates *Sulfolobus solfataricus* alcohol dehydrogenase and increases its thermal stability. Biochem 38: 3043-3054

Giordano A, Febbraio F, Russo C, Rossi M, Raia CA (2005) Evidence for co-operativity in coenzyme binding to tetrameric *Sulfolobus solfataricus* alcohol dehydrogenase and its structural basis: fluorescence, kinetic and structural studies of the wild-type enzyme and non-co-operative N249Y mutant. Biochem J 388: 657-667

Glasfeld A, Benner SA (1989) The stereospecificity of the ferrous-ion-dependent alcohol dehydrogenase from *Zymomonas mobilis*. Eur J Biochem 180: 373-375

Godfroy A, Raven NDH, Sharp RJ (2000) Physiology and continuous culture of the hyperthermophilic deep-sea vent archaeon *Pyrococcus abyssi* ST549. FEMS Microbiol Lett 186: 127-132.

Goihberg E, Dym O, Tel-Or S, Levin I, Peretz M, Burstein Y (2007) A single proline substitution is critical for the thermostabilization of *Clostridium beijerinckii* alcohol dehydrogenase. Proteins: Structure, Function and Bioinformatics 66: 196-204

Gong CS, Gao NJ, Du J, Tsao GT (1999) Ethanol production from renewable resources. Adv Biochem Eng Biotechnol 65: 207-241

González E, Fernández MR, Larroy C, Solà L, Pericàs MA, Parés X, Biosca JA (2000) Characterization of a (*2R*, *3R*)-2, 3-butanediol dehydrogenase as the *Saccharomyces cerevisiae YAL060W* gene product. J Biol Chem 275: 35876-35885

González JM, Masuchi Y, Robb FT, Ammerman JW, Maeder DL, Yanagibayashi M, Tamaoka J, Kato C (1998) *Pyrococcus horikoshii* sp. nov., a hyperthermophilic archaeon isolated from a hydrothermal vent at the Okinawa Trough. Extremophiles 2: 123-130

González JM, Sheckells D, Viebahn M, Krupatkina D, Borges KM, Robb FT (1999) *Thermococcus waiotapuensis* sp. nov., an extremely thermophilic archaeon isolated from a freshwater hot spring. Arch Microbiol 172: 95-101

Goodlove PE, Cunningham PR, Parker J, Clark DP (1989) Cloning and sequence analysis of fermentative alcohol dehydrogenase-encoding gene of *Escherichia coli*. Gene 85: 209-214

Grassia GC, McLean KM, Glénat P, Bauld J, Sheehy A (1996) A systematic survey for thermophilic fermentative bacteria and archaea in high temperature petroleum reservoirs. FEMS Microbiol Ecol 21: 47-58

Grogan DW (1989) Phenotypic characterization of the archaebacterial genus *Sulfolobus*: comparison of five wild-type strains. J Bacteriol 171: 6710-6719

Guagliardi A, Martino M, Iaccarino I, Rosa MD, Rossi M, Bartolucci S (1996) Purification and characterization of the alcohol dehydrogenase from a novel strain of *Bacillus stearothermophilus* growing at 70°C. Int J Biochem Cell Biol 28: 239-246

Guex N, Peitsch MC (1997) SWISS-MODEL and the Swiss-PdbViewer: An environment for comparative protein modelling. Electrophoresis 18: 2714-2723

Guy JE, Isupov MN, Littlechild JA (2003) The structure of an alcohol dehydrogenase from the hyperthermophilic archaeon *Aeropyrum pernix*. J Mol Biol 331: 1041-1051

Haki GD, Rakshit SK (2003) Developments in industrially important thermostable enzymes: a review. Bioresource Technol 89: 17-34

Hamelinck CN, van Hooijdonk G, Paaij APC (2005) Ethanol from lignocellulosic biomass: techno-economic performance in short-, middle- and long-term. Biomass Bioenergy 28: 384-410

Heiss C, Laivenieks M, Zeikus JG, Phillips RS (2001a) Mutation of cysteine-295 to alanine in secondary alcohol dehydrogenase from *Thermoanaerobacter ethanolicus* affects the enantioselectivity and substrate specificity of ketone reductions. Bioorg Med Chem 9: 1659-1666

Heiss C, Laivenieks M, Zeikus JG, Phillips RS (2001b) The stereospecificity of secondary alcohol dehydrogenase from *Thermoanaerobacter ethanolicus* is partially determined by active site water. J Am Chem Soc 123: 345-346

Hensgens CMH, Jansen M, Nienhuis-Kuiper ME, Boekema EJ, Van Breemen JFL, Hansen TA (1995) Purification and characterization of an alcohol dehydrogenase from 1, 2-propanediol-grown *Desulfovibrio* strain HDv. Arch Microbiol 164: 265-270

Herrero AA, Gomez RF (1980) Development of ethanol tolerance in *Clostridium thermocellum*: effect of growth temperature. Appl Environ Microbiol 40: 571-577

Higashi N, Fukada H, Ishikawa K (2005) Kinetic study of thermostable $_{L}$-threonine dehydrogenase from an archaeon *Pyrococcus horikoshii*. J Biosci Bioeng 99: 175-180

Hirakawa H, Kamiya N, Kawarabayashi Y, Nagamune T (2004) Properties of an alcohol dehydrogenase from the hyperthermophilic archaeon *Aeropyrum pernix* K1. J Biosci Bioeng 97: 202-206

Hirel PH, Schmitter JM, Dessen P, Fayat G, Blanquet S (1989) Extent of N-terminal methionine excision from *Escherichia coli* proteins is governed by the side-chain length of the penultimate amino acid. Proc Natl Acad Sci 86: 8247-8251

Holden JF, Baross JA (1993) Enhanced thermotolerance and temperature-induced changes in protein composition in the hyperthermophilic archaeon ES4. J Bacteriol 175: 2839-2843

Huber H, Hohn MJ, Rachel R, Fuchs T, Wimmer VC, Stetter KO (2002) A new phylum of archaea represented by a nanosized hyperthermophilic symbiont. Nature 417: 63-67

Huber R, Kurr M, Jannasch HW, Stetter KO (1989) A novel group of abyssal methanogenic archaebacteria (*Methanopyrus*) growing at 100°C. Nature 342: 833-834

Huber R, Langworthy TA, König H, Thomm M, Woese M, Sleytr UB, Stetter KO (1986) *Thermotoga maritima* sp. nov. represents a new genus of unique extremely thermophilic eubacteria growing up to 90°C. Arch Microbiol 144: 324-333.

Huber R, Stetter KO (2001) Discovery of hyperthermophilic microorganisms. Methods Enzymol 330: 11-24

Hummel W (1997) New alcohol dehydrogenases for the synthesis of chiral compounds. Adv Biochem Eng Biotechnol 58: 145-184

Hummel W (1999) Large-scale applications of NAD(P)-dependent oxidoreductases: recent developments. Trends Biotechnol 17: 487-492

Hummel W, Kula MR (1989) Dehydrogenases for the synthesis of chiral compounds. Eur J Biochem 184: 1-13

Ingram LO, Aldrich HC, Borges ACC, Causey TB, Martinez A, Morales F, Saleh A, Underwood SA, Yomano LP, York SW, Zaldivar J, Zhou S (1999) Enteric bacterial catalysts for fuel ethanol production. Biotechnol Prog 15: 855-866

Ishikawa K, Higashi N, Nakamura T, Matsuura T, Nakagawa A (2007) The first crystal structure of $_{L}$-threonine dehydrogenase. J Mol Biol 366: 857-867

Itoh T (2003) Taxonomy of nonmethanogenic hyperthermophilic and related thermophilic archaea. J Biosci Bioeng 96: 203-212

Jannasch HW, Huber R, Belkin S, Stetter KO (1988) *Thermotoga neapolitana* sp. nov. of the extremely thermophilic eubacterial genus *Thermotoga*. Arch Microbiol 150: 103-104

Jeanthon C, Reysenbach AL, L'Haridon S, Gambacorta A, Pace NR, Glenat P, Prieur D (1995) *Thermotoga subterranean* sp. nov., a new thermophilic bacterium isolated from a continental oil reservoir. Arch Microbiol 164: 91-97

Jochimsen B, Peinemann-Simon S, Völker H, Stüben D, Botz R, StoVers P, Dando PR, Thomm M (1997) *Stetteria hydrogenophila*, gen. nov. and sp. nov., a novel mixotrophic sulfur-dependent *crenarchaeote* isolated from Milos, Greece. Extremophiles 1: 67-73

Johnson AR, Dekker EE (1998) Site-directed mutagenesis of histidine-90 in *Escherichia coli* $_{L}$-threonine dehydrogenase alters its substrate specificity. Arch Biochem Biophy 351: 8-16

Jörnvall H, Persson B, Jeffery J (1987) Characteristics of alcohol/polyol dehydrogenases: the zinc-containing long-chain alcohol dehydrogenases. Eur J Biochem 167: 195-201

Kanai T, Imanaka H, Nakajima A, Uwamori K, Omori Y, Fukui T, Atomi H, Imanaka T (2005) Continuous hydrogen production by the hyperthermophilic archaeon, *Thermococcus kodakaraensis* KOD1. J Biotechnol 116: 271-282

Kanehisa M, Goto S, Kawashima S, Nakaya A (2002) The KEGG databases at GenomeNet. Nucl Acids Res 30: 42-46

Kannan V, Mutharasan R (1985) Ethanol fermentation characteristics of *Thermoanaerobacter ethanolicus*. Enzyme Microb Technol 7: 87-89

Karakashev D, Thomsen AB, Angelidaki I (2007) Anaerobic biotechnological approaches for production of liquid energy carriers from biomass. Biotech Lett 29: 1005-1012

Karlsson A, El-Ahmad M, Johansson K, Shafqat J, Jornvall H, Eklund H, Ramaswamy S (2003) Tetrameric NAD-dependent alcohol dehydrogenase. Chem Biol Interact 143-144: 239-245

Kashefi K, Lovley DR (2003) Extending the upper temperature limit for life. Science 301: 934

Kataoka M, Rohani LPS, Wada M, Kita K, Yanase H, Urabe I, Shimizu S (1998) *Escherichia coli* transformant expressing the glucose dehydrogenase gene from *Bacillus megaterium* as a co-factor regenerator in a chiral alcohol production system. Biosci Biotech Biochem 62: 167-169

Kawarabayasi Y, Hino Y, Horikawa H, Jin-no K, Takahashi M, Sekine M, Baba S, Ankai A, Kosugi H, Hosoyama A, Fukui S, Nagai Y, Nishijima K, Otsuka R, Nakazawa H, Takamiya M, Kato Y, Yoshizawa T, Tanaka T, Kudoh Y, Yamazaki J, Kushida N, Oguchi A, Aoki K, Masuda S, Yanagii M, Nishimura M, Yamagishi A, Oshima T, Kikuchi H (2001) Complete genome sequence of an aerobic thermoacidophilic crenarchaeon, *Sulfolobus tokodaii* strain 7. DNA Res 8: 123-140

Kawarabayasi Y, Hino Y, Horikawa H, Yamazaki S, Haikawa Y, Jin-no K, Takahashi M, Sekine M, Baba S, Ankai A, Kosugi H, Hosoyama A, Fukui S, Nagai Y, Nishijima K, Nakazawa H, Takamiya M, Masuda S, Funahashi T, Tanaka T, Kudoh Y, Yamazaki J, Kushida N, Oguchi A, Kikuchi H (1999) Complete genome sequence of an aerobic hyper-thermophilic crenarchaeon, *Aeropyrum pernix* K1. DNA Res 6: 83-101

Kawarabayasi Y, Sawada M, Horikawa H, Haikawa Y, Hino Y, Yamamoto S, Sekine M, Baba S, Kosugi H, Hosoyama A, Nagai Y, Sakai M, Ogura K, Otuka R, Nakazawa H, Takamiya M, Ohfuku Y, Funahashi T, Tanaka T, Kudoh Y, Yamazaki J, Kushida N, Oguchi A, Aoki K, Nakamura Y, Robb TF, Horikoshi K, Masuchi Y, Shizuya H, Kikuchi H (1998) Complete sequence and gene organization of the genome of a hyper-thermophilic archaebacterium, *Pyrococcus horikoshii* OT3. DNA Res. 5: 55-76

Kelly RM, Adams MWW (1994) Metabolism in hyperthermophilic microorganisms. Antonie Van Leeuwenhoek 66: 247-270

Keinan E, Seth KK, Lamed R (1986) Organic synthesis with enzymes. 3. TBADH-catalyzed reduction of chloro ketones. Total synthesis of (+)-(*S*, *S*)-(*cis*-6-methyltetrahydropyran-2-yl)-acetic acid: a civet constituent. J Am Chem Soc 108: 3473-3480

Kengen SWM, de Bok FAM, van Loo ND, Dijkema C, Stams AJM, de Vos WM (1994) Evidence for the operation of a novel Embden–Meyerhof pathway that involves ADP-dependent kinases during sugar fermentation by *Pyrococcus furiosus*. J Biol Chem 269: 17537-17541

Kengen SWM, Stams AJM, de Vos WM (1996) Sugar metabolism of hyperthermophiles. FEMS Microbiol Rev 18: 119-137

Kengen SW, Tuininga JE, de Bok FA, Stams AJ, de Vos WM (1995) Purification and characterization of a novel ADP-dependent glucokinase from the hyperthermophilic archaeon *Pyrococcus furiosus*. J Biol Chem 270: 30453-30457

Kessler D, Herth W, Knappe J (1992) Ultrastructure and pyruvate formate-lyase radical quenching property of the multienzymatic AdhE protein of *Escherichia coli*. J Biol Chem 267: 18073-18079

Kim S, Kee SB (2006) Rare codon clusters at 5'-end influence heterologous expression of archaeal gene in *Escherichia coli*. Protein Expression Purification 50: 49-57

Kizaki N, Yasohara Y, Hasegawa J, Wada M, Kataoka M, Shimizu S (2001) Synthesis of optically pure ethyl (*S*)-4-chloro-3-hydroxybutanoate by *Escherichia coli* transformant cells coexpressing the carbonyl reductase and glucose dehydrogenase genes. Appl Microbiol Biotechnol 55: 590-595

Klages KU, Morgan HW (1994) Characterization of an extremely thermophilic sulphur-metabolizing archaebacterium belonging to the *Thermococcales*. Arch Microbiol 162: 261-266

Klapatch TR, Hogsett DAL, Baskaran S, Pal S, Lynd LR (1994) Organism development and characterization for ethanol production using thermophilic bacteria. Appl Biochem Biotechnol 45-46: 209-223

Kleifeld O, Shi SP, Zarivach R, Eisenstein M, Sagi I (2003) The conserved Glu-60 residue in *Thermoanaerobacter brockii* alcohol dehydrogenase is not essential for catalysis. Protein Sci 12: 468-479

Klenk HP, Clayton RA, Tomb JF, White O, Nelson KE, Ketchum KA, Dodson RJ, Gwinn M, Hickey EK, Peterson JD, Richardson DL, Kerlavage AR, Graham DE, Kyrpides NC, Fleischmann RD, Quackenbush J, Lee NH, Sutton GG, Gill S, Kirkness EF, Dougherty BA, McKenney K, Adams MD, Loftus B, Peterson S, Reich CI, McNeil LK, Badger JH, Glodek A, Zhou L, Overbeek R, Gocayne JD, Weidman JF, McDonald L, Utterback T, Cotton MD, Spriggs T, Artiach P, Kaine BP, Sykes SM, Sadow PW, D'Andrea KP, Bowman C, Fujii C, Garland SA, Mason TM, Olsen GJ, Fraser CM, Smith HO, Woese CR, Venter JC (1997) The complete genome sequence of the hyperthermophilic, sulphate-reducing archaeon *Archaeoglobus fulgidus*. Nature 390: 364-370

Kobayashi T, Kwak YS, Akiba T, Kudo T, Horikoshi K (1994) *Thermococcus profundus* sp. nov., a new hyperthermophilic archaeon isolated from a deep-sea hydrothermal vent. Syst Appl Microbiol 17: 232-236

Kobs G (1997) Cloning blunt-end DNA fragments into the pGEM-T vector systems. Promega Notes Magazine 62: 15

Kopp J, Schwede T (2004) The SWISS-MODEL repository of annotated three-dimensional protein structure homology models. Nucl Acids Res 32: D230-D234

Korkhin Y, Kalb (Gilboa) AJ, Peretz M, Bogin O, Burstein Y, Frolow F (1998) NADP-dependent bacterial alcohol dehydrogenases: crystal structure, cofactor-binding and cofactor specificity of the ADHs of *Clostridium beijerinckii* and *Thermoanaerobacter brockii*. J Mol Biol 278: 967–981

Kort R, Liebl W, Labedan B, Forterre P, Eggen RIL, de Vos WM (1997) Glutamate dehydrogenase from hyperthermophilic bacterium *Thermotoga maritima*: molecular characterization and phylogenetic implications. Extremophiles 1: 52-60

Kostyukova AS, Gongadze GM, Polosina YY, Bonch Osmolovskaya EA, Miroshnichenko ML, Chernyh NA, Obraztsova MV, Svetlichny VA, Messner P, Sleytr UB, S. LH, Jeanthon C, Prieur D (1999) Investigation of structure and antigenic capacities of Thermococcales cell envelopes and reclassification of "*Caldococcus litoralis*" Z-1301 as *Thermococcus litoralis* Z-1301. Extremophiles 3: 239-245

Kroutil W, Mang H, Edegger K, Faber K (2004a) Recent advances in the biocatalytic reduction of ketones and oxidation of *sec*-alcohols. Curr Opin Chem Biol 8: 120-126

Kroutil W, Mang H, Edegger K, Faber K (2004b) Biocatalytic oxidation of primary and secondary alcohols. Adv Synth Catal 346: 125-142

Kube J, Brokamp C, Machielsen R, van der Oost J, Märkl H (2006) Influence of temperature on the production of an archaeal thermoactive alcohol dehydrogenase from *Pyrococcus furiosus* with recombinant *Escherichia coli*. Extremophiles 10: 221-227

Kuhad RC, Singh A (1993) Lignocellulose biotechnology: current and future prospects. Crit Rev Biotechnol 13: 151-172

Kumar S, Tsai CJ, Nussinov P (2000) Factors enhancing protein thermostability. Protein Eng. 13: 179-191

Labes A, Schönheit P (2001) Sugar utilization in the hyperthermophilic, sulfate-reducing archaeon *Archaeoglobus fulgidus* strain 7324: starch degradation to acetate and CO_2 *via* a

modified Embden–Meyerhof pathway and acetyl-CoA synthetase (ADP-forming). Arch Microbiol 176: 329-338

Laemmli UK (1970) Cleavage of structural proteins during assembly of the head of bacteriophage T4. Nature 227: 680-685

Lamed R, Zeikus JG (1980a) Glucose fermentation pathway of *Thermoanaerobium brockii*. J Bacteriol 141: 1251-1257

Lamed R, Zeikus JG (1980b) Ethanol production by thermophilic bacteria: relationship between fermentation product yields of the catabolic enzyme activities in *Clostridium thermocellum* and *Thermoanaerobium brockii*. J Bacteriol 144: 569-578

Larsen L, Nielsen P, Ahring BK (1997) *Thermoanaerobacter mathranii* sp. nov., an ethanol-producing, extremely thermophilic anaerobic bacterium from a hot spring in Iceland. Arch Microbiol 168: 114-119

Larroy C, Fernández MR, González E, Parés X, Biosca JA (2002) Characterization of the *Saccharomyces cerevisiae YMR318C* (*ADH6*) gene product as a broad specificity NADPH-dependent alcohol dehydrogenase: relevance in aldehyde reduction. Biochem J 361: 163-172

Legin E, Copinet A, Duchiron F (1998) Production of thermostable amylotic enzymes by *Thermococcus hydrothermalis*. Biotech Lett 20: 363-367

Leonardo MR, Cunningham PR, Clark DP (1993) Anaerobic regulation of the *adhE* gene, encoding the fermentative alcohol dehydrogenase of *Escherichia coli*. J Bacteriol 175: 870-878

L'Haridon S, Reysenbach A-L, Glénat P, Prieur D, Jeanthon C (1995) Hot subterranean biosphere in a continental oil reservoir. Nature 377: 223-224

Li C, Heatwole J, Soelaiman S, Shoham M (1999) Crystal structure of a thermophilic alcohol dehydrogenase substrate complex suggests determinants of substrate specificity and thermostability. Proteins: structure, function and genetics 37: 619-627

Li D, Stevenson KJ (1997) Purification and sequence analysis of a novel NADP(H)-dependent type III alcohol dehydrogenase from *Thermococcus* strain AN1. J Bacteriol 179: 4433-4437

Li WF, Zhou XX, Lu P (2005) Structural features of thermozymes. Biotech Adv 23: 271-281

Lien T, Madsen M, Rainey FA, Birkeland N (1998) *Petrotoga mobilis* sp. nov., from a North Sea oil-production well. Int J Syst Bacteriol 48: 1007-1013

Littlechild JA, Guy JE, Isupov MN (2004) Hyperthermophilic dehydrogenase enzymes. Biochem Soc Trans 32: 255-258

Lowe SE, Jain MK, Zeikus JG (1993) Biology, ecology, and biotechnological applications of anaerobic bacteria adapted to environmental stresses in temperature, pH, salinity, or substrates. Microbiol Rev 57: 451-509

Lu Z, Cabiscol E, Obradors N, Tamarit J, Ros J, Aguilar J, Lin ECC (1998) Evolution of an *Escherichia coli* protein with increased resistance to oxidative stress. J Biol Chem 273: 8308-8316

Lynd LR (1990) Large-scale fuel ethanol from lignocellulose. Appl Biochem Biotechnol 24-25: 695-719

Ma K, Adams MWW (1999) An unusual oxygen-sensitive, iron and zinc-containing alcohol dehydrogenase from the hyperthermophilic archaeon *Pyrococcus furiosus*. J Bacteriol 181: 1163-1170

Ma K, Dhanjoon J, Yang X, Ying X, Zhu H (2005) Ethanol and hydrogen production from agricultural residues by hyperthermophiles. Biocap Canada Foundation 1st National Conference. February 2nd - 3rd, Ottawa, Ontario, Canada. Poster presentation.

Ma K, Hutchins A, Sung SJS, Adams MWW (1997) Pyruvate ferrodoxin oxidoreductase from the hyperthermophilic archaeon, *Pyrococcus furiosus*, functions as a CoA-dependent pyruvate decarboxylase. Proc Natl Acad Sci 94: 9608-9613

Ma K, Loessner H, Heider J, Johnson MK, Adams MWW (1995) Effects of elemental sulfur on the metabolism of the deep-sea hyperthermophilic archaeon *Thermococcus* strain ES-1: characterization of a sulfur-regulated, non-heme iron alcohol dehydrogenase. J Bacteriol 177: 4748-4756

Ma K, Robb FT, Adams MWW (1994) Purification and characterization of NADP-specific alcohol dehydrogenase and glutamate dehydrogenase from the hyperthermophilic archaeon *Thermococcus litoralis*. Appl Environ Microbiol 60: 562-568

Machielsen R, Uria AR, Kengen SWM, van der Oost J (2006) Production and characterization of a thermostable alcohol dehydrogenase that belongs to the aldo-keto reductase superfamily. Appl Environ Microbiol 72: 233-238

Machielsen R, van der Oost J (2006) Production and characterization of a thermostable L-threonine dehydrogenase from the hyperthermophilic archaeon *Pyrococcus furiosus*. FEBS 273: 2722-2729

Mackenzie KF, Eddy CK, Ingram LO (1989) Modulation of alcohol dehydrogenase isoenzyme levels in *Zymononas mobilis* by iron and zinc. J Bacteriol 171: 1063-1067

McFall SM, Montville TJ (1989) pH-mediated regulation of pyruvate catabolism in *Lactobacillus plantarum* chemostat cultures. J Industrial Microbiol 4: 335-340

Magonet E, Hayen P, Delforge D, Delaive E, Remacle J (1992) Importance of the structural zinc atom for the stability of yeast alcohol dehydrogenase. Biochem J 287: 361-365

Makrides SC (1996) Strategies for achieving high-level expression of genes in *Escherichia coli*. Micrbiol Rev 60: 512-538

Marchler-Bauer A, Bryant SH (2004) CD-Search: protein domain annotations on the fly. Nucl Acids Res 32: 327-331

Membrillio-Hernández J, Lin ECC (1999) Regulation of expression of the *adhE* gene, encoding ethanol oxidoreductase in *Escherichia coli*: transcription from a downstream promoter and regulation by Fnr and RpoS. J Bacteriol 181: 7571-7579

Mertens R, Greiner L, van den Ban ECD, Haaker HBCM, Liese A (2003) Practical applications of hydrogenase I from *Pyrococcus furiosus* for NADPH generation and regeneration. J Mol Catalysis B: Enzymatic 24-25: 39-52

Mertens R, Liese A (2004) Biotechnological applications of hydrogenases. Curr Opin Biotechnol 15: 343-348

Mikulskis A, Aristarkhov A, Lin ECC (1997) Regulation of expression of the ethanol dehydrogenase gene (*adhE*) in *Escherichia coli* by catabolite repressor activator protein Cra. J Bacteriol 179: 7129-7134

Miroshnichenko ML, Bonch-Osmolovskaya EA (2006) Recent developments in the thermophilic microbiology of deep-sea hydrothermal vents. Extremophiles 10: 85-96

Miroshnichenko ML, Bonch-Osmolovskaya EA, Neuner A, Kostrikina NA, Chernych NA, Alekseev VA (1989) *Thermococcus stetteri* sp. nov., a new extremely thermophilic marine sulfur-metabolizing archaebacterium. Syst Appl Microbiol 12: 257-262

Miroshnichenko ML, Gongadze GM, Rainey FA, Kostyukova AS, Lysenko AM, Chernyh NA, BonchOsmolovskaya EA (1998) *Thermococcus gorgonarius* sp. nov. and

Thermococcus pacificus sp. nov.: heterotrophic extremely thermophilic archaea from New Zealand submarine hot vents. Int J Syst Bacteriol 48: 23-29

Miroshnichenko ML, Hippe H, Stackebrandt E, Kostrikina NA, Chernyh NA, Jeanthon C, Nazina TN, Belyaev SS, Bonch-Osmolovskaya EA (2001) Isolation and characterization of *Thermococcus sibiricus* sp. nov. from a Western Siberia high-temperature oil reservoir. Extremophiles 5: 85-91

Montella C, Bellsolell L, Pérez-Luque R, Badía J, Baldoma L, Coll M, Aguilar J (2005) Crystal structure of an iron-dependent group III dehydrogenase that interconverts $_{L}$-lactaldehyde and $_{L}$ -1,2-propanediol in *Escherichia coli*. J Bacteriol 187: 4957-4966

Moracci M, Cobucci-Ponzano B, Trincone A, Fusco S, De Rosa M, van der Oost J, Sensen CW, Charlebois RL, Rossi M (2000) Identification and molecular characterization of the first α-xylosidase from an archaeon. J Biol Chem 275: 22082-22089

Murali C, Creaser EH (1986) Protein engineering of alcohol dehydrogenase -1. Effects of two amino acid changes in the active site of yeast ADH-1. Prot Engineer 1: 55-57

Musa MM, Ziegelmann-Fjeld KI, Vieille C, Zeikus JG, Phillips RS (2007) Asymmetric reduction and oxidation of aromatic ketones and alcohols using W110A secondary alcohol dehydrogenase from *Thermoanaerobacter ethanolicus*. J Org Chem 72: 30-34

Neale AD, Scopes RK, Kelly JM, Wettenhall RE (1986) The two alcohol dehydrogenases of *Zymomonas mobilis*. Purification by differential dye ligand chromatography, molecular characterisation and physiological roles. Eur J Biochem 154: 119-124

Nelson KE, Clayton R, Gill SR, Gwinn ML, Dodson RJ, Haft DH, Hickey EK, Peterson J, Nelson WC, Ketchum KA, McDonald L, Utterback TR, Malek JA, Linher KD, Garrett MM, Stewart AM, Cotton MD, Pratt MS, Phillips CA, Richardson D, Heidelberg J, Sutton GG, Fleischmann RD, White O, Salzberg SL, Smith HO, Venter JC, Fraser CM (1999) Evidence for lateral gene transfer between archaea and bacteria from genome sequence of *Thermotoga maritima*. Nature 399: 323-329

Neuner A, Jannasch HW, Belkin S, Stetter KO (1989) *Thermococcus litoralis* sp. nov.: a new species of extremely thermophilic marine archaebacteria. Arch Microbiol 153: 205-207

Ng TK, Ben-Bassat A, Zeikus JG (1981) Ethanol production by thermophilic bacteria: fermentation of cellulosic substrates by cocultures of *Clostridium thermocellum* and *Clostridium thermohydrosulfuricum*. Appl Environ Microbiol 41: 1337-1343

Nishikubo T, Nakagawa N, Kuramitsu S, Masui R (2005) Improved heterologous gene expression in *Escherichia coli* by optimization of AT-content of codons immediately downstream of the initiation codon. J Biotech 120: 341-346

Nishio N, Nakashimada Y (2004) High rate production of hydrogen/methane from various substrates and wastes. Recent Prog Biochem Biomed Eng Japan I 90: 63-87

Olsson L, Hahn-Hagerdal B (1996) Fermentation of lignocellulosic hydrolysates for ethanol production. Enzyme Microb Technol 18: 312-331

Olofsson L, Nicholls NA, Wikman S (2005) TBADH activity in water-miscible organic solvents: correlations between enzyme performance, enantioselectivity and protein structure through spectroscopic studies. Org Biomol Chem 3: 750-755

Orphan VJ, Taylor LT, Hafenbradl D, Delong EF (2000) Culture-dependent and culture-independent characterization of microbial assemblages associated with high-temperature petroleum reservoirs. Appl Environ Microbiol 66: 700-711

Pan N, Imlay JA (2001) How does oxygen inhibit central metabolism in the obligate anaerobe *Acteroides thetaiotaomicron*? Mol Microbiol 39: 1562-1571

Patel BKC, Morgan HW, Daniel RM (1985) *Fervidobacterium nodosum* gen. nov. and spec. nov. a new chemoorganotrophic, caldoactive, anaerobic bacterium. Arch Microbiol 141: 63-69

Peitsch MC (1995) Protein modeling by E-mail. Bio/Technology 13: 658-660

Peretz M, Weiner LM, Burstein Y (1997) Cysteine reactivity in *Thermoanaerobacter brockii* alcohol dehydrogenase. Protein Sci 6: 1074-1083

Persson B, Krook MK, Jörnvall H (1991) Characteristics of short-chain alcohol dehydrogenases and related enzymes. Eur J Biochem 200: 537-543

Pham VT, Phillips RS, Lungdahl LG (1989) Temperature-dependent enantiospecificity of secondary alcohol dehydrogenase from *Thermoanerobacter ethanolicus*. J Am Chem Soc 111: 1935-1936

Phillips RS (2002) Tailoring the substrate specificity of secondary alcohol dehydrogenase. Can J Chem 80: 680-685

Pikuta EV, Marsic D, Itoh T, Bej AK, Tang J, Whitman WB, Ng JD, Garriott OK, Hoover RB (2007) *Thermococcus thioreducens* sp. nov., a novel hyperthermophilic, obligately sulfur-reducing archaeon from a deep-sea hydrothermal vent. Int J Syst Evol Microbiol 57: 1612-1618

Pledger RJ, Baross J (1989) Characterization of an extremely thermophilic archaebacterium isolated from a black smoker polychaete (Paralvinella, sp.) at the Juan de Fuca Ridge. Syst Appl Microbiol 12: 249-256

Pollastri G, Przybylski D, Rost B, Baldi P (2002) Improving the prediction of protein secondary structure in three and eight classes using recurrent neural networks and profiles. Proteins, 47: 228-235

Postec A, Pignet P, Cueff-Gauchard V, Schmitt A, Querellou J, Godfroy A (2005) Optimisation of growth conditions for continous culture of the hyperthermophilic archaeon *Thermococcus hydrothermalis* and development of sulphur-free defined and minimal media. Res Microbiol 156: 82-87

Prelog V (1964) Specification of the stereospecificity of some oxido-reductases by diamond lattice sections. Pure Appl Chem 9: 119-130

Prieur D, Erauso G, Jeanthon C (1995) Hyperthermophilic life at deep-sea hydrothermal vents. Planet Space Sci 43: 115–122

Radianingtyas H, Wright PC (2003) Alcohol dehydrogenases from thermophilic and hyperthermophilic archaea and bacteria. FEMS Microbiol Rev 794: 1–24

Radianingtyas H, Wright PC (2003) 2-propanol degradation by *Sulfolobus solfataricus*. Biotech Lett 25: 579-583

Raia CA, Giordano A, Rossi M (2001) Alcohol dehydrogenase from *Sulfolobus solfataricus*. Methods Enzymol 331: 176-195

Ranford JC, Coates AR, Henderson B (2000) Chapeonins are cell-signalling proteins: the unfolding biology of molecular chaperones. Expert Rev Mol Med 2: 1-17

Raven N, Ladwa N, Sharp R (1992) Continuous culture of the hyperthermophilic archaeum *Pyrococcus furiosus*. Appl Microbiol Biotechnol 38: 263-267

Raven NDH, Sharp RJ (1997) Development of defined and minimal media for the growth of the hyperthermophilic archaeon *Pyrococcus furiosus* Vc1. FEMS Microbiol Lett 146: 135-141.

Ravot G, Magot M, Fardeau ML, Patel BKC, Prensier G, Egan A, Garcia JL, Ollivier B (1995) *Thermotoga elfii* sp. nov., a novel thermophilic bacterium from an African oil-producing well. Int J Syst Bacteriol 45: 308-314

Ravot G, Ollivier B, Fardeau ML, Patel BKC, Andrews KT, Magot M, Garcia JL (1996) $_{L}$-Alanine production from glucose fermentation by hyperthermophilic members of the domains bacteria and archaea: a remnant of an ancestral metabolism? Appl Environ Microbiol 62: 2657-2659

Ravot G, Ollivier B, Magot M, Patel BKC, Crolet JL, Fardeau ML, Garcia JL (1995) Thiosulfate reduction, an important physiological feature shared by members of the order *Thermotogales*. Appl Environ Microbiol 61: 2053-2055

Reid MF, Fewson CA (1994) Molecular characterization of microbial alcohol dehydrogenases. Crit Rev Microbiol 20: 13-56

Reiter WD, Palm P, Zillig W (1988) Transcription termination in the archaebacterium *Sulfolobus*: signal structures and linkage to transcription initiation. Nucl Acids Res 16: 2445-2459

Rella R, Raia CA, Pensa M, Pisani FM, Gambacorta A, De Rosa M, Rossi M (1987) A novel archaebacterial NAD^+-dependent alcohol dehydrogenase: purification and properties. Eur J Biochem 167: 475-479

Riebel BR, Gibbs PR, Wellborn WB, Bommarius AS (2003) Cofactor regeneration of both NAD^+ from NADH and $NADP^+$ from NADPH:NADH oxidase from *Lactobacillus sanfranciscensis*. Adv Synth Catal 2003, 345: 707-712

Riebel BR, Gibbs PR, Wellborn WB, Bommarius AS (2002) Cofactor regeneration of NAD^+ from NADH: novel water-forming NADH oxidases. Adv Synth Cat 344: 1156-1169

Rinker KD, Han CJ, Kelly RM (1999) Continuous culture as a tool for investigating the growth physiology of heterotrophic hyperthermophiles and extreme thermoacidophiles, J Appl Microbiol (Suppl S) 85: 118S-127S

Rinker KD, Kelly RM (2000) Effect of carbon and nitrogen sources on growth dynamics and exopolysaccharide production for the hyperthermophilic archaeon *Thermococcus litoralis* and bacterium *Thermotoga maritima*. Biotechnol Bioeng 69: 537-547

Rinker KD, Kelly RM (1996) Growth physiology of the hyperthermophilic Archaeon *Thermococcus litoralis*: development of a sulfur-free defined medium, characterization of an exopolysaccharide, and evidence of biofilm formation. Appl Environ Microbiol 62: 4478-4485

Robb FT, Clark DS (1999) Adaptation of proteins from hyperthermophiles to high pressure and high temperature. J Mol Microbiol Biotechnol 1: 101-105

Robb FT, Maeder DL (1998) Novel evolutionary histories and adaptive features of proteins from hyperthermophiles. Curr Opin Biotech 9: 288-291

Robb FT, Maeder DL, Brown JR, DiRuggiero J, Stump MD, Yeh RK, Weiss RB, Dunn DM (2001) Genomic sequence of hyperthermophile, *Pyrococcus furiosus*: Implications for physiology and enzymology. Methods Enzymol 330: 134-157

Robb FT, Park JB, Adams MWW (1992) Characterization of an extremely thermostable glutamate dehydrogenase: a key enzyme in the primary metabolism of the hyperthermophilic archaebacterium, *Pyrococcus furiosus*. Biochim Biophys Acta 1120: 267-272

Robb FT, Maeder DL, DiRuggiero J, Borges KM, Tolliday N (2001) Glutamate dehydrogenases from hyperthermophiles. Methods Enzymol 331: 26-41

Ronimus, R. S. and Morgan, H. W. (2003) Distribution and phylogenies of enzymes of the Embden–Meyerhof–Parnas pathway from archaea and hyperthermophilic bacteria support a gluconeogenic origin of metabolism. Archaea 1: 199-221

Ronimus RS, Reysenbach AL, Musgrave DR, Morgan HW (1997) The phylogenetic position of the *Thermococcus* isolate AN1 based on 16S rRNA gene sequence analysis: a proposal that AN1 represents a new species, *Thermococcus zilligii* sp. nov. Arch Microbiol 168: 245-248.

Ruzheinikov SN, Burke J, Sedelnikova S, Baker PJ, Taylor R, Bullough PA, Muir NM, Gore MG, Rice DW (2001) Glycerol dehydrogenase: structure, specificity and mechanism of a family III polyol dehydrogenase. Structure 9: 789-802.

Sakuraba H, Goda S, Ohshima T (2004) Unique sugar metabolism and novel enzymes of hyperthermophilic archaea. Chem Rec 3: 281-287

Sælensminde G, Halskau Ø, Helland R, Willassen NP, Jonassen I (2007) Structure-dependent relationships between growth temperature of prokaryotes and the amino acid frequency in their proteins. Extremophiles 11: 585-596

Sambrook J, Fritsch EF, Maniatis T (1989) Molecular Cloning: A Laboratory Manual (second edition). Cold Spring Harbor Laboratory Press, Cold Spring Harbor, New York, pp 25-28

Schiraldi C, Rosa D (2002) Perspectives on biotechnological application of archaea. Archaea 1: 75-86

Schönheit P, Schäfer T (1995) Metabolism of hyperthermophiles. World J Microbiol Biotechnol 11: 26-57

Schwarzenbacher R, von Delft F, Canaves JM, Brinen LS, Dai X, Deacon AM, Elsliger MA, Eshaghi S, Floyd R, Godzik A, Grittini C, Grzechnik SK, Guba C, Jaroszewski L, Karlak C, Klock HE, Koesema E, Kovarik JE, Kreusch A, Kuhn P, Lesley SA, McMullan D, McPhillips TM, Miller MA, Miller MD, Morse A, Moy K, Ouyang J, Page R, Robb A, Rodrigues K, Selby TL, Spraggon G, Stevens RC, van den Bedem H, Velasquez J, Vincent J, Wang X, West B, Wolf G, Hodgson KO, Wooley J, Wilson IA (2004) Crystal structure of an iron-containing 1,3-propanediol dehydrogenase (TM0920) from *Thermotoga maritima* at 1.3 Å resolution. Proteins 54: 174-177

Schwede T, Kopp J, Guex N, Peitsch MC (2003) SWISS-MODEL: an automated protein homology-modeling server. Nucl Acids Res 31: 3381-3385

Scopes PK (1983) An iron-activated alcohol dehydrogenase. FEBS Lett 156: 303-306

Seelbach K, Riebel B, Hummel W, Kula MR, Tishkov VI, Egorov AM, Wandrey C, Kragl U (1996) A novel, efficient regenerating method of NADPH using a new formate dehydrogenase. Tetrahedron Lett 37: 1377-1380

Selig M, Xavier KB, Santos H, Schönheit P (1997) Comparative analysis of Embden–Meyerhof and Entner–Doudoroff glycolytic pathways in hyperthermophilic archaea and the bacterium *Thermotoga*. Arch Microbiol 167: 217-232

Seo JS, Chong H, Park HS, Yoon KO, Jung C, Kim JJ, Hong JH, Kim H, Kim JH, Kil JI, Park CJ, Oh HM, Lee JS, Jin SJ, Um HW, Lee HJ, Oh SJ, Kim JY, Kang HL, Lee SY, Lee KJ, Kang HS (2005) The genome sequence of the ethanologenic bacterium *Zymomonas mobilis* ZM4. Nat Biotechnol 23: 63-68

She Q, Singh RK, Confalonieri F, Zivanovic Y, Allard G, Awayez MJ, Chan-Weiher CCY, Clausen IG, Curtis BA, Moors AD, Erauso G, Fletcher S, Gordon PMK, Jong IH, Jeffries AC, Kozera CJ, Medina N, Peng X, Thi-Ngoc HP, Redder P, Schenk ME, Theriault C, Tolstrup N, Charlebois RL, Doolittle WF, Duguet M, Gaasterland T, Garrett RA, Ragan MA, Christoph W. Sensen CW, van der Oostg J (2001) The complete genome of the crenarchaeon *Sulfolobus solfataricus* P2. Proc Natl Acad Sci 98: 7835-7840

Sheehan JJ (1994) Bioconversion for production of renewable transportation fuels in the United States: a strategic perspective. In: Himmel ME, Baker JO, Overend RP (eds) Enzymatic conversion of biomass for fuels production, ACS symposium series 566. American Chemical Society, Washington DC, pp 1-53

Shevchenko A, Wilm M, Vorm O, Mann M (1996) Mass spectrometric sequencing of proteins from silver-stained polyacrylamide gels. Anal Chem 68: 850-858

Siebers B, Hensel R (1993) Glucose catabolism of the hyperthermophilic archaeum *Thermoproteus tenax*. FEMS Microbiol Lett 111: 1-8

Siebers B, Schönheit P (2005) Unusual pathways and enzymes of central carbohydrate metabolism in archaea. Curr Opin Microbiol 8: 695-705

Snijders APL, Walther J, Peter S, Kinnman I, de Vos MGJ, van de Werken HJG, Brouns SJJ, van der Oost J, Wright PC (2006) Reconstruction of central carbon metabolism in *Sulfolobus solfataricus* using a two-dimensional gel electrophoresis map, stable isotope labeling and DNA microarray analysis. Proteomics 6: 1518-1529

Sommer P, Georgieva T, Ahring BK (2004) Potential for using thermophilic anaerobic bacteria for bioethanol production from hemicellulose. Biochem Soc Trans 32: 283-289

Sonnleitner B, Fiechter A, Giovannini F (1984) Growth of *Thermoanaerobium brockii* in batch and continuous culture at supraoptimal temperatures. Appl Microbiol Biotechnol 19: 326-334

Spencer P, Bown KJ, Scawen MD, Atkinson T, Gore MG (1989) Isolation and characterization of the glycerol dehydrogenase from *Bacillus stearothermophilus*. Biochim Biophys Acta 994: 270-279.

Stadtman ER (1993) Oxidation of free amino acids and amino acid residues in proteins by radiolysis and by metal-catalyzed reactions. Annu Rev Biochem 62: 797-821

Starrenburg MJC, Hugenholtz J (1991) Citrate fermentation by *Lactococcus* and *Leuconostoc spp*. Appl Environ Microbiol 57: 3535-3540

Sterner R, Liebl W (2001) Thermophilic adaptation of proteins. Crit Rev Biochem Mol Biol 36: 39-106

Stetter KO (1989) Extremely thermophilic chemolithoautotrophic archaebacteria. In: Schlegel HG, Bowien B (eds) Autotrophic bacteria. Science Tech Publishers/Springer, Madison/Berlin, pp 167-176

Stetter KO (1996) Hyperthermophilic prokaryotes. FEMS Microbiol Rev 18: 149-158

Stetter KO (2006) History of discovery of the first hyperthermophiles. Extremophiles 10: 357-362

Stetter KO, Fiala G, Huber G, Huber R, Segerer A (1990) Hyperthermophilic microorganisms. FEMS Microbiol Rev 75: 117-124

Stetter KO, Huber R, Blöchl E, Kurr M, Eden RD, Fielder M, Cash H, Vance I (1993) Hyperthermophilic archaea are thriving in deep North Sea and Alaskan oil reservoirs. Nature 365: 743-745

Stetter KO, Thomm M, Winter J, Wildgruber G, Huber H, Zillig W, Janecovic D, König H, Palm P, Wunderl S (1981) *Methanothermus fervidus*, sp. nov., a novel extremely thermophilic methanogen isolated from an Icelandic hot spring. System Appl Microbiol 2: 166-178

Stothard P (2000) The Sequence manipulation suite: JavaScript programs for analyzing and formatting protein and DNA sequences. Biotechniques 28: 1102-1104

Sulzenbacher G, Alvarez K, van den Heuvel RHH, Versluis C, Spinelli S, Campanacci V, Valencia C, Cambillau C, Eklund H, Tegoni M (2004) Crystal structure of *E. coli* alcohol dehydrogenase YqhD: Evidence of a covalently modified NADP coenzyme. J Mol Biol 342: 489-502

Sun H, Plapp B (1992) Progressive sequence alignment and molecular evolution of the Zn-containing Adh family. J Mol Evol 34: 522-535

Takahata Y, Nishijima M, Hoaki T, Maruyama T (2001) *Thermotoga petrophila* sp. nov. and *Thermotoga naphthophila* sp. nov., two hyperthermophilic bacteria from the Kubiki oil reservoir in Niigata, Japan. Int J Syst Evol Microbiol 51: 1901-1909

Takahata Y, Nishijima M, Hoaki T, Maruyama T (2000) Distribution and physiological characteristics of hyperthermophiles in the Kubiki oil reservoir in Niigata, Japan. Appl Environ Microbiol 66: 73-79

Takai K, Sugai A, Itoh T, Horikoshi K (2000) *Palaeococcus ferrophilus* gen. nov., sp. nov., a barophilic, hyperthermophilic archaeon from a deep-sea hydrothermal vent chimney. Int J Syst Evol Microbiol 50 Pt 2: 489–500

Tamarit J, Cabiscol E, Aguilar J, Ros J (1997) Differential inactivation of alcohol dehydrogenase isoenzymes in *Zymomonas mobilis* by oxygen. J Bacteriol 179: 1102-1104

Thompson JD, Higgins DG, Gibson TJ (1994) CLUSTAL W: improving the sensitivity of progressive multiple sequence alignment through sequence weighting, position-specific gap penalties and weight matrix choice. Nucl Acids Res 22: 4673-4680

Tishkov VI, Galkin AG, Fedorchuk VV, Savitsky PA, Rojkova AM, Gieren H, Kula MR (1999) Pilot scale production and isolation of recombinant NAD^+- and $NADP^+$-specific formate dehydrogenases. Biotechnol Bioeng 64: 187-193

Triglia T, Peterson M, Kemp D (1988) A procedure for *in vitro* amplification of DNA segments that lie outside the boundaries of known sequences. Nucl Acids Res 16: 8186

Tripp AE, Burdette DS, Zeikus JG, Phillips RS (1997) Mutation of serine-39 to threonine in thermostable secondary alcohol dehydrogenase from *Thermoanaerobacter ethanolicus* changes enantiosepecificity. J Am Chem Soc 120: 5137-5141

Ueda K, Yamashita A, Ishikawa J, Shimada M, Watsuji TO, Morimura K, Ikeda H, Hattori M, Beppu T (2004) Genome sequence of *Symbiobacterium thermophilum*, an uncultivable bacterium that depends on microbial commensalisms. Nucl Acids Res 32: 4937-4944

Unden G, Becker S, Bongaerts J, Schirawski J, Six S (1994) Oxygen regulated gene expression in facultatively anaerobic bacteria. Antonie Leeuwenhoek 66: 3-23

Vallee H, Auld DS (1990) Zinc coordination, function, and structure of zinc enzymes and other proteins. Biochemistry 29: 5647-5659

van der Oost J, Voorhorst WGB, Kengen SWM, Geerling ACM, Wittenhorst V, Gueguen Y, de Vos WM (2001) Genetic and biochemical characterization of a short-chain alcohol dehydrogenase from the hyperthermophilic archaeon *Pyrococcus furiosus*. Eur J Biochem 268: 3062-3068

van Ooteghem SA, Beer SK, Yue PC (2002) Hydrogen production by the thermophilic bacterium *Thermotoga neapolitana*. Appl Biochem Biotechnol 98-100: 177-189.

van Ooteghem SA, Jones A, Van Der Lelie D, Dong B, Mahajan D (2004) H_2 production and carbon utilization by *Thermotoga neapolitana* under anaerobic and microaerobic growth conditions. Biotechnol Lett 26: 1223-1232.

Verhees CH, Kengen SW, Tuininga JE, Schut GJ, Adams MW, de Vos WM, van der Oost J (2003) The unique features of glycolytic pathways in archaea. Biochem J 375: 231-246

Vieille C, Zeikus GJ (2001) Hyperthermophilic enzymes: sources, uses, and molecular mechanisms for thermostability. Microbiol Mol Biol Rev 65: 1-43

Völkl P, Huber R, Drobner E, Rachel R, Burggraf S, Trincone A, Stetter KO (1993) *Pyrobaculum aerophilum* sp. nov., a novel nitrate-reducing hyperthermophilic archaeum. Appl Environ Microbiol 59: 2918-2926

de Vos WM, Kengen SWM, Voorhorst WGB, van der Oost J (1998) Sugar utilization and its control in hyperthermophiles. Extremophiles 2: 201-205

Walter KA, Bennett GN, Papoutsakis ET (1992) Molecular characterization of two *Clostridium acetobutylicum* ATCC 824 butanol dehydrogenase isozyme genes. J Bacteriol 174: 7149-7158

Walter S (2002) Structure and function of the GroE chaperone. Cell Mol Life Sci 59: 1589-1597

Ward OP, Singh A (2002) Bioethanol technology: developments and perspectives. Adv Appl Microbiol 51: 53-80

Watrin L, Martin-Jezequel V, Prieur D (1995) Minimal amino acid requirements of the hyperthermophilic archaeon *Pyrococcus abyssi*, isolated from deep-sea hydrothermal vents. Appl Environ Microbiol 61: 1138-1140

Weckbecker A, Hummel W (2005) Glucose dehydrogenase for the regeneration of NADPH and NADH. In: Barredo JL (ed) Microbial enzymes and biotransformations. Humana Press, Totowa, NJ, pp 225-238

Weinhold EG, Glasfeld A, Ellington AD, Benner SA (1991) Structural determinants of stereospecificity in yeast alcohol dehydrogenase. Proc Natl Acad Sci 88: 8420-8424

Wheals AE, Basso LC, Alves DMG, Amorium HV (1999) Fuel ethanol after 25 years. TIBTECH 17: 482-487

Wichmann R, Vasic-Racki (2005) Cofactor regeneration at the lab scale. Adv Biochem Engin/Biotechnol 92: 225-260

Widdel F, Wolfe RS (1989) Expression of secondary alcohol dehydrogenase in methanogenic bacteria and purification of the F_{420}-specific enzyme from *Methanogenium thermophilum* strain TCI. Arch Microbiol 152: 322-328

Wiegel J, Ljungdahl LG, Rawson JR (1979) Isolation from soil and properties of the extreme thermophile *Clostridium thermohydrosulfuricum*. J Bacteriol 139: 800-810

Wiegel J, Ljungdahl LG (1981) *Thermoanaerobacter ethanolicus* gen. nov., spec. nov., a new, extremely thermophilic, anaerobic bacterium. Arch Microbiol 128: 343-348

Wiegel J, Ljungdahl LG (1986) The importance of thermophilic bacteria in biotechnology. Crit Rev Biotechnol 3: 39-108

Williamson VM, Paquin CE (1987) Homology of *Saccharomyces cerevisiae* ADH4 to an iron-activated alcohol dehydrogenase from *Zymomonas mobilis*. Mol Gen Genet 209: 374-381

Windberger E, Huber R, Trincone A, Fricke H, Stetter KO (1989) *Thermotoga thermarum* sp. nov. and *Thermotoga neapolitana* occurring in African continental solfataric springs. Arch Microbiol 151: 506-512

Worthington P, Blum P, Perez-Pomares F, Elthon T (2003) Large-scale cultivation of acidophilic hyperthermophiles for recovery of secreted proteins. Appl Environ Microbiol 69: 252-257

Wright HT (1991) Nonenzymatic deamidation of asparaginyl and glutaminyl residues in proteins. Crit Rev Biochem Mol Biol 26: 1-52

Wyman CE (1999) Biomass ethanol: technical progress, opportunities, and commercial challenges. Annu Rev Energy Environ 24: 189-226

Xavier KB, Peist R, Kossmann M, Boos W, Santos H (1999) Maltose metabolism in the hyperthermophilic archaeon *Thermococcus litoralis*: purification and characterization of key enzymes. J Bacteriol 181: 3358-3367

Yan RT, Chen JS (1990) Coenzyme A-acylating aldehyde dehydrogenase from *Clostridium beijerinckii* NRRL B592. Appl Environ Microbiol 56: 2591-2599

Yang X, Ma K (2005) Purification and characterization of an NADH oxidase from extremely thermophilic anaerobic bacterium *Thermotoga hypogea*. Arch Microbiol 183: 331-337

Ying X, Wang Y, Badiei HR, Karanassios V, Ma K (2007) Purification and characterization of an iron-containing alcohol dehydrogenase in extremely thermophilic bacterium *Thermotoga hypogea*. Arch Microbiol 187: 499-510

Yokoyama S, Yokoyama R, Kinlaw CS, Harry DE (1990) Molecular evolution of the zinc-containing long-chain alcohol dehydrogenase genes. Mol Biol Evol 7: 143-154

Zaldivar J, Nielsen J, Olsson L (2001) Fuel ethanol production from lignocellulose: a challenge for metabolic engineering and process integration. Appl Microbiol Biotechnol 56: 17-34

Zeikus JG, Hegge PW, Anderson MA (1979) *Thermoanaerobium brockii* gen. nov. and sp. nov., a new chemoorganotrophic, caldoactive, anaerobic bacterium. Arch Microbiol 122: 41-48

Zeikus JG, Vieille C, Savchenko A (1998) Thermozymes: biotechnology and structure-function relationships. 2: 179-183

Zheng Y, Cao Y, Fang B (2004) Cloning and sequence analysis of the *dhaT* gene of the 1,3-propanediol regulon from *Klebsiella pneumoniae*. Biotechnol Lett 26: 251-255

Zheng CS, Pham VT, Phillips RS (1992) Asymmetric reduction of ketoesters with alcohol dehydrogenase from *Thermoanaerobacter ethanolicus*. Bio Med Chem Letts 2: 619-622

Zheng CS, Pham VT, Phillips RS (1994) Asymmetric reduction of aliphatic and cyclic ketones with secondary alcohol dehydrogenase from *Thermoanaerobacter ethanolicus*: effects of substrate structure and temperature. Catalysis Today 22: 607-620

Zhu D, Malik HT, Hua L (2006) Asymmetric ketone reduction by a hyperthermophilic alcohol dehydrogenase: the substrate specificity, enantioselectivity and tolerance of organic solvents. Tetrahedron Asymmetry 17: 3010-3014

Ziegelmann-Fjeld KI, Musa MM, Phillips RS, Zeikus JG, Vieille C (2007) A *Thermoanaerobacter ethanolicus* secondary alcohol dehydrogenase mutant derivative highly active and stereoselective on phenylacetone and benzylacetone. Protein Engineering, Design and Selection 20: 47-55

Ziegenhorn J, Senn M, Bücher T (1976) Molar absorptivities of β-NADH and β-NADPH. Clin Chem 22: 151-160

Zillig W, Holz I, Janekovic D, Klenk H, Imsel E, Trent J, Wunderl S, Forjaz VH, Coutinho R, Ferreira T (1990) *Hyperthermus butylicus*, a hyperthermophilic sulfur-reducing archaebacterium that ferments peptides. J Bacteriol 172: 3959-3965

Zillig W, Holz I, Klenk HP, Trent J, Wunderl S, Janekovic D, Imsel E, Haas B (1987) *Pyrococcus woesei*, sp. nov., an ultra-thermophilic marine archaebacterium, representing a novel order, Thermococcales. Syst Appl Microbiol 9: 62–70

Zillig W, Janekovic D, Schafer W, Reiter WD (1983) The archaebacterium *Thermococcus celer* represents, a novel genus within the thermophilic branch of the archaebacteria. Syst Appl Microbiol 4: 88-94